SCUOLA DI DOTTORATO
UNIVERSITÀ DEGLI STUDI DI MILANO-BICOCCA

Department of Medicine and Surgery

PhD program in Translational and Molecular Medicine (DIMET)
Cycle XXXVIII

Phagocytic macrophages mitigate α-Synuclein pathology in an astrocyte-driven model of neurodegeneration

Surname **NANNONI** Name **MELANIA**

Registration number **896575**

Tutor: Prof. Rocco Giovanni Piazza

Co-tutor: Dr. Vania Broccoli

Supervisor: Dr. Vania Broccoli

Coordinator: Prof. Francesco Mantegazza

ACADEMIC YEAR 2024/2025

Table of Contents

Acronyms and Abbreviations

6-OHDA: 6-hydroxydopamine
αSYN: Alpha-Synuclein
AADC: L-amino-acid decarboxylase
AD: Alzheimer's disease
APCs: Antigen-presenting cells
BBB: Blood-brain barrier
CAMs: CNS-associated macrophages
CNS: Central nervous system
CSF: Cerebrospinal fluid
CSPα: Cysteine-string protein-α
DALYs: Disability-adjusted life years
DAT-SPECT: Dopamine transporter single-photon emission computed tomography
DAT: Dopamine transporter
DBS: Deep brain stimulation
DTI: Diffusion tensor imaging
EMPs: Erythro-myeloid progenitors
ER: Endoplasmic reticulum
GFAP: Glial fibrillary acidic protein
GPe: External segment of the globus pallidus
GPi: Internal segment of the globus pallidus
GWAS: Genome-wide association studies
HSCs: Hematopoietic stem cells
IPMDS: International Parkinson and Movement Disorder Society
L-DOPA: Levodopa
LBs: Lewy bodies
LNs: Lewy neurites
LPS: Lipopolysaccharide
MDS-PD: Movement Disorder Society Clinical Diagnostic Criteria for Parkinson's Disease
METH: Methamphetamine
MPTP: 1-metil 4-fenil 1,2,3,6-tetraidro-piridina
MS: Multiple sclerosis
MSNs: Medium spiny neurons
NAC: Non-amyloid-β component
NSAID: Non-steroidal anti-inflammatory drugs
PD: Parkinson's Disease
PET: Positron emission tomography
PFFs: Preformed fibrils
PP2A: Phosphatase 2A
PTMs: Post-translational modification
RBD: REM sleep behaviour disorder

ROS: Reactive oxygen species
SAAs: Alpha-Synuclein seed amplification assays
SASP: Senescence-associated secretory phenotype
SN: Substantia nigra
SNpc: Subtantia nigra pars compacta
SNpr: Substantia nigra pars reticulata
SPECT: Single photon emission computed tomography
STN: Subthalamic nucleus
STR: Striatum
TCR: T cell receptor
TH: Tyrosine Hydroxylase
TNTs: Tunnelling Nanotubes
Treg: Regulatory T cell
UPR: Unfolded protein response
VAMP2: Vesicle-associated membrane protein 2
VMAT2: Vesicular monoamine transporter 2

1. INTRODUCTION

1.1 Epidemiology

Parkinson's disease (PD) is the second most common neurodegenerative disorder after Alzheimer's disease (AD) and represents a major global health and socioeconomic challenge (Dorsey et al., 2007).

Over the past decades, its global burden has risen markedly, with more than 211,000 deaths (95 % UI: 167,771–265,160) and 3.2 million disability-adjusted life years (DALYs) (95 % UI: 2.6–4.0) reported in 2016, a 2.5-fold increase since 1990. This upward trend is expected to continue, with demographic models estimating that over 25 million individuals will be affected by 2050, primarily as a consequence of population aging (WHO, 2022; Dorsey and Bloem, 2018).

Epidemiological data show wide variation in PD prevalence and incidence across age, sex and geography (Ascherio and Schwarzschild, 2016; de Lau and Breteler, 2006). Annual incidence ranges from 5 to over 35 cases per 100,000 persons in the general population (Fig.1). As with incidence, prevalence also rises sharply with age, from about 0.3% in the general population to 1–2% in adults over 80 years (de Lau and Breteler, 2006; Poewe et al., 2017; GBD 2016 Collaborators, 2018). Overall, age remains the strongest risk factor for the onset and the progression of PD.

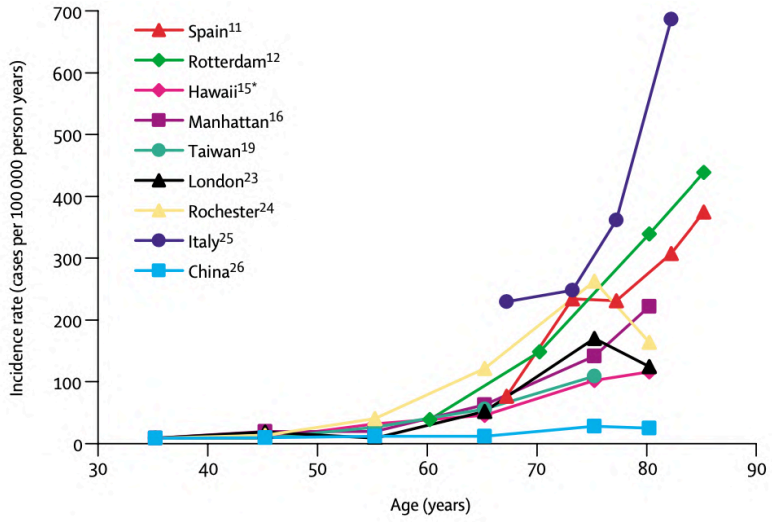

Figure 1. Age-specific incidence rates of Parkinson's disease in population-based prospective studies. Incidence rates of PD rise exponentially with age, confirming age as the strongest risk factor for disease onset and progression. Data come from population-based cohorts conducted in Spain, Rotterdam, Hawaii, Manhattan, Taiwan, London, Rochester, Italy, and China. Each line represents a separate study, highlighting geographical variability in PD incidence across populations (adapted from de Lau and Breteler, 2006). **Study restricted to men.*

While aging and longer disease duration account for part of the observed rise, other determinants also contribute (Dorsey et al, 2018). Men are more frequently affected than women, with pooled male-to-female incidence ratios of about 1.4: 1 (Hirsch et al., 2016; GBD 2016 Collaborators, 2018). These sex differences may reflect greater environmental exposures among men, neuroprotective effects of female sex hormones (oestrogens, progesterone), and disparities in healthcare access, as women and minority groups are less likely to receive specialist care (Sawada and Shimohama, 2003; Willis et al., 2011).

Ethnicity and geography also influence the epidemiology of PD, although findings remain heterogeneous. Incidence appears to be higher among Hispanic and non-Hispanic White populations than among Asian and Black groups (Mayeux et al., 1995), although robust data are largely limited to high-income countries. Reported prevalence is generally lower in sub-Saharan Africa, comparable or slightly lower in Asia, and similar in Latin America (Barbosa et al., 2006; Okubadejo et al., 2006; Zhang et al., 2005). Such variability likely reflects a complex combination of genetic susceptibility, environmental exposures, differences in life expectancy, healthcare access, and methodological inconsistencies, as well as the limited availability of primary epidemiological data in many low- and middle-income regions.

A large-scale genetic study spanning more than 40 countries confirmed substantial variation in the distribution of PD-associated mutations across ethnic groups (Vollstedt et al., 2019). Mutations in PD-related genes, such as *LRRK2* and *GBA*, are more common in certain populations, including Ashkenazi Jews (Chillag-Talmor et al., 2011). Evidence from international, multi-ethnic cohorts further indicates that both the frequency (Healy et al., 2008; Sidransky et al., 2009) and the penetrance (Trinh et al., 2014) of PD-related genetic variants differ across populations, underscoring the role of genetic diversity in shaping global heterogeneity in disease risk and burden.

1.2 Pathophysiology of Parkinson's disease

PD is a multifactorial neurodegenerative disorder characterized by the selective degeneration of dopaminergic neurons in the substantia nigra pars compacta (SNpc), which provides the major dopaminergic input to the basal ganglia (Dauer and Przedborski, 2003; Obeso et al., 2017; Zeng et al., 2018).

Two pathological hallmarks define the disease: the accumulation of α-synuclein (αSYN) in intracytoplasmic inclusions known as Lewy bodies (LBs) and Lewy neurites (LNs), and the progressive degeneration of dopaminergic neurons in the SNpc (Polymeropoulos et al., 1997; Spillantini et al., 1997). The resulting neuronal death causes the characteristic loss of pigmentation in the SNpc, due to the high neuromelanin content present in these cells (Marsden et al., 1983).

Neurodegeneration in PD extends beyond the SNpc. Other regions, including the ventral tegmental area, brainstem nuclei, the olfactory bulb, and cortical structures, may also be affected, reflecting the widespread distribution of αSYN pathology (Braak et al., 2003; Del Tredici and Braak, 2016). This broader involvement explains the complex clinical spectrum of PD, encompassing both motor and non-motor symptoms, such as cognitive decline, mood and sleep disorders, and autonomic dysfunction (Chaudhuri and Schapira, 2009; Schapira et al., 2017).

A growing body of evidence supports the prion-like propagation hypothesis, suggesting that misfolded αSYN can spread between interconnected neurons, driving the characteristic spatiotemporal progression of pathology (Brundin and Melki, 2017; Prusiner et al., 2012). Multiple cellular mechanisms converge to promote neuronal loss, including mitochondrial dysfunction, oxidative stress, impaired protein clearance, and neuroinflammation, all interacting to sustain disease progression (Henchcliffe and Beal, 2008; Schapira and Gegg, 2011).

1.2.1 Selective degeneration of dopaminergic neurons

Dopaminergic neurons constitute a heterogeneous population primarily located in the midbrain, diencephalon, and olfactory bulb, representing the major source of dopamine in the CNS. Among

these, the nigrostriatal pathway, a key component of the mesencephalic dopaminergic system, originates from neurons in the SNpc and projects to the caudate-putamen, a principal structure of the basal ganglia (Dauer and Przedborski, 2003). Although the neuronal cell bodies are located in the SNpc, their axonal projections are most abundant in the striatum (STR), while additional, sparser innervations target other basal ganglia nuclei, limbic areas, and cortical regions. Within the substantia nigra (SN), dopaminergic neurons represent approximately 3–5 % of the total neuronal population (German and Manaye, 1993).

In PD, the selective degeneration of SNpc dopaminergic neurons causes dopamine depletion in STR, which underlies the classical motor symptoms such as akinesia, bradykinesia, and resting tremor (Chinta and Andersen, 2005). Evidence indicates that at the onset of motor manifestations, dopamine loss in the caudate-putamen is more pronounced than the actual neuronal loss in the SNpc (Pakkenberg et al., 1991; Scherman et al., 1989). Consistently, Bernheimer and colleagues observed that motor symptoms typically emerge after an approximately 80% reduction of striatal dopamine content (Bernheimer et al., 1973; Dauer and Przedborski, 2003).

The remarkable vulnerability of SNpc dopaminergic neurons is thought to derive from their distinct phenotypic and anatomical features, including extensive axonal arborization, high synaptic density, and elevated metabolic demand. A single SNpc neuron can form 200,000–600,000 synapses within the STR, placing considerable stress on axonal transport and protein degradation systems (Bolam and Pissadaki, 2012).

This extreme branching, together with continuous synaptic activity, imposes substantial bioenergetic requirements, largely met through mitochondrial oxidative phosphorylation (Wong et al., 2019). However, this sustained mitochondrial activity results in higher basal superoxide production, promoting oxidative stress and presynaptic dysfunction (Wong et al., 2019).

Moreover, these neurons possess long, partially unmyelinated axonal segments, further increasing metabolic costs and exposure to oxidative insults. Cytosolic dopamine, when not sequestered in vesicles, can undergo auto-oxidation, generating reactive quinones that impair mitochondrial function and lysosomal degradation, thereby amplifying neuronal vulnerability (Wong et al., 2019; Zeng et al., 2018).

Under such conditions, disturbances such as protein aggregation or mitochondrial dysfunction, both typical of PD, can compromise neuronal homeostasis and ultimately lead to irreversible cell loss and neurodegeneration.

1.2.2 Basal ganglia circuits

The classical Albin–DeLong model of the basal ganglia (Fig. 2) proposes that parkinsonian motor dysfunction arises from an imbalance between two reciprocally organized striatal circuits: the direct and indirect pathways (Albin et al., 1989; Alexander et al., 1986).

Dopaminergic projections from the SNpc modulate striatal output by stimulating D1 receptor–expressing medium spiny neurons (MSNs) of the direct pathway and inhibiting D2 receptor–expressing MSNs of the indirect pathway. This dual modulation maintains the functional balance between movement facilitation and suppression (Albin et al., 1989; Alexander and Crutcher, 1990).

The direct pathway facilitates voluntary movement by reducing inhibition of thalamocortical neurons, thereby enhancing cortical motor activation. In contrast, the indirect pathway suppresses competing or context-inappropriate motor programs by increasing thalamic inhibition (Kravitz et al., 2010).

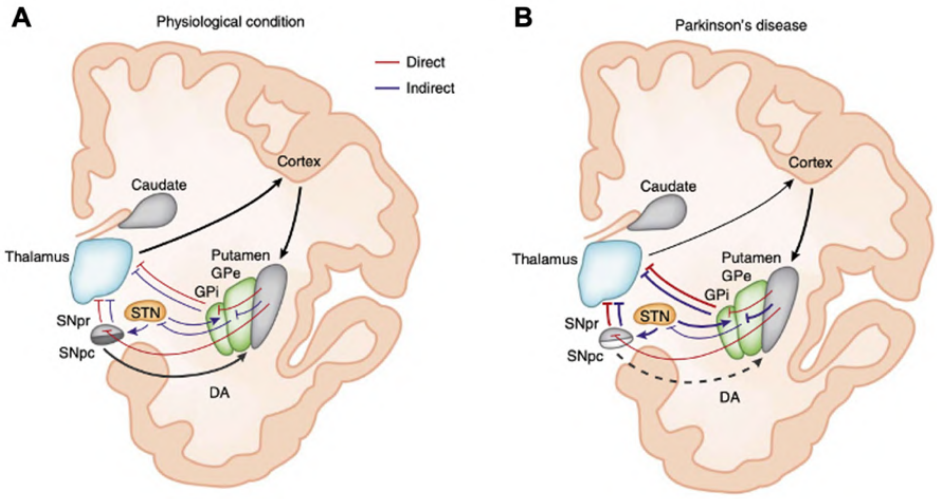

Figure 2. Schematic representation of basal ganglia circuitry under physiological conditions (A) and in Parkinson's disease (B). (A) Under normal conditions, dopaminergic projections from SNpc modulate striatal activity through two opposing pathways: the direct (red) and indirect (blue) circuits. Activation of the direct pathway facilitates movement by decreasing thalamic inhibition and enhancing cortical motor output. (B) In PD, the loss of dopaminergic input from the SNpc disrupts this balance, resulting in overactivation of the indirect pathway and excessive inhibition of thalamocortical projections. The net effect is a reduction in cortical motor activity, leading to the characteristic bradykinesia and rigidity of PD (adapted from Calabresi et al., 2014).

Within the indirect circuit, the external segment of the globus pallidus (GPe) inhibits the subthalamic nucleus (STN) via GABAergic projections, whereas the STN reciprocally excites the GPe through glutamatergic neurons (Castle et al., 2005; Parent et al., 2000).

The internal segment of the globus pallidus (GPi) and the substantia nigra pars reticulata (SNpr) constitute the main output nuclei of the basal ganglia, sending inhibitory projections to motor thalamic and brainstem targets (Grofova and Zhou, 1998). These thalamic structures, in turn, relay excitatory input back to the motor cortex, completing the basal ganglia–thalamo–cortical loop.

In PD, dopamine deficiency disrupts this modulatory equilibrium, reducing excitation of the direct pathway while enhancing activity in the indirect pathway. The resulting imbalance increases inhibitory outflow from the GPi and SNpr, leading to pathological suppression of thalamocortical and brainstem motor circuits (Alexander et al., 1986; Bergman et al., 1990; DeLong, 1990).

Empirical support for this model derives from lesion and neuromodulatory studies targeting the STN or GPi, which alleviate motor symptoms and restore cortical activation patterns in PD.

In animal models of parkinsonism (e.g., MPTP-treated primates), neuronal recordings reveal hyperactivity of the STN and GPi and hypoactivity of the GPe, consistent with excessive inhibitory output from the basal ganglia (Bergman et al., 1994; Filion and Tremblay, 1991). Similar alterations have been observed in PD patients through intraoperative recordings and functional imaging, confirming the translational relevance of these findings (Hammond et al., 2007; Hutchison et al., 1994). Optogenetic studies further demonstrated that activation of the direct pathway (D1-MSNs) facilitates, whereas activation of the indirect pathway (D2-MSNs) suppresses, movement (Kravitz et al., 2010). Moreover, lesions or inactivation of the STN or GPi alleviate bradykinesia and tremor while increasing cortical metabolic activity, reinforcing the role of excessive

inhibitory output in PD motor symptoms (Bergman et al., 1990; Grafton et al., 1995; Vitek et al., 2003).

Collectively, electrophysiological and imaging studies consistently indicate that increased STN/GPi activity and reduced GPe activity are key correlates of motor impairment (Bergman et al., 1994; Filion and Tremblay, 1991; Hutchison et al., 1994).

The Albin–Alexander–DeLong framework therefore remains the cornerstone for understanding basal ganglia dysfunction and guiding therapeutic strategies such as deep brain stimulation (DBS) targeting the STN or GPi.

Recent work has expanded this model to include dynamic network mechanisms. An additional "hyperdirect" pathway, linking cortical pyramidal neurons directly to the STN, provides a rapid route for global motor inhibition (Nambu et al., 2002). Furthermore, abnormal beta-band (13–30 Hz) oscillations within the STN–GPi–cortical loop correlate with bradykinesia and rigidity, reflecting pathological synchrony enhanced by dopamine loss (Brown et al., 2003; Hammond et al., 2007). DBS of the STN or GPi reduces these oscillations and restores flexible, desynchronized cortical activity (Eusebio et al., 2012; Little and Brown, 2014). Thus, Parkinsonian motor symptoms arise not only from altered firing rates within basal ganglia circuits, but also from aberrant network oscillations, the physiological basis for modern neuromodulatory therapies (Benabid et al., 1987; Wichmann and DeLong, 2016).

1.2.3 Pathological and clinical progression of Parkinson's disease: from early non-motor features to late-stage neurodegeneration

PD is a progressive neurodegenerative disorder historically defined by its motor manifestations. However, increasing clinical and pathological evidence indicates that these motor symptoms represent only the late expression of a complex, multisystem process that begins many years before diagnosis (Poewe et al., 2017; Spillantini et al., 1997).

A central pathological feature of PD is the accumulation of misfolded αSYN within neurons, forming LBs and LNs, the principal histopathological hallmarks of the disease (Goedert et al., 2013; Spillantini et al., 1997; Spillantini et al., 1998).

The pathogenic role of αSYN is further supported by genetic evidence, including *SNCA* gene duplications, triplications, and point mutations, as well as by experimental models that reproduce key pathological and behavioural features of PD (Feany et al., 2000; Xu et al., 2002; Zhou et al., 2000).

The anatomical progression of αSYN pathology was elegantly described by Braak and colleagues, who proposed a staging system (I–VI) paralleling the clinical course of the disease (Braak et al., 2003). In Braak stages I–II, αSYN aggregates first appear in the dorsal motor nucleus of the vagus, intermediate reticular zone, and olfactory structures, including the anterior olfactory nucleus and olfactory bulb (Fig. 3).

During the prodromal phase, patients remain free of overt motor deficits; however, a range of non-motor symptoms, including hyposmia, constipation, anxiety, depression, and REM sleep behaviour disorder (RBD), may develop years before motor onset (Ascherio et al., 2016; Faivre et al., 2019; Savica et al., 2010). While these features lack diagnostic specificity, they reflect early involvement of brainstem and olfactory circuits. Current research efforts aim to identify reliable prodromal biomarkers, including αSYN detection in cerebrospinal fluid (CSF) (Mollenhauer et al.,

2019), molecular neuroimaging such as PET-based dopaminergic and synaptic tracers (Brooks and Pavese, 2011), and digital phenotyping approaches (Arora et al., 2019), to enable earlier and more accurate diagnosis (Postuma and Berg, 2016).

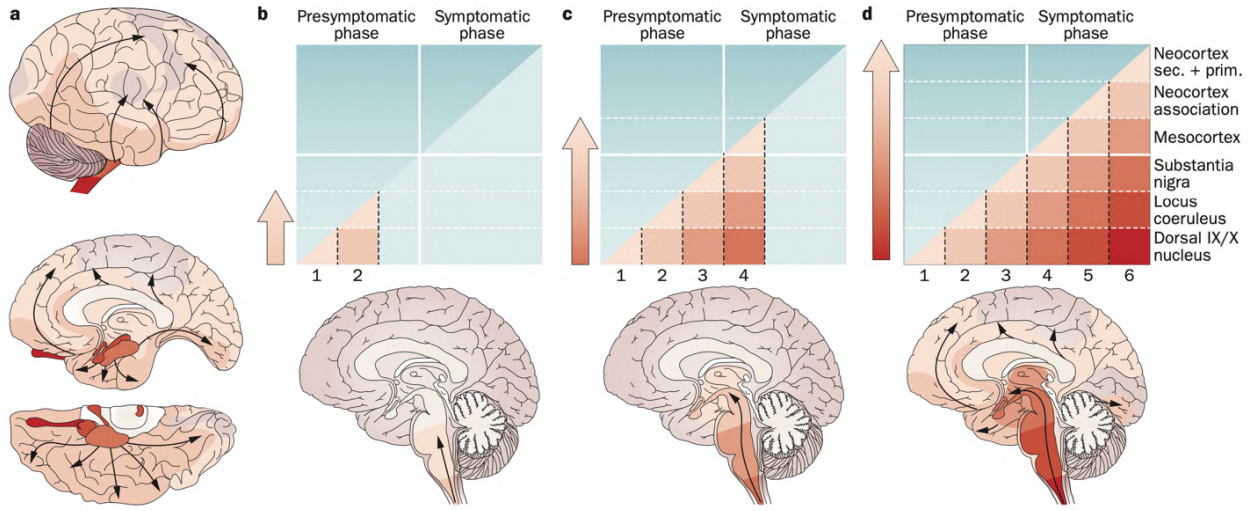

Figure 3. Anatomical progression of α-Synuclein pathology in Parkinson's disease. a) Rostro-caudal progression of pathology (arrows), with red shading indicating ascending severity. b) Stage 1: Lesions in the olfactory bulb, anterior olfactory nucleus, and/or dorsal motor nuclei of vagal and glossopharyngeal nerves. Stage 2: Lesions in the pontine tegmentum (locus coeruleus, magnocellular reticular nucleus, lower raphe nuclei). c) Stages 3–4: Lesions reach the pedunculopontine nucleus, basal forebrain cholinergic nuclei, and SNpc (stage 3), then hypothalamus, parts of the thalamus, and the anteromedial temporal mesocortex (stage 4). Initial PD symptoms appear during early stage 4. d) Stages 5–6: Lesions spread to neocortical high-order association areas (stage 5) and then first-order association and primary cortical fields (stage 6). Figure from (Goedert et al., 2013).

As PD advances to Braak stages III–IV, αSYN inclusions spread to the midbrain, particularly the SNpc, and to the basal forebrain. Neuronal loss in the SNpc, especially in its posterior regions, corresponds to the onset of classical motor symptoms: bradykinesia, rigidity, and resting tremor (Fig. 4). Motor features typically emerge when a substantial proportion, estimated at 40–60% of dopaminergic neurons, has been lost, accompanied by a marked reduction in striatal dopamine content (Bernheimer et al., 1973; Dauer and Przedborski, 2003). Bradykinesia presents as generalised slowness and difficulty initiating voluntary movement; rigidity causes resistance to passive movement with a cogwheel quality; and resting tremor usually begins unilaterally at 4–6 Hz, diminishing during voluntary activity or sleep (Jankovic et al., 2008; Postuma et al., 2015).

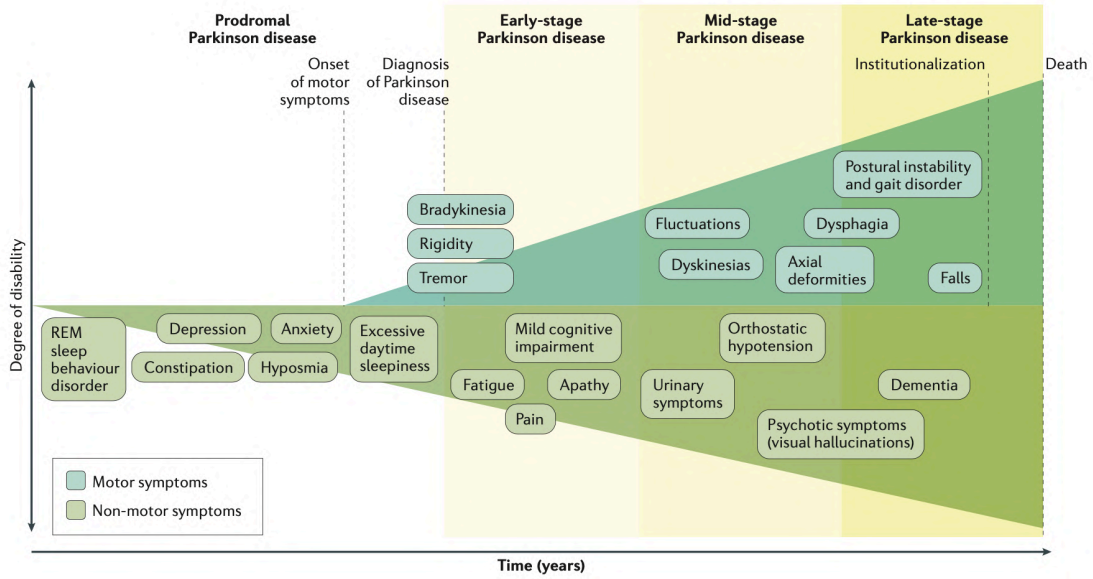

Figure 4. Motor and non-motor symptoms of Parkinson's disease across clinical stages. The figure illustrates the progression of PD over time, from the prodromal to the late stage, in relation to increasing degrees of disability. During the prodromal phase, predominantly non-motor symptoms (light green) are present, including REM sleep behaviour disorder, depression, anxiety, constipation, hyposmia, and excessive daytime sleepiness. With the onset of motor symptoms such as bradykinesia, rigidity, and tremor, the disease enters the early stage, which corresponds to the typical time of clinical diagnosis. As the disease progresses to the mid stage, both motor and non-motor symptoms worsen, with the emergence of fluctuations, dyskinesias, axial deformities, orthostatic hypotension, urinary disturbances, pain, fatigue, apathy, and mild cognitive impairment. In the late stage, severe disability develops due to postural instability, gait disorders, dysphagia, and frequent falls, often accompanied by psychotic symptoms and dementia, eventually leading to institutionalization and death (Poewe et al., 2017).

In Braak stages V–VI, αSYN pathology extends to limbic and neocortical regions, paralleling the onset of cognitive impairment and dementia, which affect approximately 50–60% of patients within 20–25 years, though higher rates have been reported in some long-term cohorts (Aarsland et al., 2017; Gibson et al., 2024; Perez et al., 2010).

Non-dopaminergic symptoms also become increasingly prominent, including autonomic dysfunction (gastrointestinal, urinary, sexual, and thermoregulatory), as well as dysarthria, dysphagia, speech impairment, gait disturbances, and episodes of choking, all contributing to progressive disability (McGregor et al., 2019; Sethi et al., 2008; Sveinbjornsdottir et al., 2016). In the advanced stages, patients experience motor fluctuations, L-DOPA-induced dyskinesias, and a progressive reduction in responsiveness to dopaminergic therapy, posing major therapeutic challenges.

Taken together, PD evolves as a pathological continuum: from early non-motor symptoms linked to αSYN pathology in brainstem and olfactory structures, through motor dysfunction caused by nigrostriatal degeneration, to widespread cortical and limbic neurodegeneration.

This evolving framework underscores the need to shift from purely symptomatic treatment towards early detection and disease-modifying interventions, supported by the development of stage-specific biomarkers and personalised therapeutic strategies that target PD in its earliest and potentially most modifiable phases (Poewe et al., 2017).

1.2.4 Diagnosis

The diagnosis of PD currently relies primarily on clinical evaluation. According to the International Parkinson and Movement Disorder Society (IPMDS), PD is defined as “a core clinical motor syndrome (parkinsonism) accompanied by SNpc neurodegeneration and synuclein deposition” (Postuma et al., 2015). However, as synuclein pathology cannot yet be verified *in vivo*, diagnosis remains based on the recognition of typical parkinsonian motor features, provided that red flags for alternative conditions, such as atypical parkinsonian syndromes, are absent (Kalia and Lang, 2015; Marsili et al., 2018).

The most widely adopted clinical framework is the Movement Disorder Society Clinical Diagnostic Criteria for Parkinson’s Disease (MDS-PD), designed to integrate both motor and non-motor features across disease stages and reduce misdiagnosis (Homayoun et. al, 2018; Postuma et al., 2015; Postuma et al., 2018). Genetic testing is not routinely included in diagnostic protocols but may be indicated in selected cases, such as early-onset PD or a strong family history, where monogenic forms are suspected (Poewe et al., 2017; Schapira et al., 2023).

In recent years, increasing efforts have focused on identifying molecular biomarkers capable of supporting clinical diagnosis and enabling earlier detection. Among these, αSYN seed amplification assays (SAAs) have shown high diagnostic accuracy in distinguishing PD from healthy controls and may provide insights into disease staging (Russo et al., 2021; Siderowf et al., 2023). Nevertheless, the ability of currently available molecular biomarkers, including SAAs, to reliably distinguish PD from other parkinsonian syndromes remains under investigation.

In parallel, several biofluid biomarkers are being evaluated for their diagnostic utility. In particular, oligomeric and phosphorylated αSYN species in CSF or plasma are being explored as markers to distinguish PD from atypical parkinsonisms, based on differences in protein conformation and concentration (Fairfoul et al., 2016). Moreover, neurofilament light chain (NfL) levels, typically elevated in progressive supranuclear palsy (PSP) and multiple system atrophy (MSA), may serve as negative biomarkers for PD (Hansson et al., 2017). Additional candidates, including glial fibrillary acidic protein (GFAP) and tau protein, are also being studied for their potential to improve differential diagnosis (Che et al., 2024).

While biofluid biomarkers hold promise for molecular-level diagnosis, neuroimaging continues to play a crucial role in assessing structural and functional brain alterations in vivo. Conventional MRI helps exclude structural abnormalities and may assist in distinguishing PD from atypical parkinsonian syndromes based on region-specific atrophy (Paviour et al., 2006; Quattrone et al., 2008). Advanced MRI approaches, such as resting-state functional MRI (rs-fMRI), can assess alterations in functional connectivity (Prodoehl et al., 2014), while diffusion-weighted and diffusion tensor imaging (DWI/DTI) reveal microstructural and white-matter integrity changes (Cochrane and Ebmeier, 2013).

Molecular imaging plays a complementary role, particularly through dopamine transporter single-photon emission computed tomography (DAT-SPECT), which evaluates the integrity of presynaptic dopaminergic terminals. DAT, a membrane transporter specific to dopaminergic neurons, serves as a robust imaging biomarker in both early and advanced PD (Huang et al., 2003; Piccini and Brooks, 2006). Positron emission tomography (PET) and single photon emission computed tomography (SPECT) imaging can also monitor disease progression and neurotransmitter system activity (Kalia and Lang, 2015; Politis and Piccini, 2015). Despite these advances, more than 75% of definitive PD diagnoses are still confirmed only post-mortem (Gibb and Lees, 1988; Hughes et al., 1992; Rajput

et al., 1991), underscoring the urgent need for reliable biomarkers enabling early and accurate diagnosis. Future diagnostic strategies are likely to integrate molecular, imaging, and digital biomarkers to achieve earlier and more precise disease stratification.

1.2.5 Current therapies: symptomatic and disease modifying therapies

The therapeutic management of PD primarily relies on symptomatic treatments, as no intervention has yet demonstrated definitive disease-modifying efficacy in pivotal trials (Poewe et al., 2017). Since the 1960s, the main approach has focused on restoring cerebral dopamine levels, with levodopa (L-DOPA) administration remaining the gold standard treatment, particularly during the early stages of the disease (Cotzias et al., 1967; Haddad et al., 2018).

Prolonged L-DOPA exposure, however, is frequently associated with motor complications, L-DOPA-induced dyskinesia, wearing-off, and on–off fluctuations, often emerging within a few years of treatment initiation (Poewe et al., 2017). To improve clinical management, L-DOPA is commonly co-administered with inhibitors of dopa decarboxylase (benserazide, carbidopa), catechol-O-methyltransferase (entacapone, tolcapone), and monoamine oxidase type B (selegiline, rasagiline), which enhance its bioavailability and prolong its half-life (Pålhagen et al., 2006; Tetrud and Langston, 1989). Dopamine receptor agonists and anticholinergic agents are also employed to ameliorate motor fluctuations and tremor control, respectively, although their use is limited by cognitive side effects (Moore et al., 2014; Poewe et al., 2017).

Introduced in the 1990s, DBS has revolutionized the treatment of medication-refractory motor symptoms by delivering electrical stimulation via implanted electrodes in the STN or GPi, thereby modulating aberrant motor circuit activity (Chiken and Nambu, 2016). Although DBS has demonstrated considerable efficacy**,** long-term neuropsychological side effects have been reported (Merola et al., 2011). Currently, adaptive “closed-loop” DBS systems are under investigation, aiming to dynamically adjust stimulation in response to real-time neural activity to optimize therapeutic outcomes and minimize adverse effects (Guidetti et al., 2021).

Beyond symptomatic strategies, increasing efforts aim to develop disease-modifying therapies capable of slowing or halting neurodegeneration. Among these, immunotherapies targeting αSYN have advanced the furthest. Monoclonal antibodies such as prasinezumab and cinpanemab were evaluated for their ability to neutralise toxic αSYN aggregates. Although phase-II trials did not meet their primary efficacy endpoints, exploratory and post-hoc analyses suggested possible signals of reduced motor progression in selected patient subgroups (Lang et al., 2022; Pagano et al., 2022; Siderowf et al., 2023), prompting further investigation. Several small-molecule compounds that inhibit αSYN aggregation or promote its clearance are also under evaluation, but consistent clinical evidence of benefit is still lacking (Chen et al., 2015).

Gene therapy represents another innovative avenue, designed to restore dopaminergic function by delivering genes encoding key enzymes involved in dopamine biosynthesis, such as aromatic L-amino-acid decarboxylase (AADC) or tyrosine hydroxylase (TH). Early-phase clinical trials have reported encouraging symptomatic improvements and durable expression of transgenes, though confirmatory, large-scale studies are still required to establish long-term efficacy and safety (LeWitt et al., 2011; Palfi et al., 2014). Likewise, cell-based therapies, involving the transplantation of dopaminergic neurons derived from embryonic or induced pluripotent stem cells, aim to replace lost

neuronal populations and restore nigrostriatal connectivity. Preliminary clinical experiences indicate feasibility and potential benefit, while long-term integration, immune compatibility and sustained safety remain active areas of research (Barker et al., 2015; González et al., 2016).
Ultimately, the central goal of current research is to move beyond symptomatic relief toward genuine neuroprotection, ideally intervening during the prodromal stages of the disease. Progress in this direction will depend on the identification of reliable biomarkers capable of detecting early pathology and predicting treatment response, thereby enabling timely and personalised therapeutic interventions. Despite substantial advances, the development of therapies that can truly alter PD progression remains one of the foremost challenges in modern neurodegenerative medicine *(*Heinzel et al., 2019; Mahlknecht et al., 2022*).*

1.3 Genetic and environmental interplay in Parkinson's disease

PD is a complex neurodegenerative disorder arising from the interaction of genetic susceptibility, environmental exposures, and aging-related processes. In approximately 90% of cases, the aetiology remains idiopathic, meaning that no single causative mutation or environmental factor can be clearly identified (Klein and Westenberger, 2012).
Roughly 10% of PD cases are associated with identifiable mutations in genes that regulate critical aspects of neuronal homeostasis, including *SNCA*, *LRRK2*, *PRKN* (*PARK2*), *PINK1*, and *GBA*. These genes are involved in fundamental cellular pathways such as protein folding and degradation, mitochondrial quality control, and lysosomal-autophagic clearance, processes essential for the survival of dopaminergic neurons (Blauwendraat et al., 2020; Poewe et al., 2017).
Disruptions in these mechanisms lead to the accumulation of misfolded proteins, oxidative stress, and impaired energy metabolism, which together drive neuronal vulnerability in PD.
To date, more than 20 genes have been implicated in monogenic or familial forms of PD. However, these account for only a minor proportion of all cases, around 30% of familial PD and 3–5% of sporadic PD, where no clear family history is present (Blauwendraat et al., 2020; Klein and Westenberger, 2012; Tansey and Romero-Ramos, 2019). The best-characterised genetic forms include autosomal dominant variants in *SNCA* and *LRRK2*, and autosomal recessive mutations in *PRKN*, *PINK1*, and *DJ-1*. In addition, mutations or risk variants in *GBA*, which encodes the lysosomal enzyme glucocerebrosidase, have been identified as one of the most frequent genetic risk factors, present in up to 10–15% of PD patients, especially in certain populations (Gan-Or et al., 2018).
Importantly, many PD-associated mutations show incomplete penetrance and variable expressivity, meaning that not all mutation carriers develop PD, and those who do may present with markedly different clinical trajectories. This variability suggests that additional genetic modifiers, epigenetic regulation, and environmental influences, such as pesticide exposure, smoking, or head injury, modulate the individual risk and timing of disease onset (Goldman, 2019; Poewe et al., 2017). Consequently, even individuals carrying the same pathogenic variant can differ substantially in age at onset, motor and non-motor symptoms, and disease progression rate.
This heterogeneity supports the current understanding of PD not as a single disease entity but as a spectrum of related disorders that share overlapping molecular and clinical features (Pajares et al., 2020). In keeping with this multifactorial model, twin studies have estimated the heritability of PD,

(i.e. the proportion of disease risk attributable to genetic factors alone) at approximately 25–30%, underscoring the predominant contribution of non-genetic and sporadic influences in most patients (Goldman et al., 2019; Keller et al., 2012).
Collectively, these findings emphasise that PD represents a continuum between genetic predisposition and environmental susceptibility, with aging acting as the major catalyst that ultimately tips cellular homeostasis toward neurodegeneration.

1.3.1 Environmental determinants and protective modulators of Parkinson's disease

PD results from a complex interplay between intrinsic risk factor, such as genetic variants and metabolic profile and extrinsic element, including environmental toxicants, infections, and lifestyle-related behaviours. These variables do not act in isolation but rather interact at the molecular level, influencing epigenetic programs, inflammatory responses, and the gut microbiome (Ascherio and Schwarzschild, 2016; Marras et al., 2018).
Among the most extensively studied environmental risk factors, exposure to pesticides and herbicides has received particular attention. Compounds such as rotenone, paraquat, maneb, and organochlorines are strongly associated with an increased risk of PD. Rotenone, a mitochondrial complex I inhibitor, induces selective dopaminergic degeneration in animal models that reproduce key pathological features of PD (Martinez and Greenamyre, 2012). Similarly, paraquat exposure enhances oxidative stress and promotes αSYN aggregation, supporting a mechanistic link between environmental toxins and synucleinopathy (Berry et al., 2010).
The role of mitochondrial toxins in PD pathogenesis was first recognised following the discovery of MPTP-induced parkinsonism in illicit drug users, where inhibition of complex I caused rapid nigrostriatal degeneration (Langston et al., 1983). Likewise, methamphetamine (METH) abuse has been linked to increased neurodegeneration due to dopaminergic axon loss, microglial activation, and reductions in striatal dopamine, TH and dopamine transporter (DAT) levels, resembling MPTP toxicity (Guilarte et al., 2003).
Occupational exposure to heavy metals (such as manganese, lead, and copper) and chlorinated solvents has also been associated with elevated PD risk, likely mediated by mitochondrial dysfunction, oxidative stress, and chronic neuroinflammation (Racette et al., 2012). Moreover, repeated head trauma is emerging as an independent risk factor, as traumatic brain injury may disrupt the blood-brain barrier (BBB) and facilitate αSYN misfolding and propagation (Jafari et al., 2013).
Beyond environmental toxins, lifestyle and hormonal factors can influence susceptibility. High dairy consumption has been linked to a modestly increased PD incidence, potentially reflecting pesticide contamination in milk or altered urate metabolism (Ascherio and Schwarzschild, 2016). In women, early menopause and reduced oestrogen levels are associated with greater risk, supporting a neuroprotective role for oestrogens in dopaminergic systems (Rocca et al., 2008).
Conversely, several behaviours appear protective against PD. Numerous epidemiological studies have demonstrated an inverse association between cigarette smoking and PD incidence, possibly due to nicotine's effects on dopaminergic neurotransmission, monoamine oxidase-B inhibition, and anti-inflammatory actions (Grandinetti et al., 1994; Hernán et al., 2001; Quik et al., 2004). Similarly, caffeine consumption has been consistently linked to a reduced PD risk, most likely through antagonism of the adenosine A2A receptor, which enhances dopaminergic signalling. This

effect seems more pronounced in men, possibly due to interactions between caffeine and oestrogen metabolism (Ascherio et al., 2004; Ross et al., 2000; Xu et al., 2006).
Elevated serum urate levels have also been associated with lower PD risk and slower disease progression, likely reflecting urate's antioxidant capacity (Weisskopf et al., 2007). However, therapeutic urate elevation remains controversial, as it may increase cardiovascular risk.
Finally, non-steroidal anti-inflammatory drugs (NSAIDs) have been investigated as potential modulators of PD risk due to their ability to suppress neuroinflammation. While preclinical studies demonstrate neuroprotective effects on dopaminergic neurons (Teismann and Ferger, 2001), clinical data remain mixed (Becker et al., 2011; Ren et al., 2018). Given the growing recognition of immune mechanisms in PD pathogenesis (Hirsch and Hunot, 2009), the potential of NSAIDs and related agents to prevent or delay disease onset remains an active and promising area of research.
In summary, PD results from the dynamic interaction of genetic predisposition, environmental exposure, and lifestyle factors. Understanding both risk and protective influences provides crucial insight into disease pathogenesis and may guide the development of preventive and disease-modifying interventions in the future.

1.3.2 Genetic determinants and pathogenic mechanisms in Parkinson's disease

PD was long considered a paradigmatic example of a non-genetic neurodegenerative disorder. This view changed in 1997 with the discovery of the A53T mutation in the *SNCA* gene, encoding αSYN, which established a clear genetic basis for PD pathogenesis (Polymeropoulos et al., 1997). Since then, more than 20 genes and loci have been implicated in monogenic forms of PD, including autosomal dominant mutations (*SNCA*, *LRRK2*) and autosomal recessive mutations (*PRKN*, *PINK1*, *DJ-1*) (Blauwendraat et al., 2020; Bonifati et al., 2003; Klein and Westenberger, 2012; Kitada et al., 1998; Valente et al., 2001). Although these discoveries revolutionized our understanding of PD, monogenic forms account for only a small minority of cases, highlighting the multifactorial nature of the disease, which arises from the interplay of genetic susceptibility, environmental exposures, and age-related mechanisms (Billingsley et al., 2018). The nomenclature for PD-linked loci follows the "PARK" convention, numbered in order of discovery (e.g., *PARK1*, *PARK2*). *PARK1/SNCA* and *PARK8/LRRK2* mutations are autosomal dominant, while *PARK2/PRKN*, *PARK6/PINK1*, *PARK7/DJ-1,* and *PARK9/ATP13A2* follow autosomal recessive inheritance (Klein and Westenberger, 2012).
Following the initial identification of the A53T mutation, other missense variants such as A30P, E46K, H50Q, G51D and A53E were described, all clustering in the N-terminal region involved in membrane binding and fibril formation (Zeng et al., 2018). In addition to these point mutations, *SNCA* duplications and triplications are pathogenic, and increased gene dosage correlates with earlier onset and more rapid disease progression (Singleton et al., 2003).
The *LRRK2* gene (*PARK8*) encodes a large multidomain protein with GTPase and kinase activities. Pathogenic variants such as G2019S, R1441C/G and Y1699C account for approximately 5% of familial PD cases, although their frequency varies across populations (Ferreira and Massano, 2017). These mutations enhance LRRK2 kinase activity, disrupt protein–protein interactions and impair vesicular trafficking and autophagy, ultimately compromising dopaminergic signalling and neuronal viability (Yoon et al., 2017). PINK1 *(PARK6)* and PRKN *(PARK2)* act in the same mitochondrial quality-control pathway: under conditions of mitochondrial depolarization, PINK1 accumulates on the

outer mitochondrial membrane and recruits the E3 ubiquitin ligase Parkin, which mediates the selective degradation of damaged mitochondria through mitophagy (Narendra et al., 2009). Loss-of-function mutations in either gene are major causes of autosomal recessive early-onset PD, collectively accounting for up to 20–40% of these cases, depending on ethnic background, and leading to impaired mitophagy, mitochondrial dysfunction and increased oxidative stress (Huang et al., 2017; Zhuang et al., 2016). Similarly, *DJ-1 (PARK7)* encodes a redox-sensitive chaperone involved in oxidative stress defence and mitochondrial homeostasis. Mutations such as L166P and M26I abolish its antioxidant and neuroprotective functions, contributing to early-onset parkinsonism (Biosa et al., 2017; Ishikawa et al., 2009; Malgieri et al., 2008).

Beyond these rare familial mutations, genome-wide association studies (GWAS) have identified over ninety susceptibility loci associated with sporadic PD (Blauwendraat et al., 2020; Nalls et al., 2019). Among the most significant are variants in *MAPT*, *SNCA*, *LRRK2*, *GBA*, *HLA-DRA*, *INPP5F* and *BST1* (Benitez et al., 2016; Nalls et al., 2019). Individually, these loci confer modest effects on disease risk, but their cumulative and epistatic interactions, further shaped by environmental and epigenetic influences, can significantly modify disease onset and clinical course.

Among the susceptibility genes, *GBA* mutations have particular clinical relevance. *GBA* encodes β-glucocerebrosidase (GCase), a lysosomal enzyme responsible for sphingolipid degradation. Heterozygous carriers of *GBA* mutations have a four- to five-fold higher risk of developing PD and often display earlier onset and faster cognitive decline (Anheim et al., 2012; Sidransky et al., 2009; Simon et al., 2020). Loss-of-function variants such as N370S decrease GCase activity, leading to lysosomal lipid accumulation, impaired protein degradation and autophagy stress that promotes αSYN aggregation. This establishes a vicious cycle in which lysosomal dysfunction exacerbates αSYN pathology and neurodegeneration (Pang et al., 2022).

Other genetic polymorphisms affecting xenobiotic metabolism and neuroinflammatory regulation, including *NAT2*, *MAOB*, *GSTT1* and *APOE ε2*, have also been reported to influence PD risk in some populations, although their effects remain inconsistent and appear to depend on gene–environment interactions (de Lau and Breteler, 2006). Altogether, these findings illustrate a continuum of genetic influence in PD, ranging from rare, high-penetrance mutations to common, low-risk polymorphisms. The interaction between these genetic factors and environmental modifiers contributes to the remarkable clinical heterogeneity of the disease and supports the current view of PD as a multifactorial spectrum disorder rather than a single nosological entity.

1.3.3 Molecular and cellular effects of the A53T α-Synuclein mutation

The human *SNCA* gene, located on chromosome 4q22.1, encodes a 140-amino acid presynaptic protein predominantly expressed in neurons, where it plays roles in synaptic vesicle trafficking and neurotransmitter release (Maroteaux et al., 1988). In 1997, the first missense mutation in *SNCA*, known as A53T, was identified; this substitution replaces alanine with threonine at position 53 (Polymeropoulos et al., 1997). In the same year, αSYN was recognized as the major fibrillar component of LBs, the pathological hallmark of PD (Spillantini et al., 1997).

The A53T mutation profoundly alters both the structure and function of αSYN. This amino acid substitution introduces a hydroxyl group into the N-terminal amphipathic region, increasing the protein's propensity to form β-sheet conformations that promote aggregation (Coskuner and Wise Scira, 2013). Molecular dynamics simulations indicate that A53T disrupts long-range interactions

with the non-amyloid-β component (NAC) domain, exposing hydrophobic residues that facilitate oligomer formation and reduce conformational flexibility, thus favouring aggregation-prone states (Coskuner and Wise Scira, 2013). Compared with wild-type αSYN, the A53T variant exhibits accelerated aggregation kinetics and forms more stable, degradation-resistant fibrils (Conway et al., 1998; Li et al., 2001; Ono et al., 2011).

Functionally, A53T impairs αSYN's physiological association with synaptic vesicle membranes, disrupting vesicular trafficking and promoting cytosolic accumulation of the protein. It also interferes with cellular degradation pathways, including autophagy and mitophagy, resulting in inefficient clearance of misfolded proteins and damaged organelles. This impairment exacerbates mitochondrial dysfunction and oxidative stress (Minakaki et al., 2018; Smith et al., 2005; Pupyshev et al., 2018). At the cellular level, A53T expression is associated with deficits in mitochondrial bioenergetics, including decreased respiratory efficiency and increased reactive oxygen species (ROS) production, which create a pro-oxidant environment favouring neuronal vulnerability (Pozo Devoto et al., 2020). In parallel, the mutation disturbs proteostatic balance by inhibiting autophagic flux, leading to the accumulation of autophagic vacuoles and protein aggregates, consistent with defective lysosomal degradation (Minakaki et al., 2018). Moreover, A53T-expressing neurons display chronic endoplasmic reticulum (ER) stress and sustained activation of the unfolded protein response (UPR). Persistent activation of this pathway triggers pro-apoptotic cascades, aggravating proteotoxic stress and contributing to dopaminergic neurodegeneration (Ryu et al., 2021).

Collectively, these findings demonstrate that the A53T mutation accelerates αSYN pathology through converging mechanisms, such as structural destabilization, aggregation propensity, mitochondrial dysfunction, impaired proteostasis, and ER stress, conferring a highly neurotoxic phenotype to the mutant protein.

1.4 Alpha-Synuclein

1.4.1 Structure of α-Synuclein

Structurally, αSYN is composed of three major domains. The N-terminal region (residues 1–60) contains amphipathic repeats that adopt an α-helical conformation upon binding to membrane lipids, mediating interaction with synaptic vesicles. The central NAC region (non-amyloid-β component, residues 61–95) is highly hydrophobic and essential for β-sheet formation and aggregation. Finally, the C-terminal domain (residues 96–140), enriched in acidic residues, confers conformational flexibility and modulates protein–protein interactions as well as calcium binding (Lautenschläger et al., 2018; Fonseca et al., 2015; Vamvaca et al., 2009).

Building on these structural properties (Fig. 5), accumulating evidence indicates that pathological aggregation of αSYN is a central event in PD-related neurodegeneration. Among the aggregated species, soluble oligomers, rather than mature fibrils, are considered the most neurotoxic. Their small size (<200 nm) enables efficient interaction with cellular membranes, leading to membrane disruption, mitochondrial impairment, and activation of inflammatory responses (Cocozza et al., 2022).

This aggregation propensity is largely driven by the NAC region, particularly by a hydrophobic stretch of residues (71–82) crucial for fibril formation. Mutagenesis studies introducing charged residues into

this segment disrupt amyloid formation, highlighting its essential role in aggregation (Uversky et al., 2001). Insights from recent cryo-electron microscopy analyses reveal that αSYN fibrils can adopt distinct polymorphic conformations with variable pathogenic potential. Notably, intramolecular salt bridges, such as those between residues K45 and E57, contribute to conformational stability and may underlie phenotypic variability among different synucleinopathies (Guerrero-Ferreira et al., 2018).

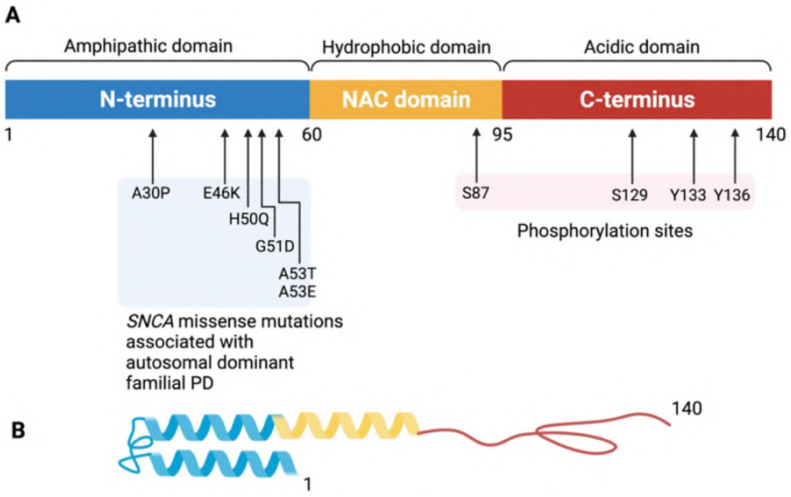

Figure 5. Structural organization of α-Synuclein and pathogenic mutations associated with Parkinson's disease. (A) Linear structure of αSYN showing its three main domains (N-terminus, NAC, C-terminus), *SNCA* missense mutations associated with familial PD, and key phosphorylation sites. (B) Schematic 3D representation of αSYN domains (Fan et al., 2021).

In addition to protein-centric mechanisms, recent studies have identified RNA-based regulatory elements that influence αSYN pathology. Specifically, RNA G-quadruplex (G4) structures located in the 3' untranslated region (3'UTR) of *SNCA* mRNA facilitate αSYN phase separation in the presence of calcium ions. Pharmacological inhibition of these G4 structures, for example, using 5-aminolevulinic acid, reduces αSYN aggregation and improves dopaminergic neuron survival in PD mouse models (Matsuo et al., 2024).

The C-terminal domain of αSYN also exhibits distinctive structural and functional properties compared to β- and γ-synuclein isoforms. This negatively charged, acidic region mediates nuclear localization and interactions with numerous proteins (Masliah et al., 1996; Ulmer et al., 2005). It enhances protein solubility and inhibits aggregation, whereas C-terminal truncations result in increased fibrillization, suggesting a protective role of the intact domain.

Furthermore, long-range intramolecular interactions between the C-terminal, NAC, and N-terminal regions help maintain αSYN's dynamic and disordered conformation. This structural plasticity acts as a regulatory mechanism to prevent excessive oligomerization and fibril formation (Bertoncini et al., 2005; Dedmon et al., 2005).

Together, these structural insights highlight αSYN as a highly dynamic and multifaceted protein whose conformational flexibility, regulated at multiple levels, determines its physiological functions as well as its pathological aggregation potential (Fan et al., 2021).

1.4.2 Physiological function of α-Synuclein

αSYN is a multifunctional protein whose physiological role remains partially undefined, yet it is involved in numerous critical cellular processes, including synaptic transmission, intracellular calcium regulation, mitochondrial homeostasis, and modulation of gene expression (Benskey et al., 2016).

At the synaptic level, αSYN organizes the vesicular pool by promoting clustering, docking, and recycling of synaptic vesicles through interactions with synapsins and cholesterol-enriched lipid rafts, membrane microdomains essential for efficient neurotransmission (Burré et al., 2010; Burré, 2015; Fortin et al., 2004).

It also interacts with crucial presynaptic components such as TH, protein phosphatase 2A (PP2A), vesicular monoamine transporter 2 (VMAT2), and the SNARE complex, highlighting its central role in dopaminergic modulation.

Under basal conditions, αSYN fine-tunes dopamine transmission by acting as a negative regulator of synthesis, storage, and release. It inhibits TH and AADC activity via PP2A-mediated dephosphorylation, reduces VMAT2-dependent vesicular loading, and slows synaptic vesicle recycling through interference with clathrin-mediated endocytosis (Benskey et al., 2016). During neuronal activation, αSYN transiently redistributes away from the active zone, lifting its inhibitory effect and enhancing DA release in response to stimulation (Fig. 6; Benskey et al., 2016).

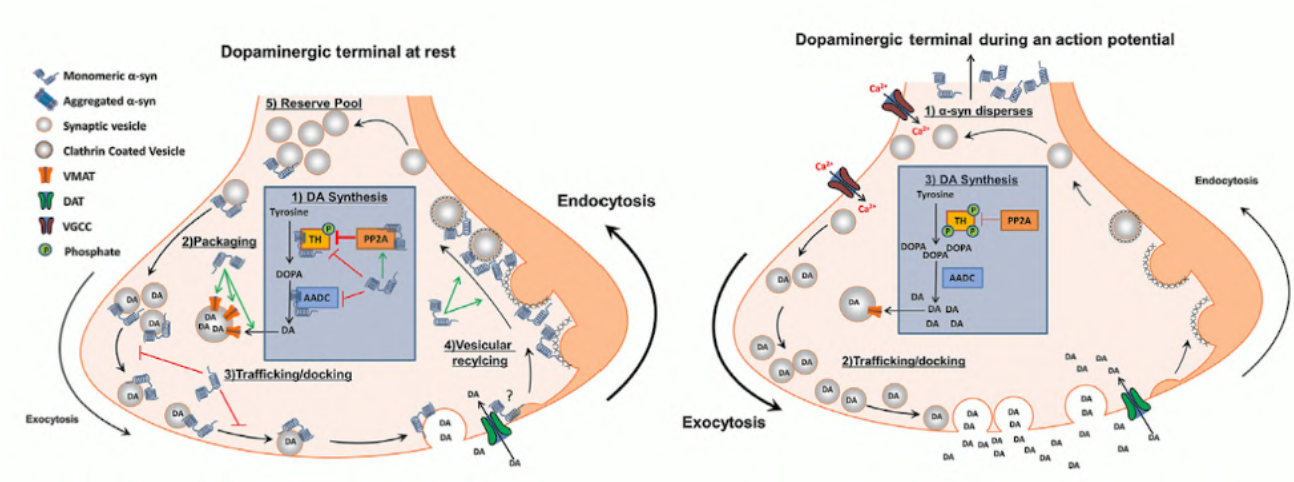

Figure 6. **Proposed model of α-Synuclein function in dopaminergic terminals at rest and during neuronal activity.** Resting state: αSYN is concentrated at the presynaptic terminal, where it regulates dopaminergic homeostasis. Specifically, it inhibits dopamine (DA) synthesis by modulating the activity of tyrosine hydroxylase (TH) and aromatic L-amino acid decarboxylase (AADC), with the involvement of the phosphatase PP2A. In addition, αSYN promotes vesicular DA storage through interaction with the vesicular monoamine transporter (VMAT), while restraining vesicle trafficking and docking at the plasma membrane. These functions contribute to maintaining the reserve pool of synaptic vesicles and supporting efficient vesicle recycling through endocytosis. During an action potential**:** Calcium (Ca^{2+}) influx through voltage-gated calcium channels (VGCCs) triggers αSYN dispersion, relieving its inhibitory actions and facilitating vesicle trafficking, docking, and exocytosis of DA. Elevated intracellular calcium also enhances DA synthesis and mobilization of vesicles from the reserve pool. Following membrane repolarization, αSYN reassociates with synaptic vesicles, restoring the presynaptic organization and regulatory functions characteristic of the resting state (adapted from Benskey et al., 2016).

The interaction of αSYN with vesicle exocytosis machinery is mediated by domain-specific contacts: the C-terminal region binds vesicle-associated membrane protein 2 (VAMP2), while the N-terminal associates with the SNARE complex, promoting vesicle docking and fusion (Burré et al., 2010; Lashuel et al., 2013). In cysteine-string protein-α (CSPα) knockout models, overexpression of αSYN rescues SNARE assembly and neurotransmission, suggesting it acts downstream of CSPα (Chandra et al., 2005).

Beyond the presynaptic terminal, αSYN localizes to mitochondria, where it modulates fission–fusion dynamics, oxidative phosphorylation and calcium buffering (Devi et al., 2008; Li et al., 2007; Parihar et al., 2008). While physiological levels support mitochondrial integrity, αSYN accumulation or misfolding perturbs energy production and promotes oxidative stress, contributing to neurodegenerative cascades (Choubey et al., 2011; Nakamura et al., 2011; Zaichick et al., 2017).

Emerging evidence also implicates αSYN in nuclear and transcriptional regulation. Nuclear αSYN binds DNA and histones, modulating transcription factors linked to mitochondrial function and synaptic plasticity. Its interaction with histones suppresses acetylation and may promote neurotoxicity (Goers et al., 2003; Kontopoulos et al., 2006; Villar-Piqué et al., 2016). In addition, αSYN associates with RNA and RNA-binding proteins, potentially influencing mRNA processing and translation (Gonçalves and Outeiro, 2013; Siwecka et al., 2023).

Overall, these findings define αSYN as a dynamic regulator of neuronal homeostasis. Its physiological versatility enables fine control of synaptic and mitochondrial function, but also makes it particularly vulnerable, when dysregulated, to initiating pathogenic cascades underlying PD.

1.4.3 Pathological aggregation of α-Synuclein: from oligomers to fibrils

αSYN is an intrinsically disordered and highly dynamic protein whose structural flexibility allows it to interact with a wide range of cellular partners. This same conformational plasticity, while essential for its physiological functions, also makes the protein susceptible to misfolding and aggregation. These processes are finely regulated by post-translational modifications (PTMs) that influence αSYN's conformation, aggregation kinetics, and neurotoxic potential, representing crucial determinants in the pathogenesis of PD.

Among the best-characterized PTMs, phosphorylation plays a central role. It predominantly occurs at serine and tyrosine residues in the C-terminal region, notably S87, Y125, Y133, and Y136. Phosphorylation at serine 129 (pS129) is particularly relevant, as it is found in more than 90% of αSYN within Lewy bodies, the pathological hallmark of PD (Fujiwara et al., 2002; Oueslati et al., 2010). Although several studies have associated pS129 with enhanced aggregation, others indicate that its effect may depend on the specific cellular context, reflecting a more complex regulatory role (Anderson et al., 2006; Fujiwara et al., 2002; Meade et al., 2019). Another frequent modification observed in PD brains is C-terminal truncation, which occurs in approximately 15% of αSYN species within Lewy bodies. These truncated forms exhibit increased aggregation propensity and act as nucleating seeds for full-length αSYN, potentially accelerating disease progression (Li et al., 2005; Murray et al., 2003). Conversely, N-terminal acetylation, a constitutive modification present in physiological conditions, stabilizes α-helical structures and enhances membrane affinity, often resulting in decreased aggregation rates (Kang et al., 2012; Maltsev et al., 2012).

Oxidative and nitrative modifications further modulate αSYN structure and function. Oxidation of methionine residues (M1, M5, M116, M127) increases conformational disorder and inhibits fibril

formation, suggesting a potential protective role (Hokenson et al., 2004). In contrast, nitration at tyrosine residues, particularly Y39, can prevent fibril elongation while stabilizing oligomeric intermediates that are potentially toxic (Giasson et al., 2000; Souza et al., 2000). These diverse PTMs highlight how the fine-tuning of αSYN chemistry critically shapes its aggregation behaviour.

Structurally, αSYN exists in dynamic equilibrium between unstructured monomers in the cytosol, α-helical multimers upon membrane binding, and β-sheet–rich aggregates. Membrane association promotes transient multimerization necessary for its normal function in synaptic vesicle trafficking (Burré et al., 2014; Eliezer et al., 2001; Trexler and Rhoades, 2009).

Pathological conditions, including altered pH, metal ion exposure, and familial PD mutations such as A30P, E46K, and A53T, disrupt these equilibria, destabilizing native conformations and promoting misfolded β-sheet assemblies (Bertoncini et al., 2005; Conway et al., 1998; Lashuel et al., 2002).

The aggregation process of αSYN follows a nucleation-dependent mechanism, characterized by a lag phase, elongation phase, and stationary phase. During the lag phase, soluble oligomeric nuclei form from monomeric precursors, serving as seeds for subsequent fibril growth. The elongation phase involves rapid monomer addition to growing protofibrils, while the stationary phase reflects a dynamic equilibrium among monomers, oligomers, and mature fibrils (Mehra et al., 2019; Wood et al., 1999). In addition to primary nucleation, secondary mechanisms, including fibril fragmentation and surface-catalysed nucleation, amplify aggregate propagation by generating new seeding sites, explaining the self-perpetuating nature of αSYN pathology (Buell et al., 2014; Knowles et al., 2009).

Although mature fibrils were long considered the main toxic species, converging evidence identifies soluble oligomers as the principal neurotoxic forms. These small, β-sheet–rich assemblies exhibit a “hollow-cylinder” morphology and can permeabilize membranes, disrupt mitochondrial function, impair proteasomal and ER activity, and activate neuroinflammatory pathways via TLR2 (Chen et al., 2015; Choi et al., 2013; Cremades et al., 2012; Ghosh et al., 2015; Hoffmann et al., 2016). Distinct oligomeric populations have been identified, with variable stability and toxicity, underscoring the structural heterogeneity of αSYN aggregates.

Recent studies have expanded our understanding of αSYN aggregation dynamics. O-GlcNAcylation has been shown to attenuate aggregation and reduce seeding capacity, suggesting a neuroprotective role and potential therapeutic target (Levine et al., 2022).

Furthermore, cross-seeding between αSYN and tau proteins has been demonstrated, supporting a synergistic mechanism in mixed neurodegenerative disorders (Hoffmann et al., 2023). Advances in cryo-electron microscopy have revealed that patient-derived fibrils exhibit distinct structural polymorphs, potentially explaining the heterogeneity of clinical phenotypes across synucleinopathies (Schweighauser et al., 2021).

Collectively, these findings illustrate that αSYN aggregation is governed by a complex interplay of PTMs, genetic mutations, and environmental factors. The ability of αSYN to transition between physiological and pathological conformations defines its dual nature as both a critical regulator of neuronal function and a central driver of neurodegeneration. Understanding how each modification modulates this equilibrium will be essential for developing strategies aimed at stabilizing functional αSYN while preventing its pathological aggregation.

1.4.4 Pathological propagation of α-Synuclein: mechanisms of intercellular transfer

The pathological spreading of misfolded αSYN is a central event in PD progression. Increasing evidence indicates that intercellular transmission of misfolded αSYN species contributes to the multisystem degeneration characteristic of PD. The prion-like hypothesis proposes that misfolded αSYN acts as a seed, inducing conformational changes in native αSYN and promoting aggregation and propagation across interconnected brain regions.

Clinical support for this model comes from observations in PD patients who received fetal dopaminergic neuron grafts. Years after transplantation, these grafted neurons developed LBs–like inclusions and degenerative changes, indicating host-to-graft propagation of pathology (Kordower et al., 2008; Kurowska et al., 2011; Li et al., 2008; Mendez et al., 2008). Similar findings have been reproduced in animal models, where host-to-graft transmission of αSYN was observed in murine and rat dopaminergic neurons transplanted into αSYN-overexpressing hosts (Angot et al., 2012; Desplats et al., 2009; Hansen et al., 201; Rey et al., 2013). These studies collectively demonstrate that healthy neurons can acquire αSYN aggregates from neighbouring affected cells, thereby becoming susceptible to degeneration.

Further experimental evidence was provided by Luk and colleagues, who showed that brain homogenates from aged αSYN (A53T) transgenic mice induced widespread αSYN inclusions when injected into young mice, reproducing LB-like pathology and glial activation (Luk et al., 2012). The same effect was achieved with recombinant preformed fibrils (PFFs**)**, which are internalized by neurons and trigger aggregation of endogenous αSYN into insoluble, phosphorylated, and ubiquitinated forms (Luk et al., 2009; Volpicelli-Daley et al., 2011).

Misfolded αSYN can spread through several complementary routes. It can travel along axons, be released via non-classical exocytosis, or be taken up by neighbouring cells, including neurons, astrocytes, and microglia (Freundt et al., 2012; Lee et al., 2005; Lee et al., 2010). Uptake occurs via multiple mechanisms, such as macropinocytosis, receptor-mediated endocytosis, or passive diffusion, suggesting that αSYN propagation does not depend on a single receptor (Angot et al., 2012; Desplats et al., 2009; Mao et al., 2016). When intracellular degradation is overwhelmed (Fig.7), αSYN is released extracellularly through exosomes, lysosomal exocytosis, or non-vesicular pathways, facilitating its dissemination (Alvarez-Erviti et al., 2011; Emmanouilidou et al., 2010).

Once released, extracellular αSYN can be internalized by neighbouring neurons through receptor-mediated mechanisms. Identified neuronal receptors involved in αSYN uptake include LRP1, which binds monomeric and oligomeric species; LAG3, which preferentially recognizes preformed fibrils; HSPGs, which facilitate aggregate internalization in cooperation with other receptors (Chen et al., 2022; Mao et al., Science, 2016); and the recently proposed FAM171A2, implicated in the selective uptake of fibrillar αSYN (Wu et al., 2025).

Glial cells also play an active role in αSYN propagation. Microglia internalize extracellular αSYN and can re-release it via exosomes, amplifying its spread (George et al., 2019; Guo et al., 2020). Fibrillar αSYN activates microglia through TLR2/TLR4 and the NLRP3 inflammasome, inducing secretion of pro-inflammatory cytokines such as IL-1β, TNF-α, and IL-6, and promoting the formation of truncated αSYN species with enhanced seeding potential (Danzer et al., 2012; Emmanouilidou et al., 2010; Henderson et al., 2019).

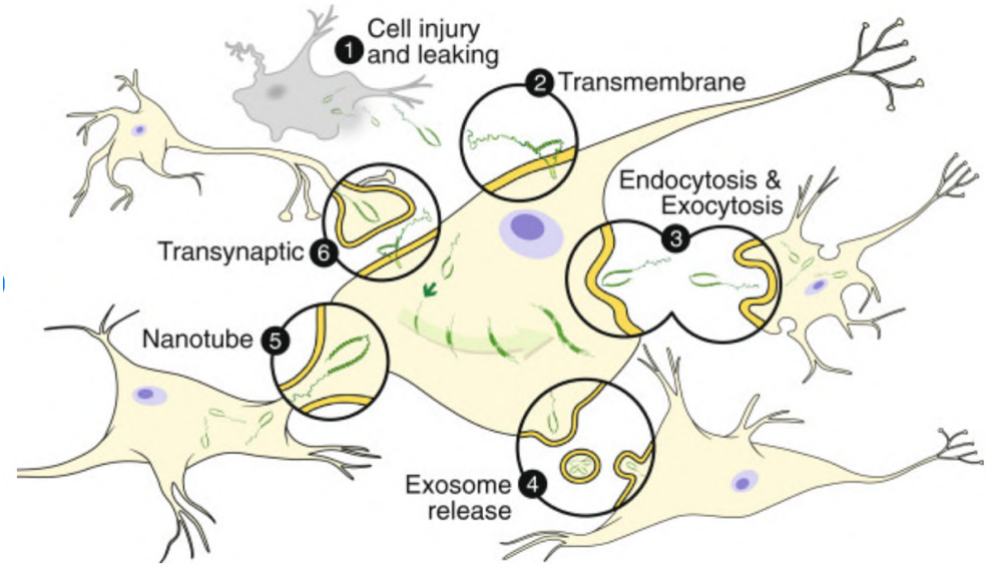

Figure 7. Potential mechanisms of α-Synuclein transmission: (1) leakage from damaged cells, (2) direct membrane translocation, (3) conventional exocytosis/endocytosis, (4) release and uptake via exosomes, (5) transfer through tunnelling nanotubes, (6) direct synaptic contact (Lee et al., 2013).

Astrocytes exert a dual role: under physiological conditions, they internalize and degrade αSYN, but under lysosomal stress, for instance, in the presence of GBA1 mutations or excessive αSYN load, they lose clearance efficiency, accumulate aggregates, and release inflammatory mediators (Alvarez-Erviti et al., 2011; di Domenico et al., 2022). Moreover, astrocytes can transfer αSYN to neurons or other glial cells via exosomes or direct contact, amplifying neuroinflammation and neuronal injury (Loria et al., 2021; Wang et al., 2023). Tunneling nanotubes (TNTs), actin-based cytoplasmic bridges, further facilitate direct intercellular transfer of αSYN aggregates, bypassing extracellular degradation routes (Abounit et al., 2016; Rostami et al., 2017).

An additional clearance route is provided by the glymphatic system, a perivascular CSF circulation that removes extracellular solutes and neurotoxic proteins, including αSYN, through AQP4-dependent flow along astrocytic endfeet (Iliff et al., 2012; Mestre et al., 2018). Aging and PD-associated glymphatic dysfunction impair αSYN clearance, resulting in its accumulation and facilitating neurodegeneration (Rasmussen et al., 2018; Smith et al., 2021). Neuroimaging studies using diffusion tensor imaging (DTI) have revealed reduced glymphatic efficiency in PD patients, correlating with disease severity (Bae et al., 2023; Chen et al., 2025).

In summary, αSYN spreading is a multifactorial process involving neurons, glial cells, and clearance systems. Under physiological conditions, microglia and astrocytes contribute to αSYN degradation, but when proteostasis fails, they shift from protective to pathogenic, releasing and propagating toxic aggregates and sustaining chronic neuroinflammation. Understanding these interconnected mechanisms will be essential for designing strategies that interrupt disease propagation and slow PD progression.

1.5 Neuroinflammation in Parkinson's disease

1.5.1 Insights from human and experimental studies

The involvement of inflammatory processes in PD has been consistently supported by both clinical and experimental evidence. The first indication of microglial activation in the SN of PD patients was reported in 1988, with the identification of HLA-DR+ reactive microglia (McGeer et al., 1988). This foundational observation was later complemented by findings of increased astrocytic reactivity, with about a 30% rise in GFAP immunoreactivity in PD post-mortem brains compared to controls (Damier et al., 1993).

Alongside glial changes, post-mortem analyses have revealed a clear infiltration of immune cells in the brains of PD patients. Both cytotoxic (CD8+) and helper (CD4+) T cells have been found in increased numbers in the SN, indicating an active adaptive immune response (Brochard et al., 2009). Sulzer and colleagues provided a pivotal mechanistic link by showing that T cells from PD patients respond to αSYN peptides, indicating antigen-specific activation (Sulzer et al, 2017). Although regulatory T cells are present in the PD brain, their suppressive function is impaired, which might contribute to ongoing neuroinflammation (Bas et al., 2001; Saunders et al., 2012). The role of the adaptive immune system is underscored by experiments in immunodeficient mice. *Rag1*−/− and *Tcrb*−/− mice exhibit resistance to MPTP-induced degeneration, which is reversed upon transfer of T cells, particularly CD4+ cells, highlighting their pathogenic potential (Gelders et al., 2018).

Humoral immunity is also implicated. Autoantibodies targeting PD-related antigens such as αSYN, neuromelanin, and GM1 gangliosides have been found in patient sera. Furthermore, IgG immunoreactivity has been detected within dopaminergic neurons in PD brains, suggesting a potential role in neuronal damage (Double et al., 2009; Papachroni et al., 2007; Yanamandra et al., 2011).

Disruption of BBB is another key pathological feature, potentially facilitating peripheral immune cell entry. Inflammatory mediators such as TNF-α, IL-1β, and IFN-γ, produced by glial and infiltrating immune cells, may contribute to BBB permeability (Block et al., 2007; Gelders et al., 2018; Harms et al., 2018). In parallel, CSF analysis in PD patients has shown elevated levels of cytokines like IL-1, IL-2, IL-6, and TNF, further confirming systemic and central inflammation (De Virgilio et al., 2016; Fiszer et al., 1994; Liu et al., 2003).

Animal models have provided essential insights into how inflammation contributes to neurodegeneration. For instance, in the 6-hydroxydopamine (6-OHDA) model, there is a notable increase in microglial numbers following lesioning, though the rapid neuronal death suggests that inflammation might be a consequence rather than a cause (Gelders et al., 2018). In contrast, in the MPTP model, microglial activation occurs before substantial neuronal loss, hinting at a causative role (Liberatore et al., 1999; Wu et al., 2002). Transgenic and viral-vector models overexpressing αSYN show early and sustained microglial and astrocytic activation, often prior to neuronal loss (Bido et al., 2021; Chesselet et al., 2012; Dawson and Chesselet, 2010; Su et al., 2008). Targeted overexpression of αSYN in glial populations has revealed that intracellular accumulation in microglia and astrocytes actively drives neurodegeneration. In microglia, αSYN accumulation induces a chronic inflammatory phenotype, reduced phagocytic capacity, and recruitment of T cells, culminating in dopaminergic neuron loss (Bido et al., 2021; Choi et al., 2020). Astrocyte-specific expression of the $SNCA^{A53T}$ under the *GFAP* promoter causes pronounced

astrogliosis, impaired glutamate transporter function, vascular alterations, and secondary microgliosis, ultimately leading to motor deficits and nigral degeneration (Gu et al., 2010).
Together, these findings from human and animal studies demonstrate that neuroinflammation is not merely a by-product of neuronal loss but an active contributor to PD progression. Both innate and adaptive immune mechanisms, mediated by microglia, astrocytes, T cells, and circulating antibodies, interact to create a self-sustaining inflammatory milieu. This growing body of evidence provides a strong rationale for therapeutic approaches targeting neuroimmune pathways to slow or halt disease progression.

1.5.2 Astrocytes in health and disease

1.5.2.1 Morphological and functional heterogeneity of astrocytes

Astrocytes, first identified by Rudolf Virchow in 1858 under the term “neuroglia”, were historically regarded as mere structural support for neurons (Allen and Barres et al., 2009; Parpura and Verkhratsky et al., 2012). Over the past decades, however, they have emerged as highly specialized glial cells essential for CNS homeostasis, synaptic modulation, and metabolic regulation. Astrocytes are now recognized as the most abundant cell type in the CNS, outnumbering neurons by approximately 10:1, and are involved in a broad range of physiological processes (Herculano-Houzel et al., 2009).
In their quiescent, homeostatic state, often referred to as A2 astrocytes, these cells regulate ionic and water balance, maintain neurotransmitter homeostasis, and contribute to the formation and maintenance of the BBB. They also modulate cerebral blood flow and provide critical metabolic support by storing glycogen, supplying neurons with energy substrates, and releasing neurotrophic and antioxidant factors. Furthermore, astrocytes clear metabolic waste and participate in synaptic remodelling, thereby supporting neuronal survival and plasticity (Miyazaki and Asanuma et al., 2018; Tremblay et al., 2019; Verkhratsky and Nedergaard et al., 2018).
Astrocyte ontogenesis begins during embryonic development, when neural stem cells in the ventricular zone first generate neurons and later macroglial lineages, including astrocytes and oligodendrocytes (Kang and Zheng, 2021). This neurogenic-to-gliogenic switch marks a key developmental transition, driven by intrinsic transcriptional programs and epigenetic repression of proneural genes such as *Neurog1* and *Neurog2* (Anderson et al., 2016; Miller et al., 2007).
In the mouse brain, astrocytes arise in two main waves. The first starts around embryonic day 16.5, when radial glial cells detach from the ventricular surface, upregulate *Egfr*, and generate astrocyte progenitors that populate the cortical gray matter (Li et al., 2021; Noctor et al., 2004). A second, broader wave occurs postnatally from multipotent subventricular progenitors expressing both astrocytic (*Slc1a3*, *Mfge8*) and oligodendrogenic (*Olig1*, *Olig2*) markers (Huang et al., 2020; Weng et al., 2019).
Maturation involves downregulation of progenitor genes (*Egfr*, *Olig1/2*) and activation of transcriptional regulators *Id1/3*and *Hes1/5*, reflecting BMP and Notch pathway activity (Zamboni et al., 2020). Postnatal astrocyte progenitors proliferate until about postnatal day 6, reaching approximately 50% of the mature population by day 28 (Ge et al., 2012). Differentiated astrocytes express *GLT1*, *Kir4.1*, *Cx30/43*, *AQP4*, and cytoplasmic markers such as *GFAP*, *AldoC*, and *GS*, while secreting synaptogenic and homeostatic factors including Thbs1, Gpc4, and hevin (Akdemir et al., 2020).

In the adult human brain, astrocytes represent roughly 30% of all cells and exhibit significant morphological and functional diversity. Traditionally, two main subtypes are recognized: protoplasmic astrocytes, found in the gray matter, and fibrous astrocytes, located in the white matter (Ben Haim and Rowitch, 2017). Protoplasmic astrocytes extend fine perisynaptic processes that ensheath synapses and contact blood vessels, while fibrous astrocytes display elongated processes aligned with myelinated axons and nodes of Ranvier. These subtypes also differ transcriptionally: fibrous astrocytes exhibit high *GFAP* expression, whereas protoplasmic astrocytes are enriched in *GS*, reflecting their metabolic role in glutamine synthesis (Bayraktar et al., 2020).

Morphologically, astrocytes are characterized by intricate, highly branched processes extending from the soma and permeating the surrounding neuropil. Early studies based on GFAP immunolabeling captured only the major branches, representing about 15% of total astrocytic volume (Chen et al., 2015). Advanced imaging techniques have revealed that a single mature rodent astrocyte occupies a domain of 20,000–80,000 μm³, contacts hundreds of dendrites, and associates with up to 100,000 synapses (Chen et al., 2015; Clarke et al., 2018). In humans, this complexity is magnified, each astrocyte is estimated to interact with nearly two million synapses and span a territory almost thirty times larger than its rodent counterpart (Matias et al., 2019).

Developmentally, astrocytic processes emerge during the first postnatal week as dynamic filopodia-like projections. By the third to fourth postnatal week, these extensions become thinner and highly ramified, adopting a sponge-like architecture indicative of structural and functional maturity (Das et al., 2019).

This progressive structural specialization mirrors the functional diversification of astrocytes, laying the foundation for their dynamic responses to injury and disease that will be discussed in the following section.

1.5.2.2 Astrocytic dynamics in Parkinson's disease

Astrocytes are highly specialized and abundant glial cells of the CNS, essential for maintaining neuronal homeostasis, regulating synaptic activity, modulating cerebral blood flow, and preserving the integrity of the BBB (Sofroniew and Vinters, 2010; Verkhratsky and Nedergaard, 2018).

Under physiological conditions, they maintain extracellular ion balance and recycle neurotransmitters, particularly glutamate, through excitatory amino acid transporters EAAT1 and EAAT2 (also known as GLAST and GLT-1) (Verkhratsky and Nedergaard, 2018).

Astrocytes also provide neurons with metabolic support through the astrocyte–neuron lactate shuttle, a mechanism coupling neuronal activity to glucose utilization (Pellerin and Magistretti, 1994; Bélanger et al., 2011). In addition, they secrete trophic and synaptogenic molecules, including thrombospondins (Thbs1, Thbs2), hevin, and glypicans, that promote synapse formation and neuronal survival (Allen and Eroglu, 2017; Christopherson et al., 2005).

In response to pathological stimuli such as trauma, infection, or neurodegeneration, astrocytes undergo profound morphological and molecular remodelling, a process known as astrogliosis. This state is characterized by cellular hypertrophy, increased expression of intermediate filaments such as GFAP, vimentin, and nestin, proliferation, and transcriptional reprogramming associated with inflammatory and oxidative stress responses. Historically, reactive astrocytes were classified into two phenotypes: A1 astrocytes, neurotoxic and induced by pro-inflammatory factors (TNF, IL-1α, C1q) released by activated microglia, and A2 astrocytes, considered neuroprotective. However, this

binary model has been challenged by single-cell transcriptomic studies, which have revealed a continuum of reactive states influenced by stimulus type, duration, brain region, sex, and disease stage (Liddelow and Barres, 2017).

Although αSYN is predominantly neuronal, astrocytic αSYN accumulation is a hallmark of synucleinopathies (Lee et al., 2010). The precise mechanisms mediating αSYN uptake and the consequences of defective proteostasis in astrocytes remain partially unresolved (Guo et al., 2013). αSYN inclusions have been identified in astrocytes in PD (Colosimo et al., 2003), particularly in white matter and Bergmann glia, as well as in cortical and nigral regions (Braak et al., 2003; Wakabayashi et al., 2000).

Current evidence indicates that astrocytes internalize αSYN released from neurons or through direct cell–cell contact (Desplats et al., 2009). αSYN propagation can also occur via TNTs or exosomes, serving as vehicles for intercellular transmission (Danzer et al., 2012; Emmanouilidou et al., 2010). Once internalized, αSYN interacts with pattern recognition receptors such as TLR4, triggering inflammatory cascades (Lee et al., 2010; Fellner et al., 2013). Reactive astrocytes subsequently secrete pro-inflammatory cytokines (IL-1β, IL-6, TNF-α) and chemokines (CCL2, CXCL10), express antigen-presentation molecules (MHC class I and II), and upregulate oxidative stress markers including iNOS and HO-1. This inflammatory phenotype is accompanied by mitochondrial dysfunction, decreased ATP production, and elevated ROS generation (Gu et al., 2010; Rannikko et al., 2015).

Single-cell RNA sequencing has identified disease-associated astrocytes characterized by overexpression of inflammatory (*Il6*, *Ccl2*), lipid metabolism (*ApoE*, *Lpl*), and lysosomal (*Lamp1*) genes (Escartin et al., 2021; Habib et al., 2020). These subtypes exhibit functional heterogeneity and may exert either neuroprotective or neurotoxic effects (Hasel et al., 2021). While similar transcriptional profiles appear in AD, Multiple sclerosis (MS), and stroke, in PD they are thought to arise primarily from chronic αSYN exposure and dopaminergic vulnerability (Yun et al., 2023).

Transgenic mouse models have confirmed that astrocytic pathology can directly drive neurodegeneration. Animals overexpressing A53T-mutated αSYN in astrocytes develop extensive intracellular inclusions, astrocyte loss, and dopaminergic neuron degeneration (Gu et al., 2010). Double-mutant A30P/A53T models show parkinsonian motor symptoms even in the absence of neuronal loss, indicating that astrocytic dysfunction alone can disrupt neuronal circuitry (Rannikko et al., 2015). Astrocytic accumulation of αSYN is a consistent feature of synucleinopathies and has been linked to astrocyte dysfunction and oxidative stress. Emerging evidence also suggests that glial αSYN may contribute to the intercellular dissemination of pathogenic aggregates, although the underlying mechanisms remain incompletely understood (Altay et al., 2022; Jan et al., 2021; Sorrentino et al., 2019). Normally, astrocytic αSYN clearance occurs through lysosomal and cathepsin-dependent degradation; however, PD-related mutations in *LRRK2*, *GBA*, *PARK2*, and *PINK1* compromise these pathways, exacerbating protein aggregation and cellular stress (Nirujogi et al., 2018). Moreover, astrocyte–neuron crosstalk can establish a self-perpetuating pathogenic loop: dysfunctional astrocytes release αSYN via TNTs or exosomes, propagate toxic aggregates, impair dopamine uptake, and fail to regulate glutamate homeostasis. Under chronic stress, antioxidant defences become insufficient, but activation of the Nrf2 signalling pathway emerges as a crucial compensatory response, enhancing antioxidant capacity, suppressing inflammation, and promoting neuronal survival (Gan et al., 2012; Lastres-Becker et al., 2012).

Altogether, these findings indicate that astrocytic pathology in PD is not merely secondary to neuronal degeneration but constitutes a primary pathogenic mechanism driving disease progression. Therapeutic strategies should therefore avoid nonspecific suppression of astrogliosis and instead aim to reprogram astrocytes toward protective phenotypes, restoring their neuro-supportive functions while curbing their role in αSYN propagation and chronic neuroinflammation. Understanding the molecular checkpoints that govern this duality is essential for designing innovative, targeted interventions in PD.

1.5.3 Microglia: a double-edged sword

1.5.3.1 Microglia ontogeny and functional heterogeneity

Microglia, first described by Pío del Río-Hortega in the early 20th century, have undergone profound conceptual re-evaluation. Initially considered static and quiescent, they are now recognized as highly dynamic components of the CNS, constantly surveilling the brain parenchyma and responding rapidly to physiological and pathological stimuli (Tremblay et al., 2015).

Accounting for approximately 10% of total CNS cells (Lawson et al., 1990), microglia express a repertoire of molecular markers that distinguish them from peripheral macrophages, including CD11b, CSF1R, CX3CR1, and CD200R (Gautier et al., 2012; Jung et al., 2000). More specific identifiers such as IBA1, TMEM119, FCRLS, and Siglec-H further define microglial subsets according to functional state and anatomical localization (Bennett et al., 2016; Imai et al., 1996; Konishi et al., 2017).

Microglia derive from primitive myeloid progenitors originating in the yolk sac during early embryogenesis (around E7.5 in mice), which invade the developing brain prior to BBB formation (E9.5–E10.5) and complete colonization by E13.5–E14.5 (Ginhoux et al., 2010; Schulz et al., 2012). Under homeostatic conditions, the population is maintained through local self-renewal, independent of bone marrow-derived hematopoietic input (Prinz et al., 2019). Their survival is critically dependent on CSF1R signalling, as mice lacking CSF1R exhibit a complete absence of microglia (Elmore et al., 2014). IL-34 partially compensates for CSF1 deficiency (Greter et al., 2012; Wang et al., 2012), while TGF-β acts as a pivotal regulator of microglial identity and homeostasis, its deletion results in microglial loss (Butovsky et al., 2014).

During development, microglia express gene programs aligned with the maturation stage of the brain: early signatures include genes related to proliferation and the cell cycle, whereas later profiles are enriched in those mediating synaptic remodelling, homeostasis and immune tolerance (Gosselin et al., 2014; Lavin et al., 2014; Matcovitch-Natan et al., 2016). Functionally, microglia orchestrate neurogenesis, prune redundant synapses, promote myelination, and release neurotrophic factors such as thrombospondin (Chamak et al., 1994; Ferrer et al., 1990; Marín-Teva et al., 2004).

Environmental and neuronal signals dynamically modulate microglial morphology and function. For instance, sensory deprivation or visual stimuli reshape their phagocytic behaviour and synaptic interactions in the visual cortex (Tremblay et al., 2010). Synaptic pruning depends on molecular cues such as “eat me” signals (phosphatidylserine, C1q, Gas6) and “don’t eat me” signals (CD47), maintaining circuit refinement and stability (Elward and Gasque, 2003; Lehrman et al., 2018; Neniskyte and Gross, 2017).

In the adult brain, microglia perform dual roles: immune surveillance and metabolic support. The transcription factor MafB is essential in maintaining this equilibrium (Matcovitch-Natan et al., 2016).

Even under basal conditions, microglia retain phagocytic capacity (“phagoptosis”), crucial for clearing debris and apoptotic cells via receptors such as Axl and MerTK (Fourgeaud et al., 2016; Ji et al., 2013). They are also responsive to neuronal activity through neurotransmitter receptors (AMPA, NMDA, mGluR), linking neural transmission with immune function (Pocock and Kettenmann, 2007). Upon injury, ATP released by damaged neurons activates P2Y12 receptors, inducing rapid chemotaxis and transition to an amoeboid phenotype (Haynes et al., 2006). Following resolution, activated microglia undergo apoptosis or return to a homeostatic ramified morphology.

Microglial heterogeneity is evident across brain regions, reflecting both developmental and environmental influences. Even under steady-state conditions, microglia in the hippocampus, cortex, and cerebellum exhibit distinct transcriptional and morphological profiles (De Biase et al., 2017). Although regional diversity is most pronounced during development, single-cell RNA sequencing (scRNA-seq) studies indicate that transcriptional heterogeneity persists into adulthood, with distinct subpopulations specialized for synaptic, metabolic, or immune functions (Hammond et al., 2019).

Recent scRNA-seq analyses have refined this view, identifying region- and disease-specific microglial subtypes that vary with injury stage, sex, and CNS location. For example, $CD45^{high}/STAT1^{+}$ microglia predominate in male mice after ischemic stroke, suggesting sexually dimorphic immune responses. Comparative studies in AD, MS, and PD have further demonstrated that microglia exhibit context-dependent activation states, adopting distinct transcriptional signatures rather than a uniform reactive profile (Masuda et al., 2019; Prater et al., 2023; Russo et al., 2022). As a result, the traditional M1/M2 dichotomy is now regarded as overly simplistic. Categories such as disease-associated microglia (DAM) and microglial neurodegenerative phenotype (MGnD) capture some pathological states but are not universally applicable, since each neurodegenerative condition elicits unique, temporally dynamic microglial responses (Dadwal et al., 2024).

Overall, microglia represent a highly plastic, multifunctional cell population that integrates immune, metabolic, and synaptic functions. Their diversity allows them to adapt rapidly to changes in the neural environment but also renders them susceptible to maladaptive activation during neurodegeneration. This functional duality underlies their role as both protectors and potential amplifiers of pathology.

1.5.3.2 Microglial dynamics in health and Parkinson’s disease

A substantial body of evidence from neurodegenerative disorders such as MS and AD has underscored the central role of neuroinflammation, and particularly microglial activation, in neuronal degeneration (Stephenson et al., 2018). These findings have progressively directed scientific attention toward the mechanisms of microglial activation in PD, where immune–glial interactions critically influence disease progression.

The first evidence of microglial activation in PD dates back to the late 1980s, when McGeer and colleagues identified HLA-DR–positive reactive microglia in the SN of post-mortem PD brains (McGeer et al., 1988). Subsequent studies confirmed that microglial activation increases proportionally with dopaminergic neuronal loss along the nigrostriatal pathway, supporting a causative rather than purely reactive role (Imamura et al., 2003).

Activated microglia represent a major source of pro-inflammatory mediators, including cytokines such as TNF-α, IL-1β, IL-6, and TGF-β, as well as reactive oxygen and nitrogen species (ROS and NO). Elevated concentrations of these molecules have been detected in the SNpc, STR, and CSF

of PD patients (Harms et al., 2021; Nagatsu et al., 2000). These findings emphasize that microglia are not merely passive responders but active participants in neurodegenerative pathology.

A key mediator in this immune–neuronal interface is αSYN. Released by neurons in a calcium-dependent manner, oligomeric αSYN species are particularly immunogenic. They engage pattern-recognition receptors such as TLR2 and TLR4 on microglial surfaces, triggering NF-κB–mediated inflammatory cascades and cytokine release (Kwon et al., 2019; Lee et al., 2010b; Letiembre et al., 2009).

Persistent exposure to aggregated, truncated, or mutant αSYN variants promotes chronic microglial activation, excessive cytokine secretion, and oxidative stress (Fellner et al., 2013; Grozdanov et al., 2019). Over time, these conditions drive microglia toward a dysfunctional phenotype characterized by impaired phagocytic activity and reduced clearance of pathological proteins, including αSYN itself. The interplay among genetic predispositions, αSYN conformation, and inflammatory cues contributes to the maintenance of a self-perpetuating neurotoxic milieu, linked to dopaminergic neurodegeneration and the recruitment of peripheral immune cells such as T lymphocytes (Bido et al., 2021; Choi et al., 2020; Tremblay et al., 2019).

Beyond Toll-like receptors, the NLRP3 inflammasome, a cytosolic multiprotein complex, has emerged as a central mediator of microglial inflammatory signalling. Activation of NLRP3 by αSYN results in the maturation and secretion of IL-1β and IL-18 and, in some models, the degradation of αSYN aggregates, suggesting a dual role in both host defence and neurotoxicity (Gordon et al., 2018; Piancone et al., 2021; Scheiblich et al., 2021).

Experimental paradigms have shown that stimulation with lipopolysaccharide (LPS) and interferon-γ (IFNγ) induces potent microglial activation marked by elevated iNOS expression and NADPH oxidase (NOX) activity (DeLeo et al., 1998; Lehnardt et al., 2003). NOX-derived superoxide amplifies cytokine output and oxidative stress–related neuronal injury (Shimohama et al., 2000; Qian et al., 2010), while TNF-α further sustains chronic microglial activation via autocrine feedback (Qin et al., 2007).

Microglia also modulate astrocyte activity by releasing IL-1α, TNF, and C1q, which promote the conversion of homeostatic astrocytes into A1 neurotoxic phenotypes, exacerbating neuronal injury (Liddelow et al., 2017). Furthermore, impaired lysosomal function and defective protein degradation compromise glial phagocytic capacity, aggravating αSYN accumulation and neuroinflammation.

Recent single-cell RNA sequencing studies have redefined the understanding of microglial biology. Rather than conforming to the simplistic M1/M2 polarization model, microglia display a spectrum of activation states influenced by sex, brain region, disease stage, and local microenvironmental factors (Depp et al., 2025). These transcriptionally distinct subpopulations assume context-specific functional phenotypes, reflecting the dynamic adaptability of microglia during neurodegeneration.

In conclusion, current evidence supports a model in which αSYN-induced microglial overactivation, amplified by inflammatory signals and genetic susceptibilities, acts as a central driver of neurodegeneration in PD. Elucidating the molecular pathways that govern microglial activation, and heterogeneity will be essential for designing targeted immunomodulatory therapies aimed at interrupting this self-reinforcing cycle and slowing disease progression.

1.5.4 Brain-resident and infiltrating macrophages

PD is a complex neurodegenerative disorder increasingly recognised as the result of a dynamic interaction between neurodegeneration and inflammation, both central and peripheral. Historically, the CNS was regarded as an immunologically privileged site; however, accumulating evidence has challenged this view, revealing an extensive interplay between the CNS and the peripheral immune system, particularly under pathological conditions such as PD (Ransohoff et al., 2009). In patients with PD, elevated levels of pro-inflammatory cytokines have been detected in both CSF and serum (Reale et al., 2009), together with systemic immune imbalances including altered lymphocyte subpopulations (Kustrimovic et al., 2016) and monocyte dysfunction (Grozdanov et al., 2014).
Monocytes are circulating myeloid cells produced in the bone marrow that contribute to immune surveillance and inflammatory responses under physiological conditions (Fig. 8). They are generally classified into three major subsets: classical ($CD14^{+}CD16^{-}$), intermediate ($CD14^{+}CD16^{+}$), and non-classical ($CD14^{low}CD16^{+}$) monocytes (Ziegler-Heitbrock et al., 2010).

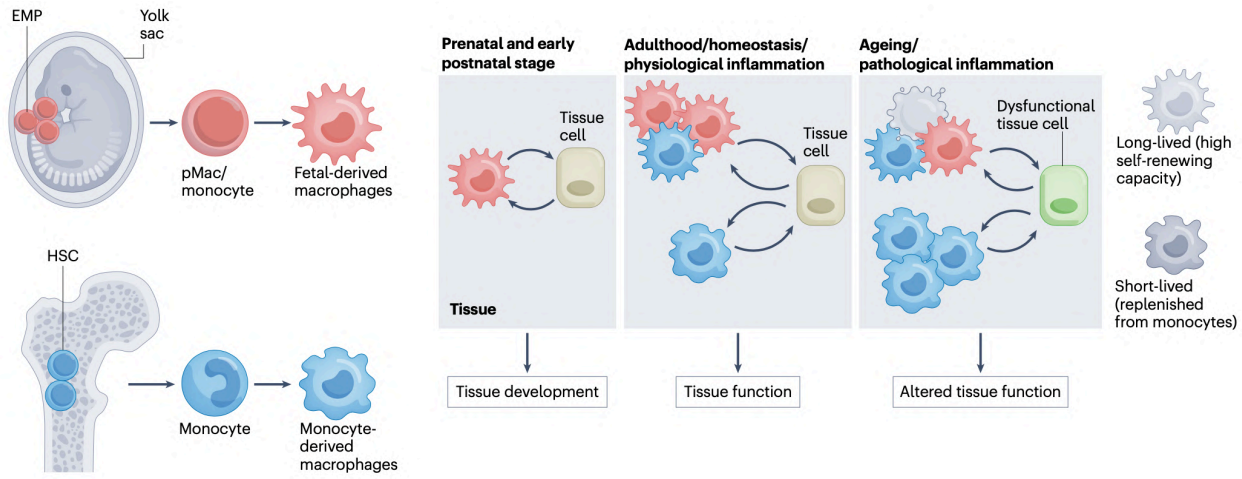

Figure 8. Origin and dynamics of tissue macrophage populations across development and ageing. Erythro-myeloid progenitors (EMPs) in the yolk sac give rise to pMac/monocyte precursors that differentiate into fetal-derived macrophages, while hematopoietic stem cells (HSCs) generate monocytes that give rise to monocyte-derived macrophages. During prenatal and early postnatal stages, fetal-derived macrophages contribute to tissue development. In adulthood, under homeostatic or physiological inflammatory conditions, both fetal- and monocyte-derived macrophages cooperate with tissue cells to maintain physiological function. With ageing or in pathological inflammation, macrophages undergo functional changes that contribute to tissue dysfunction. Some macrophage populations are long-lived with high self-renewing capacity, whereas others are short-lived and continuously replenished from circulating monocytes. (Elvira et al., 2023).

Recent scRNA-sequencing analyses of peripheral blood have refined our understanding of the immune landscape in PD. These studies have identified transcriptional remodelling within the peripheral immune compartment, including enrichment of interferon-responsive and inflammatory programmes in specific monocyte subsets. Such molecular signatures correlate with clinical measures of disease severity, supporting the concept of a peripheral immune “priming” in PD (Moquin-Beaudry et al., 2025; Pajares et al., 2020; Xiong et al., 2024).
Beyond their inflammatory role, monocytes are also proposed to interact directly with circulating αSYN. Although human data remain heterogeneous, several studies indicate that

monocytes and macrophages can internalise αSYN and modulate autophagy and inflammatory signalling pathways (Limanaqi et al., 2024). However, there is still no definitive evidence that impaired peripheral clearance by monocytes directly drives disease propagation. More plausibly, the interaction between αSYN and the monocytic compartment contributes to peripheral immune dysregulation, thereby amplifying neuroinflammatory responses (Pajares et al., 2020; Wijeyekoon et al., 2020).

In preclinical mouse models of PD, infiltration of $TREM1^+$ monocytes into the SN has been observed, correlating with dopaminergic neuronal loss. Both pharmacological and genetic inhibition of TREM1 markedly reduce neuroinflammation and preserves neuronal integrity, whereas adoptive transfer of $TREM1^+$ monocyte into naïve mice induces dopaminergic neuron damage and motor deficits (Song et al., 2025). Similarly, under conditions of neuronal stress or inflammation, $CCR2^+$ monocytes can cross the BBB and differentiate locally into inflammatory macrophages (Harms et al., 2018; Xu et al., 2022). Their transcriptional profile and lifespan differ from those of resident border-associated macrophages, suggesting complementary rather than overlapping roles (Schonhoff et al., 2023).

Beyond infiltrating monocytes, the brain harbours long-lived resident macrophages that maintain tissue homeostasis and immune surveillance. During embryogenesis, these cells arise primarily from yolk sac–derived erythron-myeloid progenitors (EMPs), giving rise to both parenchymal microglia and CNS-associated macrophages (CAMs) independently of adult haematopoietic stem cells (Mass et al., 2016; Sheng et al., 2015). More recent ontogenetic and transcriptomic studies have identified three major CAM subsets (perivascular, meningeal, and choroid plexus macrophages) each characterised by distinct spatial distribution and transcriptional identity (Mass et al., 2023).

Unlike parenchymal microglia, which express *Tmem119*, *P2ry12*, and *Sall1* and are maintained in a homeostatic state via *Cx3cr1*–fractalkine signalling, CAMs display distinct gene expression profiles, including *Mrc1* (CD206), *Lyve1*, *Cd163*, *Ms4a7*, and *Spp1*. These signatures reflect roles in barrier maintenance, antigen presentation, and immune drainage. *Cx3cr1* expression in CAMs is more heterogeneous and region-dependent, implying variable signalling functions across compartments. In adult tissues, local macrophage populations are largely self-renewing but can be replenished by bone marrow–derived cells under inflammatory or injurious conditions (Hashimoto et al., 2013). Their proliferation and differentiation depend on growth factors such as M-CSF (CSF-1), G-CSF, GM-CSF (CSF-2), IL-6, and IL-34, along with their respective receptors; the absence of any of these signals impairs macrophage survival and differentiation (Boulakirba et al., 2018; Dai et al., 2002; Duplomb et al., 2008; Sakagami et al., 2009; Wang et al., 2012;).

Functionally, macrophages exhibit remarkable plasticity and can polarise towards pro-inflammatory (M1-like) or anti-inflammatory/repair-associated (M2-like) phenotypes depending on local cues (Mantovani et al., 2004; Murray et al., 2011). However, recent studies have shown that this dichotomy is overly simplistic, as immune cells in both the CNS and periphery display a continuum of intermediate and dynamic activation states (Ma et al., 2024). Single-cell transcriptomic studies further reveal that CNS macrophages express genes associated with neurodegenerative-linked phenotypes, including *ApoE*, *Trem2*, *Lgals3*, and *Clec7a*, indicating partial functional overlap with disease-associated microglia (Silvin and Ginhoux, 2023).

With ageing, macrophages acquire a pro-inflammatory senescence-associated secretory phenotype (SASP), contributing to chronic low-grade inflammation and impaired immune regulation (Pajares et al., 2020).

A pivotal study by Schönhoff et al. (2023) demonstrated that CAMs act as key antigen-presenting cells (APCs) in PD, mediating recruitment of $CD4^+$ T lymphocytes into the CNS. In a murine model with αSYN overexpression in dopaminergic neurons of the SNpc, these macrophages expressed MHC class II molecules and upregulated inflammatory genes such as *Il1b*, *Ccl5*, and *Cxcl10*. Post-mortem analyses of PD patient brains confirmed the spatial association between CAMs ($CD68^+$) and $CD3^+$ T lymphocytes (Schönhoff et al., 2023).

Spatial multi-omic profiling of human PD and other synucleinopathy brains has further identified perivascular macrophage subtypes with high TREM2/ApoE expression, linked to lipid phagocytosis and tissue remodelling programmes (Sankowski et al., 2024). Chronic exposure to fibrillar αSYN can drive these macrophages towards pro-inflammatory states characterized by elevated IL-1β and TNF-α expression, thereby amplifying neuroinflammation (Condolo et al, 2013).

Taken together, current evidence supports a model in which infiltrating monocytes and resident macrophages cooperate within a dynamic immunological network that bridges peripheral and central inflammation. Their interactions with microglia, endothelial cells, and T lymphocytes shape the neuroimmune landscape of PD and highlight novel therapeutic targets aimed at modulating macrophage polarisation, antigen presentation, and αSYN–mediated inflammation. Understanding the signals controlling these interactions, such as TREM2, CCR2, and CSF1R, may open new avenues for immunomodulatory strategies designed to restore neuroimmune balance and slow neurodegeneration.

1.5.5 Pathogenic T cell responses and adaptive immune imbalance in Parkinson's disease

Mounting evidence indicates that the adaptive immune system contributes actively to the pathogenesis of PD, challenging the traditional view that inflammation is a secondary epiphenomenon of neuronal loss. The landmark neuropathological study by McGeer and colleagues (1988) first revealed the presence of infiltrating $CD3^+$ T lymphocytes within the CNS of individuals with PD, paving the way for subsequent work that established the functional significance of this adaptive response. These initial findings were later confirmed by multiple studies reporting increased numbers of both $CD4^+$ and $CD8^+$ T cells in the SNpc compared with healthy controls (Brochard et al., 2009; Fiszer et al., 1994; Sommer et al., 2018), suggesting that immune activation is not merely a secondary reaction but an integral component of neurodegeneration.

Such immune alterations are detectable even during the prodromal stages of the disease. Individuals with RBD, a recognised prodromal manifestation of PD, display persistent transcriptional reprogramming within the T cell compartment, which remains evident after conversion to clinically manifest PD (De Francesco et al., 2020). These alterations include increased expression of interferon-stimulated genes and activation markers, supporting the concept of peripheral immune priming prior to dopaminergic neurodegeneration.

Detailed immunophenotyping of peripheral lymphocytes has revealed a functional imbalance characterised by an increased proportion of IFNγ-producing cells, a reduction in IL-4-secreting cells, and a decreased CD4/CD8 ratio (Baba et al., 2005). This Th1-skewed profile promotes chronic microglial activation and amplifies oxidative stress within the SNpc, thereby contributing to dopaminergic neuron vulnerability. A major conceptual advance came from Sulzer et al. (2017), who demonstrated that $CD4^+$ T cells recognise peptides derived from αSYN, confirming the existence of

an antigen-specific adaptive immune response in PD. This discovery linked peripheral immune activation directly to a central neuronal antigen, establishing a mechanistic bridge between innate and adaptive immunity. Subsequent T cell receptor (TCR) sequencing studies identified αSYN-specific clonal expansions detectable even at early stages of the disease (Lindestam Arlehamn et al., 2020), reinforcing the notion that adaptive immunity participates from the onset of pathology.

The immune imbalance in PD is further aggravated by regulatory T cell (Treg) dysfunction, resulting in insufficient suppression of pro-inflammatory activity. Concurrently, Th1 and Th17 effector populations expand and release neurotoxic cytokines (Alvarez-Luquin et al., 2019; Contaldi et al., 2022; Thome et al., 2021; Sommer et al., 2018). Defective Treg-mediated control permits persistent immune activation, fostering a pro-inflammatory milieu that promotes neuronal loss.

In preclinical models, αSYN–specific T cells display pronounced cytotoxicity towards dopaminergic neurons (Bido et al., 2024; Karikari et al., 2022; Reynolds et al., 2010). Mechanistically, $CD8^+$ cytotoxic T cells can directly recognise dopaminergic neurons through MHC-I interactions. Although MHC-I expression is typically low in neurons, inflammatory stimuli can induce its upregulation, rendering them susceptible to immune-mediated killing via granzyme/perforin release or Fas/FasL pathways (Cebrián et al., 2014; Galiano-Landeira et al., 2020; Medana et al., 2000; Meuth et al., 2009). In parallel, $CD4^+$ helper T cells, once activated through MHC-II–dependent antigen presentation, amplify the inflammatory cascade by secreting IFNγ, IL-5, IL-10, and particularly IL-17, which promotes NF-κB activation and contributes to neuronal apoptosis and glial activation (Lindestam Arlehamn et al., 2019; Sommer et al., 2018).

The widespread microgliosis observed in PD and related neurodegenerative conditions further supports the existence of a pathogenic glia–lymphocyte crosstalk (Brochard et al., 2009; Kouli et al., 2020; Williams et al., 2018). Microglia and astrocytes are central to sustaining this inflammatory network. When exposed to aggregated αSYN, microglia adopt an activated phenotype characterised by increased expression of MHC-II, CD68, and pro-inflammatory cytokines, acting as APC that perpetuate T cell activation (Almolda et al., 2015; Harms et al., 2013). Astrocytes, upon exposure to aggregated αSYN, upregulate immune-related genes such as MHC-II and secrete cytokines and chemokines including IL-6, TNF-α, and MCP-1. These mediators enhance microglial activation, promote peripheral immune cell recruitment, and disrupt BBB integrity, collectively sustaining a pro-inflammatory microenvironment (Huang et al., 2025; Liddelow et al., 2017; Wang et al., 2021; Weiss et al., 2024).

The inflammatory milieu generated by activated glia and infiltrating lymphocytes also promotes BBB disruption, a crucial step that enables further immune cell entry into the CNS. Systemic inflammation enhances BBB permeability through the induction of endothelial adhesion molecules such as ICAM-1 and VCAM-1, facilitating leukocyte adhesion and transmigration (Banks et al., 2015; Liebner et al., 2018; Varatharaj et al., 2017). Once within the brain parenchyma, T cells interact with resident glia and neurons to establish a self-perpetuating cycle of neuroinflammation and degeneration, sustaining chronic immune activation even in the absence of persistent peripheral stimuli.

Taken together, current evidence converges on the notion that T cells are central to the initiation and maintenance of chronic inflammation in PD. Through intricate interactions with microglia, astrocytes, and neurons, they contribute to the establishment and perpetuation of a pathogenic neuroimmune environment. The polarisation towards Th1 and Th17 phenotypes, combined with Treg dysfunction and direct cytotoxicity of αSYN–specific T cells, collectively drives sustained

inflammation, further exacerbated by immunosenescence and disruption of protective CNS barriers. These findings reinforce the view that adaptive immunity, and T cells in particular, are active drivers of neurodegenerative progression in PD, providing a rationale for the exploration of immunomodulatory therapeutic strategies aimed at restoring immune homeostasis and limiting neuronal loss.

2. AIM

Parkinson's disease (PD) is a chronic and progressive neurodegenerative disorder primarily characterized by the loss of dopaminergic neurons in the substantia nigra pars compacta (SNpc) and by the presence of intracellular inclusions known as Lewy bodies, mainly composed of misfolded and aggregated α-synuclein (αSYN). Traditionally, PD pathogenesis has been interpreted through a neuron-centric perspective, focusing on the intrinsic vulnerability of dopaminergic neurons and on mechanisms such as oxidative stress, mitochondrial dysfunction, and abnormal protein aggregation. However, increasing evidence over the past two decades has redefined this view, highlighting the contribution of non-neuronal cells to disease progression and the pivotal role of neuroinflammation as an active component of PD pathology.

Among glial cells, astrocytes represent the most abundant population in the central nervous system and are essential for neuronal homeostasis, synaptic regulation, and metabolic support. In pathological conditions, astrocytes can undergo profound functional and morphological changes, leading to a reactive phenotype associated with inflammation and altered intercellular communication. While microglia have long been considered the principal mediators of neuroinflammation in PD, the contribution of astrocytes has remained largely unexplored, despite post-mortem studies reporting astrocytic reactivity and the presence of αSYN-positive inclusions in these cells. The mechanisms through which astrocytic αSYN accumulation influences neuronal survival and immune activation are therefore critical to understanding PD pathogenesis but remain poorly defined.

The overarching aim of this thesis is to elucidate the pathogenic role of astrocytic αSYN accumulation and to determine how this glial pathology contributes to dopaminergic neurodegeneration and immune activation in PD. Specifically, the work seeks to address whether selective expression of human αSYN in striatal astrocytes is sufficient to induce neuronal loss in the SNpc and to trigger inflammatory and immune responses, both within the central nervous system and through the recruitment of peripheral immune cells.

To investigate these questions, we employed a transgenic mouse model engineered to overexpress human αSYN exclusively in astrocytes, allowing the study of cell-type–specific mechanisms of neurodegeneration independently of neuronal αSYN expression. Through a multidisciplinary experimental design combining histological, immunofluorescence, and flow cytometric analyses, we examined dopaminergic neuron survival, glial activation, and immune cell infiltration in the nigrostriatal system. In parallel, bulk RNA sequencing of isolated astrocytes was used to profile the transcriptional landscape associated with astrocytic αSYN accumulation, with a particular focus on inflammatory signalling pathways and chemokine networks potentially responsible for immune cell recruitment.

To dissect the interaction between astrocytes and microglia in this context, we depleted microglia through chronic treatment with Pexidartinib (PLX3397), a CSF1R inhibitor. This approach enables the assessment of whether microglia are required for astrocyte-induced immune activation or if astrocytes can autonomously orchestrate the infiltration of peripheral immune cells. Furthermore, it allows evaluation of how the absence of microglia affects αSYN aggregation dynamics and dopaminergic neuron vulnerability, shedding light on potential compensatory roles of other myeloid populations.

Finally, single-cell RNA sequencing of $CD45^+$ immune cells isolated from the brain was conducted to characterize the heterogeneity and functional states of the infiltrating immune compartment. This high-resolution analysis aims to uncover the molecular signatures associated with immune cell activation, exhaustion, or repair programs, providing insight into how the immune landscape is reshaped under conditions of astrocyte-driven pathology and microglial modulation.

Overall, this thesis aims to provide an integrated and comprehensive understanding of astrocyte-mediated mechanisms underlying neurodegeneration in PD. By investigating how astrocytic αSYN accumulation affects neuronal survival and immune responses, and by exploring how the balance between resident microglia and peripheral immune cells influences the progression or resolution of neuroinflammation, this work seeks to redefine astrocytes as active and autonomous contributors to PD pathogenesis. The findings derived from this research are expected to deepen our understanding of glia–immune interactions within an inflamed environment and to identify novel therapeutic avenues aimed at modulating astrocyte activity, immune cell recruitment, and proteostatic clearance in order to slow or prevent dopaminergic neurodegeneration.

Unpublished work

Phagocytic macrophages mitigate α-Synuclein pathology in an astrocyte-driven model of neurodegeneration

Melania Nannoni [1,2,3], Giorgia Ruffini[2], Sharon Muggeo[2,3], Thomas Bahrens[2], Andrea Cugurra[2], Matteo Iannacone[2], Giosuè Moscato[2,3], Mirko Luoni[2,3], Serena Giannelli[2], Vania Broccoli[2,3]

[1]University of Milano-Bicocca, Milan, 20126, Italy; [2]San Raffaele Scientific Institute, Milan, 20132, Italy; [3]National Research Council (CNR), Institute of Neuroscience, Milan, 20900, Italy.

Abstract

Parkinson's disease (PD), a chronic and progressive neurodegenerative disorder, has long been studied from a neuron-centric perspective. However, more recent research indicates that neuroinflammation plays a key role in the pathological process, shifting the focus toward non-neuronal cells such as astrocytes, which are no longer seen as mere passive bystanders.

In this study, we investigated the role of α-Synuclein (αSYN) accumulation in astrocytes as a trigger of neurodegeneration and immune responses in PD, isolating and examining the specific consequences of astrocytic pathology in the absence of direct neuronal αSYN expression. Our results demonstrate that astrocyte-specific αSYN accumulation is sufficient to induce significant dopaminergic neuronal loss in the substantia nigra pars compacta (SNpc), accompanied by strong glial activation and widespread recruitment of peripheral immune cells into the brain parenchyma.

Transcriptomic analysis revealed a pro-inflammatory profile, characterized by increased expression of chemokines and immune-related signalling pathways, suggesting that astrocytes actively participate in shaping the neuroimmune environment. To determine whether these effects depend on the presence of microglia, we chronically depleted microglial cells using the PLX3397 compound. Surprisingly, T cell infiltration persisted even in the absence of microglia, providing strong evidence that astrocytes are capable of orchestrating peripheral immune recruitment. Interestingly, microglia depletion also led to a reduction in αSYN aggregate burden, suggesting a complex and potentially dual role of microglia in both the clearance and maintenance of protein pathology.

Single-cell RNA sequencing of $CD45^+$ immune cells from the striatum (STR) revealed a novel macrophage subpopulation with high phagocytic activity, alongside immunologically "exhausted" lymphocytes. This co-occurrence indicates a shift toward a tolerogenic, clearance-oriented immune state in the context of microglial depletion.

Our findings demonstrate that astrocytic αSYN is not merely a byproduct of pathology but a key driver of neurodegeneration and neuroinflammation. Astrocytes actively recruit immune cells and reshape the brain's immune landscape. In the absence of microglia, a distinct population of phagocytic macrophages emerges as powerful clean-up cells, opening new avenues to enhance proteostasis and restrain inflammation. Together with the central role of astrocytes in PD–associated

neurodegeneration, these findings point to novel strategies for protecting dopaminergic neurons and restoring neuroimmune balance.

Introduction

PD research has traditionally focused on neuronal pathology, with experimental paradigms modelling αSYN accumulation in neurons and investigating the resulting neuroinflammatory and immune responses (Chesselet et al., 2012; Gómez-Benito et al., 2020; Kirik et al., 2003; Rockenstein et al., 2002). A paradigm shift occurred after the first report of microglial activation in the SNpc (McGeer et al., 1988), establishing neuroinflammation as a key pathogenic driver (García-Revilla et al., 2022; Tansey and Romero-Ramos, 2022). Since then, the field has increasingly recognized glial and immune responses as active contributors to disease progression. Despite extensive investigation into microglial mechanisms, the role of astrocytes remains comparatively underexplored, even though early histopathological studies documented their reactivity in PD brains (Damier et al., 1993; Viejo et al., 2022). Astrocytes are essential regulators of CNS homeostasis, synaptic function, and neuroimmune signalling (Liu et al., 2021; Verkhratsky et al., 2023; Won et al., 2023), yet their contribution to αSYN-driven pathology and dopaminergic neuron vulnerability remains poorly understood (Ozoran and Srinivasan, 2023).

Although αSYN is predominantly neuronal, astrocytic αSYN inclusions are a distinct hallmark of α-synucleinopathies and PD (Braak and Del Tredici, 2008; Lee et al., 2008; Wakabayashi et al., 2000). The mechanisms underlying αSYN uptake by astrocytes and its downstream consequences are still not fully understood (Lindström et al., 2017). Current evidence suggests that astrocytes internalize extracellular αSYN released by degenerating neurons (Lee et al., 2010), although additional routes such as tunnelling nanotubes (TNTs) (Rostami et al., 2017) and exosomes (Mavroeidi, 2022) have also been described. Once internalized, αSYN activates pattern recognition receptors, including TLR4, triggering pro-inflammatory signalling cascades (Lee et al., 2010; Rannikko et al., 2015). Consequently, astrocytes acquire a reactive phenotype characterized by increased expression of IL-1β, IL-6, and TNF-α, secretion of chemokines such as CCL2 and CXCL10, and induction of antigen-presentation molecules (MHC I/II) (Rostami et al., 2020). These features resemble an A1-like pro-inflammatory state, although the classical A1/A2 dichotomy likely oversimplifies astrocyte heterogeneity (Escartin et al., 2021; Liddelow et al., 2017).

Such astrocytic polarization not only fosters a neurotoxic milieu but may also recruit and activate adaptive immune cells. Through chemokines secretion and antigen presentation, astrocytes could directly promote T-cell infiltration and activation within the CNS (Rostami et al., 2020), thereby bridging innate and adaptive immunity, a function traditionally ascribed primarily to microglia. Since the seminal observation of microglial HLA-DR$^+$ activation in PD (McGeer et al., 1988), accumulating evidence has highlighted the involvement of adaptive immunity. In particular, CD4$^+$ and CD8$^+$ T-cell infiltration into the substantia nigra (Brochard et al., 2009), altered peripheral T-cell subsets (Fiszer

et al., 1994), and Th17-mediated neurotoxicity (Sommer et al., 2018) underscore a multifaceted immune contribution to PD. Remarkably, immune perturbations are evident even during the prodromal phase: patients with idiopathic REM sleep behaviour disorder exhibit transcriptional and quantitative T-cell changes indicative of early adaptive immune activation (De Francesco et al., 2021; Zheng et al., 2024).

Beyond numerical imbalances, PD T cells display functional polarization toward Th1 responses and impaired regulatory activity (Álvarez-Luquín et al., 2019; Kustrimovic et al., 2018). $CD8^+$ T cells can recognize dopaminergic neurons via MHC-I and exert cytotoxicity through granzyme and Fas/FasL signalling (Cebrián et al., 2014; Galiano-Landeira et al., 2020), whereas αSYN-reactive $CD4^+$ T cells amplify inflammation via IFN-γ release (Lindestam Arlehamn et al., 2020). Importantly, αSYN itself functions as an autoantigen, eliciting $CD4^+$ T-cell responses in prodromal and early PD (Lindestam Arlehamn et al., 2020; Sulzer et al., 2017).

Myeloid cells, including microglia, border-associated macrophages (BAMs), and infiltrating monocytes, serve as central regulators of neuroinflammation. Microglia are long-lived, yolk sac–derived macrophages that self-renew locally, whereas bone marrow–derived monocytes can infiltrate the CNS under pathological conditions (Epelman et al., 2014; Hashimoto et al., 2013; Sheng et al., 2015; Silvin et al., 2023). Both resident and infiltrating myeloid populations exhibit remarkable plasticity and can polarize toward pro- or anti-inflammatory phenotypes depending on microenvironmental cues (Mantovani et al., 2004; Murray et al., 2011). Notably, BAMs have been shown to present αSYN-derived antigens via MHC-II and promote $CD4^+$ T-cell recruitment (Schonhoff et al., 2023), while monocytes in PD display enhanced migratory and antigen-presenting capacities (Farmen et al., 2021; Nissen et al., 2022). Experimental depletion of infiltrating monocytes mitigates dopaminergic neuron loss in toxin models, underscoring their neurotoxic potential (Song et al., 2025).

Collectively, these findings support a paradigm in which microglia and infiltrating myeloid cells orchestrate a self-perpetuating inflammatory circuit with T cells (Harms et al., 2013; Roodveldt et al., 2024). Within this framework, astrocytes have often been relegated to a secondary role, viewed mainly as responders to neuronal damage or microglial signals.

However, this perspective carries a critical limitation: most existing models include coexisting microglia, astrocytes, monocytes, and lymphocytes, making it difficult to disentangle the autonomous contribution of each population. Notably, astrocytes, but not microglia, consistently accumulate αSYN inclusions in human PD brains (Otero-Jiménez et al., 2025), suggesting that astrocytic αSYN pathology may independently shape neuroimmune interactions.

Here, we demonstrate that selective astrocytic αSYN accumulation is sufficient to induce neurodegeneration, immune infiltration and inflammation, recapitulating key pathological features of PD. Moreover, microglial depletion using PLX3397 reveals the emergence of a previously unrecognized macrophage population with reparative, immunoregulatory and phagocytic properties,

indicating a functional remodelling of the CNS immune landscape. The identification of this macrophage subset unveils a potential compensatory axis within the brain's immune network and opens new therapeutic avenues aimed at enhancing neuroprotective and clearance mechanisms in PD.

Results

Astrocytic α-Synuclein accumulation triggers the A1-reactive switch *in vivo*

Astrocytic overexpression of αSYN has been shown to trigger neuroinflammation and dopaminergic neuronal loss in murine models (Gu et al., 2010). Furthermore, exposure of astrocytes to monomeric, oligomeric, or fibrillar forms of αSYN induces their activation and promotes neurotoxic effects (Chavarría et al., 2018; Chou et al., 2021). However, to our knowledge, the specific contribution of adult striatal astrocytes remains unexplored. To date, no study has utilized an inducible, astrocyte-specific mouse line such as *Aldh1l1*-CreERT2 crossed with the Ai9 reporter (*Rosa26-LSL-tdTomato*; JAX 007909), which enables selective and permanent tdTomato labelling of recombined astrocytes (Fig. 1B and Fig. S1A) to address this question (Srinivasan et al., 2016).

To fill this gap, we performed a comprehensive characterization of striatal astrocytes accumulating the A53T-mutated form of αSYN.

We employed a lentiviral vector (LV) encoding the human A53T-SNCA gene under the control of an inducible EF1α promoter. In this construct, gene expression is triggered by Cre recombinase upon flipping of the αSYN gene in a sense orientation relative to the upstream promoter (Fig.1A). To achieve selective *SNCA*^{A53T} overexpression in striatal astrocytes, the LV:Astro-A53TαSYN vector was stereotaxically injected into the STR of *Aldh1l1*-CreERT2;Ai9 mice, whereas LV:Mock–injected mice were used as controls. To avoid confounding effects in the control group, GFP was not included in the construct, as both previous reports (Ansari et al., 2016) and our own data (Fig. S1, E-F) demonstrate its toxicity to dopaminergic neurons and strong immunogenicity. Control mice underwent the same surgical procedures and were infected with the corresponding empty lentiviral vector.

The viral construct was first validated using GFP as a reporter (Fig. S1, B-D), confirming selective expression in astrocytes, as shown by the co-localization of GFP with tdT+ astrocytes (96.7 ± 0.2%, mean ± SEM) and GFAP+ astrocytes (75.2 ± 3.1%, mean ± SEM). Once validated, GFP was replaced with the human *SNCA*^{A53T} transgene. BaseScope analysis confirmed its selective expression in Sox9^{+} astrocytes and its absence in NeuN^{+} neurons (Fig. 1C). In parallel, immunofluorescence revealed pSYN accumulation within GFAP^{+} cells (Fig. 1D).

Six weeks after transgene expression, striatal tissue injected with the LV:Astro-A53TαSYN construct exhibited a marked astrocytic activation (Fig. 1, E–G). Quantitative analysis revealed a significant increase in GFAP staining in LV:Astro-A53TαSYN–injected mice (13.0 ± 1.4%, mean ± SEM) compared to controls (7.5 ± 0.6%, mean ± SEM). Consistently, the tdT signal increases substantially, rising from 3.6 ± 1.5% to 17.3 ± 4.7% (mean ± SEM). Importantly, this reactive state was not

accompanied by changes in the number of $Sox9^+$ cells within the striatal compartment (Fig. S1, G-H), indicating that αSYN overexpression does not affect astrocyte number.

To characterize the signature of these cells following αSYN accumulation**,** striatal astrocytes were isolated from three LV:Astro-A53TαSYN–injected mice and three LV:Mock–injected controls and subjected to total RNA-sequencing analysis six weeks after transduction (Fig. 1, H-I). The accumulation of αSYN in astrocytes led to a robust enrichment of A1-reactive genes, including *Gfap, Vim, Serping1, Ggta1, Il1gp1, Gbp2, Fbln5, Fkbp5, Psmb8*, and *Srgn*. The upregulation of several of these genes was independently validated by targeted qPCR (Fig. 1J).

To further explore transcriptional alterations induced by αSYN accumulation, we performed a comprehensive bioinformatic analysis of the RNA-seq data. Principal component analysis (Fig. S3A) revealed a clear separation between αSYN-overexpressing and control astrocytes, accounting for 44% of total variance along PC1. Differential expression analysis identified a broad set of significantly modulated transcripts (Fig. S3B). Consistently, pathway analysis revealed enrichment in type I interferon signalling, TNF and IL-6 production, cytokine/chemokine-mediated cascades, inflammatory response, and ERK1/2 regulation (Fig. S3C).

Together, these data indicate that astrocytic αSYN accumulation drives a pronounced pro-inflammatory reactive state, consistent with an A1-like phenotype switch in the adult striatum.

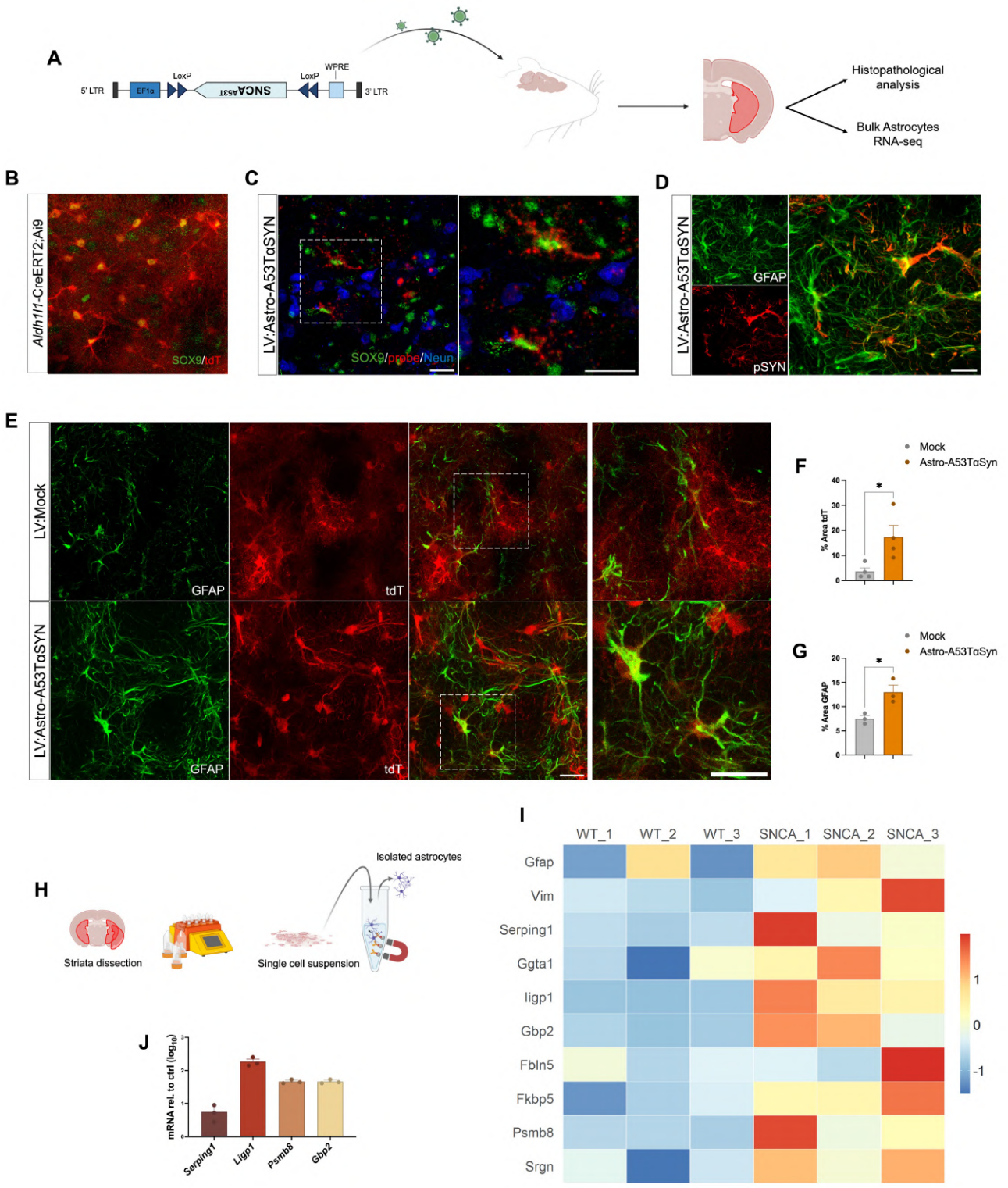

Figure 1. Astrocytic α-Synuclein drives astrocyte reactivity and inflammatory transcriptional reprogramming. (A) Schematic of the experimental design using LV:Astro-A53TαSYN to target αSYN expression in striatal astrocytes, followed by tissue collection and analysis. **(B)** Representative immunofluorescence images of using Sox9 and tdT markers to validate the *Aldh1l1*-CreERT2;Ai9 murine line. Scale bar, 25 µm. **(C)** Representative image showing the application of the BaseScope technique in slices from the LV:Astro-A53TαSYN-injected mice, displaying Sox9^{+} cells (green) co-localized with the *αSYN*^{A53T} RNA probe (red), with no signal detected in NeuN^{+} cells. The right panel shows a higher-magnification view of the boxed region. Scale bar: 25µm **(D)** Representative immunofluorescence images of GFAP and pSYN

showing co-localization (yellow) of pSYN (red) with astrocytes (green) in the mouse STR after LV:Astro-A53TαSYN injection. Scale bar, 25 µm. **(E)** Representative immunofluorescence images of GFAP and tdT showing their differential expression in the STR following LV:Astro-A53TαSYN injection, compared to the LV:Mock-injected group. Scale bar, 25 µm. **(F)** Occupied area of tdT staining (red) in the STR across the different experimental conditions. *n* = 4 striata. Data are presented as means ± SEM and were analysed using Unpaired t test. **P* < 0.01; ****P* < 0.001; *****P* < 0.0001. **(G)** Occupied area of GFAP staining (green) in the STR across the different experimental conditions. *n* = 3 striata. Data are presented as means ± SEM and were analysed using Unpaired t test. **P* < 0.01; ****P* < 0.001; *****P* < 0.0001. **(H)** Schematic of the protocol for isolating astrocytes from the mouse STR: dissection of the striata, preparation of a single-cell suspension, and magnetic separation to obtain purified astrocytes. **(I)** Heatmap depicting the expression of genes associated with the reactive state of astrocytes in striatal tissue from LV:Mock-injected (WT) and LV:Astro-A53TαSYN-injected (SNCA) mice. Rows represent astrocyte reactivity and stress-response genes, and columns correspond to individual biological replicates (n = 3 per group). Colours indicate gene-level scaled expression (z-scores). **(J)** Real-time PCR analysis of *Serping1*, *Ligp1*, *Psmb8*, and *Gbp2* transcripts in striatal astrocytes isolated from adult mice injected with LV:Astro-A53TαSYN. Data represent n=3 independent animals. STR: striatum; pSYN: phosphorylated α-Synuclein; tdT: tdTomato fluorescence expressed in astrocytes of *Aldh1l1*-CreERT2; Ai9 mice following tamoxifen-induced recombination.

Astrocyte-restricted α-Synuclein accumulation is accompanied by a robust neuroinflammatory response

Given the astrocytic activation observed following the accumulation of αSYN, we next investigated whether this was accompanied by microglial activation in the striatal compartment. Quantification of IBA1 immunoreactivity revealed a marked increase in microglial density, with the signal area rising from 12.21 ± 0.98% in control mice to 33.05 ± 0.83% (mean ± SEM) in Astro-A53TαSYN mice. CD68 immunoreactivity showed a parallel ~3.8-fold increase (0.66 ± 0.11 in controls vs 2.50 ± 0.36 in Astro-A53TαSYN, mean ± SEM; Fig. 2, A–C).

We next assessed the burden of monomeric (αSYN) and aggregated (pS129αSYN) species in Astro-A53TαSYN mice relative to controls. Immunostaining with an antibody against human αSYN, which detects the monomeric form, revealed a marked increase in the STR, with the area occupied by the signal increasing approximately 39-fold compared to control animals (Fig. S2, A-B). Notably, αSYN was distributed across multiple cell types, occupying 48.99 ± 5.62% of tdT+ astrocytes, 4.94 ± 0.57% of IBA1+ microglia, and 25.42 ± 3.64% of TH+ dopaminergic neurons (mean ± SEM, Fig. S2, C).

To specifically evaluate aggregated forms, we quantified αSYN phosphorylated at serine-129 (pS129 αSYN), a well-established marker of pathological aggregation (Fujiwara et al., 2002; Anderson et al., 2006). Independent-samples analysis confirmed a significant increase in the area occupied by pS129αSYN immunoreactivity in the Astro-A53TαSYN mice versus with Mock-injected controls, corresponding to an approximate 60.7-fold rise. Localization analyses revealed that pS129αSYN aggregates were primarily detected in astrocytes (78.94 ± 1.61% in tdT+ cells) but were also found in microglia (8.78 ± 0.51% in IBA1+ cells) and dopaminergic terminals (15.90 ± 2.78% in TH+ cells, mean ± SEM; Fig. 2, D–F).

Consistent with astrocyte-restricted transgene expression, BaseScope analysis detected *SNCA*^{A53T} mRNA exclusively in Sox9^{+} astrocytes and not in NeuN^{+} neurons (Fig. 2, G). Nevertheless, the presence of pS129αSYN aggregates in neuronal and microglial populations suggests intercellular propagation of αSYN pathology (Fig. S2, D-E).

Given the pronounced astrocytic reactivity and concomitant microglial activation observed in Astro-A53TαSYN-injected mice, we next asked whether this neuroinflammatory milieu was accompanied by infiltration of peripheral immune cells. Immunohistochemistry and immunofluorescence analyses revealed a striking accumulation of T cells within the STR, with $CD3^+$ T cells showing a 12.3 ± 1.7-fold increase relative to controls. Subtype analysis showed a 15.3 ± 5.6-fold increase in $CD4^+$ T cells and a 4.3 ± 1.0-fold increase in $CD8^+$ T cells (mean ± SEM; Fig. 2, H–I).

Prompted by this marked infiltration, we examined whether astrocytes contribute to T-cell recruitment by analysing the transcriptomic profile of striatal astrocytes from LV:Astro-A53TαSYN-injected mice using bulk RNA-sequencing data. The analysis revealed a robust induction of several chemokine genes compared with wild-type controls, with consistent upregulation of *Ccl8*, *Ccl4*, *Ccl7*, *Ccl5*, *Cxcl13*, *Cxcl16*, *Ccl3* and *Ccl2* (Fig. 2K). Among these, *Ccl8* and *Ccl2* showed the most pronounced increases, while *Ccl4*, *Ccl7* and *Cxcl16* were also strongly elevated. In contrast, wild-type samples displayed uniformly low expression of all chemokine genes analysed. Notably, selected transcripts, including *Ccl2*, *Ccl5*, *Ccl8* and *Cxcl10*, were independently validated by targeted qPCR, confirming the reliability of the sequencing data (Fig. 2J).

Consistent with these findings, gene-ontology enrichment analysis (Fig. S3D) revealed significant overrepresentation of biological processes involved in immune effector functions, regulation of T-cell activation, leukocytes proliferation, and antigen processing/presentation. These findings indicate that astrocyte-restricted αSYN overexpression elicits a pronounced neuroinflammatory milieu, characterized by microglial activation, αSYN spreading, and a pro-inflammatory transcriptional program dominated by chemokine signalling for the enhanced recruitment and activation of immune cells.

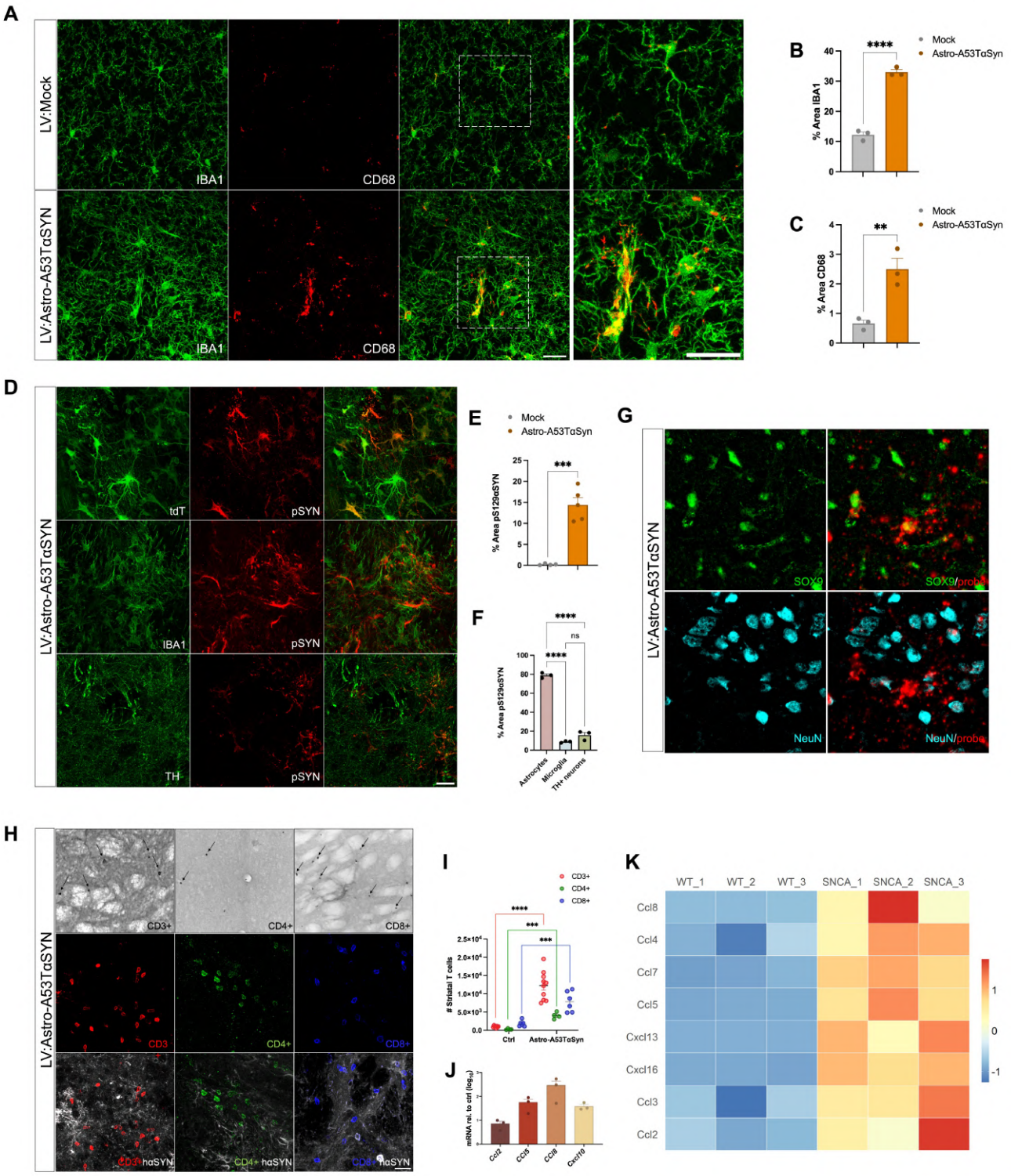

Figure 2. Astrocytic α-Synuclein drives microglial activation and T cell recruitment in the striatum. **(A)** Representative immunofluorescence images of IBA1 (green) and CD68 (red) in the mouse STR following LV:Astro-A53TαSYN injection compared to the LV:Mock group. Scale bar: 25µm **(B)** Occupied area of IBA1 staining in the STR across the different experimental conditions. *n* = 3 striata. Data are presented as means ± SEM and were analysed using Unpaired t test. *P < 0.05; **P < 0.01; ***P < 0.001; ****P < 0.0001. **(C)** Occupied area of CD68 staining in the STR across the different experimental conditions. *n* = 3 striata. Data are presented as means ± SEM and were analysed using Unpaired t test. *P < 0.05; **P < 0.01; ***P < 0.001; ****P < 0.0001. **(D)** Representative immunofluorescence images of striatal section of LV:Astro-A53TαSYN-injected mice, stained for pSYN (red) together with tdT, IBA1 and TH (green); areas where the signals overlap appears yellow

in the merged images. Scale: 25µm. **(E)** Occupied area of pS129αSYN staining in the STR across the different experimental conditions. *n* = 5 striata. Data are presented as means ± SEM and were analysed using Unpaired t test. *P < 0.05; **P < 0.01; ***P < 0.001; ****P < 0.0001. **(F)** Quantitative assessment of the percentage of pS129αSYN^{+} cells colocalizing with GFAP, IBA1 and TH. *n* = 3 striata. Values are expressed as %MOC ± SEM (Mander's Overlap Coefficient, MOC). Statistical analysis: one-way ANOVA followed by Tukey's multiple comparison test. *P < 0.05; **P < 0.01; ***P < 0.001; ****P < 0.0001. **(G)** Representative image showing the application of the BaseScope technique in slices from the LV:Astro-A53TαSYN-injected mice, displaying Sox9^{+} cells (green) co-localized with the *αSYN*^{A53T} RNA probe (red), with no signal detected in NeuN^{+} cells (cyan). Scale bar: 25µm **(H)** Representative images showing CD3+ (red), CD4+ (green) and CD8+ (blue) T cells in the presence of hαSYN (gray) in the mouse STR after LV:Astro-A53TαSYN injection. The top row displays immunohistochemistry, while the two lower rows show immunofluorescence images. Scale bar: 25µm. **(I)** Unbiased stereology count of CD3+, CD4+ and CD8+ cells in the STR (6 w.p.i.). *n* = 4 to 10 striata. Statistical analysis by one-way ANOVA followed by Tukey's multiple comparison test. **(J)** Real-time PCR of *CCl2*, *Ccl5*, *Ccl8* and *Cxcl10* transcripts in adult striatal astrocytes reported as fold change increase with respect to the control group. *n* = 3 independent samples for each condition. **(K)** Heatmap depicting the chemokines and cytokines expression (rows) in Mock-injected (WT) and Astro-A53TαSYN-injected mice (SNCA), while columns correspond to individual biological replicates (n = 3 per group). Colours indicate gene-level scaled expression (z-scores). hαSYN: monomeric human α-Synuclein; pSYN/pS129αSYN: phosphorylated α-Synuclein; STR: striatum.

Sustained T cell infiltration and recruitment of myeloid populations after microglial depletion

Given the pronounced astrocytic and microglia reactivity and the extensive lymphocytic infiltration observed in our model, we asked whether microglia or other CNS-resident factors modulate T cell recruitment.

Aldh1l1-CreERT2 mice were chronically treated with the CSF1R inhibitor Pexidartinib (PLX3397) for four weeks, resulting in a robust depletion of microglia (-96.3 ± 3.1% versus control, mean ± SEM; Fig. 3, B-C). After treatment, mice received stereotaxic injections of LV:Astro-A53TαSYN (n = 3) or LV:Mock (n = 3) and were maintained on PLX3397 until endpoint (Fig. 3A).

Strikingly, microglia depletion failed to abrogate T cell infiltration into the parenchyma. In Astro-A53TαSYN-injected mice, CD8^{+} T cell counts were comparable between untreated *Aldh1l1*-CreERT2 and PLX3397-treated animals (7839 ± 1147 vs 10902 ± 3930, mean ± SEM; Fig. 3D and F). Similarly, CD4^{+} T cell numbers did not significantly change between the two groups (4016 ± 435 vs 6309 ± 1456, mean ± SEM; Fig. 3D; G). Overall, CD8^{+} and CD4^{+} cells accounted for approximately 65% and 35% of the T-cell compartment, respectively (Fig. 3E). This suggests an autonomous, microglia-independent role for astrocytes in T cell recruitment. Notably, PLX3397 treatment further revealed the presence of CCR2^{+}/IBA1^{+} infiltrating cells in LV:Astro-A53TαSYN–injected mice, an observation confirmed using the transgenic murine *Cx3cr1*-GFP/*Ccr2*-RFP reporter line, in which GFP labels myeloid cells including resident microglia, and RFP marks peripheral CCR2^{+} monocytes (Fig. 3, H–I). To ensure selective expression of the transgene in astrocytes in a murine model lacking Cre recombinase under the *Aldh1l1* promoter, we designed a lentiviral vector incorporating a miroRNA detargeting system, in which neuron-specific miR-124, microglia-specific miR-223 and oligodendrocyte-specific miR-338 target sequences were inserted to restrict expression to astrocytes (Fig. S4A). The construct was initially validated with GFP as a reporter (Fig.

S4, B-C), showing robust and selective expression in GFAP$^+$ astrocytes. Quantitative analysis confirmed that the vast majority of transduced cells were GFAP$^+$ astrocytes (77.4 ± 2.3%, mean ± SEM), comparable to the efficiency observed with LV:Astro-GFP (Fig. S1, B–D).

In *Cx3cr1*-GFP/*Ccr2*-RFP reporter mice injected with LV:Astro-A53TαSYN, we observed RFP$^+$ monocytes infiltrating and accumulating specifically around pS129αSYN aggregates, whereas such infiltrates were absent in controls. This selective localization of CCR2$^+$ cells near pathological αSYN deposits (Fig. 3J) indicates active recruitment of peripheral immune cells despite microglial depletion.

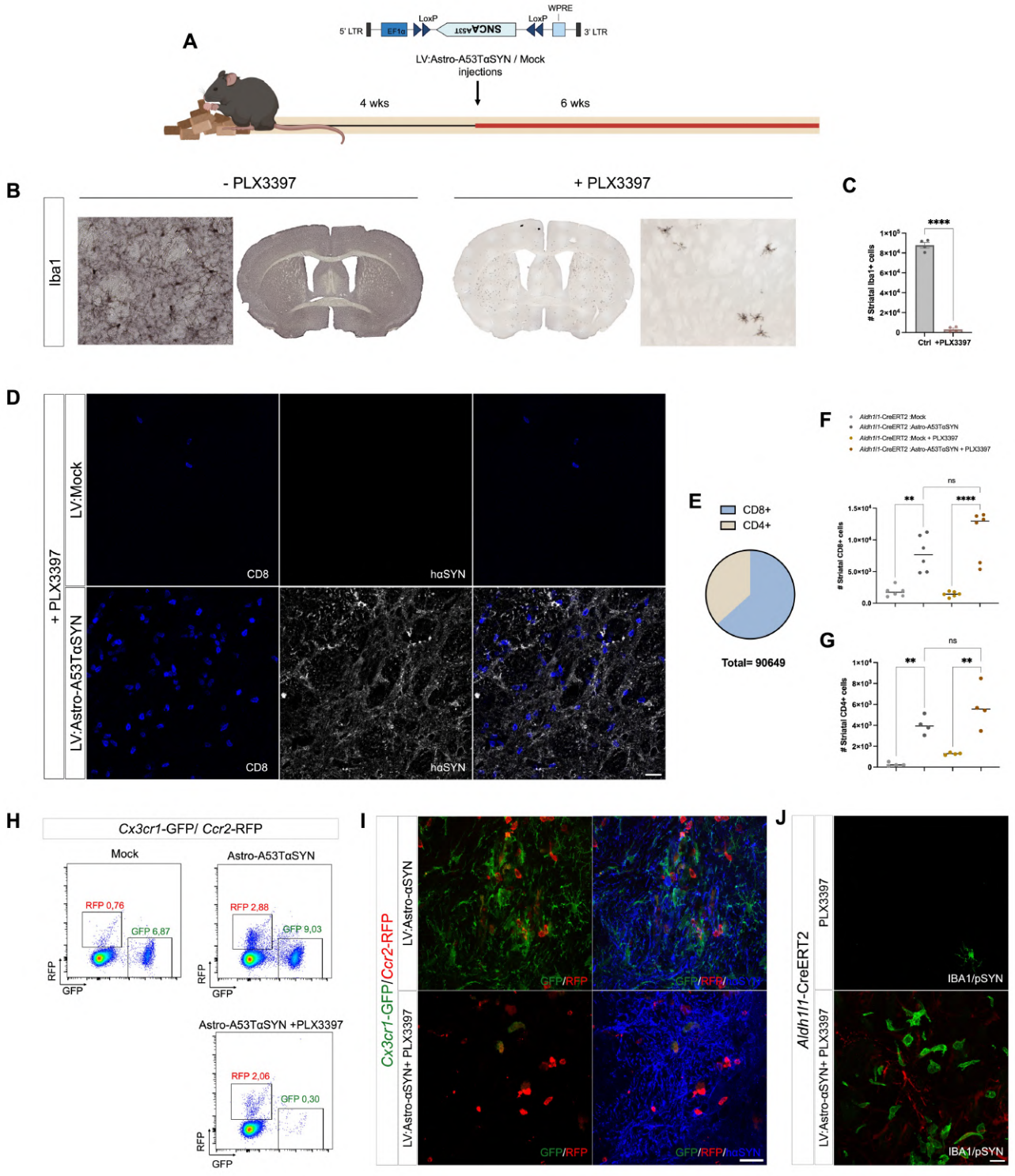

Figure 3. PLX3397-induced microglial depletion and characterization of T cell and myeloid recruitment in the striatal compartment. (A) Schematic representation of the experimental design: chronic PLX3397 administration starts 4 weeks before the intra-striatal injection of LV:Astro-A53TαSYN and continues until tissue collection (6 wpi). **(B)** IBA1 immunostaining in coronal striatal sections from untreated mice (left) and after 4 weeks of PLX3397 treatment (right), shown with corresponding magnified views. **(C)** Unbiased stereological counts of Iba1$^+$ cells in the striatum of control and PLX3397–treated mice (n = 4 striata). Data are presented as means ± SEM and were analysed using Unpaired t test. *P < 0.05; **P < 0.01; ***P < 0.001; ****P < 0.0001. **(D)** Representative immunofluorescence images showing CD8$^+$ cells (blue) in the STR of PLX3397–treated mice in the presence of hαSYN (gray) after LV:Astro-A53TαSYN injection, compared with

controls. **(E)** Pie chart showing the percentage of $CD4^+$ and $CD8^+$ cells among 90,649 counted T cells in the striatal compartment. The percentages are calculated based on the average number of T cells counted in 4–6 striata. **(F-G)** Unbiased stereological quantification of $CD4^+$ and $CD8^+$ cells in the STR of mice receiving LV:Astro-Mock or LV:Astro-A53TαSYN injections, in the presence or absence of PLX3397 treatment. n = 4–6 striata. Statistical analysis: Two-way ANOVA followed by Tukey's multiple comparison test *P < 0.05; **P < 0.01; ***P < 0.001; ****P < 0.0001. **(H)** Flow cytometry analysis of GFP^+ and RFP^+ cells in the STR of *Cx3cr1*-GFP/*Ccr2*-RFP mice across experimental conditions (LV:Astro-Mock, LV:Astro-A53TαSYN, LV:Astro-A53TαSYN + PLX3397). Percentages indicate gated populations. **(I)** Representative immunofluorescence images of GFP- (*Cx3cr1*-GFP, green) and RFP-positive cells (*Ccr2*-RFP, red) in the STR of LV:Astro-A53TαSYN–injected mice with or without PLX3397 treatment. Scale bar: 25 μm. **(J)** Representative images of $IBA1^+$ cells (green) in proximity to pSYN (red) in the STR of PLX3397–treated mice, with or without LV:Astro-A53TαSYN injection. Scale bar: 25 μm. hαSYN: monomeric human α-Synuclein; pSYN/pS129αSYN: phosphorylated α-Synuclein; STR: striatum.

Microglial depletion attenuates α-Synuclein–induced dopaminergic loss

We next investigated whether astrocyte-restricted αSYN accumulation in the striatal compartment is sufficient to elicit dopaminergic neurodegeneration and to assess the contribution of microglia to this process. We quantified TH^+ neurons in the SNpc six weeks after striatal delivery of LV:Astro-A53TαSYN. Unbiased stereological counts revealed a robust, non–cell-autonomous loss of nigral dopaminergic neurons in LV:Astro-A53TαSYN–injected mice relative to LV:Mock-injected controls, accounting for a 31.5% ± 4.6% decrease (mean ± SEM; Fig. 4, A–B).

Because the transgene is selectively expressed in astrocytes and not in neurons, this degeneration reflects a non–cell-autonomous effect, demonstrating that astrocytic αSYN accumulation alone is sufficient to compromise SNpc neuron survival. Strikingly, pharmacological depletion of microglia with PLX3397 substantially attenuated this deficit. In the absence of microglia, astrocytic αSYN expression produced only a modest reduction in TH^+ neurons (13.0% ± 7.9% deacrease) relative to the corresponding control (mean ± SEM; Fig. 4, A-B). Thus, the presence of microglia, or the inflammatory milieu they sustain, amplifies astrocyte-driven dopaminergic neuron loss. This neuroprotective effect was mirrored by a marked reduction in the pS129αSYN+ aggregate burden (14.40 ±1.69% in LV:Astro-A53TαSYN-injected mice versus 6.64% ±0.63% in microglia-depleted brains, mean ± SEM; Fig. 4, C-D). Together, these findings link astrocytic αSYN to downstream nigrostriatal degeneration and show that reactive microglia dramatically accelerate both αSYN aggregation and subsequent neurodegeneration.

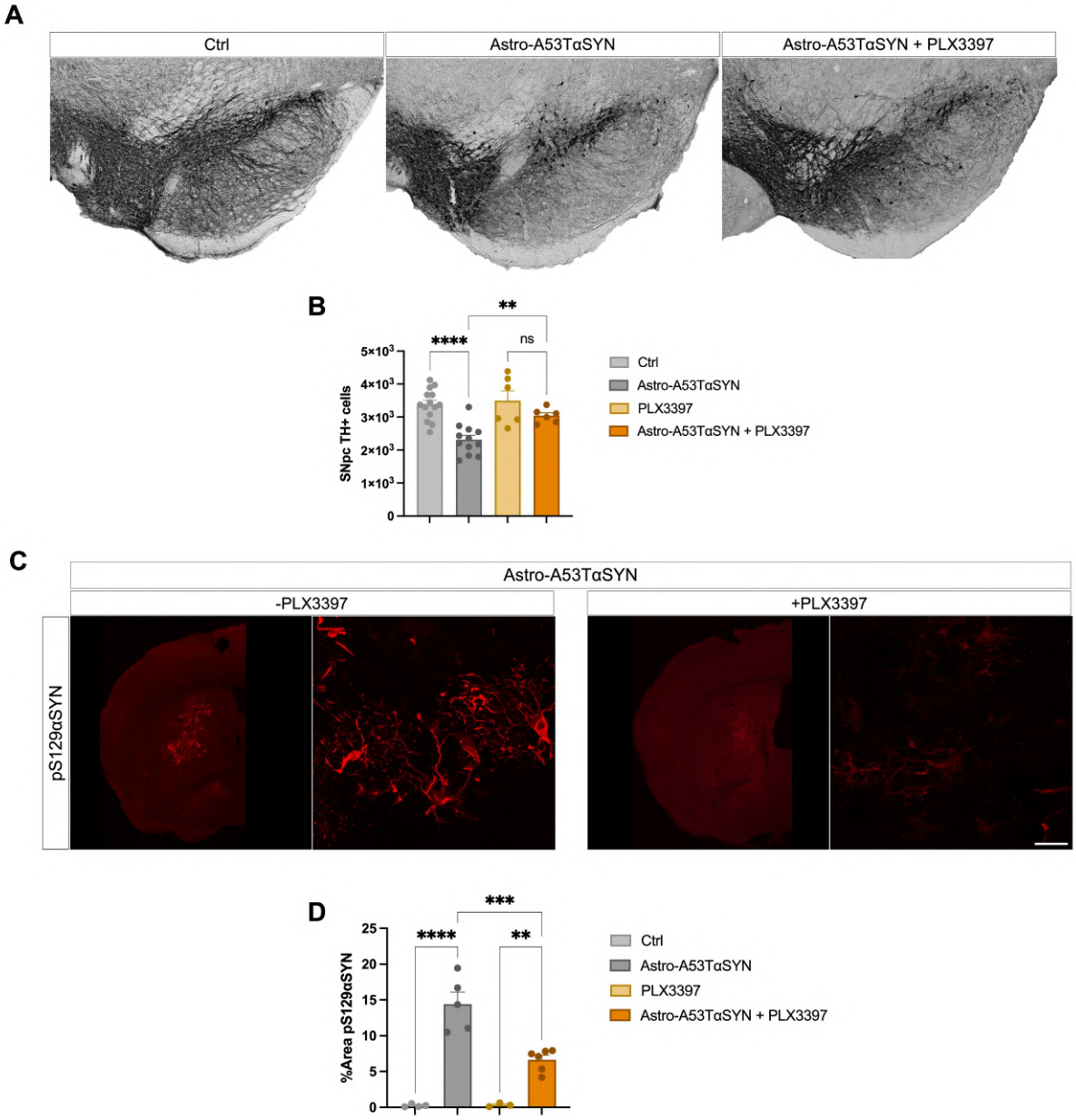

Figure 4. Microglia depletion reduces astrocytic α-Synuclein–associated pathology and preserves nigral dopaminergic neurons. (A) TH^+ immunostaining in nigral sections from mice injected with LV:Astro-Mock (Ctrl), LV:Astro-A53TαSYN, or LV:Astro-A53TαSYN combined with PLX3397 treatment. **(B)** Unbiased stereological count of TH^+ cells in the SNpc from mice injected with LV:Astro-Mock (Ctrl), LV:Astro-A53TαSYN, or LV:Astro-A53TαSYN combined with PLX3397 treatment (n = 6–14 nigra). Data are presented as means ± SEM and were analysed using two-way ANOVA followed by Tukey's multiple comparison test; *P < 0.05; **P < 0.01; ***P < 0.001; ****P < 0.0001. **(C)** Representative immunofluorescence images of pS129αSYN in the STR of PLX3397-untreated and PLX3397-treated LV:Astro-A53TαSYN–injected mice. Scale bar: 25 µm. **(D)** Quantification of pS129-$αSYN^+$ area in the STR of mice injected with LV:Astro-Mock (Ctrl) or LV:Astro-A53TαSYN, with or without PLX3397 treatment. Data are expressed as mean ± SEM. Statistical analysis: two-way ANOVA followed by Tukey's multiple comparison test; *P < 0.05; **P < 0.01; ***P < 0.001; ****P < 0.0001. pS129αSYN: phosphorylated α-Synuclein; STR: striatum.

Single-cell transcriptomics reveals myeloid compartment remodelling following microglial depletion

Building on the insights gained from microglial depletion studies, we profiled the striatal immune landscape in LV:Astro-A53TαSYN-injected mice either maintained on or withdrawn from chronic PLX3397 treatment. Six weeks after transgene delivery, $CD45^+$ cells were isolated by fluorescence-activated cell sorting (FACS) and processed for droplet-based single-cell RNA sequencing (Fig. 5A). CD45 and CD11b expression allowed us to distinguished resident microglia ($CD11b^{hi}CD45^+$), infiltrating myeloid cells ($CD11b^{int}CD45^+$) and lymphocytes ($CD11b^-CD45^+$), informing a sorting strategy to enrich myeloid and lymphocytic fractions for downstream transcriptomics (Fig. 5B).

In total, we profiled 9,347 cells isolated from LV:Astro-A53TαSYN mice and 9,194 cells from PLX3397-treated animals, with mean sequencing depth of 22,946 and 30,315 reads per cell, respectively. Quality control showed comparable distributions of detected genes, UMI counts and proportions of mitochondrial or ribosomal transcripts, indicating that sequencing depth and overall cell quality were consistent across experimental conditions (Fig. S5A).

Integrated clustering initially resolved 42 transcriptionally discrete populations. Using canonical marker genes, clusters were consolidated into broad immunological categories, including microglia, infiltrating monocytes/macrophages (Mo/MΦ), $CD4^+$ and $CD8^+$ T lymphocytes, B cells, natural killer (NK) cells, and additional myeloid subsets (Fig. 5C and Fig. S5, B–D). Microglia were defined by *P2ry12*, *Tmem119*, *Fcrls*, *Hexb*; infiltrating Mo/MΦ by *Ccr2*, *Ly6c2*, *S100a8/S100a9*, *Ms4a7*; $CD8^+$ T cells by *Cd8a/Cd8b1* with cytotoxic effectors (*Gzmb*, *Prf1*); $CD4^+$ T cells by the co-expression of *Cd3*, *Cd4, Cd28,* (Treg: *Foxp3*, *Il2ra*, *Ctla4*); B cells by *Cd19*, *Ms4a1* (CD20), *Cd79a/b*; NK cells by *Nkg7*, *Klrd1* with *Gzmb/Prf1*; dendritic-cell–like myeloid subsets by *Itgax* (CD11c), *Flt3*, and MHC-II genes (*H2-Aa/H2-Ab1*, *Cd74*); and macrophages by *Mrc1* (CD206), *Lyve1*, *Pf4*.

Direct comparison revealed a profound reorganization of the immune milieu triggered by depletion of microglia. Samples from PLX3397-treated animals exhibited a near-complete depletion of resident microglia, accompanied by the appearance of a transcriptionally distinct cluster, hereafter referred to as PLX-MΦ (Fig. 5D). To further delineate the identity of these cell types, we examined the expression of lineage-defining markers across all clusters. Microglial subsets were characterized by high levels of *Olfml3*, *Cx3cr1* and *Ccl12*, consistent with established gene signatures of homeostatic and disease-associated microglia. In contrast, infiltrating monocytes/macrophages expressed *Hp*, *Cd14* and *F10*, confirming their peripheral origin and identity (Fig. 5E).

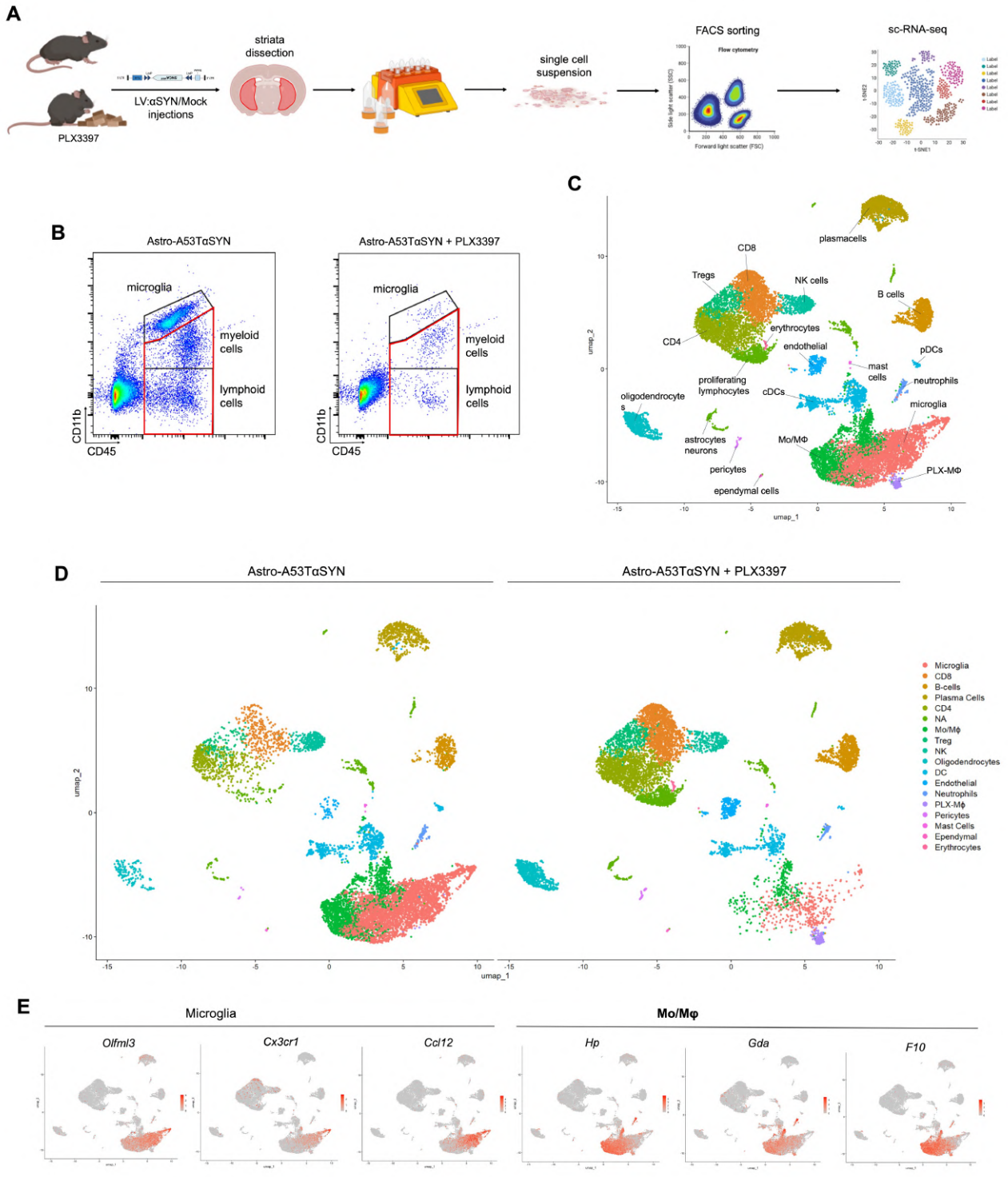

Figure 5. Remodelling of the myeloid landscape following microglial depletion revealed by single-cell transcriptomics. (A) Schematic representation of the experimental workflow. PLX3397-treated or untreated mice received striatal LV:Astro-A53TαSYN injections. Striata were dissected (6 w.p.i), processed into single-cell suspensions, and subjected to FACS sorting. Sorted cells were analysed by scRNA-seq. **(B)** Gating strategy adopted for enrichment of myeloid and lymphoid cells based on CD11b and CD45 expression in LV:Astro-A53TαSYN and LV:Astro-A53TαSYN + PLX3397 experimental groups. **(C)** UMAP projection of all sorted cells coloured by cell type, showing the distribution of major immune populations. **(D)** UMAP plots comparing cell type distribution in LV:Astro-A53TαSYN (left) and LV:Astro-A53TαSYN + PLX3397 (right) conditions. **(E)** Feature plots showing expression of representative marker genes for microglia (*Olfml3*, *Cx3cr1*, *Cst12*) and Mo/MΦ (*Hp*, *Cd14*, *F10*) across all clusters.

Microglial depletion drives the emergence of peripheral macrophages with a reparative and phagocytic phenotype

To better elucidate the functional identity of macrophages emerging in PLX3397-Astro-A53TαSYN group, we compared their transcriptional profiles with those of infiltrating Mo/MΦ from the Astro-A53TαSYN controls. The analysis revealed a marked shift in their gene expression (Fig. 6A). PLX-MΦ exhibited robust upregulation of genes liked to M2-like and tissue-repair programs (*Arg1, Chil3, Mrc1*, *Ccl6*, *Igf1*, *Lpl*, and *Tgfb1*), together with robust induction of autophagy- and phagocytosis-related transcripts (*Lamp1*, *Cd68*, *Mfge8*, *Mertk, Anpep*, *Ctss*, *Atp6v0d2*), pointing to enhanced degradative and clearance capacity.

By contrast, Mo/MΦ from control mice exhibited higher expression of classical M1-associated pro-inflammatory mediators (*Ccl3*, *Ccl4*, *Ccl5*, *Cxcl10*, *Tnf*, *Cd40*, *Nos2*, *Stat1)* underscoring a clear functional dichotomy. PLX-MΦ preferentially adopt an anti-inflammatory, reparative phenotype, whereas control Mo/MΦ retain a pro-inflammatory signature. Flow cytometric analysis confirmed a significant reduction in MHC-II$^+$ and TNFα$^+$ myeloid cells within Mo/MΦ compartment of the PLX3397-Astro-A53TαSYN group compared with control, as well as a decrease in CD80$^+$CD86$^+$ M1 markers on this myeloid subset (Fig. S6, A-C and E). These data support the view that myeloid cells in the PLX3397 condition were skewed toward a less inflammatory state.

Interestingly, within the PLX3397 condition, the population of Mo/MΦ not belonging to the PLX-MΦ cluster appeared heterogeneous, partially expressing markers shared with PLX-MΦ (*Ccl6*, *Chil3*, *Mgll*, *Tgfb1*) as well as pro-inflammatory genes (*Cd40*, *Cd36*, *Tnf*, *Cxcl10*) similar to those found in control Mo/MΦ (Fig. 6A). To further validate the distinct identity of PLX-MΦ, we examined representative M2-like and repair-associated genes among scRNA sequencing data (Fig. 6B). UMAP plots revealed *Ear2* and *Plet1*, regulators of alternative activation, highly enriched in the PLX-MΦ cluster. Genes involved in lipid metabolism and tissue repair (*Lpl*, *Igf1*) were similarly biased toward PLX-MΦ, and the canonical M2 marker Mrc1 (CD206) was selectively expressed in this population. Mgll, a lipase linked to lipid turnover and metabolic adaptation, was also markedly upregulated, suggesting a role in reshaping the local metabolic milieu.

Flow cytometric analysis revealed an increased proportion of CD68$^+$LAMP1$^+$ infiltrating myeloid cells in PLX3397-Astro-A53TαSYN mice compared with controls (31.2% vs. 17.5%), indicating enhanced lysosomal and phagocytic activity (Fig. 6C). Immunofluorescence corroborated these findings, showing IBA1$^+$CD68$^+$ macrophages, also positive for CD13, surrounding αSYN–positive aggregates in the STR of PLX3397-treated mice (Fig. 6D-E and Fig. S6D). Notably, these infiltrating cells also expressed the macrophage maturation marker F4/80, consistent with their differentiated phenotype (Fig. S6F).

Collectively, these data demonstrate that depletion of resident microglia promotes the recruitment of infiltrating macrophages exhibiting a distinct, mature phenotype, which may contribute to the phagocytosis and clearance of αSYN-laden material within the STR milieu.

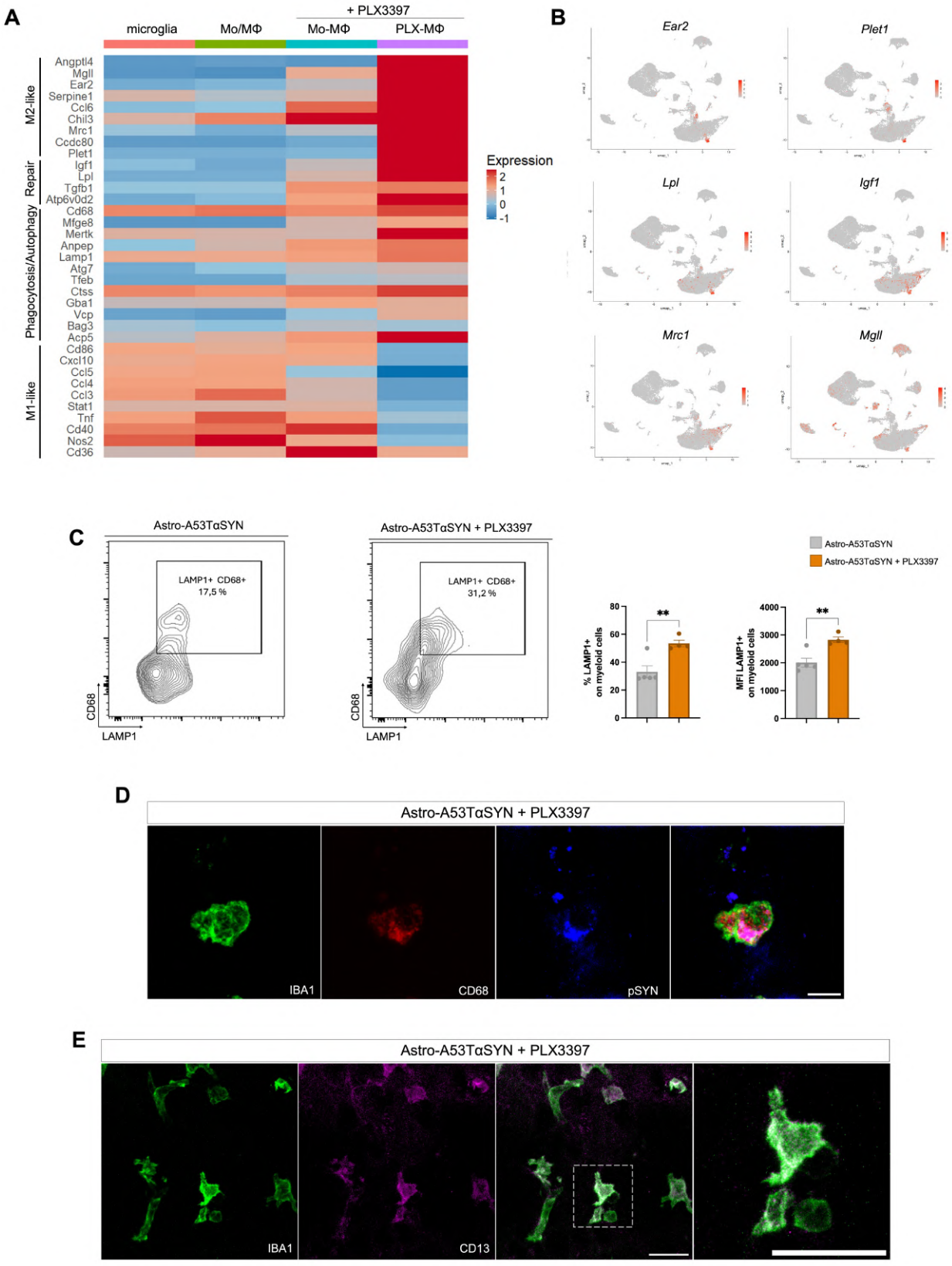

Figure 6. Monocyte-derived macrophages acquire a reparative and phagocytic phenotype following microglial depletion. (A) Heatmap of M2-like, repair-associated, phagocytosis/autophagy-related, and M1-like gene expression in microglia, Mo/MΦ, Mo/MΦ (PLX3397-treated), and PLX-MΦ cluster. **(B)** UMAP feature plots of representative PLX-MΦ M2-like and repair-associated genes (*Ear2*, *Mrc1*, *Lpl*, *Plet1*, *Igf1*, *Mgll*). **(C)** Representative FACS contour plots showing LAMP1^{+}CD68^{+} cells and quantification of LAMP1 expression in myeloid cells isolated from the striatum (STR) of LV:Astro-A53TαSYN–injected mice, with or without

PLX3397 treatment. Bar graphs show the percentage of LAMP1$^+$ myeloid cells (left) and the mean fluorescence intensity (MFI) of LAMP1$^+$ cells (right) under the two conditions. *n* = 4–5 mice per group. Data are presented as mean ± SEM. Statistical analysis was performed using an unpaired t test; *P < 0.05; **P < 0.01; ***P < 0.001; ****P < 0.0001 **(D)** Representative high-resolution confocal image showing an IBA1$^+$ cell (green) co-localizing with CD68 (red) and pSYN (blue) staining. Scale bar: 25 µm. **(E)** Representative high-resolution confocal image showing IBA1+ cells (green) co-localizing with CD13 (magenta) staining. Scale bar: 25 µm. pSYN: phosphorylated α-Synuclein; STR: striatum.

PLX-MΦ promote CD8$^+$ T-cell exhaustion through immunosuppressive pathways

Beyond their enhanced phagocytic and reparative capacity, PLX-MΦ displayed a pronounced transcriptional program of immunomodulation. To investigate the specific immunoregulatory properties of PLX-MΦ, we examined the expression of transcripts known to be linked to T cell suppression.

Heatmap analysis revealed that PLX-MΦ displayed robust induction of suppressive mediators, including *Spp1*, *Ccl6*, *Axl*, *Mrc1*, *Tgfb1*, and *Lgals9* (Fig. 7A). These genes are functionally associated with T cell inhibition, immune checkpoint engagement, and the establishment of a tolerogenic microenvironment. In contrast, infiltrating Mo/MΦ in the control group retained higher expression of M1-like pro-inflammatory mediators including *Nos2*, *Tnf*, *Ccl3*, *Ccl4*, *Ccl5*, *Cxcl10* and *Stat1*, underscoring a clear functional dichotomy between the two macrophage subsets.

Notably, within the PLX3397-treated group, we also identified monocytes/macrophages (Mo/MΦ) with a hybrid transcriptional program, partially overlapping with the PLX-MΦ signature (*Ccl6*, *Tgfb1*, *Axl*) while retaining M1-associated transcripts (*Nos2*, *Tnf*, *Ccl3*, *Cxcl10*), suggesting a transitional or mixed activation state.

Given the pronounced immunosuppressive profile of PLX-MΦ, we next asked whether these changes correlated with alterations in the T-cell population.

As we observed in scRNAseq data, flow-cytometric analysis of striatal CD45$^+$ cells confirmed a marked redistribution of lymphoid and myeloid populations upon PLX3397 treatment, with an increase in infiltrating monocytes and lymphocytes (Fig. S7, A-B). Within the lymphoid cells, PLX3397-treated mice showed a similar frequency of CD8$^+$ T cells and slightly increased in CD4$^+$ cell fraction (Fig. S7, C–E). Analysis of CD8$^+$ T cell signatures, whose identity was confirmed based on the expression of *Cd3d*, *Cd3e*, and *Cd8a/b,* revealed a strong enrichment of exhaustion-associated genes in PLX3397-treated mice (Fig. 7B). Transcripts encoding inhibitory receptors (*Pdcd1*, *Ctla4*, *Lag3*, *Tigit*) and transcriptional regulators of exhaustion (*Eomes*, *Tox*, *Prdm1*), were significantly upregulated in CD8$^+$ T cells from PLX3397-Astro-A53TαSYN mice relative to controls. Consistent with this transcriptional signature, FACS analyses confirmed a significant decrease in IFN-γ production by CD8$^+$ T cells from PLX3397-treated mice compared with controls (Fig. S7, F-G), suggesting impaired effector function.

UMAP feature plots further confirmed the contrasting transcriptional signatures of PLX3397-induced macrophages and infiltrating Mo/MΦ (Fig. 7C). Genes associated with immunosuppressive and tolerogenic activity, such as *Spp1* and *Ccl6*, were selectively enriched in the PLX-MΦ cluster, consistent with their proposed role in dampening T cell activation and promoting immune regulation.

By contrast, Mo/MΦ displayed strong expression of pro-inflammatory mediators. Nos2 was robustly expressed across this population, indicating activation of nitric oxide–dependent inflammatory pathways, while *Ccl5* was broadly distributed among infiltrating myeloid cells, in line with its role in leukocyte recruitment and amplification of neuroinflammation.

Collectively, these findings indicate that microglia depletion favours the emergence of a transcriptionally distinct macrophage population, endowed with enhanced phagocytic capacity and potent immunoregulatory features. This subset not only reshape the local immune microenvironment in α-synucleinopathy but also remodel the adaptive immune landscape by driving $CD8^+$ T cell exhaustion, suggesting a coordinated mechanism of immune suppression.

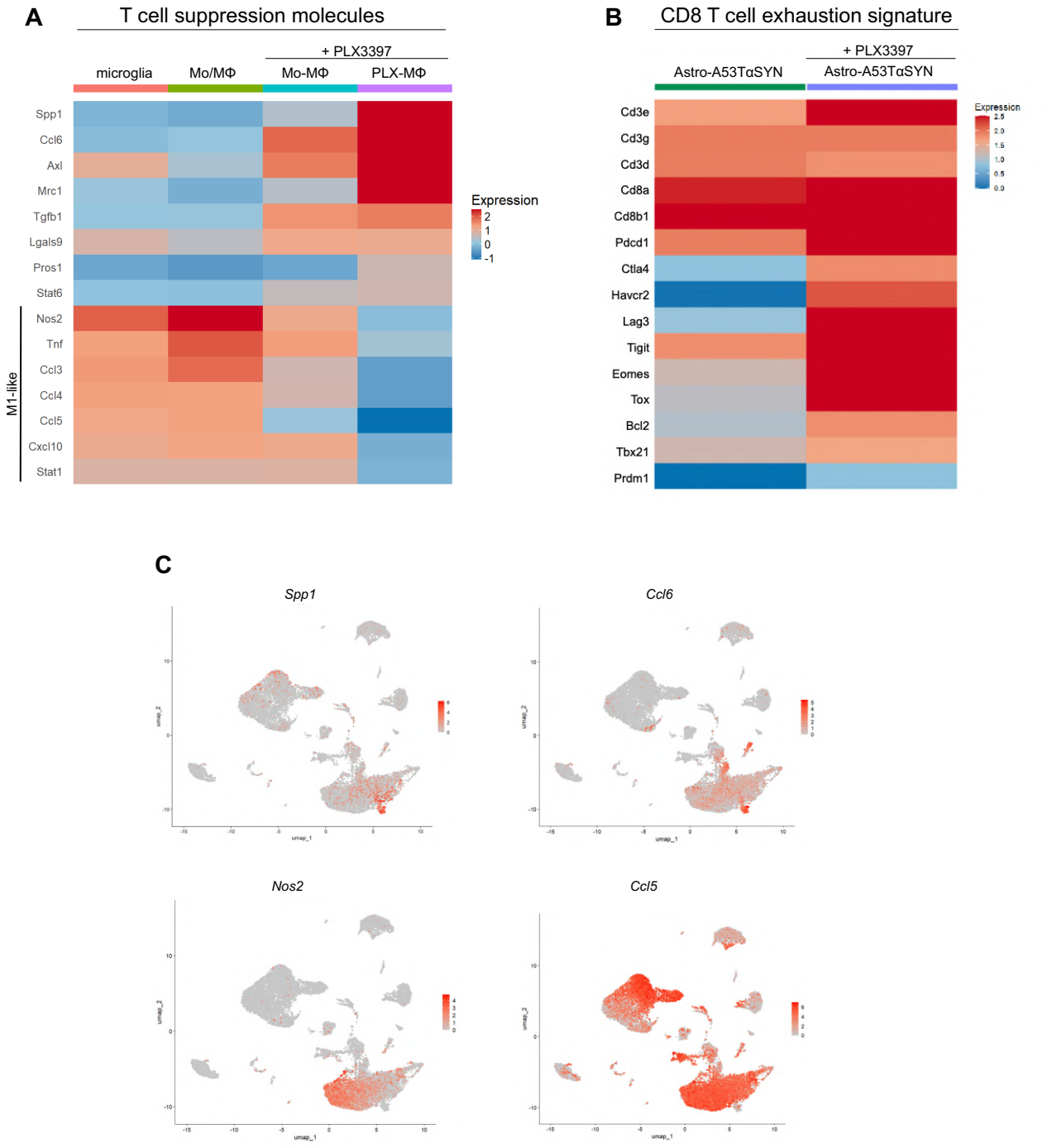

Figure 7. PLX-MΦ exhibit immunosuppressive signatures and promote CD8⁺ T cell exhaustion (A) Heatmap of T cell suppression–associated molecule gene expression in microglia, Mo/MΦ, Mo/MΦ (PLX3397-treated), and PLX-MΦ cluster. **(B)** Heatmap showing CD8⁺ T cell exhaustion gene signature in Astro-A53TαSYN compared with Astro-A53TαSYN + PLX3397 conditions. **(C)** UMAP feature plots displaying expression of representative T cell suppression genes across cell clusters.

Macrophage-mediated clearance mitigates astrocytic α-Synuclein neurotoxicity

To directly assess the functional contribution of infiltrating myeloid cells to neuroprotection, we employed *Ccr2*$^{-/-}$ mice, which lack circulating monocytes, either alone or in combination with microglia depletion using PLX3397, thereby allowing evaluation of the effects of selective or combined ablation of peripheral myeloid cells and microglia.

Previous analyses of neurodegeneration (Fig. 8, A–B) revealed a pronounced loss of TH⁺ neurons in *Aldh1l1*-CreERT2:Astro-A53TαSYN mice, representing a 31.5 ± 3.9% decrease compared with *Aldh1l1*-CreERT2:Mock controls (mean ± SEM). Microglial depletion markedly attenuated this effect, reducing the loss to 13.0 ± 2.5% in PLX3397-treated *Aldh1l1*-CreERT2:Astro-A53TαSYN mice relative to their respective controls.

In *Ccr2*$^{-/-}$ mice, TH⁺ neuronal loss reached 33.8 ± 5.9% in *Ccr2*$^{-/-}$:Astro-A53TαSYN compared with *Ccr2*$^{-/-}$:Mock (mean ± SEM). When combined with microglial depletion, neurodegeneration increased to 42.3 ± 4.3% (mean ± SEM) in PLX3397-treated *Ccr2*$^{-/-}$:Astro-A53TαSYN compared with PLX3397-treated *Ccr2*$^{-/-}$:Mock, suggesting a contribution of CCR2⁺ cells in limiting neuronal loss observed in the *Aldh1l1*-CreERT2 background mice.

pSYN staining confirmed astrocytic αSYN expression across all groups and showed that microglial depletion in *Aldh1l1*-CreERT2:Astro-A53TαSYN mice reduced the pS129αSYN burden from 14.40 ± 1.69% to 6.64 ± 0.63% relative to the corresponding PLX3397-untreated mice (mean ± SEM; Fig. 8, C–D). Similarly, the *Ccr2*$^{-/-}$:Astro-A53TαSYN group showed reduced pS129αSYN accumulation (6.02 ± 1.27% pS129αSYN occupied area); however, this decrease was accompanied by highly reactive microglial phenotype, as evidenced by elevated IBA1 levels (12.38 ± 0.93% in *Aldh1l1*-CreERT2:Astro-A53TαSYN compared with 23.20 ± 2.34% in *Ccr2*$^{-/-}$:Astro-A53TαSYN) and an 8.57-fold increase in CD68 signal (0.5 ± 0.11% in *Aldh1l1*-CreERT2:Astro-A53TαSYN compared with 4.4 ± 0.4% in *Ccr2*$^{-/-}$:Astro-A53TαSYN, mean ± SEM; Fig. S8, A–C). These data suggest that pS129αSYN levels observed in the *Ccr2*$^{-/-}$:Astro-A53TαSYN model were closely linked to an over-reactive microglial state, potentially responsible for the associated neurotoxicity.

Notably, the simultaneous loss of microglia and CCR2⁺ macrophages (PLX3397-treated *Ccr2*$^{-/-}$: Astro-A53TαSYN) resulted in a dramatic increase in pS129αSYN occupied area (27.77 ± 3.55%, mean ± SEM), underscoring the cooperative control of αSYN pathology exerted by resident and infiltrating myeloid compartments.

We next evaluated lymphocyte recruitment (Fig. S8, D–E) and found that, unlike in PLX3397-treated and untreated *Aldh1l1*-CreERT2 mice injected with LV:Astro-A53TαSYN, the absence of CCR2⁺ cells reduced T-cell infiltration. CD4+ T cells declined from 4016 ± 435 in *Aldh1l1*-CreERT2:Astro-A53TαSYN to 2651 ± 582 in *Ccr2*$^{-/-}$:Astro-A53TαSYN (34 ± 18% decrease, mean ± SEM), and CD8+

T cells dropped from 7839 ± 1147 in *Aldh1l1*-CreERT2:Astro-A53TαSYN to 5827 ± 678 in *Ccr2*$^{-}$/$^{-}$:Astro-A53TαSYN (25 ± 17% decrease, mean ± SEM), highlighting a role for CCR2^{+} macrophages in facilitating lymphocyte entry into the parenchyma.

To assess the contribution of T cells to neurodegeneration, we further employed the *Rag1*$^{-/-}$ mouse line, alone or in combination with PLX3397 treatment. In agreement with previous reports, overexpression of αSYN did not alter the number of dopaminergic neurons in the SNpc compared with controls (Fig. S9, A-C). Animals lacking T and B cells showed no neuronal loss in the presence of αSYN (3818 ± 211 TH+ cells in the Rag1$^{-/-}$:Astro-A53TαSYN compared with 3712 ± 261 in the Rag1$^{-/-}$:Mock; −2.9% ± 0.3, mean ± SEM), nor was such an effect observed in the PLX3397-treated *Rag1*$^{-/-}$ group (3719 ± 88 TH+ cells in the PLX3397-treated Rag1$^{-/-}$:Astro-A53TαSYN group compared with 3815 ± 23 in the PLX3397-treated Rag1$^{-/-}$:Mock; +2.5% ± 0.06, mean ± SEM), indicating that the absence of T cells exerts a neuroprotective effect against αSYN–induced dopaminergic loss.

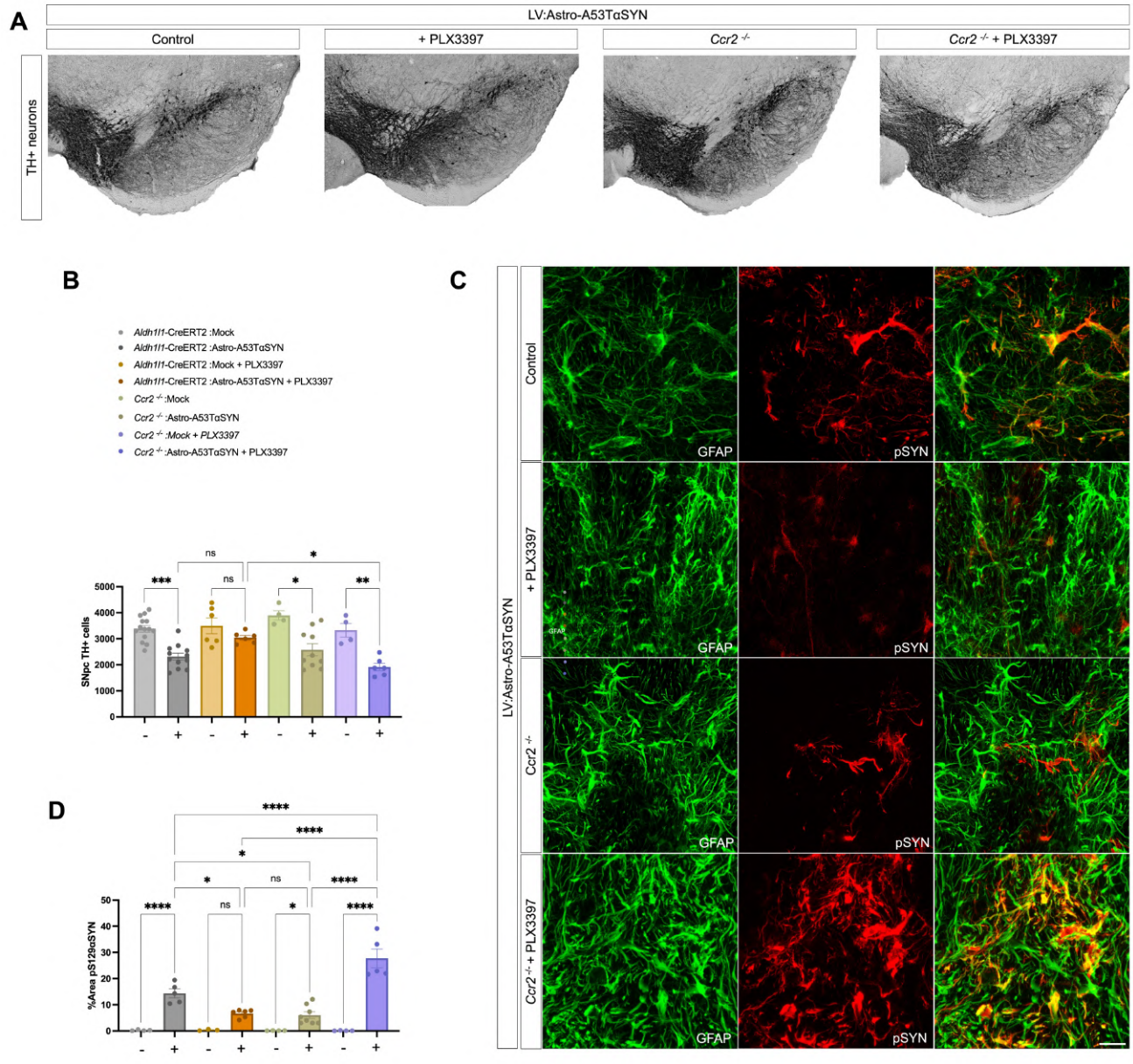

Figure 8. Impact of immune modulation on dopaminergic neurodegeneration and α-Synuclein pathology. (A) Representative immunohistochemical staining for TH in the SNpc illustrates αSYN-induced neuronal loss in *Aldh1l1*-CreERT2 (Control) and *Ccr2*$^{-/-}$ mice, with and without microglial depletion induced by PLX3397. **(B)** Unbiased stereological quantification of TH^{+} neurons in the SNpc of *Aldh1l1*-CreERT2 and *Ccr2*$^{-/-}$ mice injected with LV:Astro-A53TαSYN, with or without PLX3397 treatment. Data are expressed as mean ± SEM. Statistical analysis: two-way ANOVA followed by Tukey's multiple comparison test; *P < 0.05; **P < 0.01; ***P < 0.001; ****P < 0.0001. **(C)** Immunofluorescence analysis of the STR using astrocytic marker GFAP (green) and pS129αSYN (pSYN, red). Scale bar, 25 µm. **(D)** Quantification of pS129αSYN^{+} area in the STR across experimental groups. Data are expressed as % area ± SEM. Statistical analysis: two-way ANOVA followed by Tukey's multiple comparison test; *P < 0.05; **P < 0.01; ***P < 0.001; ****P < 0.0001. Scale bar, 25 µm. pSYN/pS129αsyn: phosphorylated α-Synuclein; STR: striatum.

In αSYN–overexpressing mice, astrocytic overexpression establishes a proinflammatory environment characterized by reactive astrocytes, activated microglia, and the recruitment of peripheral immune cells, including monocytes, macrophages and T lymphocytes. Microglial depletion with the CSF1R inhibitor PLX3397 profoundly altered this landscape, favouring the infiltration of highly phagocytic macrophages (PLX-MΦ) and a shift in T cells toward an exhausted phenotype. Notably, these changes coincided with reduced neuronal loss, suggesting that replacement of inflammatory microglia by macrophages and the attenuation of T-cell effector functions collectively promote neuronal survival. Together, these data support a model in which microglial ablation reshapes αSYN–driven neuroinflammation and mitigates its neurotoxic consequences (Fig. 9A).

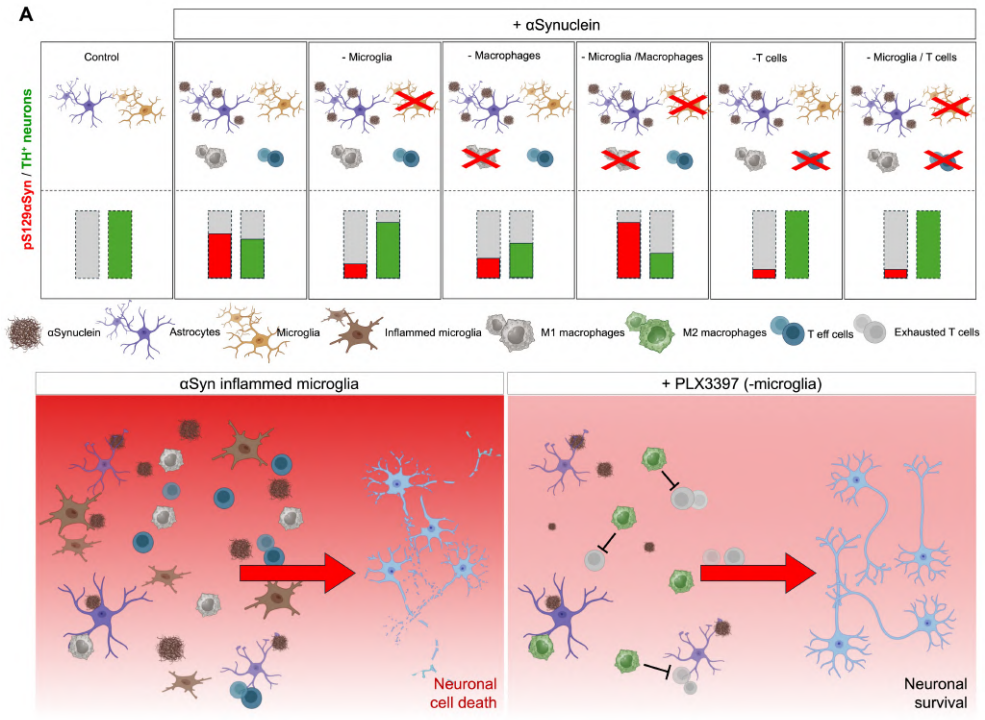

Figure 9. PLX-MΦ reshape the inflammatory environment to promote neuronal survival. Proposed mechanism schematic: Astrocytic αSYN overexpression establishes an inflammatory milieu characterized by reactive astrocytes, activated microglia, and immune cell infiltration. Upon microglial depletion with PLX3397, this environment is reshaped by the recruitment of highly phagocytic macrophages and the conversion of T cells into an exhausted state, ultimately promoting neuronal survival.

Discussion

In this study we demonstrate that pharmacological inhibition of CSF1R with PLX3397 does not merely deplete resident microglia but triggers the emergence of a reparative macrophage population, which we define as PLX-MΦ. These cells represent a novel immune entity with bifunctional properties of major relevance for α-synucleinopathies.

Our findings reveal that PLX-MΦ operate along two synergistic axes. On one hand, they act as potent proteostatic effectors endowed with an enhanced phagolysosomal machinery capable of efficiently degrading αSYN aggregates, reducing astrocytic pathology, and protecting dopaminergic neurons. On the other hand, they qualitatively modulate adaptive immunity by imposing a program of functional exhaustion on $CD8^+$ T cells, a process that in our model translates into additional neuroprotection. The identification of this population, not previously described in an astrocyte-driven context of synucleinopathy, constitutes the main novelty of our study and opens avenues for therapeutic strategies based on engineering macrophages with PLX-like phenotypes.

This discovery builds on an expanding body of literature on CSF1R inhibition as a means to manipulate microglia. Pioneering studies with PLX3397 (Elmore et al., 2014) and later with the more selective PLX5622 (Spangenberg et al., 2016) demonstrated that microglial depletion can be achieved rapidly and reversibly, providing a powerful pharmacological tool to probe microglial function in health and disease. In Alzheimer's disease models, Sosna et al. (2018) showed that early and sustained microglial ablation reduced intraneuronal Aβ accumulation, neuritic plaque formation, and soluble amyloid oligomers, resulting in improved cognitive performance, whereas late interventions were less effective. Similarly, Spangenberg et al. (2019) observed that sustained depletion with PLX5622 completely prevented parenchymal plaques formation, suggesting that amyloid deposition critically depends on microglial presence. Other studies revealed additional complexity: Unger et al. (2018) reported incomplete depletion and persistence of resistant cells around plaques in APP/PS1 mice, raising the possibility of peripheral cell involvement. More recently, Zhang et al. (2025) demonstrated in a PD mouse model induced by αSYN overexpression that microglia depletion attenuated dopaminergic neurodegeneration, reduced αSYN pathology, and remodelled the extracellular matrix. Overall, these findings suggest that CSF1R inhibition reproducibly reduces pathological protein aggregates, but do not clarify whether the benefit stems solely from the absence of resident microglia or also from active contributions of infiltrating myeloid cells.

Our work directly addresses this gap by employing a model of astrocytic αSYN accumulation, thereby isolating a context in which microglia are not the primary drivers of pathology and allowing us to dissect the effects of infiltrating cells.

PLX-MΦ differ from both resident microglia and the $CCR2^+$ macrophages that typically infiltrate brains with intact, reactive microglia. Although border-associated macrophages (BAMs) are known to contribute to neuroinflammatory responses in neurodegenerative models (Schonhoff et al., 2023; Sun et al., 2024), the cells described here display distinct transcriptional and functional hallmarks that support their autonomous identity.

At the transcriptomic level, PLX-MΦ exhibit a coordinated upregulation of genes linked to phagolysosomal function and proteostasis (*Lamp1*, *Cd68*, *Ctss*, *Mertk*, *Mfge8*), together with a reparative program defined by *Arg1*, *Chil3*, *Mrc1*, *Ccl6*, *Igf1*, *Lpl*, and *Tgfb1*. This integrated signature distinguishes them from pro-inflammatory M1-like macrophages in the control group, which express *Nos2*, *Tnf*, and chemokines such as *Ccl3*, *Ccl4*, and *Cxcl10* (Orecchioni et al., 2019; Chen et al., 2023). Such polarization indicates a shift toward anti-inflammatory and regenerative pathways, coupling degradative efficiency with tissue-repair capacity.

Within the PLX3397-treated group, a remaining heterogeneous Mo/MΦ population was also detected, partially expressing PLX-MΦ markers (*Ccl6*, *Chil3*, *Mgll*, *Tgfb1*) while retaining inflammatory transcripts (*Cd40*, *Cd36*, *Tnf*, *Cxcl10*). This hybrid subset likely represents a transitional state along the inflammatory-to-reparative continuum induced by CSF1R inhibition. In contrast, PLX-MΦ themselves maintain a coherent identity characterized by sustained lysosomal activation and immunomodulatory balance.

Consistent with these transcriptional and functional features, experiments in *Ccr2*$^{-/-}$ mice supported a contributory role of infiltrating macrophages in neuroprotection. Although TH^{+} neuronal loss in *Ccr2*$^{-/-}$:Astro-A53TαSYN mice was variable and did not reach statistical significance when compared with the *Aldh1l1*-CreERT2:Astro-A53TαSYN group, a clear exacerbation of neurodegeneration was observed when microglial depletion was combined with *Ccr2* deficiency. In this context, the concurrent loss of resident microglia and infiltrating macrophages led to increased pS129αSYN accumulation, consistent with the role of both cell populations in αSYN clearance. Moreover, the more pronounced neuronal loss observed in PLX3397-treated *Ccr2*$^{-/-}$:Astro-A53TαSYN mice compared with PLX3397-treated *Aldh1l1*-CreERT2:Astro-A53TαSYN indicates that infiltrating macrophages, rather than microglia, are the key mediators of the neuroprotective effect.

Functionally, PLX-MΦ emerge as genuine “proteostasis machines.” Their robust lysosomal machinery enables efficient degradation of toxic αSYN aggregates, leading to reduced astrocytic pathology and protection of dopaminergic neurons. These features define PLX-MΦ as a macrophage population in which degradative competence and reparative programming converge to restore homeostasis in the inflamed brain.

Alongside their proteostatic capacity, PLX-MΦ reveal an additional immunoregulatory facet, suggesting a broader role in maintaining immune homeostasis. PLX-MΦ impose a state of functional exhaustion on CD8^{+} T cells, characterized by *Pd1*, *Lag3*, *Tigit*, and *Tox* expression together with reduced IFN-γ production, sustained by macrophage-derived *Spp1*, *Lgals9*, and *Tgfβ1*. While T-cell exhaustion is generally detrimental in oncology, in which tumor-associated macrophages (TAMs) have been shown to drive CD8^{+} T cells into terminal exhaustion and thereby limit anti-tumor immunity (Kersten et al., 2022; Polania et al., 2025), in the brain the same principle acquires protective meaning by reducing cytotoxic damage while maintaining minimal surveillance compatible with neuronal integrity. This reversal of perspective suggests that T-cell exhaustion is not intrinsically pathological, but rather reflects a context-dependent adaptation of the immune system. In chronic inflammatory and autoimmune settings, including multiple sclerosis, features of T-cell exhaustion

have been proposed to limit excessive immune activation and may thus play a protective role (McLane et al., 2019).

Consistent with this concept, genetic models provide further support. In *Rag*1$^{-/-}$ mice, the absence of lymphocytes confers neuroprotection, consistent with CD8-mediated cytotoxicity playing a causal role. Indeed, CD8^{+} T cells can exert direct neurotoxic effects through release of IFN-γ, granzymes and perforin, mechanisms that compromise neuronal integrity and promote axonal degeneration. In several preclinical models, infiltration of cytotoxic CD8^{+} T cells into the brain correlates with dopaminergic neuronal loss and exacerbated αSYN pathology, underscoring the importance of immune regulation for neuronal survival (Galiano-Landeira et al., 2020; Zhang et al., 2023).

In line with this, the *Ccr2*$^{-/-}$ mouse model also enabled us to assess the contribution of these cells to the maintenance of T cells within the brain parenchyma (Schonhoff et al., 2023). Notably, regardless of PLX3397 treatment, a reduction in lymphocytic infiltration was observed in the αSYN-laden brain, which may explain why neurodegeneration in this model was less severe than expected, potentially due to limited immune cell recruitment.

These observations converge into a unified model that we define as the clearance–exhaustion axis. In the presence of astrocytic αSYN, A1-like astrocytes recruit CCR2^{+} macrophages and T cells. When microglia remain intact and reactive, pro-inflammatory modules dominate, clearance efficiency is suboptimal, and microglia progressively undergo functional exhaustion, resulting in phosphorylated αSYN accumulation and dopaminergic vulnerability. In contrast, microglial ablation reshapes the niche in favour of PLX-MΦ, which combine high lysosomal activity with immunoregulatory mediators and, in turn, impose functional exhaustion on CD8^{+} T cells, thereby reducing proteotoxic stress and neuronal loss.

However, when CCR2-dependent compensation is prevented, microglial reactivity increases and neurodegeneration accelerates, underscoring that the benefit arises from a qualitative reorganization of immune activity that maximizes proteostasis while limiting immune-mediated neuronal injury.

This conceptual framework also helps reconcile findings in other disorders. In Alzheimer's disease models, microglial depletion has been shown to reduce amyloid burden and facilitate the recruitment of peripheral myeloid cells (Spangenberg et al., 2019; Sosna et al., 2018; Unger et al., 2018), while in experimental stroke it has been specifically associated with the infiltration of GPNMB^{+}/CD63^{+} macrophages that promote remyelination and functional recovery (Zhang et al., 2025).

Overall, these observations suggest that the replacement of resident reactive microglia with reparative macrophages may constitute a protective mechanism shared across multiple neuropathologies. Our findings expand this concept to include αSYN pathology and indicate that CSF1R targeting, followed by the recruitment of reparative macrophages, could represent a strategy generalizable to different forms of neurodegeneration.

The translational implications are substantial. Pharmacological strategies capable of directing monocytes and macrophages toward a PLX-like phenotype could enhance aggregate clearance without triggering detrimental inflammation. Even more promising is the idea of ex vivo engineering macrophages using CAR-macrophage (CAR-M) platforms, which have already been shown to be feasible and therapeutically effective in oncology (Klichinsky et al., 2020). Building on this concept,

one could envision strategies to enhance lysosomal and autophagic pathways, for example through TFEB-driven lysosomal biogenesis, which has been demonstrated to boost degradative capacity in macrophages (Sergin et al., 2017; Fang et al., 2017). In parallel, phagocytic efficiency and efferocytosis could be reinforced by overexpressing receptors and bridging opsonins such as MerTK and MFGE8, both key regulators of apoptotic-cell clearance and anti-inflammatory signalling (de Couto et al., 2019; Tsai et al., 2021). Finally, the immunoregulatory arm could be strengthened by programming macrophages to release checkpoint ligands and immunosuppressive mediators such as Galectin-9 (LGALS9) and TGF-β1, both implicated in driving T-cell exhaustion and immune tolerance in chronic inflammation and cancer (Okoye et al., 2020; Wang et al., 2023).

Once reintroduced, such macrophages could act as bifunctional nodes capable of reducing protein burden and, at the same time, modulating T cells through local checkpoint mechanisms. In this perspective, CAR-macrophages could be reformulated for neuroprotection rather than cytotoxicity. Instead of pro-inflammatory, tumour-oriented CAR-M, a neuroprotective design would couple high phagocytic capacity with the induction of T-cell exhaustion and the controlled release of anti-inflammatory mediators (Bido et al., 2024) to contain bystander injury.

We nevertheless acknowledge important limitations. Our model is based on astrocytic overexpression of αSYN and does not fully capture human pathology, where neurons are the principal source and both astrocytes and microglia shape the extracellular αSYN burden through uptake and (dys)clearance. This choice was deliberate, aimed at isolating the intrinsic contribution of astrocytes and testing whether they can act as independent drivers of protein accumulation and immune remodelling. Post-mortem studies have consistently documented astrocytic αSYN inclusions astrocytes (Wakabayashi et al., 2000; Braak & Del Tredici, 2008; Lee et al., 2008), but their functional significance remained uncertain: our data fill this gap by demonstrating that striatal astrocytic αSYN accumulation is sufficient to induce widespread neuroinflammation, immune recruitment, and dopaminergic neuron loss, consistent with a dying-back process in which axonal and synaptic pathology precedes neuronal soma degeneration (Dauer and Przedborski, 2003; Ozoran et al., 2023). It remains to be clarified how different cellular sources of αSYN interact in human pathology, and to what extent cooperation or competition between neurons and astrocytes shapes protein propagation, immune responses, and neurodegeneration. Validation in combined models and human systems (patient-derived cells, organoids, humanized brains) will be essential to translate these observations into therapeutic strategies. Furthermore, the long-term stability of the PLX-MΦ phenotype and its persistence in the chronically diseased brain remain open questions. A key next step is to test whether short-course or low-dose PLX3397 can permit sufficient niche remodelling to allow PLX-MΦ to enter and persist while preserving baseline microglia, or whether alternative entry/differentiation routes, such as chemokine-guided trafficking, local delivery of differentiation cues, or ex vivo–engineered macrophages, can recruit and instruct human monocytes to adopt PLX-like states without systemic risks. In conclusion, we identify PLX-MΦ as a macrophage population capable of integrating proteostatic and immunoregulatory functions into a single trajectory. This discovery shifts the therapeutic paradigm: not microglia as the primary target, but reprogrammed macrophages as bifunctional agents, capable of containing αSYN aggregates while

modulating adaptive immunity in a neuroprotective direction. The clearance–exhaustion axis we describe provides a unifying key to interpret the effects of CSF1R inhibition across neurodegenerative models and paves the way for macrophage-centered immunotherapy strategies in synucleinopathies and beyond.

Materials and Methods

Viral vector and lentiviruses production

A third-generation lentiviral backbone with a constitutive Ef1α promoter was used for vector construction. In the LV:Astro-A53TαSYN construct and its relative control, gene expression was triggered upon flipping of the αSYN gene in a sense orientation relative to the upstream promoter. This Cre-dependent lentiviral construct contained the human *SNCA*^{A53T} gene under the control of the Ef1α promoter; the WPRE element was included to enhance transcript stability and expression efficiency. In the viral construct based on the microRNA detargeting strategy, the miRT cassette contained four tandem repeats of target sequences for three distinct microRNAs (miR-124, neuron-specific; miR-223, microglia-specific; miR-338, oligodendrocyte-specific), thereby restricting αSYN expression selectively to astrocytes.

To initially validate cell-type specificity, the green fluorescent protein (GFP) was inserted upstream of the miRT sequence as a reporter. The GFP sequence was later replaced with the coding sequence of the human SNCA^{A53T} mutant.

Lentiviral particles (LVs) were produced in 293T cells, packaging replication-incompetent virions pseudotyped with vesicular stomatitis virus glycoprotein (VSVg). Briefly, 7.5 × 10^6 293T cells were plated in a 150 mm Petri dish one day prior to transfection. Cells were transfected using the standard calcium chloride ($CaCl_2$) protocol. After 30 hours, the culture medium was collected, filtered through a 0.44 µm cellulose acetate filter, and centrifuged at 50,000 × g for 2 hours at 20 °C to obtain highly concentrated lentiviral preparations.

Animals

Eight-week-old male B6;FVB-Tg(*Aldh1l1*-Cre/ERT2)1Khakh/J, B6.129S4-Ccr2tm1Ifc/J (*Ccr2* knock-out), B6.129(Cg)-Cx3cr1tm1Litt Ccr2tm2.1Ifc/JernJ (Ccr2-RFP/Cx3cr1-GFP) and *Rag1*tm1Mom (*Rag1* knock-out) mice were purchased from Jackson Laboratories. Upon arrival, the mice were housed at the San Raffaele Hospital animal facility. The mouse lines, originally maintained on mixed genetic backgrounds (B6;129 or B6;FVB), were crossed with C57BL/6N mice at our facility, and homozygous animals for the targeted allele were selected for experiments. They were maintained under a 12 hours dark-light cycle, with controlled temperature (25 °C) and relative humidity (50–60%) and with free access to food and water. Animals subjected to chronic treatment with Pexidartinib (PLX3397) were fed with 3 grams/day of PLX3397 660 ppm diet until sacrifice. All experiments were performed in accordance with protocols approved by the internal Institutional Animal Care and Use Committee (IACUC, Ospedale San Raffaele mouse facility, Milan, Italy) and reported to the Italian Ministry of Health according to the European Commission Council Directive 2010/63/EU.

Surgery

The surgical procedure was performed under isoflurane anaesthesia, ensuring that mice were adequately anesthetized throughout the surgery. Lentiviral vectors (LVs) were bilaterally injected into the striatum (STR) at the following coordinates: anterior–posterior (AP) = −0.5 mm, medio–lateral (ML) = ±1.8 mm from bregma, and dorso–ventral (DV) = −3.27 mm from the skull surface. A volume of 3 µL of LVs was delivered to each hemisphere at a controlled flow rate of 0.5 µL/min.

Immunostaining analysis

Mice were perfused transcardially with freshly prepared 4% paraformaldehyde (PFA) in phosphate-buffered saline (PBS). Brains were collected and post-fixed overnight at 4 °C. Subsequently, brains were cryoprotected in 20% sucrose in PBS, flash-frozen, and sectioned at 50 µm thickness using a cryostat. For immunofluorescence analysis, free-floating sections were permeabilized for 10 min in

a solution containing 3% H_2O_2 and 10% methanol in PBS, followed by 20 min in 2% Triton X-100. After three washes in PBS, sections were incubated for 1 h in blocking solution containing 3% bovine serum albumin (BSA) and 0.3% Tween-20 to prevent nonspecific binding. Sections were then incubated overnight at 4 °C with the primary antibody diluted in blocking buffer (1% BSA and 0.1% Tween-20). The following day, after three PBS washes, sections were incubated for 1 h in the dark with the appropriate fluorophore-conjugated secondary antibody and then mounted for imaging.
For immunohistochemical analysis, after overnight incubation with the primary antibody, sections were incubated with a biotinylated secondary antibody, followed by the avidin–biotin complex (ABC) reagent (Vector Laboratories, Cat. PK-6100) and developed using a DAB substrate kit (Vector Laboratories, Cat. SK-4100). Details of the antibodies used in this study, including their dilutions and catalogue numbers, are provided in Supplementary Table 1 of the Supplementary Material.

Acquisition and quantification of immunofluorescent images

The immunofluorescence images were acquired with Leica TCS SP8 confocal microscope by using x40 or x63 magnification lens. Wide-field images were obtained with Mavig RS-G4 confocal microscope. Images were processed by using ImageJ software through blinded assignment of a fixed signal threshold for each experimental setup. The measurements were conducted with automated analysis run by dedicated macros. To measure the signal colocalization we use JACoP Imagej plugin to calculate the Mander's coefficient. The degree of the overlapping signals has been determined by using a fixed threshold values for both channels. The Mander's coefficient ranges between 1, total correlation, and 0, representing a random distribution.

Base scope

Mice were perfused with 4% paraformaldehyde (PFA), and brains were post-fixed overnight at 4 °C, cryoprotected in sucrose, divided into hemispheres, embedded in OCT, and stored at −80 °C. Cryosections (10 µm) were mounted on SuperFrost™ slides, fixed in 4% PFA, dehydrated, treated with H_2O_2, and subjected to antigen retrieval (RNAscope™ 1× Target Retrieval Reagent, 99 °C, 8 min) and permeabilization (RNAscope™ Manual Pretreat Pro, 30 min, 40 °C).
SNCA transcripts were detected using the BaseScope™ probe BA-Hs-SNCA-No-XMm-2zz-st, with BA-Hs-PPIB-3zz and BA-DapB-3zz as positive and negative controls. Hybridization was performed for 2 h at 40 °C. Signal amplification and detection were carried out with the BaseScope™ Detection Reagent Kit v2 – RED, with two modifications: the seventh amplification step (20 min instead of 30) and red chromogen incubation (4 min instead of 10). Sections were then processed for immunofluorescence according to the RNAscope™ Multiplex Fluorescent v2 Assay protocol.

Stereological cell counting

A series of five SNpc slices, each 50 µm thick, were collected at regular intervals of 200 µm and stained for Tyrosine Hydroxylase (TH). In parallel, for the striatum (STR), a series of six slices with a thickness of 50 µm was selected at regular intervals of 300 µm and stained for Tyrosine Hydroxylase (TH), CD3 epsilon subunit of the T-cell receptor complex (CD3), CD4 antigen (CD4), CD8 antigen alpha chain (CD8a), or ionized calcium binding adaptor molecule 1 (Iba1). Unbiased stereological cell counting was performed using a Leica DM400B motorized microscope equipped with Stereo Investigator software (MBF Bioscience) at 40x magnification. The optical fractionator probe was applied to obtain precise estimates of the total number of TH^+ cells in the SNpc and $CD3^+$, $CD4^+$, $CD8a^+$, or $Iba1^+$ cells in the STR.

Real-Time PCR

Total RNA was isolated from cells using TRI reagent (Merck) according to the manufacturer's protocol. Then, RNA was reverse transcribed in cDNA with ImProm-II Reverse Transcription System (Promega). The Real Time PCR was performed with custom- designed oligos (Supplementary table 2 in supplementary material section) using Titan HotTaq EvaGreen qPCR Mix (BioAtlas). Expression levels were normalized respect to 18S expression and results were reported as the 2−ΔCt.

FACS analysis

Striatal tissue was collected, the samples were dissociated using the *Adult Brain Dissociation Kit* and the gentleMACS Octo Dissociator with Heaters (Miltenyi Biotec) according to the manufacturer's instructions while omitting the red blood cell lysis step, cells were stained with a Live/Dead viability dye in PBS for 15 min at room temperature (RT), washed with PBS supplemented with 2% FBS (PBS-FACS) and incubated with antibodies against CD68, CD80, CD86, LAMP1, CD3, CD4, CD8, CD45, CD11b and CD25 (antibodies and dilutions in supplementary table 3 in supplementary material section), surface staining was performed for 15 min at RT in the dark, cells were then fixed with 1% PFA in PBS-FACS or permeabilized using the manufacturer's instructions when required for intracellular targets, after washing and centrifugation at 1500 rpm for 5 min the samples were acquired and analysed using *FlowJo v10*(TreeStar).

Bulk-RNA sequencing and bioinformatic analysis

Six weeks after LV injection, mice were perfused transcardially with cold saline, and brains were collected for cell isolation. The striatal region was manually dissected on ice and immediately dissociated using the Adult Brain Dissociation Kit with gentleMACS Octo Dissociator with Heaters (Miltenyi Biotec), according to the manufacturer's instructions. After debris removal, astrocytes of interest were isolated by magnetic separation by Anti-ACSA-2 MicroBead Kit (Miltenyi Biotec, cat. no. 130-097-679) according to manufacturer's instructions.Purified astrocytes were subsequently lysed in Nucleozol (macherey-nagel; Ref: 740400.250) for the RNA extraction. RNA quality was assessed by using a Tape Station instrument (Agilent). To avoid over-representation of 3'ends, only high-quality RNA with a RNA Integrity Number (RIN) ≥ 8 was used. RNA was processed according to the TruSeq Stranded mRNA Library Prep Kit protocol. The libraries were sequenced on an Illumina HiSeq *3000* (controllare nelle mail per sicurezza) with 150bp paired-end reads using Illumina TruSeq technology. Image processing and basecall was performed using the Illumina Real Time Analysis Software. Paired-end RNA-seq reads were assessed with FastQC and trimmed with Trimmomatic v0.39 to remove adapters and low-quality bases, ensuring high-quality reads for downstream analysis. Clean reads were aligned to the mouse reference genome (GRCm38.p6, UCSC mm10) using STAR v2.5.3a, and gene-level counts were generated with featureCounts v1.6.4. Downstream analyses were performed in R. Read counts were normalized and differential expression was tested with DESeq2 (Wald test; Benjamini–Hochberg adjustment). Genes with |log2 fold change| ≥ 1 and FDR < 0.05 were considered differentially expressed (DEGs). Results were visualized through an MA plot to highlight DEGs and a Principal Component Analysis (PCA) performed on the 500 most highly variable genes to assess sample clustering and variability. Gene Ontology (GO) over-representation analysis of significant DEGs was performed with the clusterProfiler package and summarized with custom R code. Additional statistical visualizations, such as heatmaps and other graphical outputs, were generated in R.

Single-cell RNA sequencing

Mice were perfused transcardially with cold saline, and brains were rapidly extracted. The striatal region was manually dissected on ice and immediately processed for single-cell isolation. Tissue was dissociated using the Adult Brain Dissociation Kit with gentleMACS Octo Dissociator with Heaters (Miltenyi Biotec), following the manufacturer's protocol. Cell suspensions were first stained with Live/Dead Nir (Thermofisher, cat no. L34994) to exclude dead cells, followed by incubation with anti-CD45 (BD Biosciences, cat. no. 563890) and CD11b (Thermofisher, cat no. 12-0112-83). $CD45^+$ cells were sorted on MACSQuant Tyto Cell Sorter (Miltenyi Biotec) and collected in PBS containing 0.04% BSA for downstream processing. Single-cell suspensions were encapsulated in droplets using the Chromium Single Cell 3′ Solution v3.0 (10x Genomics), and cDNA libraries were prepared according to the manufacturer's Single Cell 3′ Reagent Kits User Guide (v3.0). Libraries were sequenced on a NovaSeq 6000 system (Illumina) at a minimum depth of 50,000 reads per cell.

Bioinformatics analysis Single-cell RNA sequencing

Sequencing quality was assessed using FastQC v0.12.1 (Andrews, 2010), and results were aggregated with MultiQC v1.28 (Ewels et al., 2016). Raw reads were aligned, gene expression quantified, and cell barcodes called using Cell Ranger v9.0.1 from 10X Genomics (Zheng et al., 2017), mapping to the Mm39 reference genome annotated with Gencode M37 (Mudge et al., 2025), supplemented with the human *SNCA* gene. Across the two samples, 71% of reads were confidently mapped to the genome. Downstream analysis was carried out using Seurat v5.2.0 in R (Hao et al., 2024). Samples were processed separately before integration. Low-quality cells were removed by filtering out those with <500 features or <500 UMI counts, as well as cells with >5000 features to exclude potential multiplets. Cells with mitochondrial gene content >15% were also excluded. After filtering, 9347 and 9194 cells remained in the Astro-A53TαSYN and PLX3397-Astro-A53TαSYN samples, respectively.

Data were log-normalized, and the top 2000 variable genes were selected using the VST method. The data were then scaled and subjected to Principal Component Analysis (PCA). Based on the elbow plot, the top 20 principal components were used for downstream analysis. Integration was performed using the Robust PCA (RPCA) approach. Unsupervised clustering was applied using the shared nearest neighbor method via Seurat's *FindNeighbours* and *FindClusters* functions at a resolution of 2.2. Clusters were visualized with UMAP.

Marker genes were identified using *FindAllMarkers* and *FindMarkers* (Wilcoxon test). Cell-cell communication analysis was conducted using CellChat v2 (Jin et al., 2025), following the comparative workflow and excluding endothelial cells unique to the PLX3397-Astro-A53TαSYN sample. Communication probabilities and centrality scores were inferred, with condition differences tested using a paired Wilcoxon test.

Supplementary materials

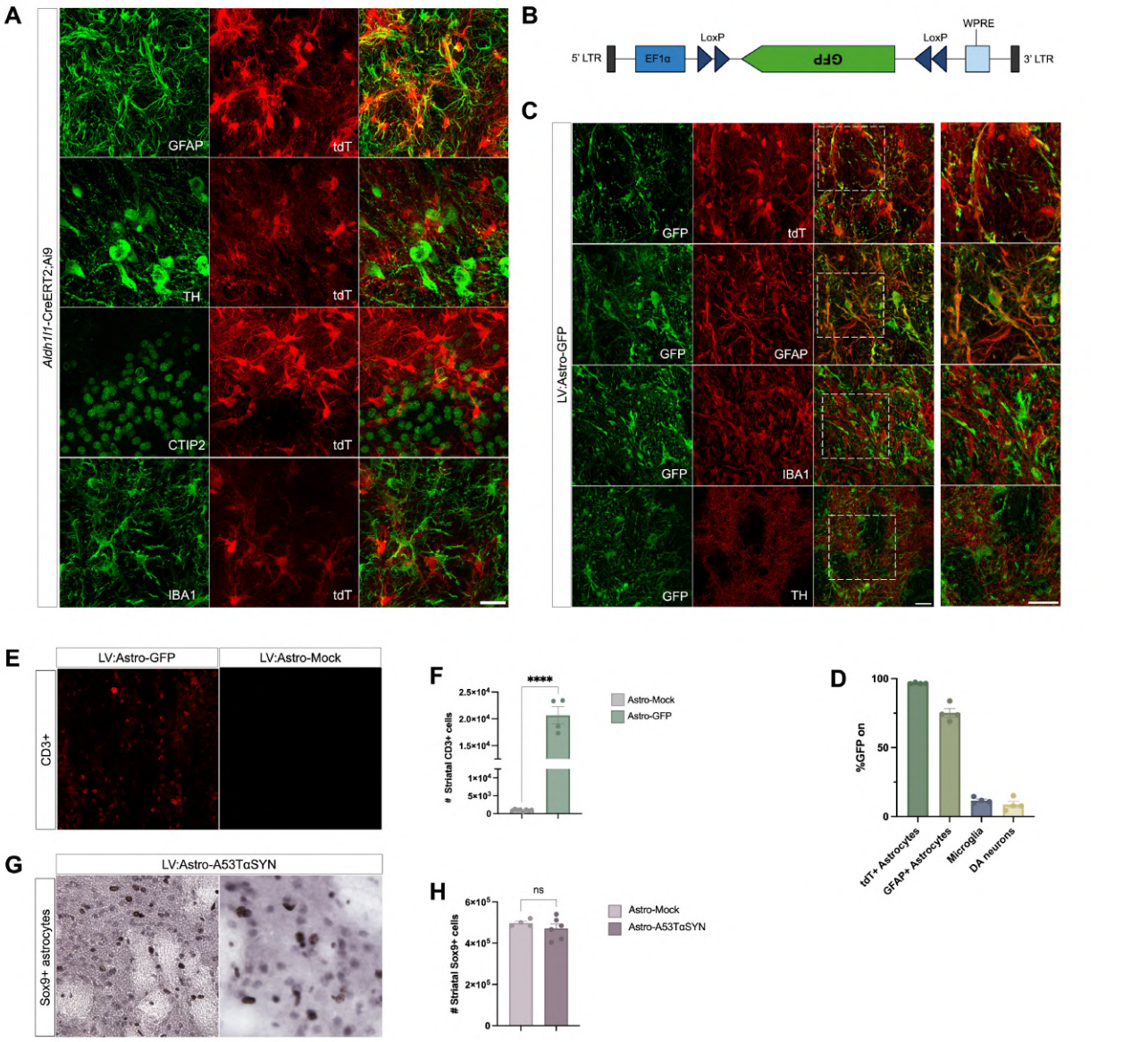

Figure S1. Characterization and validation of LV:Astro constructs in the mouse striatum.
(A) Representative immunofluorescence images showing GFP⁺ cells (green) co-stained with astrocytic (GFAP), neuronal (TH, CTIP2) and microglial (IBA1) markers (red) in striatal sections of Aldh1l1-CreERT2; Ai9 mice. Merged channel (right) demonstrate specific co-localization of astrocytic markers (GFAP⁺) with tdT+ cells. Scale bar: 25 µm. **(C)** Confocal images of striatal sections showing colocalization of GFP with astrocytic (tdT, GFAP), microglial (IBA1) and neuronal (TH) markers. Right panels: magnified views of the dashed boxes. Scale bar: 25 µm. **(D)** Percentage of GFP⁺ cells expressing astrocytic, microglial or neuronal markers. Quantification showing preferential targeting of astrocytes. Values are expressed as %MOC ± SEM (Mander's Overlap Coefficient, MOC). **(E)** Immunofluorescence for CD3 in striatal sections of mice injected with LV:Astro-GFP or LV:Astro-Mock (6 w.p.i). Scale bar: 25 µm. **(F)** Unbiased stereological count of striatal CD3+ cells in LV:Astro-GFP or LV:Astro-Mock injected mice. Data are expressed as mean ± SEM. Statistical analysis: Unpaired t test; *P < 0.05; **P < 0.01; ***P < 0.001; ****P < 0.0001. **(G)** Representative immunohistochemistry image for Sox9 in striatal sections following LV:Astro-A53TαSYN injection (n= 4-6 striata) **(H)** Unbiased stereological count of Sox9+ cells in the striatum of LV:Astro-A53TαSYN- and control-injected mice. Statistical analysis: Unpaired t test; *P < 0.05; **P < 0.01; ***P < 0.001; ****P < 0.0001.

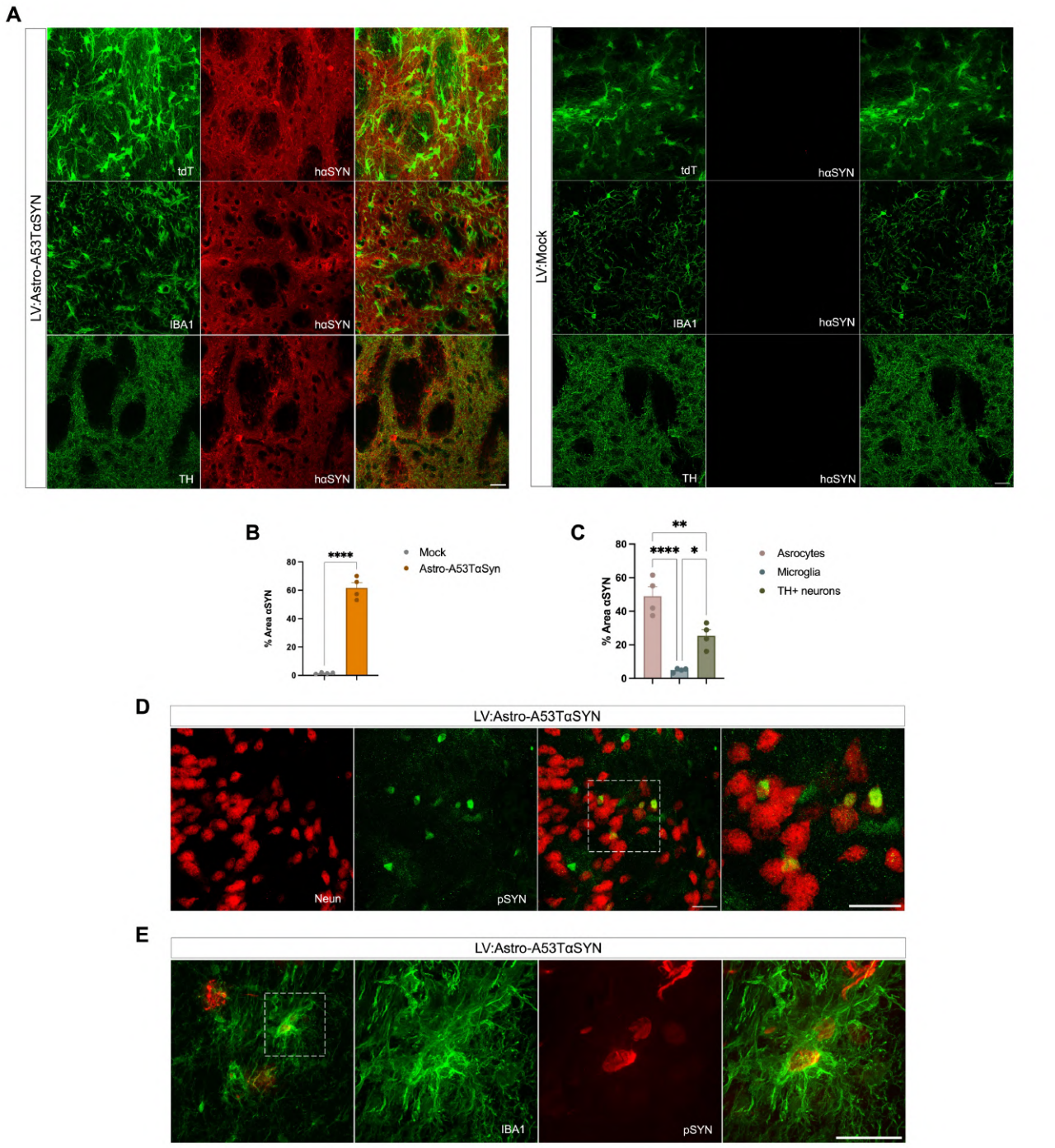

Figure S2. Cell-type specific accumulation of α-Synuclein following astrocytic A53T over-expression. **(A)** Representative immunofluorescence images of striatal section of LV:Astro-A53TαSYN-injected mice, stained for hαSYN (red) together with tdT, used as astrocytic reporter, IBA1, a microglial marker, and TH, a marker of dopaminergic neurons (green); areas where the signals overlap appears yellow in the merged images. Scale bar: 25μm. **(B)** Occupied area of hαSYN staining in the STR across the different experimental conditions. *n* = 4 striata. Data are expressed as % area ± SEM. Statistical analysis: Unpaired t test; *P < 0.05; **P < 0.01; ***P < 0.001; ****P < 0.0001. **(C)** Quantitative assessment of the percentage of hαSYN+ cells colocalizing with GFAP, IBA1 and TH. *n* = 3 independent experiments. Values are expressed as %MOC ± SEM (Mander's Overlap Coefficient, MOC). Statistical analysis: one-way ANOVA followed by Tukey's multiple comparison test; *P < 0.05; **P < 0.01; ***P < 0.001; ****P < 0.0001. **(D)** High resolution representative immunostaining for NeuN (red) and pSYN (green) showing pSYN accumulation in Neun+ neurons (yellow). Scale bar: 25μm. **(E)** IBA1 (green) and pSYN (red) immunostaining showing the presence of pSYN deposits inside microglia. Enlargements of the boxed areas are shown on the right. Scale bar: 25μm. hαSYN/αSYN:

human monomeric α-Synuclein; STR: striatum; pSYN: phosphorylated α-Synuclein; tdT: tdTomato fluorescence expressed in astrocytes of *Aldh1l1*-CreERT2; Ai9 mice following tamoxifen-induced recombination.

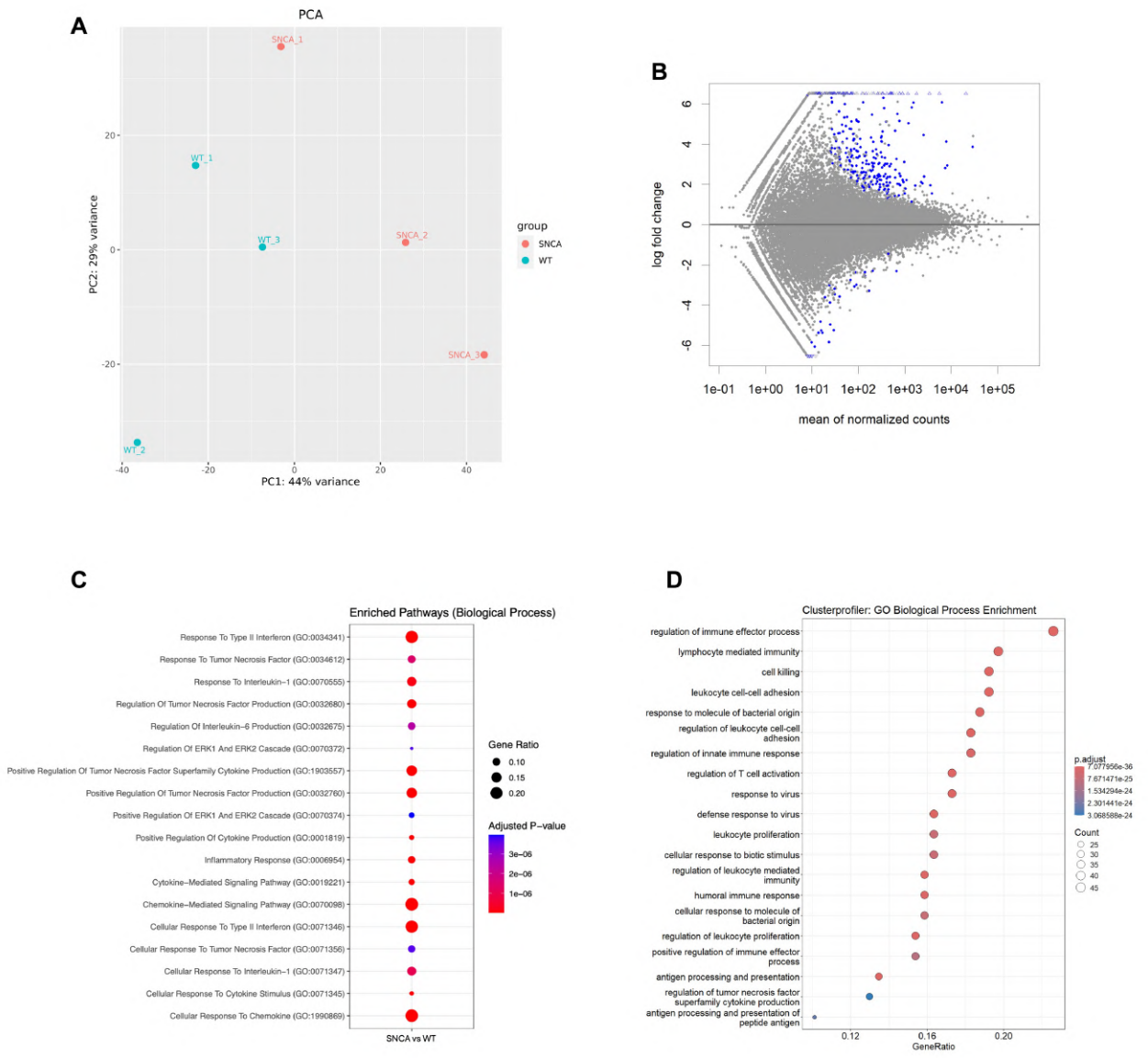

Figure S3. Transcriptomic profiling of the striatal astrocytes following LV:Astro-A53TαSYN injection. **(A)** Principal component analysis (PCA) of bulk RNA-seq data from striatal tissue of mice injected with LV:Astro-A53TαSYN (SNCA, red, n = 3) or LV:Astro-Mock (WT, blue, n = 3) showing a clear segregation along the first principal component (44% of variance) indicating a profound transcriptional impact of astrocytic A53T αSYN overexpression. **(B)** MA plot showing the relationship between log2 fold change and mean of normalized counts for differential expression analysis results between SNCA and WT samples (DESeq2). Significantly dysregulated genes (FDR < 0.05, $|\log_2$ fold change$| \geq 1$) are shown in blue. **(C)** Biological Process over-representation analysis (ORA) of differentially expressed genes (SNCA vs WT). Each dot represents an enriched biological process term; dot size indicates the Gene Ratio (fraction of query genes annotated to the term) and dot colour represent the FDR-adjusted P value, revealing robust activation of cytokine-mediated signalling in LV:Astro-A53TαSYN versus control striata, including type-I interferon and tumour necrosis factor responses, chemokine production, ERK1/2 cascade modulation, and positive regulation of inflammatory cytokines (enrichment score >2.3; adjusted p < 0.001 for the top 10 terms). **(D)** Gene Ontology (GO) enrichment analysis of the 1,327 significantly upregulated genes (FDR < 0.05; $\log_2$ fold change ≥ 1). Dot size indicates the number of enriched genes (Count), dot colour represents the FDR-adjusted P value, and the x-axis shows the GeneRatio. highlights pathways linked to immune effector regulation, lymphocyte-mediated cytotoxicity and leukocyte adhesion. SNCA: astrocyte from LV:Astro-A53TαSYN-injected mice; WT: astrocytes from LV:Mock-injected mice.

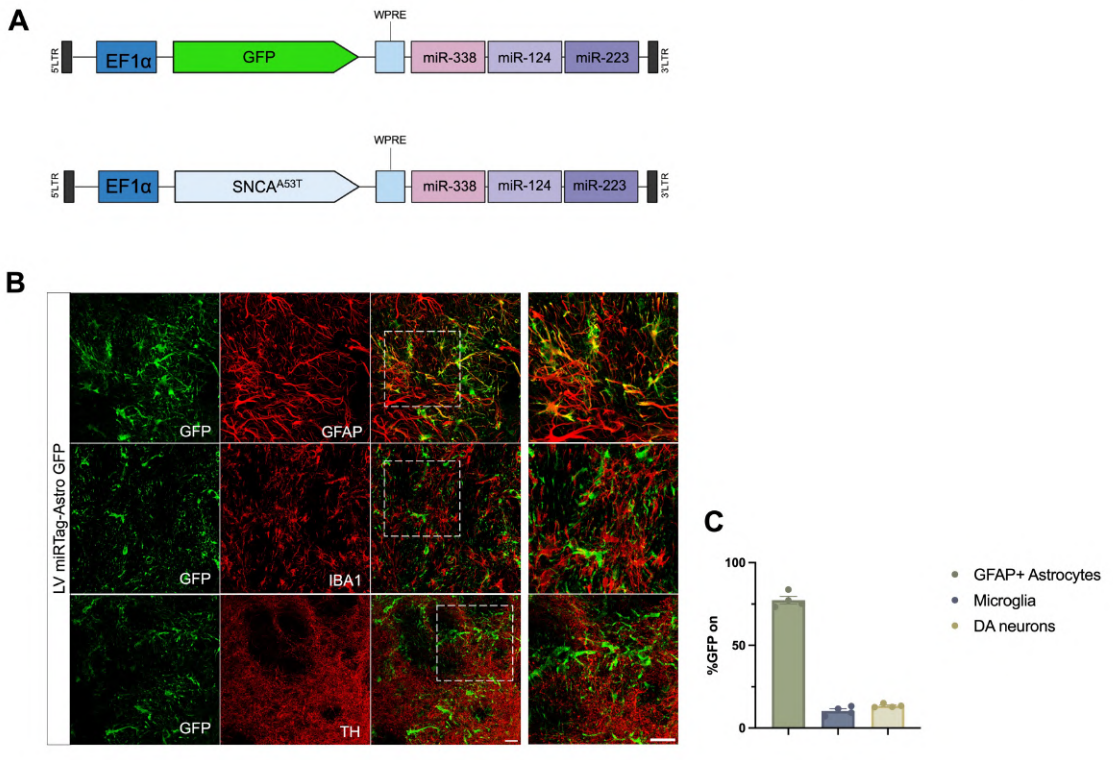

Figure S4. microRNA detargeting strategy to achieve astrocyte-specific expression. (A) Schematic representation of LV:Astro-GFP and LV:Astro-A53TαSYN vectors containing astrocyte-specific miRNA target sequences (miR-124, miR-338, miR-223) under the EF1α promoter. **(B)** Immunofluorescence analysis of striatal sections injected with LV:miRTag-Astro-GFP, stained for GFP (green) and GFAP, IBA1 or TH (red) markers. Enlarged views of the boxed regions are shown on the right. Scale bar: 25μm **(C)** Quantification of cell-type specificity of LV:Astro-GFP based on miRNA target sequences, showing high tropism for astrocytes. Values are expressed as %MOC ± SEM (Mander's Overlap Coefficient, MOC).

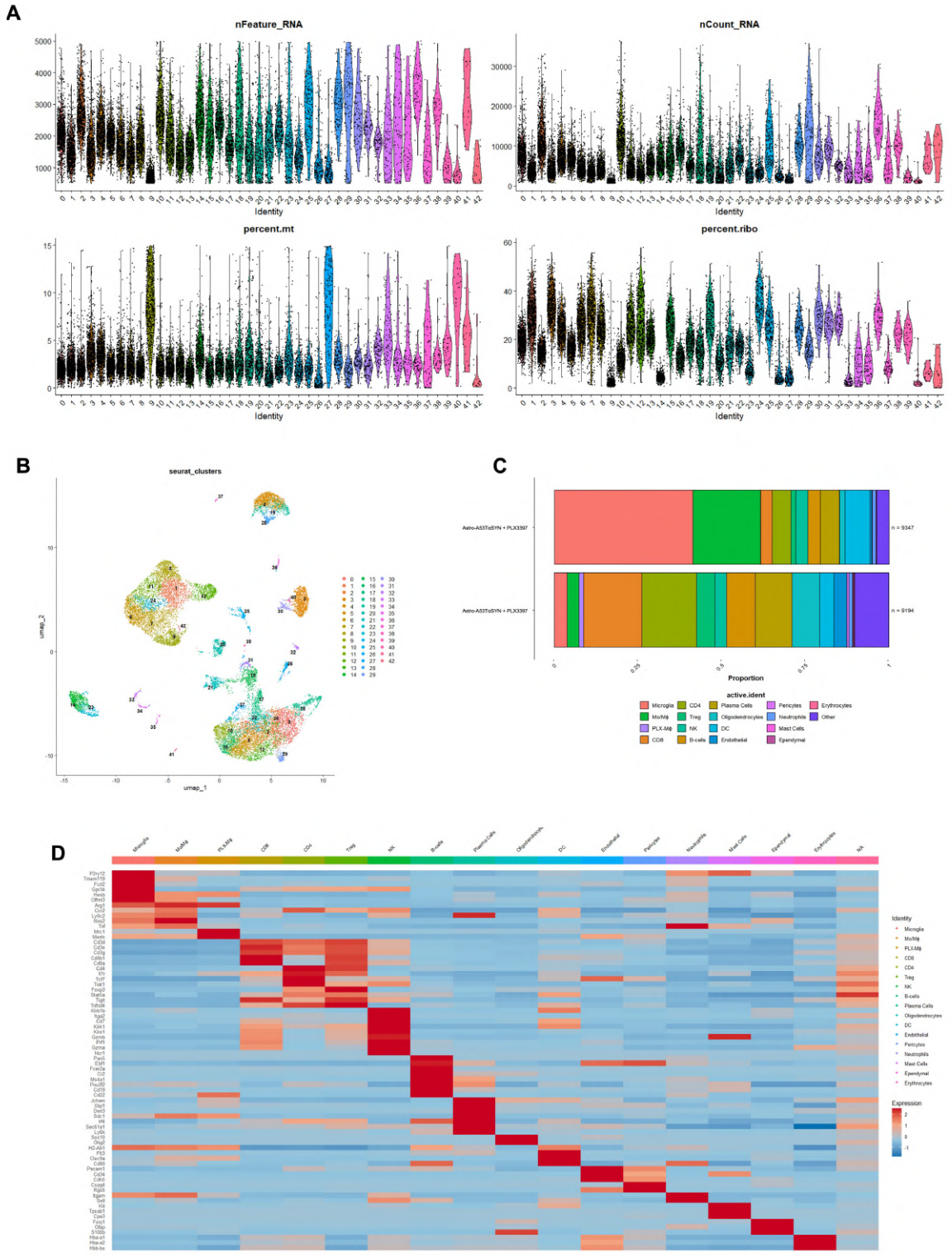

Figure S5. Single-cell transcriptomic profiling in PLX3397 treated and untreated mice. (A) Quality control metrics of single-cell RNA-seq data post-filtering, showing the distribution of detected genes per cell (nFeature_RNA), total UMI counts (nCount_RNA), mitochondrial content (percent.mt), and ribosomal content (percent.ribo) across identified clusters. **(B)** UMAP visualization of captured cells from striatal tissue of mice injected with LV:Astro-A53TαSYN (SNCA) or in combination with PLX3397 treatment (SNCA + PLX). Cells are color-coded by Seurat cluster identity generated with a resolution of 2.2 **(C)** Proportional representation of major cell types across SNCA and SNCA + PLX3397 samples, revealing shifts in cellular composition between experimental groups. **(D)** Heatmap of the relevant expressed marker genes (rows) across cell populations (columns), highlighting cluster-specific transcriptional signatures and validating the identity of the various cell types.

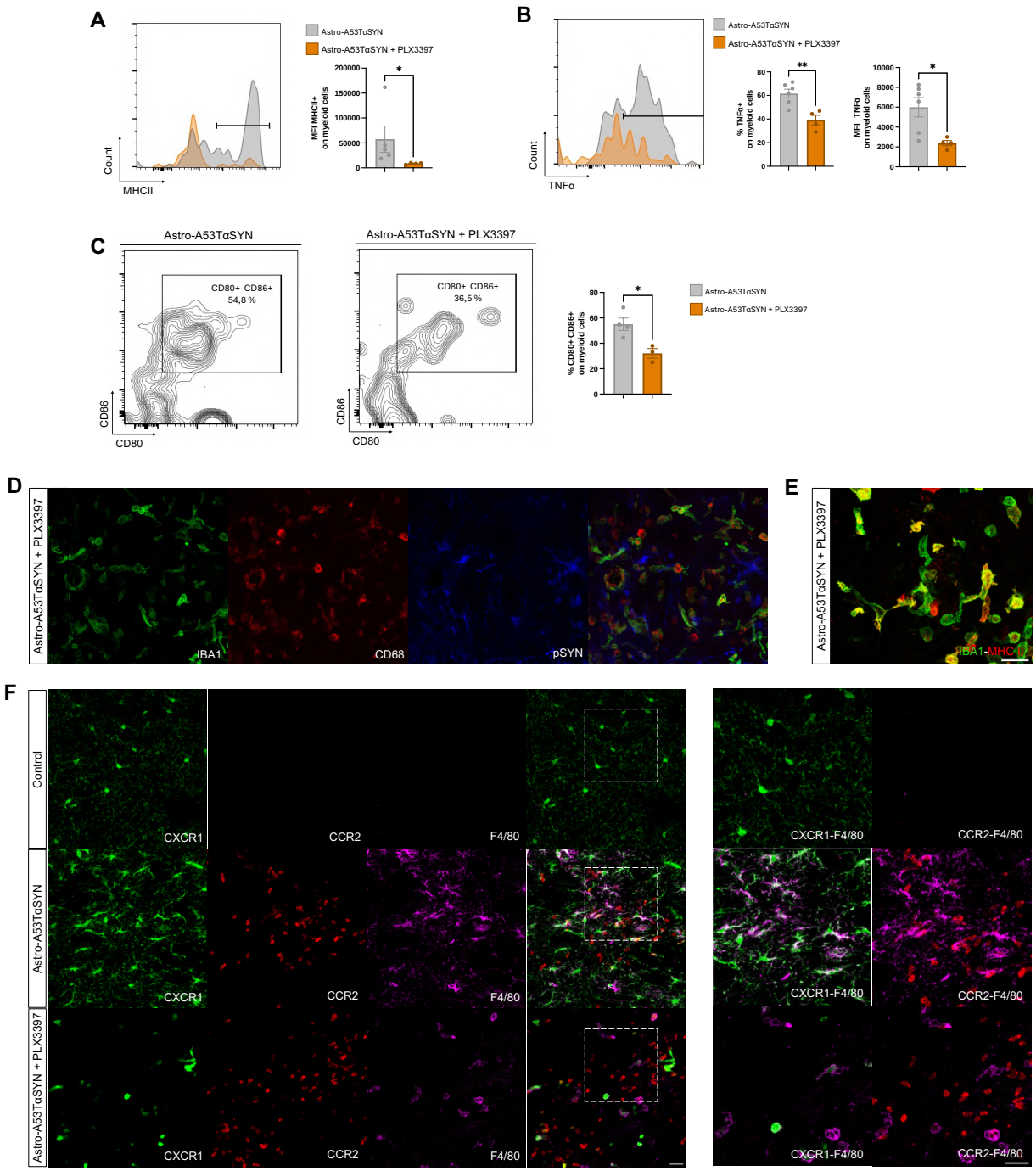

Figure S6. Microglial depletion reshapes myeloid activation and inflammatory responses in the striatum of Astro-A53TαSYN mice. (A) Flow-cytometry (FACS) analysis of striatal tissue from mice injected with LV:Astro-A53TαSYN, either untreated or treated with PLX3397. Representative histogram and quantification of MHCII expression (mean fluorescence intensity, MFI) on myeloid cells in the two groups. Data are expressed as % mean ± SEM. Statistical analysis: Unpaired t test; *P < 0.05; **P < 0.01; ***P < 0.001; ****P < 0.0001. **(B)** Representative histogram and quantification of TNFα expression, shown as mean fluorescence intensity (MFI) and percentage of TNFα$^+$ myeloid cells, in the two groups. Data are expressed as % mean ± SEM. Statistical analysis: Unpaired t test; *P < 0.05; **P < 0.01; ***P < 0.001; ****P < 0.0001. **(C)** Representative FACS contour plots and quantification of CD80$^+$CD86$^+$ myeloid cells from the STR of LV:Astro-A53TαSYN-injected mice treated or untreated with PLX3397. Bar graph shows the percentage of CD80$^+$CD86$^+$ cells among myeloid cells. *n* = 3. Data are expressed as % mean ± SEM. Statistical analysis: Unpaired t test; *P < 0.05; **P < 0.01; ***P < 0.001; ****P < 0.0001. **D)** Representative immunofluorescence images of STR sections stained for IBA1 (green), CD68 (red), and pSYN (blue), showing PLX-MΦ engulfment

of pSYN aggregates. Scale bar: 25 µm. **(E)** Confocal images of IBA1 (green) and MHCII (red) illustrating MHCII expression in PLX-MΦ. Scale bar: 25 µm. **(F)** Representative immunofluorescence images showing CXCR1 (green), CCR2 (red), and F4/80 (magenta) in striatal sections from LV:Astro-Mock (control), LV:Astro-A53TαSYN, and LV:Astro-A53TαSYN + PLX3397 mice. Insets (right) show co-localization of CXCR1 or CCR2 with F4/80^{+} microglia, highlighting changes in expression and recruitment across groups. Scale bars, 25 µm.

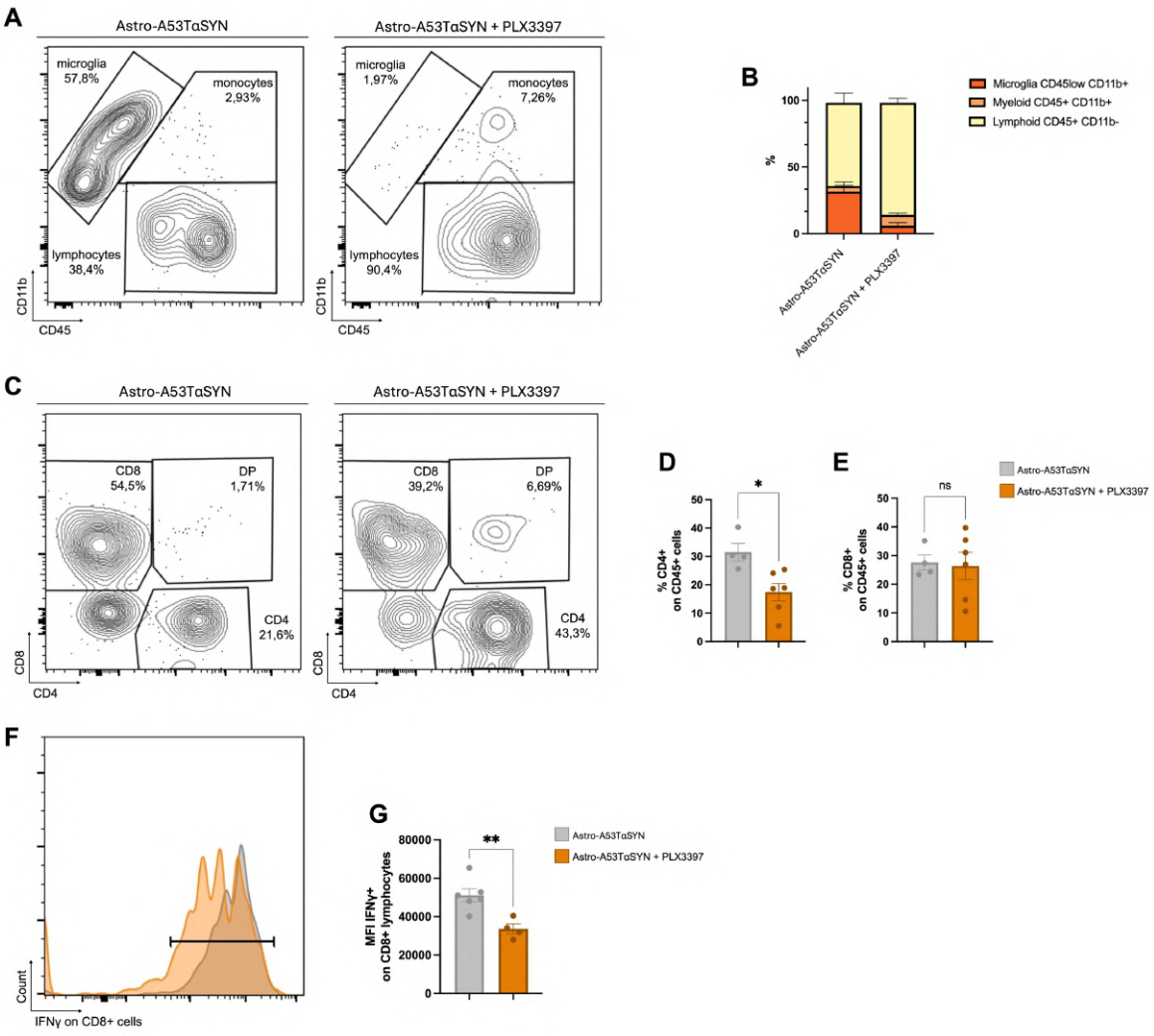

Figure S7. Microglia depletion reshapes the brain immune compartment. (A) Representative CD45/CD11b contour plots of total brain CD45$^+$ cells from Astro-A53TαSYN (left) and Astro-A53TαSYN + PLX3397 (right) group. Gates identify microglia (CD45$^+$CD11b$^+$), infiltrating myeloid cells (CD45$^+$ CD11b^{Int}), and lymphocytes (CD45$^+$CD11b$^-$). **(B)** Stacked bar graph showing the composition of the CD45$^+$ compartment by category (microglia, myeloid, lymphoid) in the two groups. Bars display mean ± SEM. **(C)** Representative CD4 vs CD8 plots gated on CD45$^+$CD11b$^-$ lymphocytes. Quadrants denote CD8$^+$, CD4$^+$ and double positive (DP, CD4$^+$CD8$^+$) subsets. **(D)** Quantification of CD4$^+$ cells among CD45$^+$ lymphocytes. Data are expressed as mean ± SEM. Statistical analysis: unpaired t test; *P < 0.05; **P < 0.01; ***P < 0.001; ****P < 0.0001. **(E)** Quantification of CD8$^+$ cells among CD45$^+$ lymphocytes for each mouse. Data are expressed as mean ± SEM. Statistical analysis: unpaired t test; *P < 0.05; **P < 0.01; ***P < 0.001; ****P < 0.0001. **(F)** Overlaid histograms showing intracellular IFN-γ levels in CD8$^+$ brain lymphocytes from the two groups. The bracket indicates the region used to calculate mean fluorescence intensity (MFI). **(G)** Quantification of IFN-γ MFI in CD8$^+$ lymphocytes for each group. Data are expressed as mean ± SEM. Statistical analysis: unpaired t test; *P < 0.05; **P < 0.01; ***P < 0.001; ****P < 0.0001.

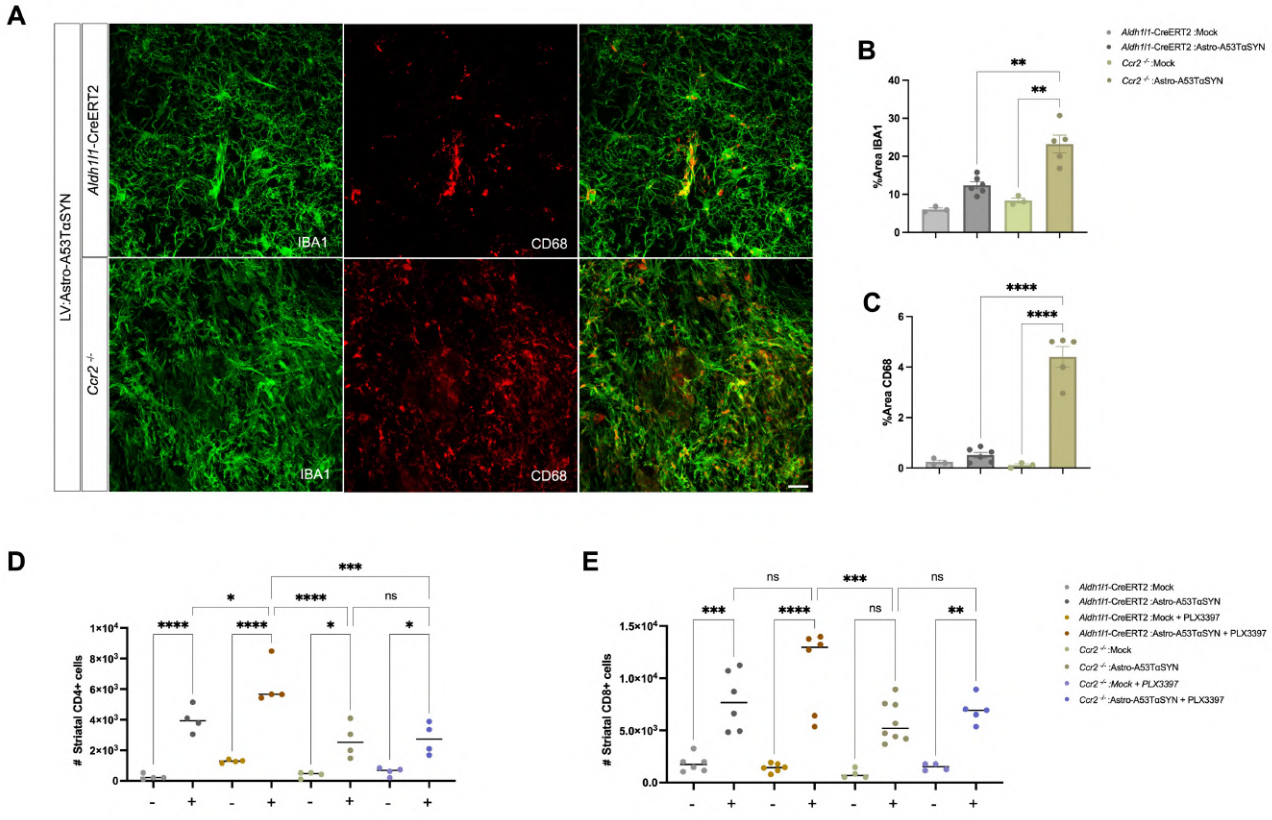

Figure S8. Microglia and lymphocyte evaluation across murine lines. (A) Representative confocal images from striatal sections immunostained for IBA1 (green) and CD68 (red), with merges shown at right. Rows display Aldh1l1-CreERT2 and Ccr2$^{-/-}$ mice under the LV:Astro-A53TαSYN condition. Scale bar: 25µm. **(B)** Occupied area of IBA1 staining (green) in the STR across the different experimental groups. *n* = 3-6 striata. Data are presented as means ± SEM and were analysed using Two-way ANOVA followed by Tukey's multiple comparison **P* < 0.01; ****P* < 0.001; *****P* < 0.0001. **(C)** Occupied area of CD68 staining (red) in the STR across the different experimental groups. *n* = 3-6 striata. Data are presented as means ± SEM and were analysed using Two-way ANOVA followed by Tukey's multiple comparison **P* < 0.01; ****P* < 0.001; *****P* < 0.0001. **(D)** Unbiased stereology count of CD4+ T cells in the STR 6 weeks after injection. *n* = 4 striata. Statistical analysis by Two-way ANOVA followed by Tukey's multiple comparison test. **(E)** Unbiased stereology count of CD8+ T cells in the STR 6 weeks after injection. *n* = 4 striata. Statistical analysis by Two-way ANOVA followed by Tukey's multiple comparison test.

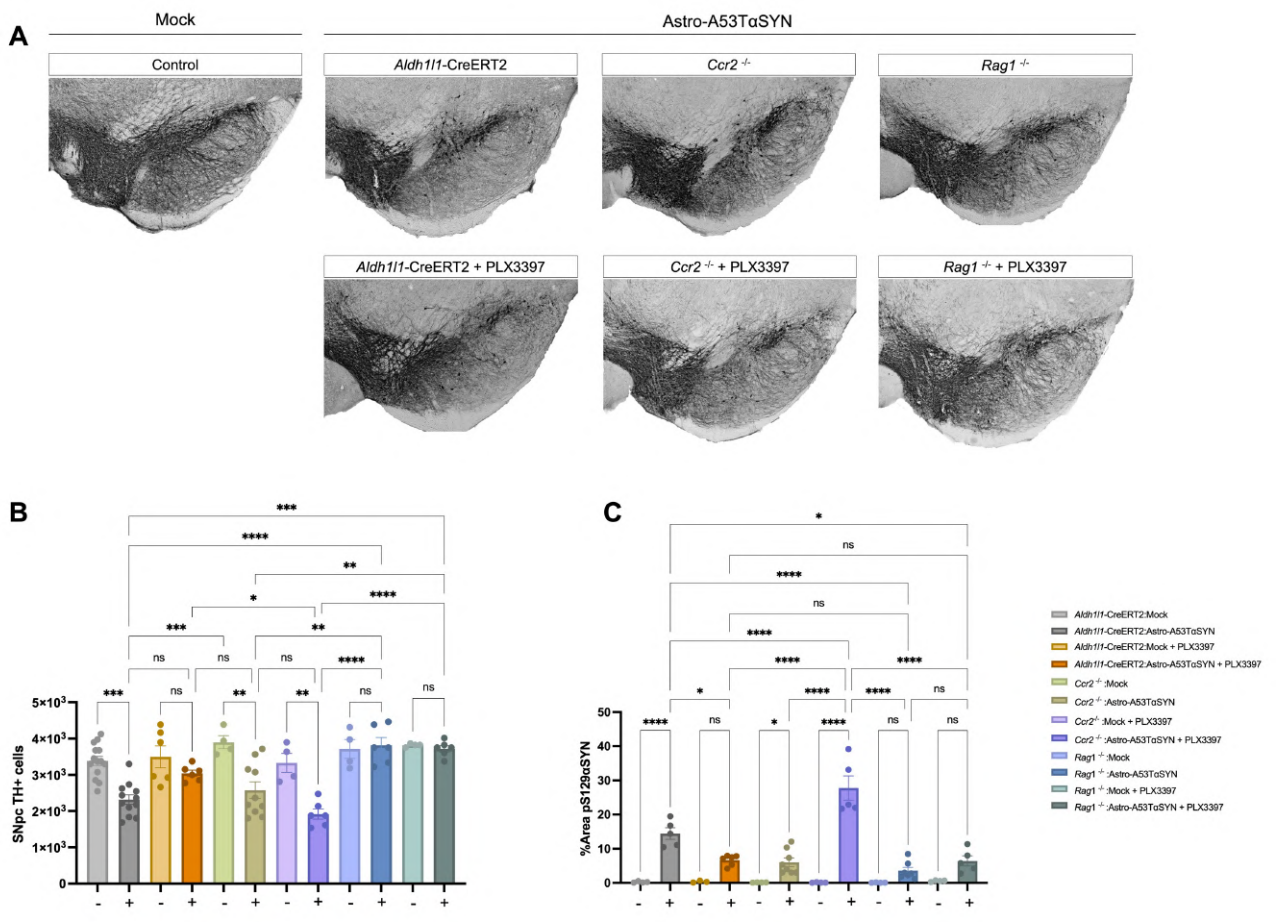

Figure S9. Microglial depletion and immune modulation influence nigral degeneration and α-Synuclein burden. (A) Representative coronal midbrain sections immunostained for TH showing the SNpc in the different experimental groups. **(B)** Unbiased stereology count of TH+ cells in the SNpc of the different experimental groups. n=4-12. Statistical analysis: two-way ANOVA followed by Tukey's multiple comparison test; *P < 0.05; **P < 0.01; ***P < 0.001; ****P < 0.0001. **(C)** Occupied area of pS129αSYN staining in the STR across the different experimental groups. *n* = 3-7 striata. Data are presented as means ± SEM and were analysed using Two-way ANOVA followed by Tukey's multiple comparison *P < 0.01; ***P < 0.001; ****P < 0.0001.

Supplementary table 1

Type	Antibody	Catalogue number	Working dilution	Company
Primary antibody	Anti-CD3	MCA-1477	1:1000	Bio-Rad Laboratories
	Anti-CD4	AB183685	1:100	Abcam
	Anti-CD8	BK98941T	1:100	Cell signalling
	Anti-CD13	AF2335	1:150	RnD
	Anti-CD68	AB53444	1:1000	Abcam
	Anti-CTIP2	AB18465	1:300	Abcam
	Anti-GFAP	Z0334	1:1000	Agilent
	Anti-GFAP	13-0300	1:1000	Thermo Fisher Scientific
	Anti-GFP	A10262	1:1000	Thermo Fisher Scientific
	Anti-IBA	019-19741	1:1000	Fujifilm Wako
	Anti-IBA	234009	1:1000	Synaptic Systems
	Anti-NeuN	AB104225	1:1000	Abcam
	Anti-human-Syn	180215	1:100	Thermo Fisher Scientific
	Anti-phosphorylated-Syn	AB51253	1:1000	Abcam
	Anti-Sox9	AB5535	1:1000	Sigma-Aldrich
	Anti-TH	AB76442	1:1000	Abcam
Secondary antibody	488 anti-Chicken	A11039	1:500	Thermo Fisher Scientific
	488 anti-Rabbit	A21206	1:500	Thermo Fisher Scientific
	488 anti-Rat	A11006	1:500	Thermo Fisher Scientific
	546 anti-Chicken	A11040	1:500	Thermo Fisher Scientific
	546 anti-Mouse	A10036	1:500	Thermo Fisher Scientific
	546 anti-Rabbit	A10040	1:500	Thermo Fisher Scientific
	546 anti-Rat	A11081	1:500	Thermo Fisher Scientific
	647 anti-Chicken	A21449	1:500	Thermo Fisher Scientific
	647 anti-Mouse	A31571	1:500	Thermo Fisher Scientific
	647 anti-Rabbit	A31573	1:500	Thermo Fisher Scientific
	647 anti-Rat	A21247	1:500	Thermo Fisher Scientific
Biotinylated antibody	Anti-Chicken	BA-9010	1:500	Vector Laboratories
	Anti-Rabbit	BA-1000	1:500	Vector Laboratories
	Anti-Rat	BA-4000	1:500	Vector Laboratories

Supplementary table 2

Gene	Forward primer	Reverse primer
Ccl2	TCACCAGCAAGATGATCCCA	CAGCACAGACCTCTCTCTTGA
Ccl5	CCCTCACCATCATCCTCACT	CACTTGCTGCTGGTGTAGAA
Ccl8	TCTACGCAGTGCTTCTTTGCC	AAGGGGGATCTTCAGCTTTAGTA
Cxcl10	CCAAGTGCTGCCGTCATTTTC	GGCTCGCAGGGATGATTTCAA
Gbp2	GGAGGAGCTGTGTGGTGAAT	TATCTGGGCCAAAGTCAGCA
Ligp1	GGGTGGGTCTCATGTGAAGA	ACAGCTGACCCATGACTTCA
Psmb8	TGGTCATGGCGTTACTGGAT	CAAAGGACCTCAGGAATGCG
Serping1	TCAGTGGCCAATGGAAGACT	CGATGAACATGCTGAGGGTG

Supplementary table 3

Type	Antibody	Conjugated dye	Cat. number	Company
Flow Cytometry Antibody	Anti-CD3e	Real Blue 705	570560	BD Pharmingen
	Anti-CD4	Real Yellow 703	571449	BD Horizon
	Anti-CD8a	Brilliant Violet 711	100759	Biolegend
	Anti-CD11b	PE-Fire 810	101285	Biolegend
	Anti-CD45	Brilliant UltraViolet 395	564279	BD Bioscience
	Anti-CD68	PE-Cy7	137015	Biolegend
	Anti-CD80	PE-Dazzle 594	104738	Biolegend
	Anti-CD86	Real Blue 613	759079	BD Bioscience
	Anti-CD107a (Lamp1)	Alexa Fluor 700	121628	Biolegend
	Anti-IFNg	Brilliant Violet 421	505830	Biolegend
	Anti-MHCII	PE-Cy7	25532180	eBio
	Anti-TNFa	Brilliant Violet 650	563943	BD Bioscences

4. SUMMARY AND CONCLUSIONS

This doctoral work provides a comprehensive dissection of the pathogenic contribution of astrocytes to PD, with particular emphasis on αSYN accumulation as a trigger of neurodegeneration and immune activation. Through the selective overexpression of human αSYN in striatal astrocytes, this research reveals a pivotal, autonomous role of astrocytic pathology in orchestrating neuroinflammatory cascades and dopaminergic neuron loss, thus disentangle the role of these cells in PD pathogenesis.

The study demonstrates that astrocytic αSYN accumulation is per se sufficient to induce a robust reactive phenotype in astrocytes, characterized by the upregulation of A1-like genes (such as *Gfap, Serping1,* and *Gbp2*) and the activation of pro-inflammatory signalling pathways involving type I interferons, TNF, and IL-6 (Liddelow and Barres, 2017). This transcriptional reprogramming is accompanied by a marked increase in chemokine production (*Ccl2*, *Ccl5*, *Ccl8*, *Cxcl10*), creating a neuroimmune milieu conducive to the recruitment of peripheral immune cells. In parallel, astrocytic αSYN overexpression leads to extensive microglial activation, pS129αSYN accumulation, and the infiltration of $CD4^+$ and $CD8^+$ T lymphocytes into the brain parenchyma, hallmarks that faithfully recapitulate human PD neuropathology. These findings position astrocytes as active participants in neuroinflammation and immune cell recruitment rather than mere passive responders.

A central question addressed in this thesis concerns the interdependence between astrocytic and microglial responses. By employing chronic microglial ablation with the CSF1R inhibitor PLX3397, the study demonstrates that T cell infiltration persists even in the absence of microglia, revealing a microglia-independent capacity of astrocytes to orchestrate adaptive immune engagement. Remarkably, microglial depletion not only failed to exacerbate pathology but instead mitigated dopaminergic neuron loss and reduced αSYN aggregate burden, highlighting the dual and context-dependent role of microglia in both propagating and constraining neurodegeneration. This observation underscores a paradigm shift: microglia are not merely neuroprotective scavengers but can, under specific inflammatory contexts, amplify astrocyte-driven toxicity.

Single-cell RNA sequencing further elucidated the profound reorganization of the brain's immune landscape following microglial depletion. The emergence of a transcriptionally distinct macrophage subset (PLX-MΦ), endowed with reparative and phagocytic properties, reveals a compensatory immune mechanism capable of mitigating αSYN pathology. PLX-MΦ express high levels of *Arg1, Mrc1*, *Chil3*, *Igf1*, and *Tgfb1,* together with autophagy- and phagocytosis-related genes (*Lamp1*, *Cd68*, *Mfge8*, *Mertk*), defining a functional program of enhanced proteostasis and tissue repair. In contrast, macrophages from control group retained a pro-inflammatory, M1-like transcriptional profile enriched for *Nos2*, *Ccl3*, *Tnf* and *Cxcl10*, indicative of sustained neuroinflammatory potential.

Confocal imaging confirmed the presence of these cells in proximity to αSYN aggregates and revealed a reduced aggregate burden, suggesting their involvement in debris clearance and a consequent decrease in neuronal vulnerability. Flow cytometric analysis further revealed an increased proportion of $CD68^+LAMP1^+$ infiltrating myeloid cells in PLX3397-Astro-A53TαSYN mice compared with controls, indicating their enhanced lysosomal and phagocytic activity.

Beyond their phagocytic competence, PLX-MΦ exhibited pronounced immunomodulatory activity. Transcriptomic profiling revealed the upregulation of *Spp1, Axl, Lgals9,* and *Tgfb1,* consistent with a tolerogenic, T cell–suppressive phenotype. Correspondingly, $CD8^+$ T cells isolated from PLX-treated brains displayed an exhaustion signature, with increased expression of inhibitory receptors (*Pdcd1,*

Ctla4, Lag3, Tigit) and decreased effector cytokine production. These findings indicate that the macrophage population emerging upon microglial depletion exerts a dual function: it promotes proteostatic clearance while simultaneously attenuating detrimental adaptive immune responses, collectively fostering a neuroprotective microenvironment.

To disentangle the non-redundant contributions of resident and infiltrating myeloid cells, the study further employed *Ccr2*$^{-/-}$ and *Rag1*$^{-/-}$ mouse lines. The absence of CCR2^{+} monocytes exacerbated αSYN accumulation and dopaminergic neuron loss when combined with microglial ablation, underscoring the cooperative role of peripheral macrophages in sustaining clearance mechanisms. Conversely, the lack of T cells conferred significant neuroprotection, confirming that lymphocytic infiltration is a crucial effector of astrocyte-induced neurotoxicity. Together, these data delineate a fine-tuned balance between inflammatory amplification and repair processes within the CNS, orchestrated by the dynamic interplay among astrocytes, microglia, macrophages, and lymphocytes.

From a conceptual standpoint, this work advances three major conclusions. First, astrocytic αSYN pathology constitutes an autonomous and sufficient trigger of neuroinflammation and neurodegeneration, independent of neuronal αSYN expression. Second, the immune landscape of the PD brain is profoundly plastic, capable of undergoing functional reprogramming in response to microglial depletion, with infiltrating macrophages assuming protective roles that counterbalance inflammation and promote αSYN clearance. Third, macrophage-centered reprogramming emerges as a promising therapeutic strategy: rather than targeting neurons directly, interventions aimed at shifting macrophages toward homeostatic, reparative states could restore immune balance, enhance αSYN clearance, and slow disease progression. In sum, this thesis provides compelling evidence that Parkinson's disease should be reinterpreted as a multicellular disorder in which astrocytes act as key regulators of neuroinflammation. The integration of bulk and single-cell transcriptomics, immunohistochemical mapping, and pharmacological manipulations reveals an intricate network of cell–cell communication underlying αSYN-driven pathology. By demonstrating that macrophage-mediated clearance and immune exhaustion can mitigate astrocyte-induced neurotoxicity, this research opens new perspectives for therapeutic intervention, shifting the focus toward immune reprogramming. Ultimately, these findings lay the groundwork for a new paradigm of PD pathogenesis, one in which the balance between inflammation, clearance, and immune tolerance determines the trajectory of neurodegeneration.

5. BIBLIOGRAPHY

Aarsland, D., Creese, B., Politis, M., Chaudhuri, K.R., Ffytche, D.H., Weintraub, D., Ballard, C., 2017. Cognitive decline in Parkinson disease. Nat. Rev. Neurol. https://doi.org/10.1038/nrneurol.2017.27

Abounit, S., Bousset, L., Loria, F., Zhu, S., de Chaumont, F., Pieri, L., Olivo-Marin, J.C., Melki, R., Zurzolo, C., 2016. Tunneling nanotubes spread fibrillar α-synuclein by intercellular trafficking of lysosomes. *EMBO Journal*35(19), 2120–2138. https://doi.org/10.15252/embj.201593411

Akdemir, E. S., Huang, A. Y., & Deneen, B. (2020). Astrocytogenesis: where, when, and how. *F1000Research*, *9*, F1000 Faculty Rev-233. https://doi.org/10.12688/f1000research.22405.1

Albin, R.L., Young, A.B., Penney, J.B., 1989. The functional anatomy of basal ganglia disorders. Trends Neurosci. https://doi.org/10.1016/0166-2236(89)90074-X

Alexander, G.E., Crutcher, M.D., 1990. Functional architecture of basal ganglia circuits: neural substrates of parallel processing. Trends Neurosci. https://doi.org/10.1016/0166-2236(90)90107-L

Alexander, G.E., DeLong, M.R., Strick, P.L., 1986. Parallel organization of functionally segregated circuits linking basal ganglia and cortex. Annu. Rev. Neurosci. https://doi.org/10.1146/annurev.ne.09.030186.002041

Allen, N. J., & Eroglu, C. (2017). Cell biology of astrocyte–synapse interactions. *Neuron, 96*(3), 697–708. https://doi.org/10.1016/j.neuron.2017.09.056

Almolda, B., González, B., Castellano, B., 2015. Are microglial cells the regulators of lymphocyte responses in the CNS? Front. Cell. Neurosci. https://doi.org/10.3389/fncel.2015.00440

Altay, M. F., et al. (2022). *Prominent astrocytic alpha-synuclein pathology with unique post-translational modification patterns in synucleinopathies. Acta Neuropathologica Communications, 10*(1), 148. https://doi.org/10.1186/s40478-022-01468-8

Alvarez-Erviti, L., Seow, Y., Schapira, A.H., Gardiner, C., Sargent, I.L., Wood, M.J.A., Cooper, J.M., 2011. Lysosomal dysfunction increases exosome-mediated alpha- synuclein release and transmission. Neurobiol. Dis. https://doi.org/10.1016/j.nbd.2011.01.029

Álvarez-Luquín, D. D., Arce-Sillas, A., Leyva-Hernández, J., Esquivel-Suárez, A. R., de la Rosa-Chávez, O., Ortuño-Sahagún, D., Adalid-Peralta, L., & Hernández-Zimbrón, L. F. (2019). *Regulatory impairment in untreated Parkinson's disease is not restricted to Tregs: Other regulatory populations are also involved.* Journal of Neuroinflammation, 16(1), 212. https://doi.org/10.1186/s12974-019-1606-1

Anderson, J. P., Walker, D. E., Goldstein, J. M., de Laat, R., Banducci, K., Caccavello, R. J., Barbour, R., Huang, J., Kling, K., Lee, M., Diep, L., Keim, P. S., Shen, X., Chataway, T., Schlossmacher, M. G., Seubert, P., Schenk, D., Sinha, S., Gai, W. P., & Chilcote, T. J. (2006). *Phosphorylation of Ser-129 is the dominant pathological modification of alpha-synuclein in familial and sporadic Lewy body disease.* Journal of Biological Chemistry, 281(40), 29739–29752. https://doi.org/10.1074/jbc.M600933200

Anderson, J.P., Walker, D.E., Goldstein, J.M., De Laat, R., Banducci, K., Caccavello, R.J., Barbour, R., Huang, J., Kling, K., Lee, M., Diep, L., Keim, P.S., Shen, X., Chataway, T., Schlossmacher, M.G., Seubert, P., Schenk, D., Sinha, S., Gai, W.P., Chilcote, T.J., 2006. Phosphorylation of Ser-129 is the dominant pathological modification of α-synuclein in familial and sporadic lewy body disease. J. Biol. Chem. https://doi.org/10.1074/jbc.M600933200

Andrews, S. (2010). FastQC: A Quality Control Tool for High Throughput Sequence Data. Available online at: http://www.bioinformatics.babraham.ac.uk/projects/fastqc/

Angot, E., Steiner, J.A., Tomé, C.M., Ekström, P., Mattsson, B., Björklund, A., Brundin, P., 2012. Alpha-synuclein cell-to-cell transfer and seeding in grafted dopaminergic neurons in vivo. PLoS One. https://doi.org/10.1371/journal.pone.0039465

Anheim, M., Elbaz, A., Lesage, S., Durr, A., Condroyer, C., Viallet, F., Pollak, P., Bonaïti, B., Bonaïti-Pellié, C., Brice, A., 2012. Penetrance of Parkinson disease in glucocerebrosidase gene mutation carriers. Neurology. https://doi.org/10.1212/WNL.0b013e318245f476

Ansari, A. M., Ahmed, A. K., Matsangos, A. E., Lay, F., Born, L. J., Marti, G., Harmon, J. W., & Sun, Z. (2016). Cellular GFP Toxicity and Immunogenicity: Potential Confounders in in Vivo Cell Tracking Experiments. *Stem cell reviews and reports*, *12*(5), 553–559. https://doi.org/10.1007/s12015-016-9670-8

Arora, S., Venkataraman, V., Zhan, A., Donohue, S., Biglan, K. M., Dorsey, E. R., & Little, M. A. (2015). Detecting and monitoring the symptoms of Parkinson's disease using smartphones: A pilot study. *Parkinsonism & related disorders*, *21*(6), 650–653. https://doi.org/10.1016/j.parkreldis.2015.02.026

Ascherio, A., Schwarzschild, M.A., 2016. The epidemiology of Parkinson's disease: risk factors and prevention. Lancet Neurol. 15, 1257–1272. https://doi.org/10.1016/S1474-4422(16)30230-7

Ascherio, A., Weisskopf, M.G., O'Reilly, E.J., McCullough, M.L., Calle, E.E., Rodriguez, C., Thun, M.J., 2004. Coffee consumption, gender, and Parkinson's disease mortality in the Cancer Prevention Study II cohort: The modifying effects of estrogen. Am. J. Epidemiol. https://doi.org/10.1093/aje/kwh312

Baba, Y., Kuroiwa, A., Uitti, R. J., Wszolek, Z. K., & Yamada, T. (2005). *Alterations of T-lymphocyte populations in Parkinson disease*. *Parkinsonism & Related Disorders, 11*(8), 493–498. https://doi.org/10.1016/j.parkreldis.2005.07.005

Bae, Y. J., Kim, J. M., Choi, B. S., Choi, J. H., Ryoo, N., Song, Y. S., Cho, S. J., & Kim, J. H. (2023). Glymphatic function assessment in Parkinson's disease using diffusion tensor image analysis along the perivascular space. *Parkinsonism & Related Disorders, 114*, 105767. https://doi.org/10.1016/j.parkreldis.2023.105767

Banks, W.A., Gray, A.M., Erickson, M.A., Salameh, T.S., Damodarasamy, M., Sheibani, N., Meabon, J.S., Wing, E.E., Morofuji, Y., Cook, D.G., Reed, M.J., 2015. Lipopolysaccharide-induced blood-brain barrier disruption: Roles of cyclooxygenase, oxidative stress, neuroinflammation, and elements of the neurovascular unit. J. Neuroinflammation. https://doi.org/10.1186/s12974-015- 0434-1

Barbosa MT, Caramelli P, Maia DP, et al. Parkinsonism and Parkinson's disease in the elderly: a community-based survey in Brazil (the Bambuí study). Mov Disord 2006; 21: 800–08.

Barker, R.A., Drouin-Ouellet, J., Parmar, M., 2015. Cell-based therapies for Parkinson disease-past insights and future potential. Nat. Rev. Neurol. https://doi.org/10.1038/nrneurol.2015.123

Bas, J., Calopa, M., Mestre, M., Molleví, D. G., Cutillas, B., Ambrosio, S., & Buendia, E. (2001). Lymphocyte populations in Parkinson's disease and in rat models of parkinsonism. *Journal of neuroimmunology*, *113*(1), 146–152. https://doi.org/10.1016/s0165-5728(00)00422-7

Bayraktar, O.A., Bartels, T., Holmqvist, S., Kleshchevnikov, V., Martirosyan, A., Polioudakis, D., Ben Haim, L., Young, A.M.H., Batiuk, M.Y., Prakash, K., Brown, A., Hutchinson, P.J., Semyanov, A., Verkhratsky, A., Haeussler, M., Ross, S.E., Bernard, A., Sloan, S.A., 2020. Astrocyte layers in the mammalian cerebral cortex revealed by a single-cell in situ transcriptomic map. *Nature Neuroscience* 23(4), 500–509. https://doi.org/10.1038/s41593-020-0602-1

Becker, C., Jick, S. S., & Meier, C. R. (2011). NSAID use and risk of Parkinson disease: a population-based case-control study. *European journal of neurology*, *18*(11), 1336–1342. https://doi.org/10.1111/j.1468-1331.2011.03399.x

Bélanger, M., Allaman, I., & Magistretti, P. J. (2011). Brain energy metabolism: Focus on astrocyte–neuron metabolic cooperation. *Cell Metabolism, 14*(6), 724–738. https://doi.org/10.1016/j.cmet.2011.08.016

Ben Haim, L., Rowitch, D.H., 2017. Functional diversity of astrocytes in neural circuit regulation. *Nature Reviews Neuroscience* 18(1), 31–41. https://doi.org/10.1038/nrn.2016.159

Benabid, A. L., Pollak, P., Louveau, A., Henry, S., & de Rougemont, J. (1987). Combined (thalamotomy and stimulation) stereotactic surgery of the VIM thalamic nucleus for bilateral Parkinson disease. *Applied neurophysiology*, *50*(1-6), 344–346. https://doi.org/10.1159/000100803

Benitez, B.A., Davis, A.A., Jin, S.C., Ibanez, L., Ortega-Cubero, S., Pastor, P., Choi, J., Cooper, B., Perlmutter, J.S., Cruchaga, C., 2016. Resequencing analysis of five Mendelian genes and the top genes from genome-wide association studies in Parkinson's Disease. Mol. Neurodegener. 11, 1–12. https://doi.org/10.1186/s13024-016-0097-0

Bennett, M.L., Bennett, F.C., Liddelow, S.A., Ajami, B., Zamanian, J.L., Fernhoff, N.B., Mulinyawe, S.B., Bohlen, C.J., Adil, A., Tucker, A., Weissman, I.L., Chang, E.F., Li, G., Grant, G.A., Hayden Gephart, M.G., Barres, B.A., 2016. New tools for studying microglia in the mouse and human CNS. Proc. Natl. Acad. Sci. U. S. A. https://doi.org/10.1073/pnas.1525528113

Benskey, M.J., Perez, R.G., & Manfredsson, F.P. (2016). The contribution of α-synuclein to neuronal survival and function – Implications for Parkinson's disease. *Journal of Neurochemistry*, 137(3), 331–359. https://doi.org/10.1111/jnc.13570

Bergman, H., Wichmann, T., DeLong, M.R., 1994. Reversal of experimental parkinsonism by lesions of the subthalamic nucleus. *Science* 249(4975), 1436–1438. https://doi.org/10.1126/science.2402638

Bernheimer, H., Birkmayer, W., Hornykiewicz, O., Jellinger, K., Seitelberger, F., 1973. Brain dopamine and the syndromes of Parkinson and Huntington Clinical, morphological and neurochemical correlations. J. Neurol. Sci. https://doi.org/10.1016/0022-510X(73)90175-5

Berry, C., La Vecchia, C., Nicotera, P., 2010. Paraquat and parkinson's disease. Cell Death Differ. 17, 1115–1125. https://doi.org/10.1038/cdd.2009.217

Bertoncini, C.W., Fernandez, C.O., Griesinger, C., Jovin, T.M., Zweckstetter, M., 2005a. Familial mutants of α-synuclein with increased neurotoxicity have a destabilized conformation. J. Biol. Chem. https://doi.org/10.1074/jbc.C500288200

Bertoncini, C.W., Jung, Y.S., Fernandez, C.O., Hoyer, W., Griesinger, C., Jovin, T.M., & Zweckstetter, M. (2005). Release of long-range tertiary interactions potentiates aggregation of natively unstructured α-synuclein.*Proceedings of the National Academy of Sciences of the United States of America*, 102(5), 1430–1435. https://doi.org/10.1073/pnas.0407146102

Bertoncini, C.W., Jung, Y.S., Fernandez, C.O., Hoyer, W., Griesinger, C., Jovin, T.M., Zweckstetter, M., 2005b. Release of long-range tertiary interactions potentiates aggregation of natively unstructured α-synuclein. Proc. Natl. Acad. Sci. U. S. A. https://doi.org/10.1073/pnas.0407146102

Bido, S., Muggeo, S., Massimino, L., Marzi, M.J., Giannelli, S.G., Melacini, E., Nannoni, M., Gambare, D., Bellini, E., Ordazzo, G., Rossi, G., Maffezzini, C., Iannelli, A., Luoni, M., Bacigaluppi, M., Gregori, S., Nicassio, F., Broccoli, V., 2021. Microglia-specific overexpression of α-synuclein leads to severe dopaminergic neurodegeneration by phagocytic exhaustion and oxidative toxicity. *Nature Communications* 12, 6237. https://doi.org/10.1038/s41467-021-26519-x.

Bido, S., Nannoni, M., Muggeo, S., Gambarè, D., Ruffini, G., Bellini, E., Passeri, L., Iaia, S., Luoni, M., Provinciali, M., Giannelli, S. G., Giannese, F., Lazarevic, D., Gregori, S., & Broccoli, V. (2024). *Microglia-specific IL-10 gene delivery inhibits neuroinflammation and neurodegeneration in a mouse model of Parkinson's disease.* Science Translational Medicine, 16(761), eadm8563. https://doi.org/10.1126/scitranslmed.adm8563

Bido, S., Nannoni, M., Muggeo, S., Gambarè, D., Ruffini, G., Bellini, E., Passeri, L., Iaia, S., Luoni, M., Provinciali, M., Giannelli, S. G., Giannese, F., Lazarevic, D., Gregori, S., & Broccoli, V. (2024). *Microglia-specific IL-10 gene delivery inhibits neuroinflammation and neurodegeneration in a mouse model of Parkinson's disease. Science Translational Medicine, 16*(737), eadk1205. https://doi.org/10.1126/scitranslmed.adk1205

Billingsley, K. J., Bandres-Ciga, S., Saez-Atienzar, S., & Singleton, A. B. (2018). Genetic risk factors in Parkinson's disease. *Cell and tissue research*, *373*(1), 9–20. https://doi.org/10.1007/s00441-018-2817-y

Biosa, A., Sandrelli, F., Beltramini, M., Greggio, E., Bubacco, L., Bisaglia, M., 2017. Recent findings on the physiological function of DJ-1: Beyond Parkinson's disease. Neurobiol. Dis. https://doi.org/10.1016/j.nbd.2017.08.005

Blauwendraat, C., Nalls, M. A., & Singleton, A. B. (2020). The genetic architecture of Parkinson's disease. *The Lancet. Neurology*, *19*(2), 170–178. https://doi.org/10.1016/S1474-4422(19)30287-X

Block, M.L., Zecca, L., Hong, J.S., 2007. Microglia-mediated neurotoxicity: Uncovering the molecular mechanisms. Nat. Rev. Neurosci. 8, 57–69. https://doi.org/10.1038/nrn2038

Bolam, J.P., Pissadaki, E.K., 2012. Living on the edge with too many mouths to feed: Why dopamine neurons die. Mov. Disord. https://doi.org/10.1002/mds.25135

Bonifati, V., Rizzu, P., Squitieri, F., Krieger, E., Vanacore, N., van Swieten, J.C., Brice, A., van Duijn, C.M., Oostra, B., Meco, G., Heutink, P., 2003. DJ-1 (PARK7), a novel gene for autosomal recessive, early onset parkinsonism. Neurol. Sci. https://doi.org/10.1007/s10072-003-0108-0

Boulakirba, S., et al. (2018). IL-34 and CSF-1 display an equivalent macrophage differentiation ability but a different polarization potential. *Scientific Reports, 8*, 256. https://doi.org/10.1038/s41598-017-18433-4

Braak, H., Del Tredici, K., Rüb, U., De Vos, R.A.I., Jansen Steur, E.N.H., Braak, E., 2003. Staging of brain pathology related to sporadic Parkinson's disease. Neurobiol. Aging. https://doi.org/10.1016/S0197-4580(02)00065-9

Braak, H., Del Tredici, K., Rüb, U., de Vos, R.A.I., Jansen Steur, E.N.H., Braak, E., 2003. Staging of brain pathology related to sporadic Parkinson's disease. *Neurobiology of Aging* 24(2), 197–211. https://doi.org/10.1016/S0197-4580(02)00065-9

Braak, H., Sastre, M., & Del Tredici, K. (2007). Development of α-synuclein immunoreactive astrocytes in the forebrain parallels stages of intraneuronal pathology in sporadic Parkinson's disease. *Acta Neuropathologica, 114*(3), 231–241. https://doi.org/10.1007/s00401-007-0244-3

Brochard, V., Combadière, B., Prigent, A., Laouar, Y., Perrin, A., Beray-Berthat, V., Bonduelle, O., Alvarez-Fischer, D., Callebert, J., Launay, J.M., Duyckaerts, C., Flavell, R.A., Hirsch, E.C., Hunot, S., 2009. Infiltration of CD4+ lymphocytes into the brain contributes to neurodegeneration in a mouse model of Parkinson disease. J. Clin. Invest. https://doi.org/10.1172/JCI36470

Brochard, V., Combadière, B., Prigent, A., Laouar, Y., Perrin, A., Beray-Berthat, V., Bonduelle, O., Alvarez-Fischer, D., Callebert, J., Launay, J. M., Duyckaerts, C., Flavell, R. A., Hirsch, E. C., & Hunot, S. (2009). *Infiltration of CD4⁺ lymphocytes into the brain contributes to neurodegeneration in a mouse model of Parkinson disease.*Journal of Clinical Investigation, 119(1), 182–192. https://doi.org/10.1172/JCI36470

Brooks, D. J., & Pavese, N. (2011). Imaging biomarkers in Parkinson's disease. *Progress in neurobiology*, *95*(4), 614–628. https://doi.org/10.1016/j.pneurobio.2011.08.009

Brown P. (2003). Oscillatory nature of human basal ganglia activity: relationship to the pathophysiology of Parkinson's disease. *Movement disorders : official journal of the Movement Disorder Society*, *18*(4), 357–363. https://doi.org/10.1002/mds.10358

Brundin, P., Melki, R., 2017. Prying into the prion hypothesis for Parkinson's disease. *Journal of Neuroscience* 37(41), 9808–9818. https://doi.org/10.1523/JNEUROSCI.1788-16.2017

Buell, A.K., Galvagnion, C., Gaspar, R., Sparr, E., Vendruscolo, M., Knowles, T.P.J., Linse, S., Dobson, C.M., 2014. Solution conditions determine the relative importance of nucleation and growth processes in α-synuclein aggregation. Proc. Natl. Acad. Sci. U. S. A. https://doi.org/10.1073/pnas.1315346111

Burré, J. (2015). The synaptic function of α-synuclein. *Journal of Parkinson's Disease, 5*(4), 699–713. https://doi.org/10.3233/JPD-150642

Burré, J., Sharma, M., & Südhof, T.C. (2010). α-synuclein promotes SNARE-complex assembly in vivo and in vitro. *Science*, 329(5999), 1663–1667. https://doi.org/10.1126/science.1195227

Burré, J., Sharma, M., Südhof, T.C., 2014. α-Synuclein assembles into higher-order multimers upon membrane binding to promote SNARE complex formation. Proc. Natl. Acad. Sci. U. S. A. https://doi.org/10.1073/pnas.1416598111

Butovsky, O., Jedrychowski, M.P., Moore, C.S., Cialic, R., Lanser, A.J., Gabriely, G., Koeglsperger, T., Dake, B., Wu, P.M., Doykan, C.E., Fanek, Z., Liu, L., Chen, Z., Rothstein, J.D., Ransohoff, R.M., Gygi, S.P., Antel, J.P., Weiner, H.L., 2014. Identification of a unique TGF-β-dependent molecular and functional signature in microglia. Nat. Neurosci. https://doi.org/10.1038/nn.3599

Calabresi, P., Picconi, B., Tozzi, A., Ghiglieri, V., Di Filippo, M., 2014. Direct and indirect pathways of basal ganglia: A critical reappraisal. Nat. Neurosci. 17, 1022–1030. https://doi.org/10.1038/nn.3743

Castle, M., Aymerich, M.S., Sanchez-Escobar, C., Gonzalo, N., Obeso, J.A., Lanciego, J.L., 2005. Thalamic innervation of the direct and indirect basal ganglia pathways in the rat: Ipsi- and contralateral projections. J. Comp. Neurol. https://doi.org/10.1002/cne.20421

Cebrián, C., Zucca, F. A., Mauri, P., Steinbeck, J. A., Studer, L., Scherzer, C. R., Kanter, E., Budhu, S., Mandelbaum, J., Vonsattel, J. P. G., Zecca, L., Loike, J. D., & Sulzer, D. (2014). *MHC-I expression renders catecholaminergic neurons susceptible to T-cell-mediated degeneration.* Nature Communications, 5, 3633. https://doi.org/10.1038/ncomms4633

Cebrián, C., Zucca, F.A., Mauri, P., Steinbeck, J.A., Studer, L., Scherzer, C.R., Kanter, E., Budhu, S., Mandelbaum, J., Vonsattel, J.P., Zecca, L., Loike, J.D., Sulzer, D., 2014. MHC-I expression renders catecholaminergic neurons susceptible to T-cell- mediated degeneration. Nat. Commun. https://doi.org/10.1038/ncomms4633

Chamak, B., Morandi, V., Mallat, M., 1994. Brain macrophages stimulate neurite growth and regeneration by secreting thrombospondin. J. Neurosci. Res. https://doi.org/10.1002/jnr.490380213

Chandra, S., Gallardo, G., Fernández-Chacón, R., Schlüter, O.M., & Südhof, T.C. (2005). α-synuclein cooperates with CSPα in preventing neurodegeneration. *Cell*, 123(3), 383–396. https://doi.org/10.1016/j.cell.2005.09.028

Chaudhuri, K.R., Schapira, A.H.V., 2009. Non-motor symptoms of Parkinson's disease: dopaminergic pathophysiology and treatment. *The Lancet Neurology* 8(5), 464–474. https://doi.org/10.1016/S1474-4422(09)70068-7

Chavarría, C., Rodríguez-Bottero, S., Quijano, C., Cassina, P., & Souza, J. M. (2018). *Impact of monomeric, oligomeric and fibrillar α-synuclein on astrocyte reactivity and toxicity to neurons.* Biochemical Journal, 475(19), 3153–3169. https://doi.org/10.1042/BCJ20180297

Che, N., Ou, R., Li, C. *et al.* Plasma GFAP as a prognostic biomarker of motor subtype in early Parkinson's disease. *npj Parkinsons Dis.* 10, 48 (2024). https://doi.org/10.1038/s41531-024-00664-8

Chen, K., Xu, H., Shen, S., Li, Q., Chen, Z., Li, Y., Cai, Y., Wang, T., … & Zhang, Q. (2025). Glymphatic dysfunction as a potential driver of cerebral iron deposition in Parkinson's disease. *Brain Communications, 7*(5), fcaf365. https://doi.org/10.1093/braincomms/fcaf365

Chen, S., Saeed, A. F. U., Liu, Q., Jiang, Q., Xiao, G., & Rao, L. (2023). *Macrophages in immunoregulation and therapeutics.* Signal Transduction and Targeted Therapy, 8, 207. https://doi.org/10.1038/s41392-023-01452-1

Chen, S.W., Drakulic, S., Deas, E., Ouberai, M., Aprile, F.A., Arranz, R., Ness, S., Roodveldt, C., Guilliams, T., De-Genst, E.J., Klenerman, D., Wood, N.W., Knowles, T.P.J., Alfonso, C., Rivas, G., Abramov, A.Y., Valpuesta, J.M., Dobson, C.M., Cremades, N., 2015. Structural characterization of toxic oligomers that are kinetically trapped during α-synuclein fibril formation. Proc. Natl. Acad. Sci. U. S. A. https://doi.org/10.1073/pnas.1421204112

Chen, W., Guo, C., Wang, F., 2015. Imaging and modeling of astrocytes in the rodent brain: morphological complexity, domain organization, and structural plasticity. *Neuroscience Bulletin* 31(5), 573–583. https://doi.org/10.1007/s12264-015-1551-0

Chen, Y., Zhang, D.Q., Liao, Z., Wang, B., Gong, S., Wang, C., Zhang, M.Z., Wang, G.H., Cai, H., Liao, F.F., Xu, J.P., 2015. Anti-oxidant polydatin (piceid) protects against substantia nigral motor degeneration in multiple rodent models of Parkinson's disease. Mol. Neurodegener. https://doi.org/10.1186/1750-1326-10-4

Chesselet, M. F., Richter, F., Zhu, C., Magen, I., Watson, M. B., & Subramaniam, S. R. (2012). A progressive mouse model of Parkinson's disease: the Thy1-aSyn ("Line 61") mice. *Neurotherapeutics : the journal of the American Society for Experimental NeuroTherapeutics*, *9*(2), 297–314. https://doi.org/10.1007/s13311-012-0104-2

Chesselet, M.F., Richter, F., Zhu, C., Magen, I., Watson, M.B., Subramaniam, S.R., 2012. A Progressive Mouse Model of Parkinson's Disease: The Thy1-aSyn ('Line 61') Mice. Neurotherapeutics. https://doi.org/10.1007/s13311-012-0104-2

Chiken, S., Nambu, A., 2016. Mechanism of Deep Brain Stimulation: Inhibition, Excitation, or Disruption? Neuroscientist. https://doi.org/10.1177/1073858415581986

Chillag-Talmor, O., Giladi, N., Linn, S., Gurevich, T., El-Ad, B., Silverman, B., Friedman, N., Peretz, C., 2011. Use of a refined drug tracer algorithm to estimate prevalence and incidence of Parkinson's disease in a large israeli population. J. Parkinsons. Dis. 1, 35–47. https://doi.org/10.3233/JPD-2011-11024

Chinta, S.J., Andersen, J.K., 2005. Dopaminergic neurons. Int. J. Biochem. Cell Biol. https://doi.org/10.1016/j.biocel.2004.09.009

Choi, I., Kim, J., Jeong, H.K., Kim, B., Jou, I., Park, M., Chen, L., Kang, U.J., Zhuang, X., Joe, E. hye, 2013. PINK1 deficiency attenuates astrocyte proliferation through mitochondrial dysfunction, reduced AKT and increased p38 MAPK activation, and downregulation of EGFR. Glia. https://doi.org/10.1002/glia.22475

Choi, I., Zhang, Y., Seegobin, S.P. *et al.* Microglia clear neuron-released α-synuclein via selective autophagy and prevent neurodegeneration. *Nat Commun* 11, 1386 (2020). https://doi.org/10.1038/s41467-020-15119-w

Chou, C. H., Lin, C. H., Lee, C. H., Wang, C. Y., Lin, K. L., & Huang, Y. C. (2021). *Fibrillar α-synuclein induces neurotoxic astrocyte activation.* Cell Death & Disease, 12, 897. https://doi.org/10.1038/s41419-021-04049-0

Choubey, V., Safiulina, D., Vaarmann, A., Cagalinec, M., Wareski, P., Kuum, M., Zharkovsky, A., & Kaasik, A. (2011). Mutant A53T α-synuclein induces neuronal death by increasing mitochondrial autophagy. *Journal of Biological Chemistry*, 286(12), 10814–10824. https://doi.org/10.1074/jbc.M110.132514

Christopherson, K. S., Ullian, E. M., Stokes, C. C. A., Mullowney, C. E., Hell, J. W., Agah, A., ... & Barres, B. A. (2005). Thrombospondins are astrocyte-secreted proteins that promote CNS synaptogenesis. *Cell, 120*(3), 421–433. https://doi.org/10.1016/j.cell.2004.12.020

Clarke, L., Barres, B. Emerging roles of astrocytes in neural circuit development. *Nat Rev Neurosci* 14, 311–321 (2013). https://doi.org/10.1038/nrn3484

Codolo, G., Plotegher, N., Pozzobon, T., Brucale, M., Tessari, I., Bubacco, L., et al. (2013). *Triggering of Inflammasome by Aggregated α–Synuclein, an Inflammatory Response in Synucleinopathies.* PLoS ONE, 8(1), e55375. https://doi.org/10.1371/journal.pone.0055375

Colosimo, C., Hughes, A.J., Kilford, L., Lees, A.J., 2003. Lewy body cortical pathology in Parkinson's disease: clinical correlations. *Brain* 126(6), 1490–1501. https://doi.org/10.1093/brain/awg150

Contaldi, E., Magistrelli, L., & Comi, C. (2022). T Lymphocytes in Parkinson's Disease. *Journal of Parkinson's disease*, *12*(s1), S65–S74. https://doi.org/10.3233/JPD-223152

Conway, K.A., Harper, J.D., Lansbury, P.T., 1998. Accelerated in vitro fibril formation by a mutant α-synuclein linked to early-onset Parkinson disease. Nat. Med. https://doi.org/10.1038/3311

Coskuner, O., Wise-Scira, O., 2013. Structures and free energy landscapes of the A53T mutant-type α-synuclein protein and impact of A53T mutation on the structures of the wild-type α-synuclein protein with dynamics. ACS Chem. Neurosci. https://doi.org/10.1021/cn400041j

Cotzias, G.C., Van Woert, M.H., Schiffer, L.M., 1967. Aromatic Amino Acids and Modification of Parkinsonism. N. Engl. J. Med. https://doi.org/10.1056/nejm196702162760703

Cremades, N., Cohen, S.I.A., Deas, E., Abramov, A.Y., Chen, A.Y., Orte, A., Sandal, M., Clarke, R.W., Dunne, P., Aprile, F.A., Bertoncini, C.W., Wood, N.W., Knowles, T.P.J., Dobson, C.M., Klenerman, D., 2012. Direct observation of the interconversion of normal and toxic forms of α-synuclein. *Cell* 149(5), 1048–1059. https://doi.org/10.1016/j.cell.2012.03.037

D. Kirik, L.E. Annett, C. Burger, N. Muzyczka, R.J. Mandel, & A. Björklund, Nigrostriatal α-synucleinopathy induced by viral vector-mediated overexpression of human α-synuclein: A new primate model of Parkinson's disease, Proc. Natl. Acad. Sci. U.S.A. 100 (5) 2884-2889, https://doi.org/10.1073/pnas.0536383100 (2003).

da Fonseca, T.L., Villar-Piqué, A., Outeiro, T.F., 2015. The interplay between alpha- synuclein clearance and spreading. Biomolecules. https://doi.org/10.3390/biom5020435

Dadwal, S., & Heneka, M. T. (2023). *Microglia heterogeneity in health and disease*. FEBS Open Bio. https://doi.org/10.1002/2211-5463.13735

Dai, X.-M., Ryan, G. R., Hapel, A. J., Dominguez, M. G., Russell, R. G., Kapp, S., Sylvestre, V., & Stanley, E. R. (2002). Targeted disruption of the mouse colony-stimulating factor 1 receptor gene results in osteopetrosis, mononuclear phagocyte deficiency, increased primitive progenitor cell frequencies, and reproductive defects. *Blood, 99*(1), 111–120. https://doi.org/10.1182/blood.v99.1.111

Damier, P., Hirsch, E.C., Zhang, P., Agid, Y., Javoy-Agid, F., 1993. Glutathione peroxidase, glial cells and Parkinson's disease. Neuroscience. https://doi.org/10.1016/0306-4522(93)90175-F

Danzer, K.M., Kranich, L.R., Ruf, W.P., Cagsal-Getkin, O., Winslow, A.R., Zhu, L., Vanderburg, C.R., McLean, P.J., 2012. Exosomal cell-to-cell transmission of α-synuclein oligomers. *Molecular Neurodegeneration* 7, 42. https://doi.org/10.1186/1750-1326-7-42

Das, S., Li, Z., Noori, A., Hyman, B. T., & Serrano-Pozo, A. (2020). Meta-analysis of mouse transcriptomic studies supports a context-dependent astrocyte reaction in acute CNS injury versus neurodegeneration. *Journal of neuroinflammation*, *17*(1), 227. https://doi.org/10.1186/s12974-020-01898-y

Dauer, W., & Przedborski, S. (2003). *Parkinson's disease: Mechanisms and models.* Neuron, 39(6), 889–909. https://doi.org/10.1016/S0896-6273(03)00568-3

De Biase, L. M., Schuebel, K. E., Fusfeld, Z. H., Jair, K., Hawes, I. A., Cimbro, R., Zhang, H. Y., Liu, Q. R., Shen, H., Xi, Z. X., Goldman, D., & Bonci, A. (2017). Local Cues Establish and Maintain Region-Specific Phenotypes of Basal Ganglia Microglia. *Neuron*, *95*(2), 341–356.e6. https://doi.org/10.1016/j.neuron.2017.06.020

de Couto, G., Jaghatspanyan, E., DeBerge, M., Liu, W., Luther, K., Wang, Y., … Marbán, E. (2019). Mechanism of enhanced MerTK-dependent macrophage efferocytosis by extracellular vesicles. *Arteriosclerosis, Thrombosis, and Vascular Biology*, 39(10), 2082–2096. https://doi.org/10.1161/ATVBAHA.119.313115

De Francesco, E., Terzaghi, M., Storelli, E., Magistrelli, L., Comi, C., Legnaro, M., Mauri, M., Marino, F., Versino, M., & Cosentino, M. (2021). *CD4⁺ T-cell transcription factors in idiopathic REM sleep behavior disorder and Parkinson's disease.* Movement Disorders, 36(1), 225–229. https://doi.org/10.1002/mds.28137

de Lau, L. M. L., & Breteler, M. M. B. (2006). Epidemiology of Parkinson's disease. *The Lancet Neurology*, 5(6), 525–535. https://doi.org/10.1016/S1474-4422(06)70471-9

De Virgilio, A., Greco, A., Fabbrini, G., Inghilleri, M., Rizzo, M.I., Gallo, A., Conte, M., Rosato, C., Ciniglio Appiani, M., de Vincentiis, M., 2016. Parkinson's disease: Autoimmunity and neuroinflammation. Autoimmun. Rev. https://doi.org/10.1016/j.autrev.2016.07.022

Dedmon, M.M., Lindorff-Larsen, K., Christodoulou, J., Vendruscolo, M., & Dobson, C.M. (2005). Mapping long-range interactions in α-synuclein using spin-label NMR and ensemble molecular dynamics simulations. *Journal of the American Chemical Society*, 127(2), 476–477. https://doi.org/10.1021/ja044834j

Del Tredici, K., Braak, H., 2016. Review: Sporadic Parkinson's disease: Development and distribution of α-synuclein pathology. *Neuropathology and Applied Neurobiology* 42(1), 33–50. https://doi.org/10.1111/nan.12298

DeLeo, F.R., Renee, J., McCormick, S., Nakamura, M., Apicella, M., Weiss, J.P., Nauseef, W.M., 1998. Neutrophils exposed to bacterial lipopolysaccharide upregulate NADPH oxidase assembly. J. Clin. Invest. https://doi.org/10.1172/JCI949

DeLong, M.R., 1990. Primate models of movement disorders of basal ganglia origin. *Trends in Neurosciences* 13(7), 281–285. https://doi.org/10.1016/0166-2236(90)90110-V

Depp, C., Doman, J. L., Hingerl, M., Xia, J., & Stevens, B. (2025). Microglia transcriptional states and their functional significance: Context drives diversity. *Immunity*, *58*(5), 1052–1067. https://doi.org/10.1016/j.immuni.2025.04.009

Desplats, P., Lee, H.J., Bae, E.J., Patrick, C., Rockenstein, E., Crews, L., Spencer, B., Masliah, E., Lee, S.J., 2009. Inclusion formation and neuronal cell death through neuron-to-neuron transmission of α-synuclein. Proc. Natl. Acad. Sci. U. S. A. https://doi.org/10.1073/pnas.0903691106

di Domenico, A., Carola, G., Calatayud, C., Pons-Espinal, M., Muñoz, J. P., Richaud-Patin, Y., Fernandez-Carasa, I., Gut, M., Faella, A., Parameswaran, J., Soriano, J., Ferrer, I., Tolosa, E., Zorzano, A., Cuervo, A. M., Raya, A., & Consiglio, A. (2019). Patient-Specific iPSC-Derived Astrocytes Contribute to Non-Cell-Autonomous Neurodegeneration in Parkinson's Disease. *Stem cell reports*, *12*(2), 213–229. https://doi.org/10.1016/j.stemcr.2018.12.011

Dorsey, E.R., Bloem, B.R., 2018. The Parkinson pandemic - A call to action. JAMA Neurol. https://doi.org/10.1001/jamaneurol.2017.3299

Dorsey, E.R., Constantinescu, R., Thompson, J.P., Biglan, K.M., Holloway, R.G., Kieburtz, K., Marshall, F.J., Ravina, B.M., Schifitto, G., Siderowf, A., Tanner, C.M., 2007. Projected number of people with Parkinson disease in the most populous nations, 2005 through 2030. Neurology. https://doi.org/10.1212/01.wnl.0000247740.47667.03

Double, K.L., Rowe, D.B., Carew-Jones, F.M., Hayes, M., Chan, D.K.Y., Blackie, J., Corbett, A., Joffe, R., Fung, V.S., Morris, J., Riederer, P., Gerlach, M., Halliday, G.M., 2009. Anti-melanin antibodies are increased in sera in Parkinson's disease. Exp. Neurol. https://doi.org/10.1016/j.expneurol.2009.03.002

Duplomb, L., Baud'huin, M., Charrier, C., Berreur, M., Trichet, V., Blanchard, F., & Heymann, D. (2008). Interleukin-6 inhibits receptor activator of nuclear factor kappaB ligand-induced osteoclastogenesis by

diverting cells into the macrophage lineage: key role of Serine727 phosphorylation of signal transducer and activator of transcription 3. *Endocrinology*, *149*(7), 3688–3697. https://doi.org/10.1210/en.2007-1719

Eliezer, D., Kutluay, E., Bussell, R., Browne, G., 2001. Conformational properties of α- synuclein in its free and lipid-associated states. J. Mol. Biol. https://doi.org/10.1006/jmbi.2001.4538

Elmore, M.R.P., Najafi, A.R., Koike, M.A., Dagher, N.N., Spangenberg, E.E., Rice, R.A., Kitazawa, M., Matusow, B., Nguyen, H., West, B.L., Green, K.N., 2014. Colony- stimulating factor 1 receptor signaling is necessary for microglia viability, unmasking a microglia progenitor cell in the adult brain. Neuron. https://doi.org/10.1016/j.neuron.2014.02.040

Elward, K., Gasque, P., 2003. 'Eat me' and 'don't eat me' signals govern the innate immune response and tissue repair in the CNS: Emphasis on the critical role of the complement system, in: Molecular Immunology. https://doi.org/10.1016/S0161- 5890(03)00109-3

Emmanouilidou, E., Melachroinou, K., Roumeliotis, T., Garbis, S.D., Ntzouni, M., Margaritis, L.H., Stefanis, L., Vekrellis, K., 2010. Cell-produced α-synuclein is secreted in a calcium-dependent manner by exosomes and impacts neuronal survival. *Journal of Neuroscience* 30(20), 6838–6851. https://doi.org/10.1523/JNEUROSCI.5699-09.2010

Epelman, S., Lavine, K. J., & Randolph, G. J. (2014). *Origin and functions of tissue macrophages.* Immunity, 41(1), 21–35. https://doi.org/10.1016/j.immuni.2014.06.013

Fairfoul, G., McGuire, L.I., Pal, S., Ironside, J.W., Neumann, J., Christie, S., Joachim, C., Esiri, M., Evetts, S.G., Rolinski, M., Baig, F., Ruffmann, C., Wade-Martins, R., Hu, M.T., Parkkinen, L., Green, A.J.E., 2016. Alpha-synuclein RT-QuIC in the CSF of patients with α-synucleinopathies. *Annals of Clinical and Translational Neurology*3(10), 812–818. https://doi.org/10.1002/acn3.338

Faivre, F., Joshi, A., Bezard, E., Barrot, M., 2019. The hidden side of Parkinson's disease: Studying pain, anxiety and depression in animal models. Neurosci. Biobehav. Rev. https://doi.org/10.1016/j.neubiorev.2018.10.004

Fang, L., Hodge, J., Saaoud, F., Wang, J., Iwanowycz, S., Wang, Y., Hui, Y., Evans, T. D., Razani, B., & Fan, D. (2017). Transcriptional factor EB regulates macrophage polarization in the tumor microenvironment. *Oncoimmunology*, *6*(5), e1312042. https://doi.org/10.1080/2162402X.2017.1312042

Farmen, K., Nido, G. S., Korkman, N., Miletic, H., Borgan, F., Selnes, P., Tysnes, O.-B., Larsen, J. P., Alves, G., & Tzoulis, C. (2021). *Monocyte markers correlate with immune and neuronal changes in a synucleinopathy-related disorder.* Proceedings of the National Academy of Sciences, 118(24), e2020858118. https://doi.org/10.1073/pnas.2020858118

Feany, M.B., Bender, W.W., 2000. A Drosophila model of Parkinson's disease. Nature. https://doi.org/10.1038/35006074

Fellner, L., Irschick, R., Schanda, K., Reindl, M., Klimaschewski, L., Poewe, W., Wenning, G.K., Stefanova, N., 2013. Toll-like receptor 4 is required for α-synuclein dependent activation of microglia and astroglia. *Glia* 61(3), 349–360. https://doi.org/10.1002/glia.22437

Ferreira, M., Massano, J., 2017. An updated review of Parkinson's disease genetics and clinicopathological correlations. Acta Neurol. Scand. https://doi.org/10.1111/ane.12616

Ferrer, I., Bernet, E., Soriano, E., Del Rio, T., Fonseca, M., 1990. Naturally occurring cell death in the cerebral cortex of the rat and removal of dead cells by transitory phagocytes. Neuroscience. https://doi.org/10.1016/0306-4522(90)90281-8

Filion M, Tremblay L. Abnormal spontaneous activity of globus pallidus neurons in monkeys with MPTP-induced parkinsonism. Brain Res. 1991 Apr 26;547(1):142-51. PMID: 1677607.

Fiszer, U., Mix, E., Fredrikson, S., Kostulas, V., Olsson, T., Link, H., 1994. γδ+ T cells are increased in patients with Parkinson's disease. J. Neurol. Sci. https://doi.org/10.1016/0022-510X(94)90154-6

Fortin, D. L., Troyer, M. D., Nakamura, K., Kubo, S.-I., Anthony, M. D., & Edwards, R. H. (2004). Lipid rafts mediate the synaptic localization of alpha-synuclein. *Journal of Neuroscience, 24*(30), 6715–6723. https://doi.org/10.1523/JNEUROSCI.1594-04.2004

Fourgeaud, L., Traves, P.G., Tufail, Y., Leal-Bailey, H., Lew, E.D., Burrola, P.G., Callaway, P., Zagorska, A., Rothlin, C. V., Nimmerjahn, A., Lemke, G., 2016. TAM receptors regulate multiple features of microglial physiology. Nature. https://doi.org/10.1038/nature17630

Fujiwara, H., Hasegawa, M., Dohmae, N., Kawashima, A., Masliah, E., Goldberg, M. S., Shen, J., Takio, K., & Iwatsubo, T. (2002). *α-Synuclein is phosphorylated in synucleinopathy lesions.* Nature Cell Biology, 4(2), 160–164. https://doi.org/10.1038/ncb748

Galiano-Landeira, J., Torra, A., Vila, M., & Bové, J. (2020). *CD8 T cell nigral infiltration precedes synucleinopathy in early stages of Parkinson's disease.* Brain, 143(11), 3717–3733. https://doi.org/10.1093/brain/awaa269

Gan-Or, Z., Liong, C., & Alcalay, R. N. (2018). GBA-Associated Parkinson's Disease and Other Synucleinopathies. *Current neurology and neuroscience reports*, *18*(8), 44. https://doi.org/10.1007/s11910-018-0860-4

Gan, L., Vargas, M.R., Johnson, D.A., Johnson, J.A., 2012. Astrocyte-specific overexpression of Nrf2 delays motor pathology and synuclein aggregation throughout the CNS in the α-synuclein mutant (A53T) mouse model. *Journal of Neuroscience* 32(49), 17775–17787. https://doi.org/10.1523/JNEUROSCI.3049-12.2012

García-Revilla, J., Herrera, A. J., de Pablos, R. M., & Venero, J. L. (2022). Inflammatory Animal Models of Parkinson's Disease. *Journal of Parkinson's disease*, *12*(s1), S165–S182. https://doi.org/10.3233/JPD-213138

Ge, W.-P., Miyawaki, A., Gage, F.H., Jan, Y.N., Jan, L.Y., 2012. Local generation of glia is a major astrocyte source in the developing postnatal cortex. *Nature* 484(7394), 376–380. https://doi.org/10.1038/nature10959

Gelders, G., Baekelandt, V., Van der Perren, A., 2018. Linking neuroinflammation and neurodegeneration in Parkinson's disease. *Journal of Immunology Research* 2018, 4784268. https://doi.org/10.1155/2018/4784268

GENCODE 2025: reference gene annotation for human and mouse. Mudge JM, Carbonell-Sala S, Diekhans M, Martinez JG, Hunt T, Jungreis I, Loveland JE, Arnan C, Barnes I, Bennett R, Berry A, Bignell A, Cerdán-Vélez D, Cochran K, Cortés LT, Davidson C, Donaldson S, Dursun C, Fatima R, Hardy M, Hebbar P, Hollis Z, James BT, Jiang Y, Johnson R, Kaur G, Kay M, Mangan RJ, Maquedano M, Gómez LM, Mathlouthi N, Merritt R, Ni P, Palumbo E, Perteghella T, Pozo F, Raj S, Sisu C, Steed E, Sumathipala D, Suner MM, Uszczynska-Ratajczak B, Wass E, Yang YT, Zhang D, Finn RD, Gerstein M, Guigó R, Hubbard TJP, Kellis M, Kundaje A, Paten B, Tress ML, Birney E, Martin FJ, Frankish A. Nucleic Acids Res 2025 : 53 ; d1 ; D966-D975. PUBMED: 39565199; PMC: PMC11701607; DOI: 10.1093/nar/gkae1078

George, S., Rey, N.L., Tyson, T., Esquibel, C., Meyerdirk, L., Schulz, E., Pierce, S., Burmeister, A.R., Madaj, Z., Steiner, J.A., Brundin, P., 2019. Microglia affect α-synuclein cell-to-cell transfer in a mouse model of Parkinson's disease. *Molecular Neurodegeneration* 14, 34. https://doi.org/10.1186/s13024-019-0335-3

German DC, Manaye KF. (1993). *Midbrain dopaminergic neurons (nuclei A8, A9, and A10): three-dimensional reconstruction in the human brain.* Journal of Comparative Neurology, 331(3), 297–309. https://doi.org/10.1002/cne.903310302

Ghosh, A., Roy, A., Liu, X., Kordower, J.H., Mufson, E.J., Hartley, D.M., Ghosh, S., Mosley, R.L., Gendelman, H.E., Pahan, K., 2015. Selective inhibition of NF-κB activation prevents dopaminergic neuronal loss in a mouse

model of Parkinson's disease. *Proceedings of the National Academy of Sciences of the United States of America (PNAS)* 104(47), 18754–18759. https://doi.org/10.1073/pnas.0704908104

Giasson, B.I., Duda, J.E., Murray, I.V.J., Chen, Q., Souza, J.M., Hurtig, H.I., Ischiropoulos, H., Trojanowski, J.Q., Lee, V.M.Y., 2000. Oxidative damage linked to neurodegeneration by selective α-synuclein nitration in synucleinopathy lesions. Science (80-.). https://doi.org/10.1126/science.290.5493.985

Gibb, W.R.G., Lees, A.J., 1988. The relevance of the Lewy body to the pathogenesis of idiopathic Parkinson's disease. *Journal of Neurology, Neurosurgery & Psychiatry* 51(6), 745–752. https://doi.org/10.1136/jnnp.51.6.745

Ginhoux, F., Greter, M., Leboeuf, M., Nandi, S., See, P., Gokhan, S., Mehler, M.F., Conway, S.J., Ng, L.G., Stanley, E.R., Samokhvalov, I.M., Merad, M., 2010. Fate mapping analysis reveals that adult microglia derive from primitive macrophages. Science. https://doi.org/10.1126/science.1194637

Global Burden of Disease Study 2016 Parkinson's Disease Collaborators. (2018). Global, regional, and national burden of Parkinson's disease, 1990–2016: a systematic analysis for the Global Burden of Disease Study 2016. *The Lancet Neurology, 17*(11), 939–953. https://doi.org/10.1016/S1474-4422(18)30295-3

Goedert, M., Spillantini, M.G., Del Tredici, K., Braak, H., 2013. 100 years of Lewy pathology. *Nature Reviews Neurology* 9(1), 13–24. https://doi.org/10.1038/nrneurol.2012.242

Goers, J., Manning-Bog, A. B., McCormack, A. L., Millett, I. S., Doniach, S., Di Monte, D. A., Uversky, V. N., & Fink, A. L. (2003). Nuclear localization of alpha-synuclein and its interaction with histones. *Biochemistry*, *42*(28), 8465–8471. https://doi.org/10.1021/bi0341152

Goldman, S.M., Marek, K., Ottman, R., Meng, C., Comyns, K., Chan, P., Ma, J., Marras, C., Langston, J.W., Ross, G.W., Tanner, C.M., 2019. Concordance for Parkinson's disease in twins: A 20-year update. Ann. Neurol. https://doi.org/10.1002/ana.25441

Gómez-Benito, M., Granado, N., García-Sanz, P., Michel, A., Dumoulin, M., & Moratalla, R. (2020). *Modeling Parkinson's disease with the alpha-synuclein protein: Comparative analysis of PFFs and rAAV-mediated overexpression models*. *Frontiers in Pharmacology, 11*, 356. https://doi.org/10.3389/fphar.2020.00356

Gonçalves, S., & Outeiro, T. F. (2013). Assessing the subcellular dynamics of alpha-synuclein using photoactivation microscopy. *Molecular neurobiology*, *47*(3), 1081–1092. https://doi.org/10.1007/s12035-013-8406-x

González, C., Bonilla, S., Isabel Flores, A., Cano, E., Liste, I., 2016. An Update on Human Stem Cell-Based Therapy in Parkinson';s Disease. Curr. Stem Cell Res. Ther. https://doi.org/10.2174/1574888x10666150531172612

Gordon, R., Albornoz, E.A., Christie, D.C., Langley, M.R., Kumar, V., Mantovani, S., Robertson, A.A.B., Butler, M.S., Rowe, D.B., O'Neill, L.A., Kanthasamy, A.G., Schroder, K., Cooper, M.A., Woodruff, T.M., 2018. Inflammasome inhibition prevents -synuclein pathology and dopaminergic neurodegeneration in mice. Sci. Transl. Med. https://doi.org/10.1126/scitranslmed.aah4066

Gosselin, D., Link, V.M., Romanoski, C.E., Fonseca, G.J., Eichenfield, D.Z., Spann, N.J., Stender, J.D., Chun, H.B., Garner, H., Geissmann, F., Glass, C.K., 2014. Environment drives selection and function of enhancers controlling tissue-specific macrophage identities. Cell. https://doi.org/10.1016/j.cell.2014.11.023

Grafton, S. T., Waters, C., Sutton, J., Lew, M. F., & Couldwell, W. (1995). Pallidotomy increases activity of motor association cortex in Parkinson's disease: a positron emission tomographic study. *Annals of neurology*, *37*(6), 776–783. https://doi.org/10.1002/ana.410370611

Grandinetti, A., Morens, D.M., Reed, D., Maceachern, D., 1994. Prospective study of cigarette smoking and the risk of developing idiopathic parkinson's disease. Am. J. Epidemiol. https://doi.org/10.1093/oxfordjournals.aje.a116960

Greter, M., Lelios, I., Pelczar, P., Hoeffel, G., Price, J., Leboeuf, M., Kündig, T.M., Frei, K., Ginhoux, F., Merad, M., Becher, B., 2012. Stroma-Derived Interleukin-34 Controls the Development and Maintenance of Langerhans Cells and the Maintenance of Microglia. Immunity. https://doi.org/10.1016/j.immuni.2012.11.001

Grofova I, Zhou M. Nigral innervation of cholinergic and glutamatergic cells in the rat mesopontine tegmentum: light and electron microscopic anterograde tracing and immunohistochemical studies. J Comp Neurol. 1998 Jun 8;395(3):359-79. PMID: 9596529.

Grozdanov, V., Bliederhaeuser, C., Ruf, W. P., et al. (2019). Increased immune activation by pathologic α-synuclein in Parkinson's disease. *Annals of Neurology, 86*(4), 593-606. https://doi.org/10.1002/ana.25557

Grozdanov, V., Bliederhaeuser, C., Ruf, W. P., Roth, V., Fundel-Clemens, K., Zondler, L., Brenner, D., Martin-Villalba, A., Hengerer, B., Kassubek, J., Ludolph, A. C., Weishaupt, J. H., & Danzer, K. M. (2014). Inflammatory dysregulation of blood monocytes in Parkinson's disease patients. *Acta neuropathologica*, *128*(5), 651–663. https://doi.org/10.1007/s00401-014-1345-4

Gu, X. L., Long, C. X., Sun, L., Xie, C., Lin, X., & Cai, H. (2010). *Astrocytic expression of Parkinson's disease-related A53T α-synuclein causes neurodegeneration in mice.* Molecular Brain, 3, 12. https://doi.org/10.1186/1756-6606-3-12

Guerrero-Ferreira, R., Taylor, N.M.I., Mona, D., Ringler, P., Lauer, M.E., Riek, R., Britschgi, M., & Stahlberg, H. (2018). Cryo-EM structure of α-synuclein fibrils. *eLife*, 7, e36402. https://doi.org/10.7554/eLife.36402

Guidetti, M., Marceglia, S., Loh, A., Harmsen, I. E., Meoni, S., Foffani, G., Lozano, A. M., Moro, E., Volkmann, J., & Priori, A. (2021). Clinical perspectives of adaptive deep brain stimulation. *Brain stimulation*, *14*(5), 1238–1247. https://doi.org/10.1016/j.brs.2021.07.063

Guilarte, T. R., Nihei, M. K., McGlothan, J. L., & Howard, A. S. (2003). Methamphetamine-induced deficits of brain monoaminergic neuronal markers: distal axotomy or neuronal plasticity. *Neuroscience*, *122*(2), 499–513. https://doi.org/10.1016/s0306-4522(03)00476-7

Guo, J.L., Covell, D.J., Daniels, J.P., Iba, M., Stieber, A., Zhang, B., Riddle, D.M., Kwong, L.K., Xu, Y., Trojanowski, J.Q., Lee, V.M.Y., 2013. Distinct α-synuclein strains differentially promote tau inclusions in neurons. *Cell* 154(1), 103–117. https://doi.org/10.1016/j.cell.2013.05.057

Guo, M., Wang, J., Zhao, Y., Feng, Y., Han, S., Dong, Q., Cui, M., & Tieu, K. (2020). Microglial exosomes facilitate α-synuclein transmission in Parkinson's disease. *Brain : a journal of neurology*, *143*(5), 1476–1497. https://doi.org/10.1093/brain/awaa090

Haddad, F., Sawalha, M., Khawaja, Y., Najjar, A., Karaman, R., 2018. Dopamine and levodopa prodrugs for the treatment of Parkinson's disease. Molecules. https://doi.org/10.3390/molecules23010040

Hammond, C., Bergman, H., Brown, P., 2007. Pathological synchronization in Parkinson's disease: networks, models and treatments. *Trends in Neurosciences* 30(7), 357–364. https://doi.org/10.1016/j.tins.2007.05.004

Hammond, T.R., Dufort, C., Dissing-Olesen, L., Giera, S., Young, A., Wysoker, A., Walker, A.J., Gergits, F., Segel, M., Nemesh, J., Marsh, S.E., Saunders, A., Macosko, E., Ginhoux, F., Chen, J., Franklin, R.J.M., Piao, X., McCarroll, S.A., Stevens, B., 2019. Single-Cell RNA Sequencing of Microglia throughout the Mouse Lifespan and in the Injured Brain Reveals Complex Cell-State Changes. Immunity. https://doi.org/10.1016/j.immuni.2018.11.004

Hansen, C., Angot, E., Bergström, A.L., Steiner, J.A., Pieri, L., Paul, G., Outeiro, T.F., Melki, R., Kallunki, P., Fog, K., Li, J.Y., Brundin, P., 2011. α-Synuclein propagates from mouse brain to grafted dopaminergic neurons and seeds aggregation in cultured human cells. Journal of Clinical Investigation 121(2), 715–725. https://doi.org/10.1172/JCI43366

Hansson, O., Janelidze, S., Hall, S., Magdalinou, N., Lees, A. J., Andreasson, U., Norgren, N., Linder, J., Forsgren, L., Constantinescu, R., Zetterberg, H., Blennow, K., & Swedish BioFINDER study (2017). Blood-based NfL: A biomarker for differential diagnosis of parkinsonian disorder. *Neurology*, *88*(10), 930–937. https://doi.org/10.1212/WNL.0000000000003680

Hao, Y., Stuart, T., Kowalski, M.H. et al. Dictionary learning for integrative, multimodal and scalable single-cell analysis. Nat Biotechnol 42, 293–304 (2024). https://doi.org/10.1038/s41587-023-01767-y

Harms, A. S., Cao, S., Rowse, A. L., Thome, A. D., Li, X., Mangieri, L. R., Cron, R. Q., Shacka, J. J., Raman, C., Standaert, D. G. (2013). *MHCII is required for α-synuclein-induced activation of microglia and subsequent neurodegeneration.* Journal of Neuroscience, 33(23), 9592–9600. https://doi.org/10.1523/JNEUROSCI.5610-12.2013

Harms, A. S., Cao, S., Rowse, A. L., Thome, A. D., Li, X., Mangieri, L. R., Cron, R. Q., Shacka, J. J., Raman, C., & Standaert, D. G. (2013). MHCII is required for α-synuclein-induced activation of microglia, CD4 T cell proliferation, and dopaminergic neurodegeneration. *The Journal of neuroscience : the official journal of the Society for Neuroscience*, *33*(23), 9592–9600. https://doi.org/10.1523/JNEUROSCI.5610-12.2013gene therapy for Parkinson's disease: A dose escalation, open-label, phase 1/2 trial. Lancet. https://doi.org/10.1016/S0140-6736(13)61939-X

Harms, A. S., Ferreira, S. A., & Romero-Ramos, M. (2021). Periphery and brain, innate and adaptive immunity in Parkinson's disease. *Acta neuropathologica*, *141*(4), 527–545. https://doi.org/10.1007/s00401-021-02268-5

Harms, A. S., Ferreira, S. A., Romero-Ramos, M., & Peralta Ramos, J. M. (2021). Monocytes and the pathophysiology of Parkinson's disease. *Translational Neurodegeneration, 10*(1), 26. https://doi.org/10.1186/s40035-021-00260-x

Harms, A.S., Thome, A.D., Yan, Z., Schonhoff, A.M., Williams, G.P., Li, X., Liu, Y., Qin, H., Benveniste, E.N., Standaert, D.G., 2018. Peripheral monocyte entry is required for alpha-Synuclein induced inflammation and Neurodegeneration in a model of Parkinson disease. Exp. Neurol. https://doi.org/10.1016/j.expneurol.2017.11.010

Hashimoto, D., Chow, A., Noizat, C., Teo, P., Beasley, M. B., Leboeuf, M., Becker, C. D., See, P., Price, J., Lucas, D., Greter, M., Mortha, A., Boyer, S. W., Forsberg, E. C., Tanaka, M., van Rooijen, N., García-Sastre, A., Stanley, E. R., Ginhoux, F., & Merad, M. (2013). *Tissue-resident macrophages self-maintain locally throughout adult life with minimal contribution from circulating monocytes.* Immunity, 38(4), 792–804. https://doi.org/10.1016/j.immuni.2013.04.004

Haynes, S.E., Hollopeter, G., Yang, G., Kurpius, D., Dailey, M.E., Gan, W.B., Julius, D., 2006. The P2Y12 receptor regulates microglial activation by extracellular nucleotides. Nat. Neurosci. https://doi.org/10.1038/nn1805

Healy DG, Falchi M, O'Sullivan SS, Bonifati V, Durr A, Bressman S, Brice A, Aasly J, Zabetian CP, Goldwurm S, Ferreira JJ, Tolosa E, Kay DM, Klein C, Williams DR, Marras C, Lang AE, Wszolek ZK, Berciano J, et al.; International LRRK2 Consortium. *Phenotype, genotype, and worldwide genetic penetrance of LRRK2-associated Parkinson's disease: a case–control study. Lancet Neurology.* 2008;7(7):583–590. doi:10.1016/S1474-4422(08)70117-0. https://pubmed.ncbi.nlm.nih.gov/18539534/

Heinzel, S., Berg, D., Gasser, T., Chen, H., Yao, C., Postuma, R. B., Adler, C. H., Bloem, B. R., Chan, P., Deuschl, G., Dubois, B., Goetz, C. G., Halliday, G. M., Hardy, J., Lang, A. E., Litvan, I., Marek, K., Obeso, J. A., Oertel, W., Olanow, C. W., Poewe, W., & Stern, M. (2019). Update of the MDS research criteria for prodromal Parkinson's disease. *Movement Disorders*, 34(10), 1464-1470. https://doi.org/10.1002/mds.27802

Henchcliffe, C., Beal, M.F., 2008. Mitochondrial biology and oxidative stress in Parkinson disease pathogenesis. *Nature Clinical Practice Neurology* 4(11), 600–609. https://doi.org/10.1038/ncpneuro0924

Henderson, M.X., Trojanowski, J.Q., Lee, V.M.Y., 2019. α-Synuclein pathology in Parkinson's disease and related α-synucleinopathies. Neurosci. Lett. https://doi.org/10.1016/j.neulet.2019.134316

Herculano-Houzel, S., 2009. The human brain in numbers: A linearly scaled-up primate brain. Front. Hum. Neurosci. https://doi.org/10.3389/neuro.09.031.2009

Hernán, M.A., Zhang, S.M., Rueda-DeCastro, A.M., Colditz, G.A., Speizer, F.E., Ascherio, A., 2001. Cigarette smoking and the incidence of Parkinson's disease in two prospective studies. Ann. Neurol. https://doi.org/10.1002/ana.10028

Hirsch L, Jette N, Frolkis A, Steeves T, Pringsheim T. The Incidence of Parkinson's Disease: A Systematic Review and Meta-Analysis. Neuroepidemiology. 2016;46(4):292–300. doi:10.1159/000445751.

Hirsch, E.C., Hunot, S., 2009. Neuroinflammation in Parkinson's disease: a target for neuroprotection? Lancet Neurol. https://doi.org/10.1016/S1474-4422(09)70062-6

Hoffmann, A., Ettle, B., Bruno, A., Kulinich, A., Hoffmann, A.C., von Wittgenstein, J., Winkler, J., Xiang, W., Schlachetzki, J.C.M., 2016. Alpha-synuclein activates BV2 microglia dependent on its aggregation state. Biochem. Biophys. Res. Commun. https://doi.org/10.1016/j.bbrc.2016.09.109

Hoffmann, A., Ettle, B., Gao, F., Ryazanov, S., Xin, W., Steiner, J.A., Maetzler, W., Simons, M., Schulz, J.B., 2023.Cross-seeding of α-synuclein and tau drives neurodegeneration in synucleinopathies and tauopathies. *Nature Communications* 14, 1860. https://doi.org/10.1038/s41467-023-37507-8

Hokenson, M.J., Uversky, V.N., Goers, J., Yamin, G., Munishkina, L.A., Fink, A.L., 2004. Role of Individual Methionines in the Fibrillation of Methionine-Oxidized α- Synuclein. Biochemistry. https://doi.org/10.1021/bi049979h

Homayoun, H., 2018. Parkinson disease. Ann. Intern. Med. 169, ITC33–ITC47. https://doi.org/10.7326/AITC201809040

Huang, E., Qu, D., Huang, T., Rizzi, N., Boonying, W., Krolak, D., Ciana, P., Woulfe, J., Klein, C., Slack, R.S., Figeys, D., Park, D.S., 2017. PINK1-mediated phosphorylation of LETM1 regulates mitochondrial calcium transport and protects neurons against mitochondrial stress. Nat. Commun. https://doi.org/10.1038/s41467-017-01435-1

Huang, M., Long, A., Hao, L., Shi, Z., & Zhang, M. (2025). Astrocyte in Neurological Disease: Pathogenesis and Therapy. *MedComm*, *6*(8), e70299. https://doi.org/10.1002/mco2.70299

Huang, W.S., Chiang, Y.H., Lin, J.C., Chou, Y.H., Cheng, C.Y., Liu, R.S., 2003. Crossover study of 99mTc-TRODAT-1 SPECT and 18F-FDOPA PET in Parkinson's disease patients. J. Nucl. Med.

Hughes, A. J., Daniel, S. E., Kilford, L., & Lees, A. J. (1992). Accuracy of clinical diagnosis of idiopathic Parkinson's disease: a clinico-pathological study of 100 cases. *Journal of neurology, neurosurgery, and psychiatry*, *55*(3), 181–184. https://doi.org/10.1136/jnnp.55.3.181

Hutchison, W. D., Lozano, A. M., Davis, K. D., Saint-Cyr, J. A., Lang, A. E., & Dostrovsky, J. O. (1994). Differential neuronal activity in segments of globus pallidus in Parkinson's disease patients. *Neuroreport*, *5*(12), 1533–1537. https://doi.org/10.1097/00001756-199407000-00031

Iliff, J.J., Wang, M., Liao, Y., Plogg, B.A., Peng, W., Gundersen, G.A., Benveniste, H., Vates, G.E., Deane, R., Goldman, S.A., Nagelhus, E.A., Nedergaard, M., 2012. A paravascular pathway facilitates CSF flow through the brain parenchyma and the clearance of interstitial solutes, including amyloid β. *Science Translational Medicine* 4(147), 147ra111. https://doi.org/10.1126/scitranslmed.3003748

Imamura, K., Hishikawa, N., Sawada, M., Nagatsu, T., Yoshida, M., & Hashizume, Y. (2003). Distribution of major histocompatibility complex class II-positive microglia and cytokine profile of Parkinson's disease brains. *Acta neuropathologica*, *106*(6), 518–526. https://doi.org/10.1007/s00401-003-0766-2

Ishikawa, S., Taira, T., Niki, T., Takahashi-Niki, K., Maita, C., Maita, H., Ariga, H., Iguchi- Ariga, S.M.M., 2009. Oxidative status of DJ-1-dependent activation of dopamine synthesis through interaction of tyrosine hydroxylase and 4-dihydroxy-L- phenylalanine (L-DOPA) decarboxylase with DJ-1. J. Biol. Chem. https://doi.org/10.1074/jbc.M109.019950

Jafari, S., Etminan, M., Aminzadeh, F., Samii, A., 2013. Head injury and risk of Parkinson disease: a systematic review and meta-analysis. *Movement Disorders* 28(9), 1222–1229. https://doi.org/10.1002/mds.25458

Jan, A., Gonçalves, N. P., Vaegter, C. B., Jensen, P. H., & Ferreira, N. (2021). *The prion-like spreading of alpha-synuclein in neurodegenerative diseases. International Journal of Molecular Sciences, 22*(15), 8338. https://doi.org/10.3390/ijms22158338

Jankovic, J., 2008. Parkinson's disease: Clinical features and diagnosis. J. Neurol. Neurosurg. Psychiatry. https://doi.org/10.1136/jnnp.2007.131045

Jewell, S., Herath, A. M., & Gordon, R. (2022). Inflammasome Activation in Parkinson's Disease. *Journal of Parkinson's disease*, *12*(s1), S113–S128. https://doi.org/10.3233/JPD-223338

Ji, R., Tian, S., Lu, H.J., Lu, Qingjun, Zheng, Y., Wang, X., Ding, J., Li, Q., Lu, Qingxian, 2013. TAM Receptors Affect Adult Brain Neurogenesis by Negative Regulation of Microglial Cell Activation. J. Immunol. https://doi.org/10.4049/jimmunol.1302229

Jin, S., Plikus, M.V. & Nie, Q. CellChat for systematic analysis of cell–cell communication from single-cell transcriptomics. Nat Protoc 20, 180–219 (2025). https://doi.org/10.1038/s41596-024-01045-4

Jung, S., Aliberti, J., Graemmel, P., Sunshine, M.J., Kreutzberg, G.W., Sher, A., Littman, D.R., 2000. Analysis of Fractalkine Receptor CX3CR1 Function by Targeted Deletion and Green Fluorescent Protein Reporter Gene Insertion. Mol. Cell. Biol. https://doi.org/10.1128/mcb.20.11.4106-4114.2000

Kalia, L. V., & Lang, A. E. (2015). Parkinson's disease. *Lancet (London, England)*, *386*(9996), 896–912. https://doi.org/10.1016/S0140-6736(14)61393-3

Kang, L., Moriarty, G.M., Woods, L.A., Ashcroft, A.E., Radford, S.E., Baum, J., 2012. N- terminal acetylation of α-synuclein induces increased transient helical propensity and decreased aggregation rates in the intrinsically disordered monomer. Protein Sci. https://doi.org/10.1002/pro.2088

Karikari, A. A., McFleder, R. L., Ribechini, E., Blum, R., Brüttel, V., Knorr, S., Gehmeyr, M., Volkmann, J., Brotchie, J. M., Ahsan, F., Haack, B., Monoranu, C. M., Keber, U., Yeghiazaryan, R., Pagenstecher, A., Heckel, T., Bischler, T., Wischhusen, J., Koprich, J. B., … Ip, C. W. (2022). *Neurodegeneration by α-synuclein-specific T cells in AAV-A53T-α-synuclein Parkinson's disease mice*. *Brain, Behavior, and Immunity, 101*, 194-210. https://doi.org/10.1016/j.bbi.2022.01.007

Keller, M.F., Saad, M., Bras, J., Bettella, F., Nicolaou, N., Simón-Sánchez, J., Mittag, F., Buchel, F., Sharma, M., Gibbs, J.R., Schulte, C., Moskvina, V., Durr, A., Guerreiro, R., Hernandez, D.G., Brice, A., Steffens, M., Gasser, T., Heutink, P., Wood, N.W., Hardy, J., Martinez, M., Singleton, A.B., Nalls, M.A., 2012. Using genome-wide complex trait analysis to quantify 'missing heritability' in Parkinson's disease. *Human Molecular Genetics* 21(22), 4996–5009. https://doi.org/10.1093/hmg/dds335

Kersten, K., Hu, K. H., Combes, A. J., Samad, B., Harwin, T., Ray, A., Rao, A. A., Cai, E., Marchuk, K., Artichoker, J., Courau, T., Shi, Q., Belk, J., Satpathy, A. T., & Krummel, M. F. (2022). Spatiotemporal co-dependency between macrophages and exhausted $CD8^+$ T cells in cancer. *Cancer cell*, *40*(6), 624–638.e9. https://doi.org/10.1016/j.ccell.2022.05.004

Kitada, T., Asakawa, S., Hattori, N., Matsumine, H., Yamamura, Y., Minoshima, S., Yokochi, M., Mizuno, Y., Shimizu, N., 1998. Mutations in the parkin gene cause autosomal recessive juvenile parkinsonism. Nature. https://doi.org/10.1038/33416

Klein, C., Westenberger, A., 2012. Genetics of Parkinson's disease. Cold Spring Harb. Perspect. Med. https://doi.org/10.1101/cshperspect.a008888

Klichinsky, M., Ruella, M., Shestova, O., Lu, X. M., Best, A., Zhen, L., Anderson, N. E., Petty, N., Blouch, K., Yashiro-Ohtani, Y., Wallace, S. R., Kozlowski, M. S., Marchione, D. M., Garcia, B. A., June, C. H., Gill, S. (2020). *Human chimeric antigen receptor macrophages for cancer immunotherapy. Nature Biotechnology, 38*(8), 947-953. https://doi.org/10.1038/s41587-020-0462-y

Knowles, T.P.J., Waudby, C.A., Devlin, G.L., Cohen, S.I.A., Aguzzi, A., Vendruscolo, M., Terentjev, E.M., Welland, M.E., Dobson, C.M., 2009. An analytical solution to the kinetics of breakable filament assembly. *Science* 326(5959), 1533–1537. https://doi.org/10.1126/science.1178250

Konstantin Nissen, S., Farmen, K., Carstensen, M., Schulte, C., Goldeck, D., Brockmann, K., & Romero-Ramos, M. (2022). Changes in CD163+, CD11b+, and CCR2+ peripheral monocytes relate to Parkinson's disease and cognition. *Brain, behavior, and immunity*, *101*, 182–193. https://doi.org/10.1016/j.bbi.2022.01.005

Kontopoulos, E., Parvin, J.D., & Feany, M.B. (2006). Alpha-synuclein acts in the nucleus to inhibit histone acetylation and promote neurotoxicity. *Human Molecular Genetics*, 15(20), 3012–3023. https://doi.org/10.1093/hmg/ddl243

Kordower, J.H., Chu, Y., Hauser, R.A., Freeman, T.B., Olanow, C.W., 2008. Lewy body- like pathology in long-term embryonic nigral transplants in Parkinson's disease. Nat. Med. https://doi.org/10.1038/nm1747

Kouli, A., Camacho, M., Allinson, K. *et al.* Neuroinflammation and protein pathology in Parkinson's disease dementia. *acta neuropathol commun* 8, 211 (2020). https://doi.org/10.1186/s40478-020-01083-5

Kravitz, A. V., Freeze, B.S., Parker, P.R.L., Kay, K., Thwin, M.T., Deisseroth, K., Kreitzer, A.C., 2010. Regulation of parkinsonian motor behaviours by optogenetic control of basal ganglia circuitry. Nature. https://doi.org/10.1038/nature09159

Kustrimovic, N., Comi, C., Magistrelli, L. *et al.* Parkinson's disease patients have a complex phenotypic and functional Th1 bias: cross-sectional studies of CD4+ Th1/Th2/T17 and Treg in drug-naïve and drug-treated patients. *J Neuroinflammation*15, 205 (2018). https://doi.org/10.1186/s12974-018-1248-8

Kustrimovic, N., Rasini, E., Legnaro, M., Bombelli, R., Aleksic, I., Blandini, F., Furlan, R., Comi, C., Minafra, B., Riboldazzi, G., & Marino, F. (2016). Dopaminergic receptors on $CD4^+$ T cells: Negative correlation with motor impairment in Parkinson's disease. *Scientific Reports, 6*, 33738. https://doi.org/10.1038/srep33738

Kwon, S., Iba, M., Masliah, E., Kim, C., 2019. Targeting microglial and neuronal toll-like receptor 2 in synucleinopathies. Exp. Neurobiol. https://doi.org/10.5607/en.2019.28.5.547

Lang, A. E., Siderowf, A. D., Macklin, E. A., Poewe, W., Brooks, D. J., Fernandez, H. H., Rascol, O., Giladi, N., Stocchi, F., Tanner, C. M., Postuma, R. B., Simon, D. K., Tolosa, E., Mollenhauer, B., Cedarbaum, J. M., Fraser, K., Xiao, J., Evans, K. C., Graham, D. L., Sapir, I., … SPARK Investigators (2022). Trial of Cinpanemab in Early Parkinson's Disease. *The New England journal of medicine*, *387*(5), 408–420. https://doi.org/10.1056/NEJMoa2203395

Lashuel, H.A., Overk, C.R., Oueslati, A., & Masliah, E. (2013). The many faces of α-synuclein: From structure and toxicity to therapeutic target. *Nature Reviews Neuroscience*, 14(1), 38–48. https://doi.org/10.1038/nrn3406

Lashuel, H.A., Petre, B.M., Wall, J., Simon, M., Nowak, R.J., Walz, T., Lansbury, P.T. Jr., 2002. α-Synuclein, especially the Parkinson's disease–associated mutants, forms pore-like annular and tubular protofibrils. *Journal of Molecular Biology* 322(5), 1089–1102. https://doi.org/10.1016/S0022-2836(02)00735-0

Lastres-Becker, I., Ulusoy, A., Innamorato, N.G., Sahin, G., Rábano, A., Kirik, D., Cuadrado, A., 2012. α-Synuclein expression and Nrf2 deficiency cooperate to aggravate protein aggregation, neuronal death and

inflammation in early-stage Parkinson's disease. *Human Molecular Genetics* 21(14), 3173–3192. https://doi.org/10.1093/hmg/dds143

Lautenschläger, J., Kaminski, C. F., & Kaminski Schierle, G. S. (2017). α-Synuclein - Regulator of Exocytosis, Endocytosis, or Both?. *Trends in cell biology*, *27*(7), 468–479. https://doi.org/10.1016/j.tcb.2017.02.002

Lavin, Y., Winter, D., Blecher-Gonen, R., David, E., Keren-Shaul, H., Merad, M., Jung, S., Amit, I., 2014. Tissue-resident macrophage enhancer landscapes are shaped by the local microenvironment. Cell. https://doi.org/10.1016/j.cell.2014.11.018

Lawson, L.J., Perry, V.H., Dri, P., Gordon, S., 1990. Heterogeneity in the distribution and morphology of microglia in the normal adult mouse brain. Neuroscience. https://doi.org/10.1016/0306-4522(90)90229-W

Lee, H. J., Suk, J. E., Bae, E. J., Lee, J. H., Paik, S. R., & Lee, S. J. (2008). Assembly-dependent endocytosis and clearance of extracellular alpha-synuclein. *The international journal of biochemistry & cell biology*, *40*(9), 1835–1849. https://doi.org/10.1016/j.biocel.2008.01.017

Lee, H.-J., Suk, J.-E., Bae, E.-J., Lee, J.-H., Paik, S. R., & Lee, S.-J. (2008). *Assembly-dependent endocytosis and clearance of extracellular alpha-synuclein. International Journal of Biochemistry & Cell Biology, 40*(9), 1835 1849. https://doi.org/10.1016/j.biocel.2008.01.017
Lee, H.-J., Suk, J.-E., Patrick, C., Bae, E.-J., Cho, J.-H., Rho, S., Hwang, D., Masliah, E., & Lee, S.-J. (2010). *Direct transfer of α-synuclein from neuron to astroglia causes inflammatory responses in synucleinopathies. Journal of Biological Chemistry, 285*(12), 9262–9272. https://doi.org/10.1074/jbc.M109.081125

Lee, H.J., Kim, C., Lee, S.J., 2010a. Alpha-synuclein stimulation of astrocytes: Potential role for neuroinflammation and neuroprotection. Oxid. Med. Cell. Longev. https://doi.org/10.4161/oxim.3.4.12809

Lee, H.J., Patel, S., Lee, S.J., 2005. Intravesicular localization and exocytosis of α- synuclein and its aggregates. J. Neurosci. https://doi.org/10.1523/JNEUROSCI.0692-05.2005

Lee, H.J., Suk, J.E., Patrick, C., Bae, E.J., Cho, J.H., Rho, S., Hwang, D., Masliah, E., Lee, S.J., 2010b. Direct transfer of α-synuclein from neuron to astroglia causes inflammatory responses in synucleinopathies. J. Biol. Chem. https://doi.org/10.1074/jbc.M109.081125

Lehnardt, S., Massillon, L., Follett, P., Jensen, F.E., Ratan, R., Rosenberg, P.A., Volpe, J.J., Vartanian, T., 2003. Activation of innate immunity in the CNS triggers neurodegeneration through a Toll-like receptor 4-dependent pathway. Proc. Natl. Acad. Sci. U. S. A. https://doi.org/10.1073/pnas.1432609100

Lehrman, E.K., Wilton, D.K., Litvina, E.Y., Welsh, C.A., Chang, S.T., Frouin, A., Walker, A.J., Heller, M.D., Umemori, H., Chen, C., Stevens, B., 2018. CD47 Protects Synapses from Excess Microglia-Mediated Pruning during Development. Neuron. https://doi.org/10.1016/j.neuron.2018.09.017

Letiembre, M., Liu, Y., Walter, S., Hao, W., Pfander, T., Wrede, A., Schulz-Schaeffer, W., Fassbender, K., 2009. Screening of innate immune receptors in neurodegenerative diseases: A similar pattern. Neurobiol. Aging. https://doi.org/10.1016/j.neurobiolaging.2007.08.018

Levine, P. M., Galesic, A., Balana, A. T., Mahul-Mellier, A. L., Navarro, M. X., De Leon, C. A., Lashuel, H. A., & Pratt, M. R. (2019). α-Synuclein O-GlcNAcylation alters aggregation and toxicity, revealing certain residues as potential inhibitors of Parkinson's disease. *Proceedings of the National Academy of Sciences of the United States of America*, *116*(5), 1511–1519. https://doi.org/10.1073/pnas.1808845116

LeWitt, P.A., Rezai, A.R., Leehey, M.A., Ojemann, S.G., Flaherty, A.W., Eskandar, E.N., Kostyk, S.K., Thomas, K., Sarkar, A., Siddiqui, M.S., Tatter, S.B., Schwalb, J.M., Poston, K.L., Henderson, J.M., Kurlan, R.M., Richard, I.H., Van Meter, L., Sapan, C. V., During, M.J., Kaplitt, M.G., Feigin, A., 2011. AAV2-GAD gene therapy for advanced Parkinson's disease: A double-blind, sham-surgery controlled, randomised trial. Lancet Neurol. https://doi.org/10.1016/S1474-4422(11)70039-4

Li, J., Uversky, V.N., Fink, A.L., 2001. Effect of familial Parkinson's disease point mutations A30P and A53T on the structural properties, aggregation, and fibrillation of human α-synuclein. Biochemistry. https://doi.org/10.1021/bi010616g

Li, J.Y., Englund, E., Holton, J.L., Soulet, D., Hagell, P., Lees, A.J., Lashley, T., Quinn, N.P., Rehncrona, S., Björklund, A., Widner, H., Revesz, T., Lindvall, O., Brundin, P., 2008. Lewy bodies in grafted neurons in subjects with Parkinson's disease suggest host-to-graft disease propagation. Nat. Med. https://doi.org/10.1038/nm1746

Li, W.W., Yang, R., Guo, J.C., Ren, H.M., Zha, X.L., Cheng, J.S., Cai, D.F., 2007. Localization of α-synuclein to mitochondria within midbrain of mice. Neuroreport. https://doi.org/10.1097/WNR.0b013e3282f03db4

Li, X., Liu, G., Yang, L., Li, Z., Zhang, Z., Xu, Z., Qian, J., Wang, X., Zhao, S., Liu, W., 2021. EGFR signalling regulates the generation of astrocyte progenitor cells from radial glia in the developing cerebral cortex. Mol Med. 2022 May 4;28:50. doi: 10.1186/s10020-022-00478-5

Liberatore, G.T., Jackson-Lewis, V., Vukosavic, S., Mandir, A.S., Vila, M., Mcauliffe, W.G., Dawson, V.L., Dawson, T.M., Przedborski, S., 1999. Inducible nitric oxide synthase stimulates dopaminergic neurodegeneration in the MPTP model of Parkinson disease. Nat. Med. https://doi.org/10.1038/70978

Liddelow, S. A., & Barres, B. A. (2017). Reactive Astrocytes: Production, Function, and Therapeutic Potential. *Immunity*, *46*(6), 957–967. https://doi.org/10.1016/j.immuni.2017.06.006

Liddelow, S. A., Guttenplan, K. A., Clarke, L. E., Bennett, F. C., Bohlen, C. J., Schirmer, L., Bennett, M. L., Münch, A. E., Chung, W. S., Peterson, T. C., Wilton, D. K., Frouin, A., Napier, B. A., Panicker, N., Kumar, M., Buckwalter, M. S., Rowitch, D. H., Dawson, V. L., Dawson, T. M., ... & Barres, B. A. (2017). *Neurotoxic reactive astrocytes are induced by activated microglia. Nature, 541*(7638), 481–487. https://doi.org/10.1038/nature21029

Liddelow, S.A., Guttenplan, K.A., Clarke, L.E., Bennett, F.C., Bohlen, C.J., Schirmer, L., Bennett, M.L., Münch, A.E., Chung, W.S., Peterson, T.C., Wilton, D.K., Frouin, A., Napier, B.A., Panicker, N., Kumar, M., Buckwalter, M.S., Rowitch, D.H., Dawson, V.L., Dawson, T.M., Stevens, B., Barres, B.A., 2017. Neurotoxic reactive astrocytes are induced by activated microglia. Nature. https://doi.org/10.1038/nature21029

Liebner, S., Dijkhuizen, R.M., Reiss, Y., Plate, K.H., Agalliu, D., Constantin, G., 2018. Functional morphology of the blood–brain barrier in health and disease. Acta Neuropathol. https://doi.org/10.1007/s00401-018-1815-1

Limanaqi, F., Zecchini, S., Ogno, P., Artusa, V., Fenizia, C., Saulle, I., Vanetti, C., Garziano, M., Strizzi, S., Trabattoni, D., Clerici, M., & Biasin, M. (2024). Alpha-synuclein shapes monocyte and macrophage cell biology and functions by bridging alterations of autophagy and inflammatory pathways. *Frontiers in cell and developmental biology*, *12*, 1421360. https://doi.org/10.3389/fcell.2024.1421360

Lindestam Arlehamn, C. S., Garretti, F., Sulzer, D., & Sette, A. (2020). *α-Synuclein-specific T cell reactivity is associated with preclinical and early Parkinson's disease.* Nature Communications, 11, 1875. https://doi.org/10.1038/s41467-020-15626-w

Lindestam Arlehamn, C.S., Garretti, F., Sulzer, D., Sette, A., (2019). Roles for the adaptive immune system in Parkinson's and Alzheimer's diseases. Curr. Opin. Immunol. https://doi.org/10.1016/j.coi.2019.07.004 Little, S., & Brown, P. (2014). The functional role of beta oscillations in Parkinson's disease. *Parkinsonism & related disorders*, *20 Suppl 1*, S44–S48. https://doi.org/10.1016/S1353-8020(13)70013-0

Lindström, V., Gustafsson, G., Sanders, L. H., Howlett, E. H., Sigvardson, J., Kasrayan, A., Ingelsson, M., Bergström, J., & Erlandsson, A. (2017). *Extensive uptake of α-synuclein oligomers in astrocytes results in sustained intracellular deposits and mitochondrial damage. Molecular Cell Neuroscience, 82*, 143–156. https://doi.org/10.1016/j.mcn.2017.04.009

Liu, X., Li, Y., Xu, X., & Cui, L. (2021). *Astrocytes in neural circuits: Key factors in synaptic development and plasticity. Frontiers in Molecular Neuroscience, 14*, 729273. https://doi.org/10.3389/fnmol.2021.729273

Loria, F., Vargas, J.Y., Bousset, L., Syan, S., Salles, A., Melki, R., Zurzolo, C., 2017. α-Synuclein transfer between neurons and astrocytes indicates that astrocytes play a role in the spread of α-synuclein pathology. *Acta Neuropathologica* 134(5), 789–808. https://doi.org/10.1007/s00401-017-1746-2

Luk, K.C., Kehm, V., Carroll, J., Zhang, B., O'Brien, P., Trojanowski, J.Q., Lee, V.M.Y., 2012a. Pathological α-synuclein transmission initiates Parkinson-like neurodegeneration in nontransgenic mice. Science (80-.). https://doi.org/10.1126/science.1227157

Luk, K.C., Kehm, V.M., Zhang, B., O'Brien, P., Trojanowski, J.Q., Lee, V.M.Y., 2012b. Intracerebral inoculation of pathological α-synuclein initiates a rapidly progressive neurodegenerative α-synucleinopathy in mice. J. Exp. Med. https://doi.org/10.1084/jem.20112457

Luk, K.C., Song, C., O'Brien, P., Stieber, A., Branch, J.R., Brunden, K.R., Trojanowski, J.Q., Lee, V.M.Y., 2009. Exogenous α-synuclein fibrils seed the formation of Lewy body-like intracellular inclusions in cultured cells. Proc. Natl. Acad. Sci. U. S. A. https://doi.org/10.1073/pnas.0908005106

Mahlknecht, P., Marini, K., Werkmann, M. *et al.* Prodromal Parkinson's disease: hype or hope for disease-modification trials?. *Transl Neurodegener* **11**, 11 (2022). https://doi.org/10.1186/s40035-022-00286-1

Malgieri, G., & Eliezer, D. (2008). Structural effects of Parkinson's disease linked DJ-1 mutations. *Protein science : a publication of the Protein Society*, *17*(5), 855–868. https://doi.org/10.1110/ps.073411608

Maltsev, A.S., Ying, J., Bax, A., 2012. Impact of N-terminal acetylation of α-synuclein on its random coil and lipid binding properties. Biochemistry. https://doi.org/10.1021/bi300642h

Mantovani, A., Sica, A., Sozzani, S., Allavena, P., Vecchi, A., & Locati, M. (2004). *The chemokine system in diverse forms of macrophage activation and polarization.* Trends in Immunology, 25(12), 677–686. https://doi.org/10.1016/j.it.2004.09.015

Mao, X., Ou, M.T., Karuppagounder, S.S., Kam, T.I., Yin, X., Xiong, Y., Ge, P., Umanah, G.E., Brahmachari, S., Shin, J.H., Kang, H.C., Zhang, J., Xu, J., Chen, R., Park, H., Andrabi, S.A., Kang, S.U., Gonçalves, R.A., Liang, Y., Zhang, S., Qi, C., Lam, S., Keiler, J.A., Tyson, J., Kim, D., Panicker, N., Yun, S.P., Workman, C.J., Vignali, D.A.A., Dawson, V.L., Ko, H.S., Dawson, T.M., 2016. Pathological α-synuclein transmission initiated by binding lymphocyte-activation gene 3. Science (80-.). https://doi.org/10.1126/science.aah3374

Marín-Teva, J.L., Dusart, I., Colin, C., Gervais, A., Van Rooijen, N., Mallat, M., 2004. Microglia Promote the Death of Developing Purkinje Cells. Neuron. https://doi.org/10.1016/S0896-6273(04)00069-8

Maroteaux, L., Campanelli, J.T., Scheller, R.H., 1988. Synuclein: A neuron-specific protein localized to the nucleus and presynaptic nerve terminal. J. Neurosci. https://doi.org/10.1523/jneurosci.08-08-02804.1988

Marras, C., Beck, J.C., Bower, J.H. *et al.* Prevalence of Parkinson's disease across North America. *npj Parkinson's Disease* 4, 21 (2018). https://doi.org/10.1038/s41531-018-0058-0

Marsden, C.D., 1983. Neuromelanin and Parkinson's disease. J. Neural Transm. Suppl. https://doi.org/10.1097/00008390-199409001-00069

Marsili, L., Rizzo, G., Colosimo, C., 2018. Diagnostic criteria for Parkinson's disease: From James Parkinson to the concept of prodromal disease. *Frontiers in Neurology* 9, 156. https://doi.org/10.3389/fneur.2018.00156

Martinez, T.N., Greenamyre, J.T., 2012. Toxin models of mitochondrial dysfunction in Parkinson's disease. Antioxidants Redox Signal. 16, 920–934. https://doi.org/10.1089/ars.2011.4033

Masliah, E., Rockenstein, E., Veinbergs, I., Mallory, M., Hashimoto, M., Takeda, A., ... & Mucke, L. (1996). Dopaminergic loss and inclusion body formation in α-synuclein mice: implications for neurodegenerative disorders. *Science*, 287(5456), 1265–1269. https://doi.org/10.1126/science.287.5456.1265

Mass, E., Ballesteros, I., Farlik, M., Halbritter, F., Günther, P., Crozet, L., Jacome-Galarza, C. E., Händler, K., Klughammer, J., Kobayashi, Y., & Geissmann, F. (2016). Specification of tissue-resident macrophages during organogenesis. *Science, 353*(6304), aaf4238. https://doi.org/10.1126/science.aaf4238

Mass, E., Nimmerjahn, F., Kierdorf, K., & Schlitzer, A. (2023). Tissue-specific macrophages: how they develop and choreograph tissue biology. *Nature Reviews Immunology, 23*(7), 467–486. https://doi.org/10.1038/s41577-023-00848-y

Masuda, T., Sankowski, R., Staszewski, O., Böttcher, C., Amann, L., Sagar, Scheiwe, C., Nessler, S., Kunz, P., van Loo, G., Coenen, V.A., Reinacher, P.C., Michel, A., Sure, U., Gold, R., Grün, D., Priller, J., Stadelmann, C., Prinz, M., 2019. Spatial and temporal heterogeneity of mouse and human microglia at single-cell resolution. Nature. https://doi.org/10.1038/s41586-019-0924-x

Matcovitch-Natan, O., Winter, D.R., Giladi, A., Aguilar, S.V., Spinrad, A., Sarrazin, S., Ben-Yehuda, H., David, E., González, F.Z., Perrin, P., Keren-Shaul, H., Gury, M., Lara-Astaiso, D., Thaiss, C.A., Cohen, M., Halpern, K.B., Baruch, K., Deczkowska, A., Lorenzo-Vivas, E., Itzkovitz, S., Elinav, E., Sieweke, M.H., Schwartz, M., Amit, I., 2016. Microglia development follows a stepwise program to regulate brain homeostasis. Science (80-.). https://doi.org/10.1126/science.aad8670

Matias, I., Morgado, J., & Gomes, F. C. A. (2019). Astrocyte heterogeneity: impact to brain aging and disease. *Frontiers in Aging Neuroscience, 11*, 59. https://doi.org/10.3389/fnagi.2019.00059

Matsuo, K., Asamitsu, S., Maeda, K., Suzuki, H., Kawakubo, K., Komiya, G., Kudo, K., Sakai, Y., Hori, K., Ikenoshita, S., Usuki, S., Funahashi, S., Oizumi, H., Takeda, A., Kawata, Y., Mizobata, T., Shioda, N., & Yabuki, Y. (2024). RNA G-quadruplexes form scaffolds that promote neuropathological α-synuclein aggregation. *Cell*, *187*(24), 6835–6848.e20. https://doi.org/10.1016/j.cell.2024.09.037

Mavroeidi, P., Arvanitakis, Z., & Emmanouilidou, E. (2022). *Exosomes in α-synucleinopathies: Propagators of pathology or therapeutic agents? Biomolecules, 12*(7), 957. https://doi.org/10.3390/biom12070957

Mayeux R, Marder K, Cote LJ, et al. The frequency of idiopathic Parkinson's disease by age, ethnic group, and sex in northern Manhattan, 1988-1993. Am J Epidemiol 1995; 142: 820–27.

McGeer, P. L., Itagaki, S., Boyes, B. E., & McGeer, E. G. (1988). Reactive microglia are positive for HLA-DR in the substantia nigra of Parkinson's and Alzheimer's disease brains. *Neurology*, *38*(8), 1285–1291. https://doi.org/10.1212/wnl.38.8.1285

McGregor, M.M., Nelson, A.B., 2019. Circuit Mechanisms of Parkinson's Disease. Neuron. https://doi.org/10.1016/j.neuron.2019.03.004

McLane, L. M., Abdel-Hakeem, M. S., & Wherry, E. J. (2019). CD8 T Cell Exhaustion During Chronic Viral Infection and Cancer. *Annual review of immunology*, *37*, 457–495. https://doi.org/10.1146/annurev-immunol-041015-055318

Meade, R.M., Fairlie, D.P., Mason, J.M., 2019. Alpha-synuclein structure and Parkinson's disease - Lessons and emerging principles. Mol. Neurodegener. https://doi.org/10.1186/s13024-019-0329-1

Medana, I.M., Gallimore, A., Oxenius, A., Martinic, M.M.A., Wekerle, H., Neumann, H., 2000. MHC class I-restricted killing of neurons by virus-specific CD8+ T lymphocytes is effected through the Fas/FasL, but not the perforin pathway. Eur. J. Immunol. https://doi.org/10.1002/1521-4141(200012)30:12<3623::AID-IMMU3623>3.0.CO;2-F

Mehra, S., Sahay, S., Maji, S.K., 2019. α-Synuclein misfolding and aggregation: Implications in Parkinson's disease pathogenesis. Biochim. Biophys. Acta - Proteins Proteomics. https://doi.org/10.1016/j.bbapap.2019.03.001

Mehta, A. K., Gracias, D. T., & Croft, M. (2018). TNF activity and T cells. *Cytokine*, *101*, 14–18. https://doi.org/10.1016/j.cyto.2016.08.003

Mendez, I., Sanchez-Pernaute, R., Cooper, O., Viñuela, A., Ferrari, D., Björklund, L., Dagher, A., & Isacson, O. (2005). Cell type analysis of functional fetal dopamine cell suspension transplants in the striatum and substantia nigra of patients with Parkinson's disease. *Brain : a journal of neurology*, *128*(Pt 7), 1498–1510. https://doi.org/10.1093/brain/awh510

Merola, A., Zibetti, M., Angrisano, S., Rizzi, L., Ricchi, V., Artusi, C.A., Lanotte, M., Rizzone, M.G., Lopiano, L., 2011. Parkinson's disease progression at 30 years: A study of subthalamic deep brain-stimulated patients. Brain. https://doi.org/10.1093/brain/awr121

Mestre, H., Tithof, J., Du, T., Song, W., Peng, W., Sweeney, A.M., Olveda, G., Thomas, J.H., Nedergaard, M., Kelley, D.H., 2018. Flow of cerebrospinal fluid is driven by arterial pulsations and is reduced in hypertension. *Nature Communications* 9, 4878. https://doi.org/10.1038/s41467-018-07318-3

Meuth, S.G., Herrmann, A.M., Simon, O.J., Siffrin, V., Melzer, N., Bittner, S., Meuth, P., Langer, H.F., Hallermann, S., Boldakowa, N., Herz, J., Munsch, T., Landgraf, P., Aktas, O., Heckmann, M., Lessmann, V., Budde, T., Kieseier, B.C., Zipp, F., Wiendl, H., 2009. Cytotoxic CD8+ T cell-neuron interactions: Perforin-dependent electrical silencing precedes but is not causally linked to neuronal cell death. J. Neurosci. https://doi.org/10.1523/JNEUROSCI.4339-09.2009

Minakaki, G., Menges, S., Kittel, A., Emmanouilidou, E., Schaeffner, I., Barkovits, K., Bergmann, A., Rockenstein, E., Adame, A., Marxreiter, F., Mollenhauer, B., Galasko, D., Buzás, E.I., Schlötzer-Schrehardt, U., Marcus, K., Xiang, W., Lie, D.C., Vekrellis, K., Masliah, E., Winkler, J., Klucken, J., 2018. Autophagy inhibition promotes SNCA/alpha-synuclein release and transfer via extracellular vesicles with a hybrid autophagosome-exosome-like phenotype. Autophagy. https://doi.org/10.1080/15548627.2017.1395992

Miyazaki, I., Asanuma, M., 2018. Therapeutic Strategy of Targeting Astrocytes for Neuroprotection in Parkinson's Disease. Curr. Pharm. Des. https://doi.org/10.2174/1381612823666170710163731

Mollenhauer, B., Parnetti, L., Rektorova, I., Kramberger, M.G., Farotti, L., Flach, K., Meixner, H., Hussl, A., Schmitz, M., Kraus, T., Stockner, H., Kallab, M., Katisko, K., Balint, B., Seppi, K., Huber, H., Poewe, W., Krismer, F., Mahlknecht, P., 2019. Biological confounders for the values of cerebrospinal fluid proteins in Parkinson's disease and related disorders: A large multicenter study. *Movement Disorders* 34(8), 1082–1093. https://doi.org/10.1002/mds.27708

Moore, T.J., Glenmullen, J., Mattison, D.R., 2014. Reports of pathological gambling, hypersexuality, and compulsive shopping associated with dopamine receptor agonist drugs. JAMA Intern. Med. https://doi.org/10.1001/jamainternmed.2014.5262

Moquin-Beaudry, G., Andriamboavonjy, L., Audet, S., Hamilton, L. K., Duquette, A., Chouinard, S., Panisset, M., & Tétrault, M. (2025). *Mapping the peripheral immune landscape of Parkinson's disease patients with single-cell sequencing*. Brain, 148(8), 2847-2860. https://doi.org/10.1093/brain/awaf066

Murray, I.V.J., Giasson, B.I., Quinn, S.M., Koppaka, V., Axelsen, P.H., Ischiropoulos, H., Trojanowski, J.Q., Lee, V.M.Y., 2003. Role of α-synuclein carboxy-terminus on fibril formation in vitro. Biochemistry. https://doi.org/10.1021/bi027363r

Murray, P. J., & Wynn, T. A. (2011). *Protective and pathogenic functions of macrophage subsets.* Nature Reviews Immunology, 11(11), 723–737. https://doi.org/10.1038/nri3073

Murray, P. J., Allen, J. E., Biswas, S. K., Fisher, E. A., Gilroy, D. W., Goerdt, S., Gordon, S., Hamilton, J. A., Ivashkiv, L. B., Lawrence, T., Locati, M., Mantovani, A., Martinez, F. O., Mege, J. L., Mosser, D. M., Natoli, G., Saeij, J. P., Schultze, J. L., Shirey, K. A., Sica, A., … Wynn, T. A. (2014). Macrophage activation and polarization: nomenclature and experimental guidelines. *Immunity*, *41*(1), 14–20. https://doi.org/10.1016/j.immuni.2014.06.008

Nagatsu, T., Mogi, M., Ichinose, H., & Togari, A. (2000). Cytokines in Parkinson's disease. *Journal of neural transmission. Supplementum*, (58), 143–151.

Nakamura, K., Nemani, V. M., Wallender, E. K., Kaehlcke, K., Ott, M., & Edwards, R. H. (2008). Optical reporters for the conformation of alpha-synuclein reveal a specific interaction with mitochondria. *The Journal of neuroscience : the official journal of the Society for Neuroscience*, *28*(47), 12305–12317. https://doi.org/10.1523/JNEUROSCI.3088-08.2008

Nalls, M. A., Blauwendraat, C., Vallerga, C. L., Heilbron, K., Bandres-Ciga, S., Chang, D., Tan, M., Kia, D. A., Noyce, A. J., Xue, A., Bras, J., Young, E., von Coelln, R., Simón-Sánchez, J., Schulte, C., Sharma, M., Krohn, L., Pihlstrøm, L., Siitonen, A., Iwaki, H., … International Parkinson's Disease Genomics Consortium (2019). Identification of novel risk loci, causal insights, and heritable risk for Parkinson's disease: a meta-analysis of genome-wide association studies. *The Lancet. Neurology*, *18*(12), 1091–1102. https://doi.org/10.1016/S1474-4422(19)30320-5

Nambu, A., Tokuno, H., & Takada, M. (2002). Functional significance of the cortico-subthalamo-pallidal 'hyperdirect' pathway. *Neuroscience research*, *43*(2), 111–117. https://doi.org/10.1016/s0168-0102(02)00027-5

Narendra, D., Tanaka, A., Suen, D.F., Youle, R.J., 2009. Parkin-induced mitophagy in the pathogenesis of Parkinson disease. Autophagy. https://doi.org/10.4161/auto.5.5.8505

Navarro, E., Udine, E., Lopes, K. P., Parks, M., Riboldi, G., Schilder, B. M., Humphrey, J., Snijders, G. J. L., Vialle, R. A., Zhuang, M., Sikder, T., Argyrou, C., Allan, A., Chao, M. J., Farrell, K., Henderson, B., Simon, S., Raymond, D., Elango, S., Ortega, R. A., … Raj, T. (2021). Dysregulation of mitochondrial and proteolysosomal genes in Parkinson's disease myeloid cells. *Nature aging*, *1*(9), 850–863. https://doi.org/10.1038/s43587-021-00110-x

Neniskyte, U., Gross, C.T., 2017. Errant gardeners: Glial-cell-dependent synaptic pruning and neurodevelopmental disorders. Nat. Rev. Neurosci. https://doi.org/10.1038/nrn.2017.110

Noctor, S.C., Martínez-Cerdeño, V., Ivic, L., Kriegstein, A.R., 2004. Cortical neurons arise in symmetric and asymmetric division zones and migrate through specific phases of radial glial cell division. *Nature Neuroscience* 7(2), 136–144. https://doi.org/10.1038/nn1172

Obeso, J.A., Stamelou, M., Goetz, C.G., Poewe, W., Lang, A.E., Weintraub, D., Burn, D., Halliday, G.M., Bezard, E., Przedborski, S., Lehericy, S., Brooks, D., Rothwell, J.C., Hallett, M., DeLong, M.R., Marras, C., Tanner, C.M., Ross, G.W., Langston, J.W., Klein, C., Bonifati, V., Jankovic, J., Lozano, A.M., Deuschl, G., Bergman, H., Tolosa, E., Rodriguez-Violante, M., Fahn, S., Postuma, R.B., Berg, D., 2017. Past, present, and future of Parkinson's disease: A special essay on the 200th anniversary of the shaking palsy. *Movement Disorders* 32(9), 1264–1310. https://doi.org/10.1002/mds.27115

Okoye, I., Xu, L., Motamedi, M., Parashar, P., Walker, J. W., & Elahi, S. (2020). Galectin-9 expression defines exhausted T cells and impaired cytotoxic NK cells in patients with virus-associated solid tumors. *Journal for ImmunoTherapy of Cancer*, 8(2), e001849. https://doi.org/10.1136/jitc-2020-001849

Okubadejo NU, Bower JH, Rocca WA, Maraganore DM. Parkinson's disease in Africa: a systematic review of epidemiologic and genetic studies. Mov Disord 2006; 21: 2150–56.

Ono, K., Ikeda, T., Takasaki, J. ichi, Yamada, M., 2011. Familial Parkinson disease mutations influence α-Synuclein assembly. Neurobiol. Dis. https://doi.org/10.1016/j.nbd.2011.05.025

Orecchioni, M., Ghosheh, Y., Pramod, A. B., & Ley, K. (2019). *Macrophage polarization: Different gene signatures in M1(LPS+) vs. classically and M2(LPS–) vs. alternatively activated macrophages.* Frontiers in Immunology, 10, 1084. https://doi.org/10.3389/fimmu.2019.01084

Otero-Jimenez, M., Wojewska, M.J., Binding, L.P. *et al.* Neuropathological stages of neuronal, astrocytic and oligodendrocytic alpha-synuclein pathology in Parkinson's disease. *acta neuropathol commun* 13, 25 (2025). https://doi.org/10.1186/s40478-025-01944-x

Oueslati, A., Fournier, M., & Lashuel, H. A. (2010). Role of post-translational modifications in modulating the structure, function and toxicity of alpha-synuclein: Implications for Parkinson's disease pathogenesis and therapies. *Progress in Brain Research, 183*, 115–145. https://doi.org/10.1016/S0079-6123(10)83007-9

Ozoran, H., & Srinivasan, R. (2023). *Astrocytes and alpha-synuclein: Friend or foe?* Journal of Parkinson's Disease, 13(8), 1289-1301. https://doi.org/10.3233/JPD-230284
Ozoran, H., Aydin, D., Özdemir, C., & Ulusoy, A. (2023). *Astrocytes and alpha-synuclein: Friend or foe? Frontiers in Cellular Neuroscience, 17*, 1246949. https://doi.org/10.3389/fncel.2023.1246949

Pagano, G., Taylor, K.I., Anzures-Cabada, R., Marchesi, M., Simuni, T., Marek, K., Postuma, R.B., Pavese, N., Poewe, W., Stocchi, F., Brundin, P., Lane, R., Reith, A.D., 2022. Trial of prasinezumab in early-stage Parkinson's disease. *New England Journal of Medicine* 387(5), 421–432. https://doi.org/10.1056/NEJMoa2202867

Pajares, A., Rojo, A. I., Manda, G., Boscá, L., & Cuadrado, A. (2020). Inflammation in Parkinson's disease: mechanisms and therapeutic implications. *Cells, 9*(7), 1687. https://doi.org/10.3390/cells9071687

Pakkenberg, B., Moller, A., Gundersen, H.J.G., Dam, A.M., Pakkenberg, H., 1991. The absolute number of nerve cells in substantia nigra in normal subjects and in patients with Parkinson's disease estimated with an unbiased stereological method. J. Neurol. Neurosurg. Psychiatry. https://doi.org/10.1136/jnnp.54.1.30

Palfi, S., Gurruchaga, J.M., Scott Ralph, G., Lepetit, H., Lavisse, S., Buttery, P.C., Watts, C., Miskin, J., Kelleher, M., Deeley, S., Iwamuro, H., Lefaucheur, J.P., Thiriez, C., Fenelon, G., Lucas, C., Brugières, P., Gabriel, I., Abhay, K., Drouot, X., Tani, N., Kas, A., Ghaleh, B., Le Corvoisier, P., Dolphin, P., Breen, D.P., Mason, S., Guzman, N.V., Mazarakis, N.D., Radcliffe, P.A., Harrop, R., Kingsman, S.M., Rascol, O., Naylor, S., Barker, R.A., Hantraye, P., Remy, P., Cesaro, P., Mitrophanous, K.A., 2014. Long-term safety and tolerability of ProSavin, a lentiviral vector-based

Pålhagen, S., Heinonen, E., Hägglund, J., Kaugesaar, T., Mäki-Ikola, O., Palm, R., & Swedish Parkinson Study Group (2006). Selegiline slows the progression of the symptoms of Parkinson disease. *Neurology*, *66*(8), 1200–1206. https://doi.org/10.1212/01.wnl.0000204007.46190.54

Pang, S. Y., Ho, P. W., Liu, H. F., Leung, C. T., Li, L., Chang, E. E. S., Ramsden, D. B., & Ho, S. L. (2019). The interplay of aging, genetics and environmental factors in the pathogenesis of Parkinson's disease. *Translational neurodegeneration*, *8*, 23. https://doi.org/10.1186/s40035-019-0165-9

Papachroni, K.K., Ninkina, N., Papapanagiotou, A., Hadjigeorgiou, G.M., Xiromerisiou, G., Papadimitriou, A., Kalofoutis, A., Buchman, V.L., 2007. Autoantibodies to alpha- synuclein in inherited Parkinson's disease. J. Neurochem. https://doi.org/10.1111/j.1471-4159.2006.04365.x

Parent, A., Sato, F., Wu, Y., Gauthier, J., Lévesque, M., Parent, M., 2000. Organization of the basal ganglia: The importance of axonal collateralization. Trends Neurosci. https://doi.org/10.1016/S1471-1931(00)00022-7

Parihar, M.S., Parihar, A., Fujita, M., Hashimoto, M., & Ghafourifar, P. (2008). Mitochondrial association of α-synuclein causes oxidative stress. *Journal of Biological Chemistry*, 283(14), 9089–9100. https://doi.org/10.1074/jbc.M710012200

Parpura, V., & Verkhratsky, A. (2012). The astrocyte excitability brief: from receptors to gliotransmission. *Neurochemistry international*, *61*(4), 610–621. https://doi.org/10.1016/j.neuint.2011.12.001

Paviour, D., Price, S.L., Jahanshahi, M., Lees, A.J., Fox, N.C., 2006. Regional brain volumes distinguish PSP, MSA-P, and PD: MRI-based clinico-radiological correlations. Mov. Disord. https://doi.org/10.1002/mds.20877

Pellerin, L., & Magistretti, P. J. (1994). Glutamate uptake into astrocytes stimulates aerobic glycolysis: A mechanism coupling neuronal activity to glucose utilization. *Proceedings of the National Academy of Sciences, 91*(22), 10625–10629. https://doi.org/10.1073/pnas.91.22.10625

Perez, F., Helmer, C., Dartigues, J.F., Auriacombe, S., Tison, F., 2010. A 15-year population-based cohort study of the incidence of Parkinson's disease and dementia with Lewy bodies in an elderly French cohort. J. Neurol. Neurosurg. Psychiatry. https://doi.org/10.1136/jnnp.2009.189142

Philip Ewels, Måns Magnusson, Sverker Lundin, Max Käller, MultiQC: summarize analysis results for multiple tools and samples in a single report, Bioinformatics, Volume 32, Issue 19, October 2016, Pages 3047–3048, https://doi.org/10.1093/bioinformatics/btw354

Piancone, F., La Rosa, F., Marventano, I., Saresella, M., & Clerici, M. (2021). The Role of the Inflammasome in Neurodegenerative Diseases. *Molecules (Basel, Switzerland)*, *26*(4), 953. https://doi.org/10.3390/molecules26040953

Piccini, P., Brooks, D.J., 2006. New developments of brain imaging for Parkinson's Disease and related disorders. Mov. Disord. https://doi.org/10.1002/mds.20845

Pocock, J.M., Kettenmann, H., 2007. Neurotransmitter receptors on microglia. Trends Neurosci. https://doi.org/10.1016/j.tins.2007.07.007

Poewe, W., Seppi, K., Tanner, C.M., Halliday, G.M., Brundin, P., Volkmann, J., Schrag, A.E., Lang, A.E., 2017. Parkinson disease. Nat. Rev. Dis. Prim. 3, 1–21. https://doi.org/10.1038/nrdp.2017.13

Polania, J. W., et al. (2025). *Antigen presentation by tumor-associated macrophages drives T cells from a progenitor exhaustion state to terminal exhaustion.* Immunity, 58(1), 232-246. https://doi.org/10.1016/j.immuni.2024.11.026
Polania, J. W., Liu, W., Zhang, X., Meng, J., Li, Y., & Li, M. O. (2025). *Antigen presentation by tumor-associated macrophages drives T cells from a progenitor exhaustion state to terminal exhaustion.* Immunity, 58(1), 232–246. https://doi.org/10.1016/j.immuni.2024.11.026

Polymeropoulos, M.H., Lavedan, C., Leroy, E., Ide, S.E., Dehejia, A., Dutra, A., Pike, B., Root, H., Rubenstein, J., Boyer, R., Stenroos, E.S., Chandrasekharappa, S., Athanassiadou, A., Papapetropoulos, T., Johnson, W.G., Lazzarini, A.M., Duvoisin, R.C., Di Iorio, G., Golbe, L.I., Nussbaum, R.L., 1997. Mutation in the α-synuclein gene identified in families with Parkinson's disease. Science (80-.). https://doi.org/10.1126/science.276.5321.2045

Postuma, R.B., Berg, D., 2016. Advances in markers of prodromal Parkinson disease. *Nature Reviews Neurology* 12(11), 622–634. https://doi.org/10.1038/nrneurol.2016.152

Postuma, R.B., Berg, D., Stern, M., Poewe, W., Olanow, C.W., Oertel, W., Obeso, J., Marek, K., Litvan, I., Lang, A.E., Halliday, G., Goetz, C.G., Gasser, T., Dubois, B., Chan, P., Bloem, B.R., Adler, C.H., Deuschl, G., 2015. MDS clinical diagnostic criteria for Parkinson's disease. Mov. Disord. https://doi.org/10.1002/mds.26424

Pozo Devoto, V.M., Dimopoulos, N., Alloatti, M. *et al.* αSynuclein control of mitochondrial homeostasis in human-derived neurons is disrupted by mutations associated with Parkinson's disease. *Sci Rep* 7, 5042 (2017). https://doi.org/10.1038/s41598-017-05334-9

Prater, K.E., Green, K.J., Mamde, S. *et al.* Human microglia show unique transcriptional changes in Alzheimer's disease. *Nat Aging* 3, 894–907 (2023). https://doi.org/10.1038/s43587-023-00424-y

Prinz, M., Jung, S., Priller, J., 2019. Microglia Biology: One Century of Evolving Concepts. Cell. https://doi.org/10.1016/j.cell.2019.08.053

Prodoehl, J., Burciu, R.G., Vaillancourt, D.E., 2014. Resting state functional magnetic resonance imaging in Parkinson's disease. Curr. Neurol. Neurosci. Rep. https://doi.org/10.1007/s11910-014-0448-6

Prusiner, S. B. (2012). Cell biology. A unifying role for prions in neurodegenerative diseases. *Science, 336*(6088), 1511–1513. https://doi.org/10.1126/science.1222951

Pupyshev, A.B., Korolenko, T.A., Akopyan, A.A., Amstislavskaya, T.G., Tikhonova, M.A., 2018. Suppression of autophagy in the brain of transgenic mice with overexpression of A53T-mutant α-synuclein as an early event at synucleinopathy progression. Neurosci. Lett. https://doi.org/10.1016/j.neulet.2017.12.001

Qian, L., Flood, P.M., Hong, J.S., 2010. Neuroinflammation is a key player in Parkinson's disease and a prime target for therapy. J. Neural Transm. https://doi.org/10.1007/s00702-010-0428-1

Qin, L., Wu, X., Block, M.L., Liu, Y., Breese, G.R., Hong, J.S., Knapp, D.J., Crews, F.T., 2007. Systemic LPS causes chronic neuroinflammation and progressive neurodegeneration. Glia. https://doi.org/10.1002/glia.20467

Quattrone, A., Nicoletti, G., Messina, D., Fera, F., Condino, F., Pugliese, P., Lanza, P., Barone, P., Morgante, L., Zappia, M., Aguglia, U., Gallo, O., 2008. MR imaging index for differentiation of progressive supranuclear palsy from Parkinson disease and the Parkinson variant of multiple system atrophy. Radiology. https://doi.org/10.1148/radiol.2453061703

Quik, M., 2004. Smoking, nicotine and Parkinson's disease. Trends Neurosci. https://doi.org/10.1016/j.tins.2004.06.008

Racette, B. A., Aschner, M., Guilarte, T. R., Dydak, U., Criswell, S. R., & Zheng, W. (2012). Pathophysiology of manganese-associated neurotoxicity. *Neurotoxicology*, *33*(4), 881–886. https://doi.org/10.1016/j.neuro.2011.12.010

Rajput, A. H., Rozdilsky, B., & Rajput, A. (1991). Accuracy of clinical diagnosis in parkinsonism--a prospective study. *The Canadian journal of neurological sciences. Le journal canadien des sciences neurologiques*, *18*(3), 275–278. https://doi.org/10.1017/s0317167100031814

Rannikko, E. H., Salo, V., Ryhänen, S.-J., Lotjonen, J., Vainio, S., Oksanen, M., Lehtonen, Š., & Koistinaho, J. (2015). *Exogenous α-synuclein induces toll-like receptor 4 dependent inflammatory responses in astrocytes. BMC Neuroscience, 16*, 79. https://doi.org/10.1186/s12868-015-0192-0

Rannikko, E.H., Weber, S.S., Kahle, P.J., 2015. Exogenous α-synuclein induces toll-like receptor 4 dependent inflammatory responses in astrocytes. *BMC Neuroscience* 16, 57. https://doi.org/10.1186/s12868-015-0192-0

Ransohoff, R. M., Engelhardt, B., & Owens, T. (2009). The immunology of multiple sclerosis and its animal model, experimental autoimmune encephalomyelitis. *Neuron, 64*(1), 13–24. https://doi.org/10.1016/j.neuron.2009.09.015

Rasmussen, M.K., Mestre, H., Nedergaard, M., 2018. The glymphatic pathway in neurological disorders. *Lancet Neurology* 17(11), 1016–1024. https://doi.org/10.1016/S1474-4422(18)30318-1

Reale, M., Iarlori, C., Thomas, A., Gambi, D., Perfetti, B., Di Nicola, M., Onofrj, M., & Tata, A. M. (2009). Peripheral cytokines profile in Parkinson's disease. *Brain, Behavior, and Immunity, 23*(1), 55–63. https://doi.org/10.1016/j.bbi.2008.07.003

Ren, L., Yi, J., Yang, J., Li, P., Cheng, X., Mao, P., 2018. Nonsteroidal anti-inflammatory drugs use and risk of Parkinson disease: A dose–response meta-analysis. Med. (United States). https://doi.org/10.1097/MD.0000000000012172

Rey, N. L., Steiner, J. A., Maroof, N., Luk, K. C., Madaj, Z., Trojanowski, J. Q., Lee, V. M., & Brundin, P. (2016). Widespread transneuronal propagation of α-synucleinopathy triggered in olfactory bulb mimics prodromal Parkinson's disease. *The Journal of experimental medicine*, *213*(9), 1759–1778. https://doi.org/10.1084/jem.20160368

Reynolds, A. D., Banerjee, R., Liu, Y., Gendelman, H. E., & Mosley, R. L. (2010). *Regulatory T cells attenuate Th17 cell–mediated nigrostriatal dopaminergic neurodegeneration in a model of Parkinson's disease*. *The Journal of Immunology, 184*(5), 2261-2271. https://doi.org/10.4049/jimmunol.0901852

Rockenstein, E., Mallory, M., Hashimoto, M., Song, D., Shults, C. W., Lang, I., & Masliah, E. (2002). Differential neuropathological alterations in transgenic mice expressing alpha-synuclein from the platelet-derived growth

factor and Thy-1 promoters. *Journal of neuroscience research*, *68*(5), 568–578. https://doi.org/10.1002/jnr.10231

Roodveldt, C., Bernardino, L., Oztop-Cakmak, O., Dragic, M., Fladmark, K. E., Ertan, S., Aktas, B., Pita, C., Ciglar, L., Garraux, G., Williams-Gray, C., Pacheco, R., & Romero-Ramos, M. (2024). The immune system in Parkinson's disease: what we know so far. *Brain : a journal of neurology*, *147*(10), 3306–3324. https://doi.org/10.1093/brain/awae177

Ross, G.W., Abbott, R.D., Petrovitch, H., Morens, D.M., Grandinetti, A., Tung, K.H., Tanner, C.M., Masaki, K.H., Blanchette, P.L., Curb, J.D., Popper, J.S., White, L.R., 2000. Association of coffee and caffeine intake with the risk of Parkinson disease. J. Am. Med. Assoc. https://doi.org/10.1001/jama.283.20.2674

Rostami, J., Fotaki, G., Sirois, J., Mzezewa, R., Bergström, J., Essand, M., Healy, L., … Erlandsson, A. (2020).*Astrocytes have the capacity to act as antigen-presenting cells in the Parkinson's disease brain.* Journal of Neuroinflammation, 17, 119. https://doi.org/10.1186/s12974-020-01776-7

Rostami, J., Holmqvist, S., Lindström, V., Sigvardson, J., Westermark, G. T., Ingelsson, M., Bergström, J., & Erlandsson, A. (2017). *Human astrocytes transfer aggregated α-synuclein via tunneling nanotubes. Journal of Neuroscience, 37*(49), 11835–11853. https://doi.org/10.1523/JNEUROSCI.0983-17.2017

Russo, M. J., Orru, C. D., Concha-Marambio, L., Giaisi, S., Groveman, B. R., Farris, C. M., Holguin, B., Hughson, A. G., LaFontant, D. E., Caspell-Garcia, C., Coffey, C. S., Mollon, J., Hutten, S. J., Merchant, K., Heym, R. G., Soto, C., Caughey, B., & Kang, U. J. (2021). High diagnostic performance of independent alpha-synuclein seed amplification assays for detection of early Parkinson's disease. *Acta neuropathologica communications*, *9*(1), 179. https://doi.org/10.1186/s40478-021-01282-8

Ryu, E. J., Harding, H. P., Angelastro, J. M., Vitolo, O. V., Ron, D., & Greene, L. A. (2002). Endoplasmic reticulum stress and the unfolded protein response in cellular models of Parkinson's disease. *The Journal of neuroscience : the official journal of the Society for Neuroscience*, *22*(24), 10690–10698. https://doi.org/10.1523/JNEUROSCI.22-24-10690.2002

Sakagami, T., Uchida, K., Suzuki, T., Carey, B. C., Wood, R. E., Wert, S. E., Whitsett, J. A., Trapnell, B. C., & Luisetti, M. (2009). Human GM-CSF autoantibodies and reproduction of pulmonary alveolar proteinosis. *The New England journal of medicine*, *361*(27), 2679–2681. https://doi.org/10.1056/NEJMc0904077

Sankowski, R., Süß, P., Benkendorff, A. *et al.* Multiomic spatial landscape of innate immune cells at human central nervous system borders. *Nat Med* 30, 186–198 (2024). https://doi.org/10.1038/s41591-023-02673-1

Saunders, J.A., Estes, K.A., Kosloski, L.M., Allen, H.E., Dempsey, K.M., Torres-Russotto, D.R., Meza, J.L., Santamaria, P.M., Bertoni, J.M., Murman, D.L., Ali, H.H., Mosley, R.L., Gendelman, H.E., 2012. CD4+ regulatory and effector/memory T cell subsets profile motor dysfunction in Parkinson's disease. *Journal of Neuroimmune Pharmacology* 7(4), 927–938. https://doi.org/10.1007/s11481-012-9402-z

Savica, R., Rocca, W.A., Ahlskog, J.E., 2010. When does Parkinson disease start? Arch. Neurol. https://doi.org/10.1001/archneurol.2010.135

Sawada H, Shimohama S. *Estrogens and Parkinson disease: novel approach for neuroprotection.* Endocrine. 2003;21(1):77–79. doi:10.1385/ENDO:21:1:77.

Schapira, A. H. V., Chaudhuri, K. R., & Jenner, P. (2017). Non-motor features of Parkinson disease. *Nature Reviews Neuroscience, 18*, 435–450. https://doi.org/10.1038/nrn.2017.62

Schapira, A.H.V., Gegg, M.E., 2011. Mitochondrial contribution to Parkinson's disease pathogenesis. *Parkinson's Disease* 2011, 159160. https://doi.org/10.4061/2011/159160

Scheiblich, H., Bousset, L., Schwartz, S., et al. (2021). Microglial NLRP3 inflammasome activation upon TLR2 and TLR5 ligation by distinct α-synuclein assemblies. *Journal of Immunology, 207*(8), 2143-2154. https://doi.org/10.4049/jimmunol.2100035

Scherman, D., Desnos, C., Darchen, F., Pollak, P., Javoy-Agid, F., Agid, Y., 1989. Striatal dopamine deficiency in parkinson's disease: Role of aging. Ann. Neurol. https://doi.org/10.1002/ana.410260409

Schlachetzki, J. C. M., Prots, I., Tao, J., Chun, H. B., Saijo, K., Gosselin, D., Winner, B., Glass, C. K., & Winkler, J. (2018). A monocyte gene expression signature in the early clinical course of Parkinson's disease. *Scientific reports*, *8*(1), 10757. https://doi.org/10.1038/s41598-018-28986-7

Schonhoff, A.M., Figge, D.A., Williams, G.P. *et al.* Border-associated macrophages mediate the neuroinflammatory response in an alpha-synuclein model of Parkinson disease. *Nat Commun* 14, 3754 (2023). https://doi.org/10.1038/s41467-023-39060-w

Schulz, C., Perdiguero, E.G., Chorro, L., Szabo-Rogers, H., Cagnard, N., Kierdorf, K., Prinz, M., Wu, B., Jacobsen, S.E.W., Pollard, J.W., Frampton, J., Liu, K.J., Geissmann, F., 2012. A lineage of myeloid cells independent of myb and hematopoietic stem cells. Science (80-.). https://doi.org/10.1126/science.1219179

Schweighauser, M., Shi, Y., Tarutani, A., Kametani, F., Murzin, A.G., Ghetti, B., Matsubara, T., Tomita, T., Ando, T., Hasegawa, K., Murayama, S., Yoshida, M., Ryskeldi-Falcon, B., Goedert, M., Scheres, S.H.W., 2021. Structures of α-synuclein filaments from multiple system atrophy. *Nature* 585(7825), 464–469. https://doi.org/10.1038/s41586-020-2317-6

Sergin, I., Evans, T. D., Zhang, X., Bhattacharya, S., Stokes, C. J., Song, E., Ali, S., Dehestani, B., Holloway, K. B., Micevych, P. S., Javaheri, A., Crowley, J. R., Ballabio, A., Schilling, J. D., & Razani, B. (2017). *Exploiting macrophage autophagy–lysosomal biogenesis as a therapy for atherosclerosis.* Nature Communications, 8, 15750. https://doi.org/10.1038/ncomms15750

Sethi, K., 2008. Levodopa unresponsive symptoms in Parkinson disease. Mov. Disord. https://doi.org/10.1002/mds.22049

Sheng, J., Ruedl, C., & Karjalainen, K. (2015). Most Tissue-Resident Macrophages Except Microglia Are Derived from Fetal Hematopoietic Stem Cells. *Immunity*, *43*(2), 382–393. https://doi.org/10.1016/j.immuni.2015.07.016

Shimohama, S., Tanino, H., Kawakami, N., Okamura, N., Kodama, H., Yamaguchi, T., Hayakawa, T., Nunomura, A., Chiba, S., Perry, G., Smith, M.A., Fujimoto, S., 2000. Activation of NADPH oxidase in Alzheimer's disease brains. Biochem. Biophys. Res. Commun. https://doi.org/10.1006/bbrc.2000.2897

Siderowf, A., Concha-Marambio, L., Lafontant, D. E., Farris, C. M., Ma, Y., Urenia, P. A., Nguyen, H., Alcalay, R. N., Chahine, L. M., Foroud, T., Galasko, D., Kieburtz, K., Merchant, K., Mollenhauer, B., Poston, K. L., Seibyl, J., Simuni, T., Tanner, C. M., Weintraub, D., Videnovic, A., … Parkinson's Progression Markers Initiative (2023). Assessment of heterogeneity among participants in the Parkinson's Progression Markers Initiative cohort using α-synuclein seed amplification: a cross-sectional study. *The Lancet. Neurology*, *22*(5), 407–417. https://doi.org/10.1016/S1474-4422(23)00109-6

Sidibé, M., Bevan, M.D., Bolam, J.P., Smith, Y., 2002. Functional connectivity of the globus pallidus: evidence for a dual GABAergic striato-pallidal pathway. *Journal of Neuroscience* 22(20), 8502–8510. https://doi.org/10.1523/JNEUROSCI.22-20-08502.2002

Sidransky E, Nalls MA, Aasly JO, Aharon-Peretz J, Annesi G, Barbosa ER, Bar-Shira A, Berg D, Bras J, Brice A, Chen CM, Clark LN, Condroyer C, De Marco EV, Dürr A, Eblan MJ, Fahn S, Farrer MJ, Fung HC, et al. *Multicenter analysis of glucocerebrosidase mutations in Parkinson's disease. New England Journal of Medicine.* 2009;361(17):1651–1661. doi:10.1056/NEJMoa0901281. https://pubmed.ncbi.nlm.nih.gov/19846850/

Silvin, A., Ginhoux, F., & Guilliams, M. (2023). *Brain macrophage development, diversity and neurodegenerative disease.* Cellular & Molecular Immunology, 20, 503–517. https://doi.org/10.1038/s41423-023-01053-6

Simon, D.K., Tanner, C.M., Brundin, P., 2020. Parkinson Disease Epidemiology, Pathology, Genetics, and Pathophysiology. Clin. Geriatr. Med. https://doi.org/10.1016/j.cger.2019.08.002

Singleton, A.B., Farrer, M., Johnson, J., Singleton, A., Hague, S., Kachergus, J., Hulihan, M., Peuralinna, T., Dutra, A., Nussbaum, R., Lincoln, S., Crawley, A., Hanson, M., Maraganore, D., Adler, C., Cookson, M.R., Muenter, M., Baptista, M., Miller, D., Blancato, J., Hardy, J., Gwinn-Hardy, K., 2003. α-Synuclein locus triplication causes Parkinson's disease. *Science* 302(5646), 841. https://doi.org/10.1126/science.1090278

Siwecka, N., Misiewicz, M., & Wojewódzka, A. (2023). The interplay between α-synuclein and RNA metabolism: Implications for Parkinson's disease. *Neurobiology of Disease*, 178, 106062. https://doi.org/10.1016/j.nbd.2022.106062

Smith, A. J., Yao, X., Dix, J. A., Jin, B. J., & Verkman, A. S. (2017). Test of the 'glymphatic' hypothesis demonstrates diffusive and aquaporin-4-independent solute transport in rodent brain parenchyma. *eLife*, *6*, e27679. https://doi.org/10.7554/eLife.27679

Smith, W.W., Pei, Z., Jiang, H., Moore, D.J., Liang, Y., West, A.B., Dawson, V.L., Dawson, T.M., Ross, C.A., 2005. Leucine-rich repeat kinase 2 (LRRK2) interacts with parkin, and mutant LRRK2 induces neuronal degeneration. Proc. Natl. Acad. Sci. U. S. A. https://doi.org/10.1073/pnas.0508052102

Sofroniew, M. V., & Vinters, H. V. (2010). Astrocytes: Biology and pathology. *Acta Neuropathologica, 119*(1), 7–35. https://doi.org/10.1007/s00401-009-0619-8

Sommer, A., Marxreiter, F., Krach, F., Fadler, T., Grosch, J., Maroni, M., Graef, D., Eberhardt, E., Riemenschneider, M. J., Yeo, G. W., Kohl, Z., Xiang, W., Gage, F. H., Winkler, J., & Prots, I. (2018). *Th17 lymphocytes induce neuronal cell death in a human iPSC-derived model of Parkinson's disease.* Cell Stem Cell, 23(1), 123–131.e6. https://doi.org/10.1016/j.stem.2018.06.015

Song, W., Zhou, Zm., Zhang, Ll. *et al.* Infiltrating peripheral monocyte TREM-1 mediates dopaminergic neuron injury in substantia nigra of Parkinson's disease model mice. *Cell Death Dis* 16, 18 (2025). https://doi.org/10.1038/s41419-025-07333-5

Sorrentino, Z. A., Giasson, B. I., & Chakrabarty, P. (2019). *α-Synuclein and astrocytes: Tracing the pathways from homeostasis to neurodegeneration in Lewy body disease. Acta Neuropathologica, 138*(6), 873–898. https://doi.org/10.1007/s00401-019-02067-0

Sosna, J., Philipp, S., Albay, R., Reyes-Ruiz, J. M., Baglietto-Vargas, D., LaFerla, F. M., & Glabe, C. G. (2018).*Early long-term administration of the CSF1R inhibitor PLX3397 ablates microglia and reduces accumulation of intraneuronal amyloid, neuritic plaque deposition, and pre-fibrillar oligomers in 5XFAD mouse model of Alzheimer's disease.* Molecular Neurodegeneration, 13(1), 11. https://doi.org/10.1186/s13024-018-0244-x

Souza, J.M., Giasson, B.I., Chen, Q., Lee, V.M.Y., Ischiropoulos, H., 2000. Dityrosine cross-linking promotes formation of stable α-synuclein polymers: Implication of nitrative and oxidative stress in the pathogenesis of neurodegenerative synucleinopathies. J. Biol. Chem. https://doi.org/10.1074/jbc.M000206200

Spangenberg, E. E., Lee, R. J., Najafi, A. R., Rice, R. A., Elmore, M. R. P., Blurton-Jones, M., West, B. L., & Green, K. N. (2016). *Eliminating microglia in Alzheimer's mice prevents neuronal loss without modulating amyloid-β pathology.* Brain, 139(4), 1265–1281. https://doi.org/10.1093/brain/aww016

Spangenberg, E., Green, K. N., Murphy, M. P., Hohsfield, L. A., Lambert, J. C., & Green, K. N. (2019). *Sustained microglial depletion with CSF1R inhibitor (PLX5622) reveals microglia-initiated plaque pathogenesis in Alzheimer's disease.* Nature Communications, 10, 3758. https://doi.org/10.1038/s41467-019-11674-z

Spillantini, M.G., Crowther, R.A., Jakes, R., Hasegawa, M., Goedert, M., 1998. α-Synuclein in filamentous inclusions of Lewy bodies from Parkinson's disease and dementia with Lewy bodies. *Proceedings of the National Academy of Sciences of the USA (PNAS)* 95(11), 6469–6473. https://doi.org/10.1073/pnas.95.11.6469

Spillantini, M.G., Schmidt, M.L., Lee, V.M.Y., Trojanowski, J.Q., Jakes, R., Goedert, M., 1997. α-synuclein in Lewy bodies [8]. Nature. https://doi.org/10.1038/42166

Srinivasan, R., Lu, T.-Y., Chai, H., Xu, J., Huang, B. S., Golshani, P., Coppola, G., & Khakh, B. S. (2016). *New transgenic mouse lines for selectively targeting astrocytes and studying calcium signals in astrocyte processes in situ and in vivo.* Neuron, 92(6), 1181–1195. https://doi.org/10.1016/j.neuron.2016.11.030

Stephenson, J., Nutma, E., van der Valk, P., & Amor, S. (2018). Inflammation in CNS neurodegenerative diseases. *Immunology*, *154*(2), 204–219. https://doi.org/10.1111/imm.12922.

Sulzer, D., Alcalay, R. N., Garretti, F., Cote, L., Kanter, E., Agin-Liebes, J., Liong, C., McMurtrey, C., Hildebrand, W. H., Mao, X., Dawson, T. M., Dawson, V. L., Oseroff, C., Peters, B., Sidney, J., & Sette, A. (2017). *T cells from patients with Parkinson's disease recognize α-synuclein peptides.* Nature, 546(7660), 656–661. https://doi.org/10.1038/nature22815

Sun, R., & Jiang, H. (2024). *Border-associated macrophages in the central nervous system. Journal of Neuroinflammation, 21*, 67. https://doi.org/10.1186/s12974-024-03059-x

Sveinbjornsdottir, S., 2016. The clinical symptoms of Parkinson's disease. J. Neurochem. 139, 318–324. https://doi.org/10.1111/jnc.13691

Tansey, M.G., Romero-Ramos, M., 2019. Immune system responses in Parkinson's disease: early and dynamic. *European Journal of Neuroscience* 49(3), 364–383. https://doi.org/10.1111/ejn.14290

Tansey, M.G., Wallings, R.L., Houser, M.C. *et al.* Inflammation and immune dysfunction in Parkinson disease. *Nat Rev Immunol* 22, 657–673 (2022). https://doi.org/10.1038/s41577-022-00684-6

Teismann, P., & Ferger, B. (2001). Inhibition of the cyclooxygenase isoenzymes COX-1 and COX-2 provide neuroprotection in the MPTP-mouse model of Parkinson's disease. *Synapse (New York, N.Y.)*, *39*(2), 167–174. https://doi.org/10.1002/1098-2396(200102)39:2<167::AID-SYN8>3.0.CO;2-U

Tetrud, J.W., Langston, J.W., 1989. The effect of deprenyl (selegiline) on the natural history of Parkinson's disease. Science (80-.). https://doi.org/10.1126/science.2502843

Thome, A. D., Baxter, M., Forman, T., & Gutfreund, N. (2021). Peripheral monocyte transcriptomic alterations in Parkinson's disease implicate mitochondrial, proteostatic and inflammatory pathways. *Frontiers in Immunology, 12*, 712541. https://doi.org/10.3389/fimmu.2021.712541

Thome, A.D., Faridar, A., Beers, D.R. *et al.* Functional alterations of myeloid cells during the course of Alzheimer's disease. *Mol Neurodegeneration* 13, 61 (2018). https://doi.org/10.1186/s13024-018-0293-

Tremblay, M. E., Cookson, M. R., & Civiero, L. (2019). Glial phagocytic clearance in Parkinson's disease. *Molecular neurodegeneration*, *14*(1), 16. https://doi.org/10.1186/s13024-019-0314-8

Tremblay, M.È., Lecours, C., Samson, L., Sánchez-Zafra, V., Sierra, A., 2015. From the Cajal alumni Achúcarro and Río-Hortega to the rediscovery of never-resting microglia. Front. Neuroanat. https://doi.org/10.3389/fnana.2015.00045

Trexler, A.J., Rhoades, E., 2009. α-Synuclein binds large unilamellar vesicles as an extended helix. Biochemistry. https://doi.org/10.1021/bi900114z

Trinh, J., Guella, I., & Farrer, M. J. (2014). *JAMA Neurol, 71*(12), 1535–1539. doi:10.1001/jamaneurol.2014.1909.

Tsai, W. H., … (2021). *CX3CL1(+) microparticles-induced MFG-E8 enhances macrophage phagocytic activity.* Cells, 10(10), 2583. https://doi.org/10.3390/cells10102583

Ulmer, T.S., Bax, A., Cole, N.B., & Nussbaum, R.L. (2005). Structure and dynamics of micelle-bound human α-synuclein. *Journal of Biological Chemistry*, 280(10), 9595–9603. https://doi.org/10.1074/jbc.M411805200

Unger, M. S., Schernthaner, P., Marschallinger, J., Mrowetz, H., Aigner, L. (2018). *Microglia prevent peripheral immune cell invasion and promote an anti-inflammatory environment in the brain of APP-PS1 transgenic mice.* Journal of Neuroinflammation, 15, 274. https://doi.org/10.1186/s12974-018-1304-4

Uversky, V.N., Li, J., & Fink, A.L. (2001). Evidence for a partially folded intermediate in α-synuclein fibril formation. *Journal of Biological Chemistry*, 276(14), 10737–10744. https://doi.org/10.1074/jbc.M010907200

Uversky, V.N., Li, J., Souillac, P., Millett, I.S., Doniach, S., Jakes, R., Goedert, M., Fink, A.L., 401AD. Biophysical properties of the synucleins and their propensities to fibrillate: inhibition of alpha-synuclein assembly by beta- and gamma-synucleins. J.Biol.Chem. https://doi.org/10.1074/jbc.M109541200.

Valente, E.M., Bentivoglio, A.R., Dixon, P.H., Ferraris, A., Lalongo, T., Frontali, M., Albanese, A., Wood, N.W., 2001. Localization of a novel locus for autosomal recessive early-onset parkinsonism, PARK6, on human chromosome 1p35-p36. Am. J. Hum. Genet. https://doi.org/10.1086/319522

Vamvaca, K., Volles, M.J., Lansbury, P.T., 2009. The First N-terminal Amino Acids of α- Synuclein Are Essential for α-Helical Structure Formation In Vitro and Membrane Binding in Yeast. J. Mol. Biol. https://doi.org/10.1016/j.jmb.2009.03.021

Varatharaj, A., Galea, I., 2017. The blood-brain barrier in systemic inflammation. Brain. Behav. Immun. https://doi.org/10.1016/j.bbi.2016.03.010

Verkhratsky, A., Butt, A., Li, B. *et al.* Astrocytes in human central nervous system diseases: a frontier for new therapies. *Sig Transduct Target Ther* 8, 396 (2023). https://doi.org/10.1038/s41392-023-01628-9

Verkhratsky, A., Nedergaard, M., 2018. Physiology of astroglia. Physiol. Rev. https://doi.org/10.1152/physrev.00042.2016

Viejo, L., Noori, A., Merrill, E., Das, S., Hyman, B. T., & Serrano-Pozo, A. (2022). *Systematic review of human post-mortem immunohistochemical studies and bioinformatics analyses unveil the complexity of astrocyte reaction in Alzheimer's disease*. *Neuropathology and Applied Neurobiology*, 48(1), e12753. https://doi.org/10.1111/nan.12753

Villar-Piqué, A., Lopes da Fonseca, T., & Outeiro, T.F. (2016). Structure, function and toxicity of α-synuclein: The Bermuda triangle in synucleinopathies. *Journal of Neurochemistry*, 139(S1), 240–255. https://doi.org/10.1111/jnc.13249

Vitek, J.L., Hashimoto, T., Kaneoke, Y., Roper, S.N., Bakay, R.A.E., 2003. Microelectrode recordings of pallidal neurons in Parkinson's disease: comparison with the MPTP primate model. *Journal of Neurosurgery* 98(6), 1268–1277.

Vollstedt, E.J., Kasten, M., Klein, C., Aasly, J., Adler, C., Ahmad-Annuar, A., Albanese, A., Alcalay, R.N., Al-Mubarak, B., Alvarez, V., Andree-Muñoz, B., Annesi, G., Appel- Cresswell, S., Arkadir, D., Armasu, S., Barber, T.R., Bardien, S., Barkhuizen, M., Barrett, M.J., Başak, A.N., Beach, T., Benitez, B.A., Berg, D., Bhatia, K., Binkofski, F., Blauwendraat, C., Bonifati, V., Borges, V., Bozi, M., Brice, A., Brighina, L., Brockmann, K., Brücke, T., Brüggemann, N., Camacho, M., Cardoso, F., Belin, A.C., Carr, J., Chan, P., Chang-Castello, J., Chase, B., Chen-Plotkin, A., Ju Chung, S., Cilia, R., Clarimon, J., Clark, L., Cornejo-Olivas, M., Corvol, J.C., Cosentino, C., Cras, P., Crosiers, D., Damásio, J., Das, P., de Carvalho Aguiar, P., De Michele, G., De Rosa, A., Dieguez, E., Dorszewska, J., Erer, S., Ertan, S., Farrer, M., Fedotova, E., Ferese, R., Ferrarese, C., Ferraz, H., Fiala, O., Foroud, T., Friedman, A., Frigerio, R., Funayama, M., Gambardella, S., Garraux, G., Gatto, E.M., Genç, G., Giladi, N., Goldwurm, S., Gomez-Esteban, J.C., Gómez-Garre, P., Gorostidi, A., Grosset, D., Hanagasi, H., Hardy, J., Hassan, A., Hattori, N., Hauser, R.A., Hedera, P., Hentati, F., Hertz, J.M., Holton, J.L., Houlden, H., Hutz, M.H., Ikeuchi, T., Illarioshkin, S., Inca-Martinez, M., Infante, J., Jankovic, J., Jeon, B.S., Jesús, S., Jimenez-Del-Rio, M., Kaasinen, V., Kasten, M., Kataoka, H., Kawakami, H., Kim, Y.J., Klein, C.,

Klivényi, P., Koks, S., König, I.R., Kostić, V., Koziorowski, D., Krüger, R., Krygowska-Wajs, A., Kulisevsky, J., Lai, D., Lang, A., LeDoux, M., Lesage, S., Lim, S.Y., Lin, C.H., Lohmann, K., Lopera, F., Lopez, G., Lu, C.S., Lynch, T., Machaczka, M., Madoev, H., Magalhães, M., Majamaa, K., Maraganore, D., Marder, K., Markopoulou, K., Martikainen, M.H., Mata, I., Mazzetti, P., Mellick, G., Menéndez-González, M., Micheli, F., Mirelman, A., Mir, P., Morino, H., Morris, H., Munhoz, R.P., Naito, A., Olszewska, D.A., Ozelius, L.J., Padmanabhan, S., Paisán- Ruiz, C., Payami, H., Peluso, S., Petkovic, S., Petrucci, S., Pezzoli, G., Pimentel, M., Pirker, W., Pramstaller, P.P., Pulkes, T., Puschmann, A., Quattrone, A., Raggio, V., Ransmayr, G., Rieder, C., Riess, O., Rodriguez-Porcel, F., Rogaeva, E., Ross, O.A., Ruiz-Martinez, J., Sammler, E., San Luciano, M., Satake, W., Saunders- Pullman, R., Sazci, A., Scherzer, C., Schrag, A., Schumacher-Schuh, A., Sharma, M., Sidransky, E., Singleton, A.B., Petersen, M.S., Smolders, S., Spitz, M., Stefanis, L., Struhal, W., Sue, C.M., Swan, M., Swanberg, M., Taba, P., Taipa, R., Tan, M., Tan, A.H., Tan, E.K., Tang, B., Tayebi, N., Thaler, A., Thomas, A., Toda, T., Toft, M., Torres, L., Tumas, V., Valente, E.M., Van Broeckhoven, C., Vecsei, L., Velez-Pardo, C., Vidailhet, M., Vollstedt, E.J., Warner, T.T., Williams-Gray, C.H., Winkelmann, J., Woitalla, D., Wood, N.W., Wszolek, Z.K., Wu, R.M., Wu, Y.R., Xie, T., Yoshino, H., Zhang, B., Zimprich, A., 2019. Using global team science to identify genetic parkinson's disease worldwide. Ann. Neurol. 86, 153–157. https://doi.org/10.1002/ana.25514

Volpicelli-Daley, L.A., Luk, K.C., Patel, T.P., Tanik, S.A., Riddle, D.M., Stieber, A., Meaney, D.F., Trojanowski, J.Q., Lee, V.M.Y., 2011. Exogenous α-Synuclein Fibrils Induce Lewy Body Pathology Leading to Synaptic Dysfunction and Neuron Death. Neuron. https://doi.org/10.1016/j.neuron.2011.08.033

Wakabayashi, K., Hayashi, S., Yoshimoto, M., Kudo, H., & Takahashi, H. (2000). *NACP/α-synuclein-positive filamentous inclusions in astrocytes and oligodendrocytes of Parkinson's disease brains.* Acta Neuropathologica, 99, 14–20. https://doi.org/10.1007/PL00007400

Wang, C., Yang, T., Liang, M., Xie, J., & Song, N. (2021). Astrocyte dysfunction in Parkinson's disease: from the perspectives of transmitted α-synuclein and genetic modulation. *Translational neurodegeneration*, *10*(1), 39. https://doi.org/10.1186/s40035-021-00265-y

Wang, J., … (2023). *Intricacies of TGF-β signaling in Treg and Th17 cell biology.* Cellular & Molecular Immunology. https://doi.org/10.1038/s41423-023-01036-7

Wang, P., Lan, G., Xu, B., Yu, Z., Tian, C., Lei, X., Meissner, W. G., Feng, T., Yang, Y., & Zhang, J. (2023). α-Synuclein-carrying astrocytic extracellular vesicles in Parkinson pathogenesis and diagnosis. *Translational neurodegeneration*, *12*(1), 40. https://doi.org/10.1186/s40035-023-00372-y

Wang, Y., Szretter, K., Vermi, W. *et al.* IL-34 is a tissue-restricted ligand of CSF1R required for the development of Langerhans cells and microglia. *Nat Immunol* 13, 753–760 (2012). https://doi.org/10.1038/ni.2360

Wang, Y., Szretter, K.J., Vermi, W., Gilfillan, S., Rossini, C., Cella, M., Barrow, A.D., Diamond, M.S., Colonna, M., 2012. IL-34 is a tissue-restricted ligand of CSF1R required for the development of Langerhans cells and microglia. Nat. Immunol. https://doi.org/10.1038/ni.2360

Weinberg, S. E., & Chandel, N. S. (2025). *Mitochondria reactive oxygen species signaling-dependent immune responses in macrophages and T cells. Immunity,* *58*(8), 1904-1921. https://doi.org/10.1016/j.immuni.2025.07.012

Weiss, F., Hughes, L., Fu, Y., Bardy, C., Halliday, G. M., & Dzamko, N. (2024). Astrocytes contribute to toll-like receptor 2-mediated neurodegeneration and alpha-synuclein pathology in a human midbrain Parkinson's model. *Translational neurodegeneration*, *13*(1), 62. https://doi.org/10.1186/s40035-024-00448-3

Weisskopf, M.G., O'Reilly, E., Chen, H., Schwarzschild, M.A., Ascherio, A., 2007. Plasma urate and risk of Parkinson's disease. *American Journal of Epidemiology* 166(5), 561–567. https://doi.org/10.1093/aje/kwm127

Weng, Q., Wang, J., Wang, J., He, D., Cheng, Z., Zhang, F., Verma, R., Xu, L., Dong, X., Liao, Y., He, X., Potter, A., Zhang, L., Zhao, C., Xin, M., Zhou, Q., Aronow, B. J., Blackshear, P. J., Rich, J. N., He, Q., … Lu, Q. R. (2019). Single-Cell Transcriptomics Uncovers Glial Progenitor Diversity and Cell Fate Determinants

during Development and Gliomagenesis. *Cell stem cell*, *24*(5), 707–723.e8. https://doi.org/10.1016/j.stem.2019.03.006

Wichmann, T., DeLong, M.R., 2016. Deep brain stimulation for movement disorders of basal ganglia origin: restoring function or functionality? *Neurotherapeutics* 13(2), 264–283. https://doi.org/10.1007/s13311-016-0426-6

Wijeyekoon, R. S., Kronenberg-Versteeg, D., Scott, K. M., Hayat, S., Kuan, W. L., Evans, J. R., Breen, D. P., Cummins, G., Jones, J. L., Clatworthy, M. R., Floto, R. A., Barker, R. A., & Williams-Gray, C. H. (2020). Peripheral innate immune and bacterial signals relate to clinical heterogeneity in Parkinson's disease. *Brain, behavior, and immunity*, *87*, 473–488. https://doi.org/10.1016/j.bbi.2020.01.018

William Langston, J., Ballard, P., Tetrud, J.W., Irwin, I., 1983. Chronic parkinsonism in humans due to a product of meperidine-analog synthesis. Science (80-.). 219, 979– 980. https://doi.org/10.1126/science.6823561

Williams, G. P., Schonhoff, A. M., Jurkuvenaite, A., Gallups, N. J., Standaert, D. G., & Harms, A. S. (2021). CD4 T cells mediate brain inflammation and neurodegeneration in a mouse model of Parkinson's disease. *Brain : a journal of neurology*, *144*(7), 2047–2059. https://doi.org/10.1093/brain/awab103

Willis AW, Schootman M, Kung N, Racette BA, Evanoff BA. *Neurologist care in Parkinson disease: a utilization, outcomes, and survival study.* Neurology. 2011;77(9):851–857. doi:10.1212/WNL.0b013e31822b0118.

Won, W., Park, M., Lee, S., & Lee, C. J. (2023). *Astrocytes as key regulators of neural signaling in health and disease. Annual Review of Neuroscience, 46*, 1–23. https://doi.org/10.1146/annurev-neuro-112723-035356

Wong, Y.C., Luk, K., Purtell, K., Burke Nanni, S., Stoessl, A.J., Trudeau, L.E., Yue, Z., Krainc, D., Oertel, W., Obeso, J.A., Volpicelli-Daley, L.A., 2019. Neuronal vulnerability in Parkinson disease: Should the focus be on axons and synaptic terminals? Mov. Disord. https://doi.org/10.1002/mds.27823

Wood, S.J., Wypych, J., Steavenson, S., Louis, J.-C., Citron, M., Biere, A.L., 1999. α- Synuclein Fibrillogenesis Is Nucleation-dependent. J. Biol. Chem. https://doi.org/10.1074/jbc.274.28.19509

World Health Organization. (2022). *Parkinson disease: key facts and global estimates*. World Health Organization. https://www.who.int/news-room/fact-sheets/detail/parkinson-disease

Wu, D. C., Jackson-Lewis, V., Vila, M., Tieu, K., Teismann, P., Vadseth, C., Choi, D. K., Ischiropoulos, H., & Przedborski, S. (2002). Blockade of microglial activation is neuroprotective in the 1-methyl-4-phenyl-1,2,3,6-tetrahydropyridine mouse model of Parkinson disease. *The Journal of neuroscience : the official journal of the Society for Neuroscience*, *22*(5), 1763–1771. https://doi.org/10.1523/JNEUROSCI.22-05-01763.2002

Xiong, L. L., Du, R. L., Niu, R. Z., Xue, L. L., Chen, L., Huangfu, L. R., Cai, X. X., He, X. Y., Huang, J., Huang, X. Y., Liu, J., Yu, C. Y., Wang, W. Y., & Wang, T. H. (2024). Single-cell RNA sequencing reveals peripheral immunological features in Parkinson's Disease. *NPJ Parkinson's disease*, *10*(1), 185. https://doi.org/10.1038/s41531-024-00790-3

Xu, E., Boddu, R., Abdelmotilib, H.A. *et al.* Pathological α-synuclein recruits LRRK2 expressing pro-inflammatory monocytes to the brain. *Mol Neurodegeneration* 17, 7 (2022). https://doi.org/10.1186/s13024-021-00509-5

Xu, J., Kao, S.Y., Lee, F.J.S., Song, W., Jin, L.W., Yankner, B.A., 2002. Dopamine- dependent neurotoxicity of α-synuclein: A mechanism for selective neurodegeneration in Parkinson disease. Nat. Med. https://doi.org/10.1038/nm0602-600

Xu, K., Xu, Y., Brown-Jermyn, D., Chen, J.F., Ascherio, A., Dluzen, D.E., Schwarzschild, M.A., 2006. Estrogen prevents neuroprotection by caffeine in the mouse 1-methyl- 4-phenyl-1,2,3,6-tetrahydropyridine model of Parkinson's disease. J. Neurosci. https://doi.org/10.1523/JNEUROSCI.3008-05.2006

Yanamandra, K., Gruden, M.A., Casaite, V., Meskys, R., Forsgren, L., Morozova-Roche, L.A., 2011. α-synuclein reactive antibodies as diagnostic biomarkers in blood sera of parkinson's disease patients. PLoS One. https://doi.org/10.1371/journal.pone.0018513

Yoon, J.H., Mo, J.S., Kim, M.Y., Ann, E.J., Ahn, J.S., Jo, E.H., Lee, H.J., Lee, Y.C., Seol, W., Yarmoluk, S.M., Gasser, T., Kahle, P.J., Liu, G.H., Belmonte, J.C.I., Park, H.S., 2017. LRRK2 functions as a scaffolding kinase of ASK1-mediated neuronal cell death. Biochim. Biophys. Acta - Mol. Cell Res. https://doi.org/10.1016/j.bbamcr.2017.09.001

Zaichick, S. V., McGrath, K.M., Caraveo, G., 2017. The role of Ca2+ signaling in Parkinson's disease. DMM Dis. Model. Mech. https://doi.org/10.1242/dmm.028738

Zamboni, M., Llorens-Bobadilla, E., Magnusson, J. P., & Frisén, J. (2020). A Widespread Neurogenic Potential of Neocortical Astrocytes Is Induced by Injury. *Cell stem cell*, *27*(4), 605–617.e5. https://doi.org/10.1016/j.stem.2020.07.006

Zeng, X.-S., Geng, W.-S., Jia, J.-J., Chen, L., & Zhang, P.-P. (2018). Cellular and molecular basis of neurodegeneration in Parkinson's disease. *Frontiers in Aging Neuroscience, 10*, 109. https://doi.org/10.3389/fnagi.2018.00109

Zhang ZX, Roman GC, Hong Z, et al. Parkinson's disease in China: prevalence in Beijing, Xian, and Shanghai. Lancet 2005; 365: 595–97.

Zhang, Y., Liu, S., Zhou, D., Yu, H., Zhao, J., Wang, L., & Xu, Y. (2025). *Microglia depletion reduces neurodegeneration and remodels extracellular matrix in a mouse Parkinson's disease model triggered by α-synuclein overexpression.* Acta Neuropathologica Communications, 13, 56. https://doi.org/10.1186/s40478-025-01915-x

Zhang, Z., Duan, Z., & Cui, Y. (2023). $CD8^+$ T cells in brain injury and neurodegeneration. *Frontiers in cellular neuroscience*, *17*, 1281763. https://doi.org/10.3389/fncel.2023.1281763

Zheng, G. X. Y. et al. (2017). Massively parallel digital transcriptional profiling of single cells. *Nature Communications* 8: 1-12, doi:10.1038/ncomms14049

Zheng, Y., Li, Y., Cai, H., Kou, W., Yang, C., Li, S., Wang, J., Zhang, N., Feng, T. (2024). *Alterations of peripheral lymphocyte subsets in isolated rapid eye movement sleep behavior disorder (iRBD).* Movement Disorders, 39(7), 1179-1189. https://doi.org/10.1002/mds.29798

Zhou, W., Huribert, M.S., Schaack, J., Prasad, K.N., Freed, C.R., 2000. Overexpression of human α-synuclein causes dopamine neuron death in rat primary culture and immortalized mesencephalon-derived cells. Brain Res. https://doi.org/10.1016/S0006-8993(00)02215-0

Zhuang, N., Li, L., Chen, S., Wang, T., 2016. PINK1-dependent phosphorylation of PINK1 and Parkin is essential for mitochondrial quality control. Cell Death Dis. https://doi.org/10.1038/cddis.2016.396

Ziegler-Heitbrock, L., Ancuta, P., Crowe, S., Dalod, M., Grau, V., Hart, D. N., Leenen, P. J. M., Liu, Y.-J., MacPherson, G., Randolph, G. J., Scherberich, J., Schmitz, J., Shortman, K., Sozzani, S., Strobl, H., Zembala, M., Austyn, J. M., & Lutz, M. B. (2010). Nomenclature of monocytes and dendritic cells in blood. *Blood, 116*(16), e74–e80. https://doi.org/10.1182/blood-2010-02-258558

6. ACKNOWLEDGEMENTS

At the end of this doctoral journey, I would like to express my sincere gratitude to all the people who, with their support, presence, and encouragement, made this work possible and contributed to my personal and professional growth.

First and foremost, I would like to extend my heartfelt thanks to Dr. Vania Broccoli, Head of the Stem Cells and Neurogenesis Unit, for giving me the opportunity to carry out my research in his laboratory and for believing in my abilities. His guidance, innovative scientific approach, and passion for research have been a constant source of inspiration for me.

I also want to warmly thank all the members of the lab, with whom I have shared many working days and moments of discussion, for their collaboration, solidarity, and the spirit of exchange that turned this formative experience into an enriching and unforgettable life journey.

Finally, I would like to express my deepest gratitude to my family and friends. Their unwavering support, the trust they have always placed in me, and their presence during the most challenging moments have been essential. Without them, none of this would have been possible.